Annexin-A1 signalling in Inflammation and Cancer

Lauren Kelly

BSc. (Hons)

Thesis submitted in fulfilment of the requirements for the degree of Doctor of Philosophy

College of Medical, Veterinary and Life Sciences

Institute of Infection and Immunity

University of Glasgow

September 2022

Abstract

Annexin-A1(ANXA1) is a member of the Annexin family of calcium-dependent phospholipid-binding proteins that functions in a range of biological processes from cell proliferation to apoptosis. This glucocorticoid-induced protein has a well-defined anti-inflammatory role in innate immunity, with unclear functions in adaptive immunity due to the limited, contrasting data available. A role for ANXA1 and the formyl peptide receptors (FPRs) through which it signals has been suggested in a range of inflammatory diseases and cancers. This thesis aimed to investigate the ANXA1-FPR signalling axis in two primary examples of these disease settings in which pathogenesis is far from understood: Psoriatic Arthritis (PsA) and Multiple Myeloma (MM). Moreover, this project aimed to identify the impact of addition of a novel anti-ANXA1 antibody, MDX-124, to the immune response in healthy cells.

Initial work revealed that MDX-124 could bind to a range of immune cell subsets and confirmed high binding of MDX-124 to cells known to express high amounts of ANXA1 (monocytes). Functional analysis revealed that addition of MDX-124 to both stimulated THP-1 monocytic cells and primary monocytes was associated with an increase in pro-inflammatory cytokine production. Moreover, addition of MDX-124 during the differentiation of THP-1s resulted in an increased activation of intracellular and extracellular signalling proteins associated with survival. This provided some insight into the potential mechanism of how MDX-124 could function in inflammatory settings.

To investigate the potential role for ANXA1-FPR signalling in PsA, preliminary studies characterised surface expression levels of ANXA1 and its receptors, FPR1 and FPR2 on a range of immune cell subsets in PsA and healthy control (HC) samples. This analysis confirmed altered expression of ANXA1, FPR1 and FPR2 in disease-relevant cells PsA. Moreover, analysis of RNA sequencing data form PsA lesional skin (PsA L) revealed an increase in *FPR1* and *FPR2* in these samples compared to HCs. Further analysis defined key disease-associated pathways that were enriched in the PsA L skin associated with FPR1 and FPR2 signalling. This analysis implicated involvement of the ANXA1-FPR signalling axis in both the skin

and peripheral blood compartments in PsA, however more samples are required to confirm this preliminary analysis.

To investigate the role of ANXA1-FPR signalling in MM, flow cytometric analysis of ANXA1, FPR1 and FPR2 surface expression in the immune cell compartment of of MM patient samples and HCs were assessed. Preliminary results revealed a substantial upregulation of both ANXA1 and FPR1 on the circulating B cells of MM patients in 1/3 MM samples assessed. This data was; therefore, inconclusive and further samples are required to investigate these differences expression levels of ANXA1 and FPR1 in MM circulating B cells. Analysis of genomic data from a publicly available MM database revealed that higher expression of the ANXA1 gene at baseline was associated with worst survival outcomes in the cohort of patients assessed. Moreover, high ANXA1 expression was associated with an upregulation of genes associated with worst prognosis and treatment resistance in MM. Notably, baseline *ANXA1* expression correlated with the 1q21 chromosomal amplification abnormality in this cohort of patients, which is linked to worst prognosis in MM. Additionally, high ANXA1 was associated with an upregulation of the S100 family of calcium binding proteins, located at the 1q21 chromosome locus, which, in turn, have been associated with treatment resistance and worse prognosis in MM. This preliminary data has highlighted the potential of ANXA1 signalling in treatment response pathways in MM and provides rationale for further investigation into the interactions between ANXA1 and the MM- associated upregulated genes identified in this study.

In summation, this preliminary data has identified key expression differences in ANXA1 and its receptors in both PsA and MM and highlighted potential pathways worth focusing on for future analysis. Additionally, more repeats of the experiments carried out in this study are needed to confirm the significance of these findings.

Table of Contents

Annexin-A1 signalling in Inflammation and Cancer *1*

Abstract *2*

Table of Contents *4*

List of Tables *6*

List of Figures *7*

Acknowledgements *9*

Author's declaration *11*

Abbreviations *12*

Chapter 1 Introduction *16*

1.1 Overview of the immune system **16**
1.1.1 The innate immune system 16
1.1.2 The adaptive immune system 18

1.2 Annexin-A1 ..... **21**
1.2.1 Annexin-A1 structure and function 21
1.2.2 The formyl peptide receptors 23
1.2.3 ANXA1 signalling in innate immunity 26
1.2.4 ANXA1 signalling in adaptive immunity 27

1.3 ANXA1 in inflammatory disease **28**
1.3.1 ANXA1 signalling in innate inflammation 28
1.3.2 ANXA1 signalling in adaptive inflammation 29

1.4 Psoriatic arthritis **30**
1.4.1 Symptoms and pathogenesis of Psoriatic arthritis 30
1.4.2 Current biomarkers in PsA 33
1.4.3 Current treatment strategies in PsA 36
1.4.4 A potential for ANXA1 signalling in PsA? 39

1.5 ANXA1 signalling in cancer **41**
1.5.1 The immune system in cancer 41
1.5.2 ANXA1 and FPR signalling in cancer 43

1.6 Multiple myeloma **45**
1.6.1 Symptoms and pathogenesis of Multiple Myeloma 45
1.6.2 Current biomarkers in MM 48
1.6.3 Current treatment strategies in MM 50
1.6.4 A role for ANXA1 signalling in MM? 51

1.7 Hypothesis and Aims **53**

Chapter 2 Materials and methods *55*

2.1 Patients and controls **55**

2.2 Cell isolation, culture and treatment **55**
2.2.1 Peripheral blood mononuclear cell isolation 55
2.2.2 $CD14^+$ primary monocyte isolation 56
2.2.3 Isolation of primary monocytes by CD16 and CD14 positive selection 57
2.2.4 LPS treatment of primary monocytes 58
2.2.5 Differentiation and treatment of THP-1 cell line 59

2.3 MDX-124 60
2.3.1 MDX-124 development timeline 60
2.3.2 Quality control tests carried out on MDX-124 by Medannex Limited 61
2.3.3 MDX-124 conjugation 62
2.3.4 Apoptosis assay 63
2.3.5 Seahorse metabolomics assay 65

2.4 Cell surface staining using flow cytometry 67
2.4.1 Staining protocol 67
2.4.2 Characterisation of ANXA1 surface expression on tissues from different species 68

2.5 Functional assays with MDX-124 71
2.5.1 Analysis of single cytokine production via ELISA 71
2.5.2 Proteome profiler for kinase and multi cytokine analysis 74

2.6 Analysis of RNA sequencing data 77
2.6.1 Database analysis 77

2.7 Statistical analysis 78

Chapter 3 Assessment of a novel antibody against Annexin A1 79

3.1 Introduction 79

3.2 Results 82
3.2.1 MDX-124 surface staining in animal tissue 82
3.2.2 MDX-124 batch comparisons 85
3.2.3 MDX-124 surface staining of healthy human PBMCs 87
3.2.4 Refinement of PsA flow cytometry panel 92
3.2.5 MDX-124 does not induce apoptosis in healthy cells 96
3.2.6 Assessment of the effects of MDX-124 on cellular metabolism 99

3.3 Discussion 102

Chapter 4 Annexin A1 and the Formyl peptide receptors in inflammatory disease 107

4.1 Introduction 107

4.2 Results 110
4.2.1 RNA sequencing analysis of ANXA1 and FPRs in PsA skin 110
4.2.2 Enriched signalling pathways in the PsA L skin involving FPR1 and FPR2 120
4.2.3 Analysis of ANXA1, FPR1 and FPR2 surface protein expression in PsA 124
4.2.4 Assessment of the correlative relationship between ANXA1, FPR1 and FPR2 expression and clinical markers of disease activity 139
4.2.5 Investigation of FPR1 signalling in the THP-1 cell line 143
4.2.6 MDX-124 treatment of primary monocytes 155

4.3 Discussion 159

Chapter 5 Annexin A1 and the formyl peptide receptors in cancer 170

5.1 Introduction 170

5.2 Results 172
5.2.1 Characterisation of ANXA1 and FPR1/2 surface expression in multiple myeloma 172
5.2.2 Analysis of genomic data from multiple myeloma patients using the CoMMpass database 179

5.3 Discussion 190

Chapter 6 General Discussion 198

Appendix 205

List of References 233

List of Tables

Table 1.1 Disease activity scores in PsA..... 34
Table 2.1 Antibodies for flow cytometric analysis 69

List of Figures

Figure 1.1 Human CD4+ and CD8+ T cell subsets 21
Figure 1.2 Structure of the ANXA1 protein 22
Figure 1.3 Calcium binding to ANXA1 exposes the N- terminus 23
Figure 1.4 ANXA1-FPR2 interactions have different outcomes in different immune cells 25
Figure 1.5 IL-23 and IL-12 signalling 38
Figure 1.6 MM pathogenesis 47
Figure 2.1 Principles of the Annexin V staining apoptosis assay. 64
Figure 2.2 IL-6 and TNF-α ELISA standard curves 72
Figure 2.3 ANXA1 ELISA standard curve 73
Figure 2.4 BCA assay standard curve 75
Figure 3.1 MDX-124 binds to rat lymph node and spleen cells 83
Figure 3.2 MDX-124 binds to Golden Syrian hamster cells 84
Figure 3.3 MDX-124 batch comparisons 86
Figure 3.4 Characterisation of ANXA1, FPR1 and FPR2 surface expression in healthy PBMCs 91
Figure 3.5 Characterisation of ANXA1 surface expression in PsA and HC immune cell populations 95
Figure 3.6 Apoptosis assay 98
Figure 3.7 100ng/ml MDX-124 may affect cellular respiration 101
Figure 4.1 FPR1 and FPR2 genes are expressed at significantly higher levels in PsA lesional skin 111
Figure 4.2 Multiple signalling pathways are upregulated in the PsA L skin 114
Figure 4.3 Genes in the PsA L skin with the top correlations with FPR1 and FPR2 119
Figure 4.4 FPR1 and FPR2 are involved in key signalling pathways in the PsA L skin 123
Figure 4.5 Gating strategy for flow cytometry analysis of Monocyte/DC, B cell and T cell panels 128
Figure 4.6 Expression profiles of ANXA1, FPR1 and FPR2 on peripheral blood immune cell subsets. 133
Figure 4.7 Surface expression of ANXA1 and its receptors is altered in a cell-specific manner in PsA 137
Figure 4.8 No significant difference in plasma ANXA1 expression between PsA and HC samples 138
Figure 4.9 ANXA1, FPR1 and FPR2 gene expression in PsA L skin do not correlate with clinical markers of disease activity 140
Figure 4.10 FPR1 surface expression on certain B cell subsets correlates with DAPSA 142
Figure 4.11 Differentiation of THP-1s into macrophage-like cells 144
Figure 4.12 MDX-124 has no effect on undifferentiated THP-1 cells 145
Figure 4.13 Treatment with MDX-124 during the differentiation of THP-1 cells is associated with a downregulation in surface FPR1 147
Figure 4.14 Treatment with MDX-124 during the differentiation of THP-1 cells is associated with increased production of several phosphokinases 149
Figure 4.15 Treatment with MDX-124 during the differentiation of THP-1 cells is associated with increased production of cytokines, growth factors and other soluble proteins associated with survival and inflammation 154
Figure 4.16 Figure 4.16 MDX-124 treatment enhances LPS-associated pro-inflammatory cytokine production in $CD14^{+}$monocyte populations 157

Figure 4.17 Proposed mechanism of action of MDX-124 during THP-1 differentiation 166
Figure 5.1 ANXA1 and FPR1 surface expression is increased on peripheral blood B cells in a MM patient 174
Figure 5.2 FPR1 expression is higher on peripheral blood monocytes in MM samples 178
Figure 5.3 Higher ANXA1 gene expression at baseline is associated with worst survival outcomes and an upregulation in pro-cancer pathways 184
Figure 5.4 ANXA1 expression in MM cohort correlates with several cancer-associated genes 187
Figure 5.5 Expression of ANXA1 and FPR1 at baseline is associated with chromosomal markers of unfavourable disease prognosis 189

Acknowledgements

First and foremost, I would like to thank my primary supervisor, Prof. Carl Goodyear; your guidance over the last 4 years has helped me develop as a scientist, and for that I am very grateful. I would also like to thank my supervisor Fiona, Scott, Henry and everyone else at Medannex,you have answered all of my panicked technical questions and encouraged me throughout the PhD. Additionally, I'd like to thank my supervisor Iain McInnes for his optimism and encouragement throughout all of the lab meetings.

A huge thank you to the past and present members of the Goodyear Lab. Many of you are my friends as well as colleagues, without whom I would not have finished this PhD. Huge thanks goes to Aysin, you guided me with a friendly face from the very start, and have always been there to support me and boost my confidence; I am so grateful and will miss doing science with you! Thanks to Patricia for sharing this PhD journey with me, and always making sure I got a Tinderbox coffee on the way to work. A huge thanks to Cecila, you're always there to offer sound technical and life advice-I'm lucky to know you. To Flavia-you made sure my PhD journey was full of good music, laughs and yoga-thank you! A tremendous thanks to Kieran, Maria-Laura, Shiny, Annie, Mukanthu, Carmen, Aurelie, Yuriko and Andy-you've all helped me along the way, be it with a lab crisis or assisting with some pints in the pub! Special thanks to Cameron and John, you saved me from a coding crisis and answered all of my panicked questions with ease, I'm super grateful. Thanks to the Beatson and University of Glasgow Flow facility staff for the use and guidance with all of their equipment throughout my PhD.

A big thanks to all of my friends, who have helped at various stages throughout this journey. Thanks to Gabby, Heather, Gemma and Caitlin, you've listened to me, supported me and shared all my PhD struggles, as well as being there for a casual hot-tub holiday to ease the stress! To Kirstin, thanks for tackling the madness of the world with me during lockdown, all with a Gu pot and reality TV! Huge thanks to Katy, you've been a massive support to me throughout this journey, from body balance dates to hour long chats on the phone- I'm extremely grateful.

Massive thanks to my mum, dad, granny and granda, you have supported me through the highs and lows of these last few years. To Alice-Marie, William, Ben and Alice, you've all been there for support, encouragement and plenty of laughs, I'm lucky to have you. Of course, special thanks to all of the fur babies in my life, Lúna, Koko, Leo, Poppy, Skye, Honey and Snuggles- you've been there for cuddles when life was getting me down. Special thanks to Daniel, you've been my most vital support and were able boost my confidence when I was really struggling- I'm forever grateful.

Author's declaration

I declare that this thesis is the result of my own work. No part of this thesis has been submitted for any other degree at The University of Glasgow, or any other institution.

Signature: Printed name: Lauren Kelly

Abbreviations

1p21	Deletion of the small arm of chromosome 21
1q21	Deletion of the long arm of chromosome 21
AB	Antibody
ACPA	Anti-Citrullinated Peptide Antibody
ANXA1	Annexin- A1
ANXA3	Annexin- A3
APC	Antigen Presenting Cell
ATP	Adenosine 5‘-triphosphate
BAFF	B-cell Activating Factor
BAL	Bronchoalveolar Lavage
BM	Bone Marrow
BMSCs	Bone Marrow Stromal Cells
Breg	Regulatory B cells
cAMP	Cyclic Adenosine Monophosphate
CHIPS	Chemotaxis Inhibitory Protein of S. aureus
CHO	Chinese Hamster Ovary
CIA	Collagen-Induced Arthritis
CM	Central Memory
CNS	Central Nervous System
CNV	Copy Number Variation
COPD	Chronic Obstructive Pulmonary Disease
CPII	C-propeptide of type II collagen
CRC	Colorectal Cancer
CRP	C-Reactive Protein
CSB	Cell Separation Buffer
csDMARD	Conventional Synthetic DMARD
CTC	Circulating Tumour Cell
ctDNA	Circulating Tumour DNA
CVD	Cardiovascular Disease
DAG	Diacylglycerol
DAMPS	Damage Associated Molecular Patterns
DAPSA	Disease Activity Index for Psoriatic Arthritis
DAS28	Disease Activity Score using 28 joint counts
DC	Dendritic Cell
DEFA1	Defensin A1
del 17	Deletion of Chromosome 17
DMARD	Disease Modifying Antirheumatic Drug
DN	Double Negative
DP	Double Positive

EAE	Experimental Autoimmune Encephalomyelitis
ECAR	Extracellular Acidification Rate
EM	Effector Memory
EMT	Epithelial-Mesenchymal Transition
ERK	Extracellular Regulated Kinase
ESR	Erythrocyte Sedimentation Rate
FBS	Foetal Bovine Serum
FCR	FC Receptor
FGF	Fibroblast Growth Factor
FGFR3	Fibroblast Growth Factor Receptor 3
FISH	Fluorescent In Situ Hybridisation
FLIPr	FPRL1 inhibitory Protein
fMLP	N-Formyl-Methionyl-Leucyl-Phenylalanine
FMO	fluorescence Minus One
FPR	Formyl Peptide Receptor
GC	Glucocorticoid
GD T cell	Gamma Delta T cell
GEO	Gene Expression Omnibus
GMP	Good Manufacturing Process
GTPase	Guanine Nucleotide triphosphatase
HC	Healthy Control
HDT	High Dose Therapy
HIF-1α	Hypoxia-Inducible Factor-1α
hrs	Hours
hsCRP	High Sensitivity C-reactive Protein
hu-r-ANXA1	Human Recombinant ANXA1
IBD	Inflammatory Bowel Disease
icIEF	Isoelectric Focusing
IFN	Interferon
Ig	Immunoglobulin
IgH	Immunoglobulin Heavy chain
IKZF1	Ikaros
IKZF3	Aiolos
IL	Interleukin
ITGß5	Integrin ß5
IκB	Inhibitory Kappa B
JAK	Janus Kinase
K.O	Knock-Out
LEP	Leptin
LncRNA	Long-non-coding RNAs
LPS	Lipopolysaccharide
M2BP	Mac-2-Binding Protein
Mab	Monoclonal Antibody
MAIT cells	Mucosal-Associated Invariant T cells
MAPK	Mitogen-Activated Protein Kinase
mDCs	Myeloid Dendritic Cells

MFI	Mean Fluorescent Intensity
MGUS	Monoclonal Gammopathy of Undetermined Significance
MI	Myocardial Infarction
MM	Multiple Myeloma
MMP-3	Matrix Metalloproteinase 3
MS	Multiple Sclerosis
MTORC1	MTOR complex 1 protein
NAD	Nicotinamide Adenine Dinucleotide
NADH	Reduced Nicotinamide Adenine Dinucleotide
NET	Neutrophil Extracellular Trap
NF-κB	Nuclear Factor Kappa B
NK	Natural Killer
NLRs	Nod Like Receptors
NSAID	Non-Steroidal Anti-inflammatory Drugs
OCP	Osteoclast Precursors
OCR	Oxygen Consumption Rate
OPG	Osteoprotegerin
PAMPS	Pathogen Associated Molecular Patterns
PBMC	Peripheral Blood Mononuclear Cell
PBS	Phosphate Buffered Saline
PDE4	Phosphodiesterase-4
PDL-1	Programmed Cell Death protein 1
PI	Propidium Iodide
PMA	12- Phorbol 13-Myristate Acetate
PPARγ	Peroxisome Proliferator-Activated Receptor γ
PRMs	Pattern recognition molecules
PRRs	Pattern Recognition Receptors
PS	Phosphatidyl Serine
PsA	Psoriatic Arthritis
PsA L	PsA Lesional skin
PsA U	PsA Uninvolved skin
PsO	Psoriasis
QC	Quality Control
RA	Rheumatoid Arthritis
RANKL	Receptor Activator of NF-κB Ligand
RASF	RA Synovial Fibroblasts
RNI	Reactive Nitrogen Intermediates
ROS	Reactive Oxygen Species
S. aureus	Staphylococcus aureus
SEC	Size Exclusion Chromatography
SF	Synovial Fluid
SJC	Swollen Joint Count
SLE	Systemic Lupus Erythematosus
SMM	Smouldering Multiple Myeloma
SOST	Sclerostin
SPP1	Osteopontin

STAT	Signal Transducer and Activator of Transcription
TAM	Tumour Associated Macrophage
TAN	Tumour Associated Neutrophil
Tc	Cytotoxic T cell
TCR	T Cell Receptor
TEMRA	Terminally Differentiated Effector Memory
TFCP2CPII	Alpha-globin transcription factor
TFF3	Trefoil Factor 3
TGFß	Transforming Growth Factor ß
Th	T Helper cell
TJC	Tender Joint Count
TLRs	Toll Like Receptors
TLS	Tertiary Lymphoid Structures
TNF	Tumour Necrosis Factor
TNFRSF11B	TNF Receptor Superfamily member 11B
TPM	Transcripts Per Million
Treg	Regulatory T cells
UST	Ustekinumab
VEGF	Vascular Endothelial Growth Factor
WT	Wild Type

Chapter 1 Introduction

1.1 Overview of the immune system

The human immune system is a complex network of organs, cytokines and humoral components, all working in combination to support the body in its fight against infection.

The body can be subjected daily to a diverse range of pathogenic organisms, each possessing several mechanisms to attack and invade the body's tissues. The immune system, therefore, possesses a wide range of protective functions to combat these pathogenic assaults.

As well as protecting the body against invading pathogenic organisms, the immune system must be tightly controlled to avoid responses that lead to excessive tissue damage and elimination of commensal microbes. The immune system can be separated into two groups depending on both the speed and specificity of the response to infection; the innate immune system and the adaptive immune system[1,2].

1.1.1 The innate immune system

The innate immune system is both rapid and non-specific and is widely termed the body's first line of defence[1]. Innate immunity covers several physical, chemical and microbial barriers. The primary physical barrier is the skin, consisting of a thick layer of epithelial cells producing the strong, protective protein, keratin. The skin also consists of several sweat and sebaceous glands, producing secretions containing protective lipids as well as maintaining a low pH, effectively clearing microbes away.

If an infectious organism invades past the skin, chemical barriers to infection include the production of enzymes such as lysozyme in the salivary glands and the acidic environment of the digestive tract. Microbiological barriers to infection are also present, such as the normal flora of the mucosal surfaces to prevent the colonisation of pathogens on these surfaces[3].

If any of these barriers are breached, the cellular and humoral components of the innate immune system are activated. In the first phase of the innate immune response, invading microbes, which contain pattern associated molecular patterns (PAMPS), (although not antigen specific) are recognised by pattern recognition receptors (PRRs). PAMPs can include molecules on bacteria such as lipopolysaccharide (LPS), bacterial cell wall glycolipids or viral RNA. PRRs such as toll like receptors (TLRs) may be present on the membrane of innate immune cells, however some can be soluble and present in the cytoplasm such as Nod like receptors (NLRs).

In the second phase of the innate immune response, damage associated molecular patterns (DAMPS) are released from damaged cells. DAMPs include stress molecules such as chaperone proteins or metabolic products such as uric acid. When in contact with a PAMP or DAMP, pattern recognition molecules (PRMs) trigger an intracellular signalling pathway which ultimately results in the activation of several transcription factors, including NFKB, leading to the third phase of the innate immune response. This consists of the activation of pro-inflammatory cytokines, such as Interleukin(IL)-6, Tumour Necrosis Factor (TNF), IL-18 and IL-1, and other immune cells to clear the infection[1,4-6].

Cells of the innate immune system include monocytes, macrophages, granulocytes (neutrophils, eosinophils, basophils and mast cells) and natural killer (NK) cells, with dendritic cells being seen as the ‘linkers’ between innate and adaptive immunity[4,7]. For the purpose of this project, focus will be placed on monocytes and macrophages.

Monocytes and macrophages are phagocytic cells that function to engulf invading pathogens. Monocytes are derived in the bone marrow and circulate in the blood and spleen, patrolling for foreign antigens on invading pathogens. During an infection, monocytes rapidly migrate to the site of infection upon activation by chemokines or cytokines, where they can proliferate, secrete chemokines, and phagocytose antigens.

When monocytes migrate to the tissue, they have the ability to differentiate into dendritic cells and macrophages[8]. Macrophages are tissue-resident innate

immune cells that work to clear the site of infection by engulfing pathogenic particles, dead cells and any cellular debris. They play tissue-specific roles in development, homeostasis, and repair[4,8].

The innate immune response is extremely reliant on the ability of specific innate immune cells to process foreign antigens and 'present' them on their surface for recognition by other immune cell subsets, particularly adaptive immune cells. These cells are termed 'antigen-presenting cells' (APCs) and include cells such as dendritic cells and macrophages, and aid in the cross-talk between innate and adaptive immunity[9].

1.1.2 The adaptive immune system

Although the adaptive immune response is much slower than the innate immune response, it is also more specific. Adaptive immune cells have the ability to differentiate between pathogens and mount an immune response that is antigen specific. These cells can also differentiate self from non-self-antigens and remain inert to them. Cells of the adaptive immune system also have an immunological memory, that is, they remember previous pathogens upon re-exposure and mount a stronger and more rapid immune response before the pathogen can cause significant damage[10].

The main cells of the adaptive immune system are lymphocytes, which can be subcategorised into B cells and T cells. Adaptive immune responses can also be further categorised into cellular and antibody mediated. Antibody responses are carried out by B cells[11].

Each mature B cell expresses a unique B cell receptor on its surface (containing a type M and D immunoglobulin (IgM and IgD) that is specific to an antigen of interest[12]. Before their release into the peripheral blood, immature B cells reside in the bone marrow and begin to express the B cell receptor (BCR). Transitional B cells enter the peripheral blood and develop into naïve mature B cells that are ready to respond to antigens of interest[13]. When B cells are activated via receptor binding to a specific antigen, they proliferate (aided by T cell-derived cytokines) and differentiate into either plasma cells which secrete

antibodies, or memory B cells which are activated rapidly upon re-exposure of the particular pathogenic antigen, producing antibodies and clearing the body of the pathogen. Plasma cells produce large quantities of pathogen-specific antibodies, which are released into the blood for protection against the infectious agent. These cells are not long-lived and usually die via apoptosis when the pathogen is initially cleared from the body. T cells can help B cells to proliferate and undergo genetic changes to increase their affinity for the antigen of interest. Additionally, T cells can also aid in the stimulation of the B cell receptor to trigger class switching from IgD^{+}/IgM^{+} (unswiched) to IgA, $IgE^{=}$ and IgG^{+}(switched) B cells. Each Ig is responsible for a particular function and recognises a specific type of pathogen[13,14].

The cell-mediated adaptive immune response involves T cells. T cells originate in the bone marrow and migrate to the thymus for maturation and are released into the peripheral blood[15]. Naïve T cells are activated in the peripheral blood in response to a foreign antigen that is presented to them via a host APC[11]. When T cells become activated, most are short-lived, but some differentiate into memory T cells which can work to maintain the long-term immune response[15]. The mediator of T cell stimulation is the T cell receptor (TCR) which is specific to each cell and antigen.

T cells can be broadly grouped into $CD4^{+}$ T helper (Th) cells and $CD8^{+}$ cytotoxic T cells, however, there are many other subtypes. Both $CD4^{+}$ and $CD8^{+}$ T cells can be classified according to their differentiation status based on their expression of the leukocyte marker CD45RA and the lymph node homing chemokine receptor CCR7, into (CD45RA+ CCR7+) naïve cells, (CD45RA- CCR7+) central memory (CM) cells, (CD45RA- CCR7-) effector memory (EM) cells and (CD45RA+ CCR7-) terminally differentiated effector memory (TEMRA) cells[16]. Naïve T cells express CCR7 and predominantly reside in the lymphoid organs, whereas (CCR7-) CM cells can circulate and migrate lymphoid tissues and (CCR7-) EM and TEMRA cells can traffic to multiple peripheral tissue sites[17].

As well as aiding B cells, Th cells secrete cytokines to activate nearby immune cells as well as secreting chemokines to recruit these cells to the site of infection. Th cells can be classified into distinct subtypes based on transcription

factor and cytokine profiles (Th1, Th2, Th9 Th17, Th22, follicular T cells and regulatory T cells)[18]. (CD8+) Cytotoxic T cells can also produce cytokines, but their primary function is the killing of cells infected by invading pathogens by the release of cytotoxic granules into the infected cell[19]. CD8+ T cells can also be grouped into subtypes based on their cytokine and transcription factor profile[20,21]. CD4+ and CD8+ T cell subtype functions as well as their chemokine and transcription factor profiles can be seen in Figure 1.1.

A

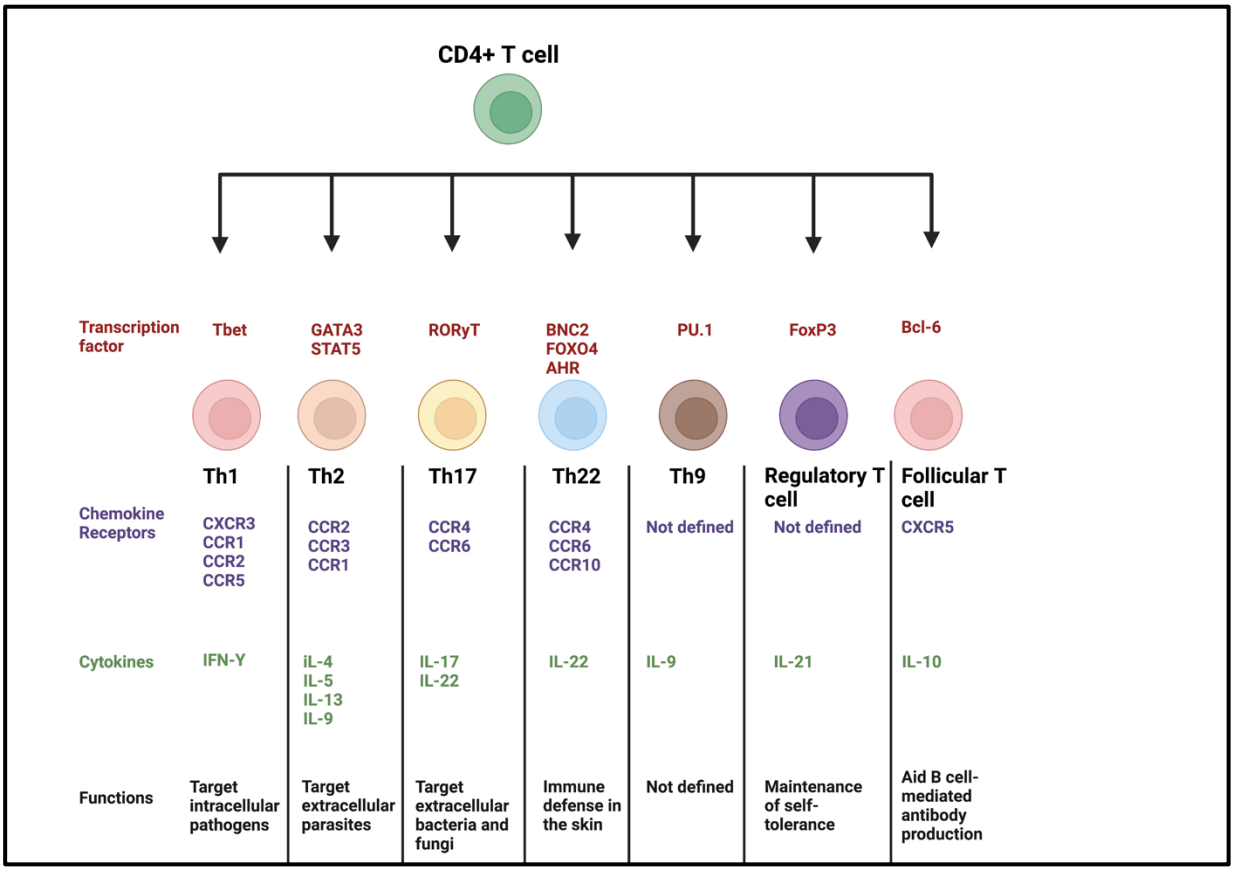

B

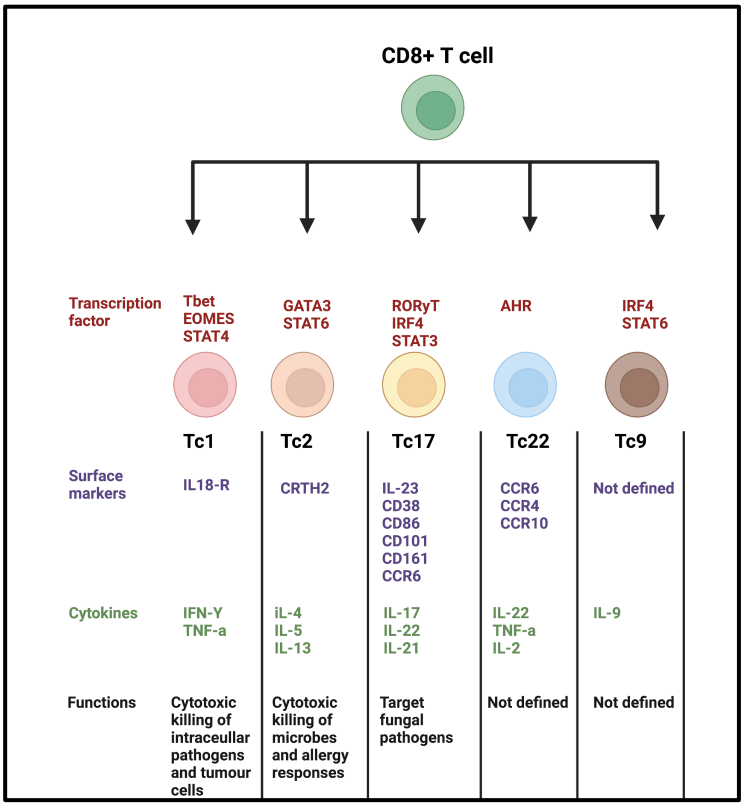

Figure 1.1 Human CD4+ and CD8+ T cell subsets

Diagram showing transcription factor profile, surface marker expression, cytokine profile and associated functions of (A) CD4+ and (B) CD8+ T cell subsets. Diagram produced using Biorender.com and adapted from St.Paul *et.al.*, 2020 and Chatzileontiadou *et.al.*, 2021.

1.2 Annexin-A1

1.2.1 Annexin-A1 structure and function

Annexin-A1 (ANXA1) is a member of the annexin family of calcium-binding proteins. There are 12 Annexins in humans (Annexin-A1-A13, with A12 unassigned), ranging in size from 15kb to 96kb, and each sharing a conserved core domain at their C-terminal. The core domain is made up of at least 4 repeats, which contain calcium binding sites. Each Annexin has a unique N-terminal domain, which differs in length, amino acid sequence and hydrophobicity between members. The N-terminal plays key functions in mediating interactions between Annexin family members and other intracellular proteins (such as the S100 calcium binding proteins). Annexin family expression can span most tissue types in a (Annexins A1,A2, A4-A7 and A11) or occur in a cell/tissue- specific manner (Annexin A3 in neutrophils and Annexin A9 in tongue tissue)[22].

ANXA1 is 37 KDa in size (346 amino acids), consisting of a homologous core region of 310 amino acid residues and a unique N- terminal region (Figure 1.2). Both the ANXA1 N-terminal peptide and the full length ANXA1 protein are capable of interacting with receptors to carry out biological functions [23-25] .

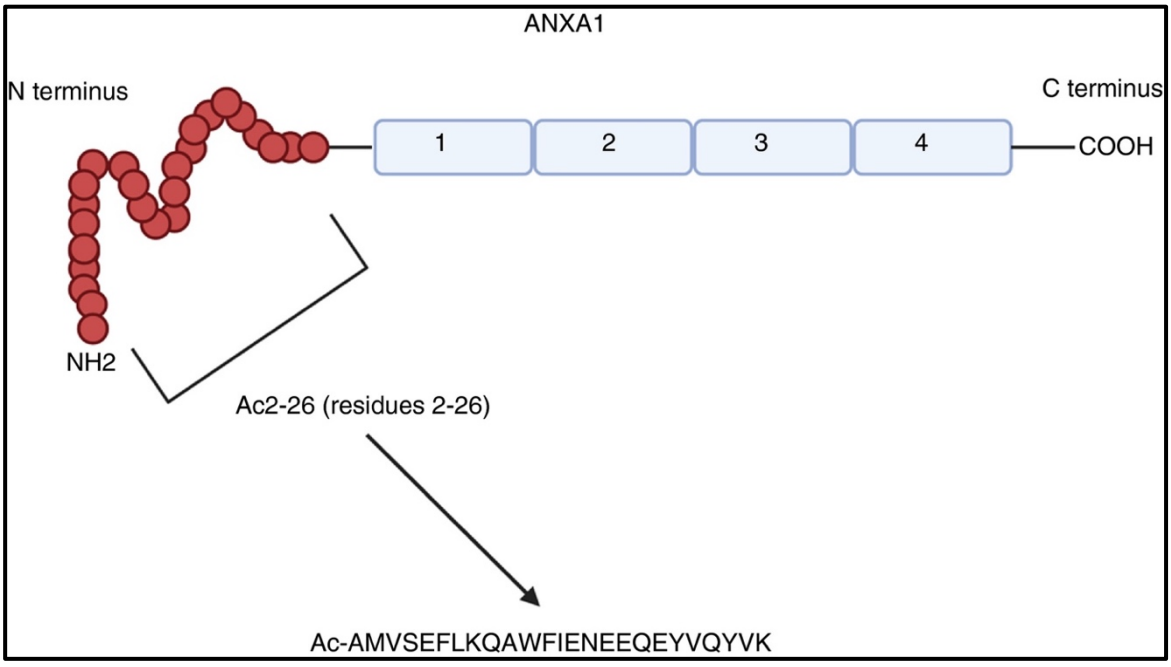

Figure 1.2 Structure of the ANXA1 protein

ANXA1 contains 4 repeating C terminal motifs attached to a unique N-terminal, containing the Ac2-26 peptide. The sequence of the Ac2-26 peptide is also shown (Kelly *et.al.*, 2022).

During homeostatic conditions, ANXA1 mainly resides in the cytosol of the cells it is contained within and is abundant in innate immune cells such as monocytes and neutrophils[26]. Upon calcium binding, the N-terminal region of ANXA1 undergoes a conformational change, exposing and activating it (Figure 1.3) [27,28]. Upon activation, ANXA1 is externalised and translocated to the cell membrane, allowing it to interact with its receptors and carry out its biological functions[28-30]. The transport mechanism of ANXA1 to the cell membrane is cell type dependent (e.g ABC transporter in the monocyte or released from gelatinase granules during neutrophil activation and mobilised to the outer leaflet of the plasma membrane[31,32]). Additionally, a 33Kda cleaved version of ANXA1 has been detected and several enzymes have been suggested to be responsible for this cleavage including elastase, metalloprotease and proteinase 3. It is not yet understood whether the cleavage is responsible for activating ANXA1 into its bioactive form or for inhibiting ANXA1 activity to maintain homeostasis[29].

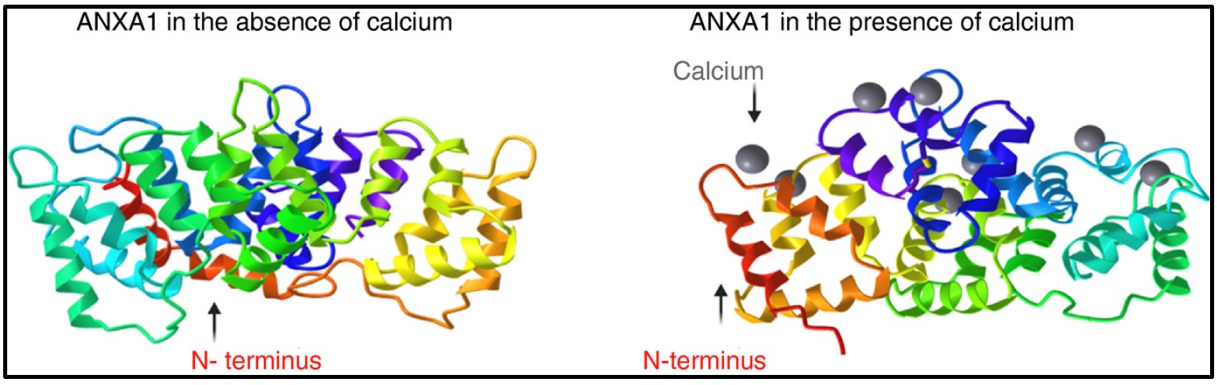

Figure 1.3 Calcium binding to ANXA1 exposes the N- terminus

Ribbon diagram showing how calcium binding causes a conformational change in the ANXA1 N-terminus, exposing it and allowing it to carry out its function. (Kelly *et.al.*, 2022).

ANXA1 is known to be induced by glucocorticoids (GCs), acting as a downstream mediator of their anti-inflammatory effects. It is believed that the anti-inflammatory effects of GCs in the innate immune system (e.g control of leukocyte responses) are mediated by release of ANXA1 and activation of its receptor (FPR1) on innate immune cells such as neutrophils and macrophages. Contrastingly, the immunosuppressive effects of GCs in adaptive immunity are believed to be initiated by inhibition of ANXA1 expression on T cells, thus reducing its stimulatory effects on these cells, highlighting the opposing effects of GCs on ANXA1 expression in innate and adaptive immunity[33,34].

ANXA1 is well-recognised as an anti-inflammatory mediator in innate immunity, however, more research is suggesting it can play a wide range of roles in adaptive immunity and homeostasis as well as being implicated in disease[23]. Most of the anti-inflammatory functions of ANXA1, (such as inhibition of leukocyte migration), are believed to be mediated through its N-terminal domain[35–37], whereas evidence suggests that the C-terminus is involved in contrasting functions such as promotion of clustering and migration across the endothelium[38]. It is evident that ANXA1 has roles that are cell-type dependent, which are mediated through interaction with its receptors; the formyl peptide receptors[29].

1.2.2 The formyl peptide receptors

The formyl peptide receptors (FPRs) are a family of G protein-coupled receptors responsible for a range of biological functions, from modulation of inflammation

to regulation of the host response to infection. There are three FPRs in humans,FPR1, FPR2 and FPR3, however, FPR1 and FPR2 are more closely related, sharing 69% sequence similarity[39,40].

Evidence suggests that ANXA1 primarily signals through FPR1 and FPR2, especially in the context of disease, therefore, this project focused primarily on FPR1/FPR2-ANXA1 interactions. Moreover, the FPRs can be activated by ANXA1 N terminal peptides Ac2-26, Ac2-12 and Ac2-6, as well as the full length ANXA1 protein [23–25].

The FPRs interact with several ligands, including microbial derived, host derived and synthetic peptides.FPR1 is known to interact with a range of N-Formyl peptides (such bacteria-derived formyl-Met-Leu-Phe, fMLP) and non-Formyl peptides (such as host-derived urokinase-type plasminogen activator receptor, uPAR88-92) as well as a range of synthetic peptides such as W peptides[39]. FPR2 being the most diverse receptor, binding a wide range of ligands that can induce opposing effects, for example, FPR2 binding to serum amyloid A (SAA) can result in pro-inflammatory activities, whereas binding to Lipoxin A4 (LXA4) can result in pro-resolving actives[29,41]. As FPRs are a promising drug target, antagonists have also been developed to inhibit FPR-induced cell responses. Amongst these, fungus-derived cyclosporin H has been shown to be one of the most potent and specific antagonists for FPR1. Additionally, the peptide WRW was found to be the most potent peptide with antagonistic activity against FPR2 agonists[39].

ANXA1 binding to the FPRs has been shown to bind its receptors in both a paracrine and juxtacrine manner[42] and trigger a downstream signalling cascade involving mitogen-activated protein kinases (MAPKs) such as extracellular regulated kinase (ERK), as well as the serine/threonine kinase Akt, which have different effects depending on the particular cell type involved[43,44](Figure 1.4). Moreover, the effects of ANXA1 mediated by FPRs appear to be both tissue specific, but also differ depending on whether full length ANXA1 or an ANXA1-derived peptide is bound[29,45–47].

FPR1-ANXA1 interactions have been shown to induce activation of TCR signalling[48] and mediation of necroptosis[49], suggesting a pro-inflammatory/stimulatory role for FPR1 on these cells. Interestingly, ANXA1-FPR1 interactions on murine dendritic cells have been shown to be essential for establishing corpse-DC synapses for clearance of apoptotic cells, highlighting a role for this pathway in non-inflammatory cell death.[50]

FPR2-ANXA1 interactions have been described as predominantly anti-inflammatory, particularly in neutrophils where it appears to play a role in inhibition of transmigration[33]. Moreover, FPR2-ANXA1 binding has been associated with an anti-viral role, through transient triggering of alveolar macrophages. These effects did not appear to be conveyed via FPR1, highlighting the differing roles of these proteins between innate and adaptive immune cells[51].

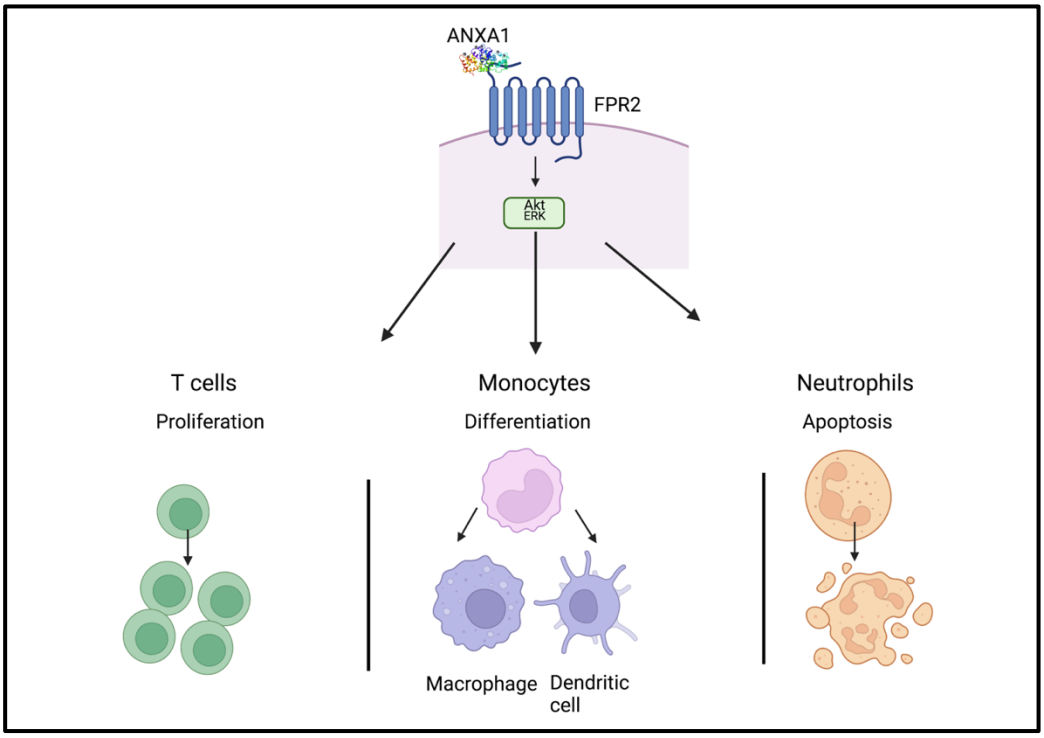

Figure 1.4 ANXA1-FPR2 interactions have different outcomes in different immune cells

ANXA1 binds to FPR2 on the plasma membrane to initiate MAPK and Akt signalling, causing cell-type dependent effects including proliferation of T cells, differentiation of monocytes and apoptosis of neutrophils. Image made on Biorender.com and adapted from Kelly *et.al.*, 2022 and D'Acquisto *et.al.*, 2013.

1.2.3 ANXA1 signalling in innate immunity

ANXA1 has been well accepted as an anti-inflammatory mediator in the innate immune system, affecting several cell types such as neutrophils and monocytes. Studies have indicated that ANXA1- mediated neutrophil apoptosis has an important role in the modulation of the inflammatory response[27,52]. Moreover, ANXA1 has been shown to counter regulate excessive neutrophil accumulation at sites of inflammation[28].

An important step in the resolution of inflammation is the clearance of apoptotic cells, a process that is mediated by phagocytic cells such as monocytes and macrophages[28]. Studies have shown that addition of the ANXA1 peptide Ac(2-26) to macrophages (at a concentration of 32 μM) triggered the engulfment of apoptotic neutrophils, highlighting a role for ANXA1 in this process[53]. An anti-inflammatory role for ANXA1 in innate immunity was also highlighted in studies showing ANXA1 knockout (-/-) mice had an enhanced inflammatory response, with inflammatory markers on monocytes and neutrophils that were more sensitive to activation. Moreover, immune responses in $ANXA1^{-/-}$ mice were not dampened in response to GCs, highlighting that the effects of ANXA1 in innate immunity are GC- dependent [54,55].

There is mounting evidence that ANXA1 mediates its anti-inflammatory actions in innate immunity through interaction both with FPR1 and FPR2. The ANXA1 peptide Ac2-26 (at a lower concentration of 33nM) is still able to carry out significant anti-inflammatory activity in neutrophils (around 50% of that seen in naïve mice) in FPR1 null mice, including induction of cell adhesion and migration. Moreover, FPR1 deficient neutrophils, still expressed significant FPR2, which was associated with induction of anti-inflammatory activity upon stimulation with high concentrations of an agonist, (fMLP, 30 μM), specifically, detachment from the endothelium[24,29]. This highlights the idea that FPR1 and FPR2 both work together in innate immunity, carrying out different functions to obtain the same anti-inflammatory goal.

1.2.4 ANXA1 signalling in adaptive immunity

ANXA1 is expressed at much lower levels on adaptive immune cells, contributing to its undefined role in adaptive immunity. Studies have shown that both ANXA1 and FPR2 expression are increased upon activation of T cells. Moreover, D'Acquisto *et.al.* showed that addition of human recombinant ANXA1 (hu-r-ANXA1) at a range of concentrations (150nM, 300nM, 600nM) to activated T cells *in vitro* enhanced their activation and proliferation. This effect was only evident when FPR2 was externalised in combination with T cell stimulation[27,34], suggesting a key role for ANXA1-FPR2 interactions in T cell activation and potentially inflammation. This group also pointed to a pro-inflammatory role of ANXA1 in T cells, and showed that T cells that were differentiated in combination with hu-r-ANXA1 (particularly at 600nM) produced more Th1-associated transcription factors (such as T-bet) compared to control cells, which are associated with increased pro-inflammatory activity[34]. FPR1 appears to also be involved in this pro-inflammatory role in T cells, as activation of FPR1 by ANXA1 in T cells was shown to increase TCR signalling[56]. Notably, much higher concentrations of hu-r-ANXA1 are needed to see this effect on T cells than seen in the Ac2-26 neutrophil studies mentioned above.

Contrasting studies have highlighted a more anti-inflammatory role for ANXA1 in T cells. Addition of (1 μM) purified ANXA1 to thymocytes was associated with a loss of their suppressor activity[57]. Moreover, ANXA1 deficiency was associated with enhanced antigen-dependent T cell proliferation and inflammation[58,59].

ANXA1 is moderately expressed on the surface of inactivated B cells, whereas FPR2 is expressed at low levels[26]. There is little evidence for what role ANXA1 and its receptors could play in B cells under homeostatic conditions, however, limited evidence has suggested that ANXA1 could play a role in B cell-associated disease[60,61]. Interestingly studies have shown that *Fpr1*-deficient mice have increased antibody responses that are protective against plague, highlighting a potential pro-inflammatory role for FPR1 in B cells, although more research is needed to determine this[62].

1.3 ANXA1 in inflammatory disease

1.3.1 ANXA1 signalling in innate inflammation

Inflammation is the body's normal mechanism of defence against invading pathogens. However, in several diseases this inflammation can persist or be uncontrolled[63]. Innate immune cells play key roles in mediating the inflammatory response through release of pro-inflammatory cytokines such as TNF, IL-6, IFNγ and IL-1ß. However, in order for the immune system to function properly, this cytokine release must be tightly controlled[64].

There are several inflammatory diseases associated with innate immune cell dysregulation and, subsequently overproduction of inflammatory cytokines. A prime and relevant example is COVID-19, which has been associated with an aberrant activation of innate immune responses and inflammatory cytokines resulting in a hyper inflamed environment in the lungs. This hyperinflammatory response is driven by aberrant activation of innate immune cells such as monocytes and macrophages[65]. Interestingly, studies have shown that patients with more severe COVID-19 had significantly lower ANXA1 levels in their serum compared to both healthy controls and those with moderate disease[66], suggesting an anti-inflammatory role for ANXA1 in this innate immune cell associated disease.

Evidence for a role of ANXA1 in modulating the activity of innate inflammatory cells has been explored in other diseases. Increased expression of ANXA1 is evident in macrophages within the active lesions in multiple sclerosis (MS)[67].Contrastingly, ANXA1 has been shown to play predominantly anti-inflammatory roles in diseases such as pleurisy, where addition of 100 µg of Ac2-26 was shown to induce neutrophil apoptosis and increase efferocytosis by macrophages[43,68,69].

The majority of evidence for a role of ANXA1 in innate inflammation is in cardiovascular disease (CVD), and the role seems to be predominantly protective. In models of myocardial infarction (MI), exposure of rat and murine hearts to 300nM of Ac2-26 at the onset of reperfusion was associated with improved recovery of left ventricle function and reduced cardiomyocyte

damage. These effects were significantly reduced upon addition of an FPR1 antagonist, but only moderately reduced upon addition of an FPR2 antagonist[70], suggesting most of the anti-inflammatory effects of ANXA1 in MI could be mediated through FPR1.

ANXA1 was also shown to have a protective effect in atherosclerosis (a leading contributor to CVD), through triggering a reduction in monocyte and neutrophil-mediated atherosclerotic plaque formation[71]. Additionally, administration of 50 μg Ac2-26 reduced both the size of accumulation of macrophages at atherosclerotic plaques in mice, which appeared to be mediated through FPR2[72]. Moreover, addition of 10nM of hu-r-ANXA1 was shown to mediate neutrophil rolling and subsequent plaque formation in murine models of atherosclerosis, which was shown to be dependent on FPR2[59,73].

1.3.2 ANXA1 signalling in adaptive inflammation

Cells of the adaptive immune system are also well-established as key players in inflammatory disease, particularly in autoimmunity[74,75]. Much evidence has highlighted a central role for T cells in autoimmunity, through aberrant production of pro-inflammatory cytokines[76]. Moreover, a role for ANXA1 and its receptors in adaptive inflammation has been predominantly discussed in the context of T cells[34,77,78].

ANXA1 has been shown to play pro-inflammatory roles in T cell-mediated inflammation in murine models of arthritis (collagen induced arthritis model). Administration of exogenous ANXA1(150-600nM) was associated with increased production of pro-inflammatory Th1 cytokines (interferon gamma,IFNγ) in these mice[34]. Moreover, ANXA1 was shown to be released from rheumatoid arthritis (RA) synovial fibroblasts (RASFs) and promoted secretion of RASF metalloproteinase-1,which is known to contribute to collagen degradation[79].

Evidence for an anti-inflammatory role for ANXA1 in the autoimmunity-associated IL-17 producing Th cells (Th17) has also been highlighted. In murine models of uveitis, knocking out ANXA1 was associated with increased eye inflammation and activation of Th17 cells[78]. Contrastingly, $ANXA1^{-/-}$ mouse

models of experimental autoimmune encephalomyelitis (EAE) produced less IL-17 compared to wild type (WT) mice.

Additional studies have suggested an anti-inflammatory role for ANXA1 in Th17 cells. Th17 cells isolated from patients with MS produced significantly less ANXA1 compared to healthy controls[80]. Additionally, deletion of ANXA1 in mice exacerbated arthritis in the K/BxN model. Moreover, addition of an FPR2 agonist was shown to reduce inflammation and osteoclastogenesis in this model[81], suggesting anti-inflammatory roles for both ANXA1 and FPR2 in RA. This data highlights both how ANXA1 could play different roles in different inflammatory diseases but also how animal model data does not always correlate with what is seen in humans.

ANXA1 dysregulation has also been implicated in diseases associated with B cell involvement, primarily through auto-antibody production. Increased levels of ANXA1 autoantibodies have been evidenced in patients with systemic lupus erythematosus (SLE)[61] and inflammatory bowel disease (IBD)[82]. ANXA1 receptor signalling has also been implicated in auto-antibody associated diseases; FPR2 has been shown to be involved in formation of intestinal fibrosis (a key finding in Crohn's disease) upon binding of antimicrobial peptides[83], highlighting potential roles for this receptor in disease that are independent of ANXA1. It is evident that further research needs to be done to define a role for ANXA1 and the FPRs in B cell associated inflammatory disease.

1.4 Psoriatic arthritis

1.4.1 Symptoms and pathogenesis of Psoriatic arthritis

Psoriatic arthritis (PsA) is a chronic, inflammatory form of arthritis that occurs in around 5-42% of people with psoriasis (PsO). PsO is a chronic inflammatory disease associated with infiltration of immune cells and thickening of the epidermal layer of the skin due to abnormal proliferation and differentiation of keratinocytes[84].

PsO clinical presentation consists of flaky patches of skin that form scales and can range from mild to severe. Patches can appear all over the body but are

most common on the elbows, scalp, knees and lower back[85].PsA disease presentation is associated with peripheral joint stiffness, with axial skeleton and connective tissue involvement[86] and is usually seronegative, allowing it to be distinct from RA. PsA is extremely variable in its presentation, ranging from relatively mild to severely destructive disease[87].

Symptoms of PsA include joint pain, stiffness and swelling, as well as complications with other organs such as the eyes, heart and digestive system. In addition, people with PsA can experience severe fatigue, depression and anxiety[88].The pathogenesis of PsA is far from understood. One hypothesis suggests a trigger could be mechanical stress to immunologically active joint tissue[89], whereas other research suggests that the disease is driven by autoimmune processes, evidenced by autoreactive cells, in particular, T cells [90,91].

On a cellular level, the immune infiltrate in PsA is predominantly in the perivascular compartment. T cells are the most common inflammatory cells in the joints and skin in PsA. CD4+ T helper (Th) cells have a prominent appearance in the tissues, whereas CD8+ cytotoxic (Tc) cells are more common in the synovial fluid and enthesis[92–95].T cells in psoriatic skin plaques have been associated with hyperproliferation of keratinocytes and granulocytes and have also been linked to triggering of pro-inflammatory cytokine production, particularly IL-17, IL-22 and IFN-γ[96,97].

Previously, it was thought that Th1 cells were responsible for driving the inflammatory response in psoriatic plaques, but recently a lot of focus has been put on the IL-17 producing T-helper (Th17) cells[98]. Elevated levels of these cells have been found in the psoriatic plaques seen in patients with PsA[99]. Furthermore, it is evident that Th17 cells play a role in chronic inflammation with IL-17 being shown to stimulate pro-inflammatory cytokine production, osteoclast activation and bone resorption[89]. Moreover, IL-17A can accelerate the proliferation of epidermal keratinocytes, which produce a range of antimicrobial peptides and chemokines, which, in turn, enhances skin inflammation[100]. Th17 cell frequency and IL-17 levels have been correlated with

disease activity as well as disease onset and progression in RA and PsA patients. These cells were also found to be prominent in the joints of these patients[101].

Recently, a subset of IL-22 producing Th cells (Th22) have been implicated in PsO. Th22 cells are recognised for their ability to produce vast amounts of IL-22 and are abundantly expressed in PsO compared to healthy controls. IL-22 triggers keratinocyte proliferation and induces PsO-associated epidermal changes, as well as sustaining the inflammatory response in the psoriatic lesions. Th22 and IL-22 levels have been shown to correlate with disease activity in PsO patients. Additionally, Th22 cells express CXCR4 and CCR10, which are skin homing receptors and play substantial roles in skin homeostasis and disease[84]. $CD8^+$ T cells can also produce IL-22 (Tc22) and higher levels than normal of these cells have been found in PsO lesions compared to healthy skin, also suggesting roles for these cells in PsO pathology[84,102].

($CD8^+CD161^+IL\text{-}17^+$) mucosal-associated invariant T (MAIT) cells have also recently been suggested as key players autoimmune disease, particularly due to their innate and adaptive immune functions, tissue homing properties and ability to produce abundant amounts of IL-17. MAIT cells were found to be enriched in the synovium of PsA patients and produced significantly more IL-17 when stimulated compared to RA or osteoarthritis (OA) MAIT cells, suggesting a more predominant role for this cells in PsA[103].

Dysregulation of B cells has also been implicated in PsA. The anti-inflammatory, IL-10 producing Regulatory B cells (Bregs) were found to be decreased in both PsA and PsO[104]. Moreover Bregs were shown to suppress IL-23-mediated psoriasis-like inflammation through inhibition of Th17 differentiation and promotion of regulatory T cell (Treg) expansion[105].This suggests a contribution of B cells to PsA pathology through reduced anti-inflammatory activity rather than enhanced pro-inflammatory activity as seen with T cells.

Whilst there is a vast amount of evidence for adaptive immune cells being key mediators in the pathogenesis of PsA, some papers support a more prominent role of innate immune cells in patients with more severe disease and co-morbidities. In particular, neutrophils and mast cells produce high amounts of IL-

17, associated with PsA pathogenesis. Furthermore, these mast cells and neutrophils were found to be the predominant sources of IL-17 production in the skin and were found at higher densities in psoriatic lesions than IL-17$^+$ T cells[106,107]. Moreover, higher than normal levels of monocytes have been found in the peripheral blood of PsA patients[108,109] and increased aggregation of monocytes has been seen in PsO[110]. It is apparent that the responsibility of PsA pathogenesis may not be placed on a single cell type, rather it appears to involve the activation and integration of several cell types.

1.4.2 Current biomarkers in PsA

There is an unmet need for appropriate diagnostic and prognostic biomarkers in PsA. There is currently no definitive diagnostic test for PsA, which can result in delayed diagnosis and poor diseases outcomes. Early diagnosis of PsA and its subtypes is key to enable treatment plans to be made and limit the damage the disease can cause[111].

To date, there are no validated biomarkers for PsA, however several disease activity scores are used to inform treatment decisions. Included in these are serum markers of inflammation such as C-reactive protein (CRP) and erythrocyte sedimentation rate (ESR). Although these markers are thought to be elevated in around 50% of patients with PsA, they are non-specific markers of disease activity[112]. Disease activity indices are also frequently used in PsA. The Disease Activity Score using 28 joint counts (DAS28) was originally developed for RA and has been shown to be useful in patients with PsA, but not as reproducible as in RA[113]. Furthermore, DAS28 does not encapsulate all the joints that could potentially be affected in PsA. DAS28 can also be used in combination with ESR (DAS28-ESR) or CRP (DAS28-CRP)[114]. The Disease Activity Index for Psoriatic Arthritis (DAPSA) is a recent, more reliable, routine measurement of disease activity in PsA. It takes into account the number of swollen (out of 66) and tender (out of 68) joints, the level of pain (in the form of a visual analogue scale or VAS) and serum markers of inflammation (CRP and ESR) [115]. Table 1.1 summarises the different disease scores mentioned above and their interpretations.

Table 1.1 Disease activity scores in PsA

Disease activity/Inflammatory marker	Score	Interpretation	Reference
DAPSA	≤ 4	Remission	Schoels, M. M., Aletaha, D., Alasti, F. & Smolen, J. S. Disease activity in psoriatic arthritis (PsA): Defining remission and treatment success using the DAPSA score. Ann. Rheum. Dis. (2016) doi:10.1136/annrheumdis-2015-207507.
	> 4 and ≤ 14	Low disease activity	
	> 14 and ≤ 28	High disease activity	
	>28	Very high disease activity	
DAS28	< 2.6	Remission	The DAS28 score | NRAS | Disease Activity Score. https://nras.org.uk/resource/the-das28-score/.
	< 3.2	Low disease activity	
	> 5.1	Active disease	
CRP	>22mm/hr (men), >29mm/hr(women)	Outside of normal range	Inflammation Blood Tests | ESR, CRP and PV Values | Patient. https://patient.info/treatment-medication/blood-tests/blood-tests-to-detect-inflammation.
ESR	>10mg/L	Outside of normal range	Inflammation Blood Tests | ESR, CRP and PV Values | Patient. https://patient.info/treatment-medication/blood-tests/blood-tests-to-detect-inflammation.
VAS	0-100 scale	0= no pain 100= severe pain	MacKenzie, H., Thavaneswaran, A., Chandran, V. & Gladman, D. D. Patient-reported outcome in psoriatic arthritis: A comparison of web-based versus paper-completed questionnaires. *J. Rheumatol.* **38**, 2619–2624 (2011).
SJC	Presence or absence of joint swelling (out of 66 joints)	Can be used to calculate DAS28 and DAPSA	Mease, P. J., Antoni, C. E., Gladman, D. D. & Taylor, W. J. Psoriatic arthritis assessment tools in clinical trials. in *Annals of the Rheumatic Diseases* vol. 64 ii49–ii54 (BMJ Publishing Group Ltd, 2005)
TJC	Presence or absence of joint tenderness (out of 68 joints)	Can be used to calculate DAS28 and DAPSA	Mease, P. J., Antoni, C. E., Gladman, D. D. & Taylor, W. J. Psoriatic arthritis assessment tools in clinical trials. in *Annals of the Rheumatic Diseases* vol. 64 ii49–ii54 (BMJ Publishing Group Ltd, 2005)

There are several proteins and currently being investigated for potential use as biomarkers PsA diagnosis. Due to their easy access, circulating peripheral blood biomarkers would be optimal for PsA diagnosis. Several studies have suggested markers involved in inflammation and cartilage or bone metabolism for the diagnosis of PsA. IL-6 is one of these and is an inflammatory cytokine shown to be increased in PsA blood compared to PsO alone. Moreover, the amount of serum IL-6 correlated with the number of joints affected with arthritis[116,117]. However, IL-6 is not specific to PsA as its secretion is increased in other diseases.

More recently, research has focused on identifying combinations of biomarkers to differentiate PsA from PsO. One study found that high sensitivity C-reactive protein (hsCRP), cartilage oligomeric matrix protein (COMP), matrix metalloproteinase 3 (MMP-3), osteoprotegerin (OPG) and the ratio of C-propeptide of type II collagen (CPII) to collagen fragment neoepitopes Col2-3/4 (C2C ratio) appeared to be biomarkers in people with PsA that had PsO[118]. Another study suggested integrin ß5 (ITGß5), Mac-2-binding protein (M2BP), and CRP as candidate biomarkers for differentiating PsA from PsO and that these were better than CRP alone at differentiating the two diseases[119].

Based on data showing that combinations of biomarkers might be the way forward in PsA diagnosis, Rahmati et al., used computational methods to identify clinical and protein markers that could best discriminate PsA from PsO. Preliminary data showed that the markers which aided the most substantial discrimination between PsA and PsO were CRP, Defensin A1 (DEFA1), Leptin (LEP), Sclerostin (SOST), Osteopontin (SPP1), Alpha-globin transcription factor CP2 (TFCP2 CPII), tumour necrosis factor receptor superfamily member 11B (TNFRSF11B), and nail psoriasis, but these results need to be validated[111,120].

In contrast to work showing that people with PsA and PsO have different levels of serum proteins, using an affinity-based proteomic platform, Leijten *et al.*, showed that these two diseases shared a similar proteomic signature, and have suggested that future work should focus on identifying markers in the skin and synovial tissues which are associated with disease progression in PsA in people with PsO[111,121].

As with diagnostic biomarkers, biomarkers predicting prognosis in PsA are not well defined. A review of current research has suggested polyarticular onset, high ESR at presentation, anti-citrullinated peptide antibody (ACPA) positivity and the presence of erosion at plan radiographs as markers of erosive and aggressive arthritis[122]. Another study has suggested plasma antibodies to carbamylated-LL37 could be markers of disease activity in PsA[123].

A systemic review which analysed prognostic biomarkers in terms of treatment response in PsA determined that firm conclusions cannot be drawn from the contrasting studies available, and that further validation is needed[124].

It is clear that biomarker identification in PsA is extremely difficult, but researchers have advised that this could be achieved successfully if future studies use a collaborative approach, looking at multiple cohorts and multiple analytes to produce robust results focused on good quality biomarkers[111].

1.4.3 Current treatment strategies in PsA

Treatment approaches in PsA can be broadly categorised into covering those with active PsA who have never been treated and those who have been treated before but still have active disease. Treatment guidelines also take into account different disease presentations within PsA (e.g whether there are any co-morbidities)[125].

Potential treatments for PsA includes non-biological agents and biological drugs. Non-biological agents include conventional disease modifying antirheumatic drugs (DMARDs), non-steroidal anti-inflammatory drugs (NSAIDs), corticosteroids, Janus kinase (JAK) inhibitors and phosphodiesterase-4 (PDE4) inhibitors[126]. Biological therapies are a type of DMARD and include TNF-inhibitors, IL-17 inhibitors and IL23/12 inhibitors.

NSAIDs are mostly focused on symptom management rather than targeting a specific part of PsA pathogenesis. Systemic administration of corticosteroids is generally not recommended in most cases but have shown promise in treating psoriatic plaques when administered topically[127].

Current treatment for moderate to severe disease involves a combination of DMARDs (such as methotrexate) and biological agents. DMARDs are immunomodulatory and immunosuppressive. There is poor evidence available for the use of conventional synthetic DMARDs (csDMARDs) in PsA, with conflicting data about their efficacy and duration of use. However, methotrexate has been shown to outperform sufasalazine, a first line DMARD[128,129].

Biological drugs such as TNF inhibitors have improved the quality of life of PsA patients but the beneficial response in patients has not been long-lasting and treatment has been associated with adverse effects[86,130,131].

Anti-IL-17 agents have been frequently used in PsA, with these therapeutics shown to be very efficacious in this disease[86,132] with most benefit being seen in the skin pathology rather than the joint pathology of the disease[132–134]. Although beneficial, the use of anti-IL-17 agents has been associated with numerous adverse effects such as upper respiratory tract infections and nausea along with more severe effects such as neutropenia[134]. It is clear that longer and larger studies are needed to investigate the use of these agents in PsA and determine optimal dosage.

As dysregulation of IL-17 signalling is a key feature of numerous inflammatory diseases, many treatments have focused on manipulating expression of this cytokine. IL-23 is a major cytokine involved in the stimulation of IL-17 production, and therapies have been developed to either block IL-17 directly or to block it upstream through IL-23 blockade. IL-12 is a key cytokine involved in Th1 differentiation which shares a p40 subunit with IL-23,but induces the differentiation of CD4+ T cells into Th1 cells rather than Th17 cells.[135,136]. Therefore, the two cytokines are closely related but trigger distinct signalling pathways. The IL-12/23 receptor is made up of a common receptor chain, IL-12RB1, which is paired with different second chains to allow the two cytokines to carry out their differential signalling (Figure 1.5).

It is thought that both IL-12/23 can drive chronic inflammation through IL-12-induced differentiation of naïve T cells into IFN-γ-producing Th1 cells and IL-23-induced expansion of Th17 cells.[137] Therefore, several treatments have been developed to target these two cytokines. The anti-IL-12/IL-23 agent, ustekinumab (UST), has been developed to treat both skin and joint pathology in PsA, and is looking comparable in terms of efficacy and safety to commonly used TNF-inhibitors[138]. In the PSUMMIT II study, people who had not received TNF inhibitors prior to UST responded better than those who had been previously treated with TNF inhibitors. This data is believed to indicate that there is a

subset of PsA patients with persistent disease mediated through mechanisms not directly linked to TNF[139].

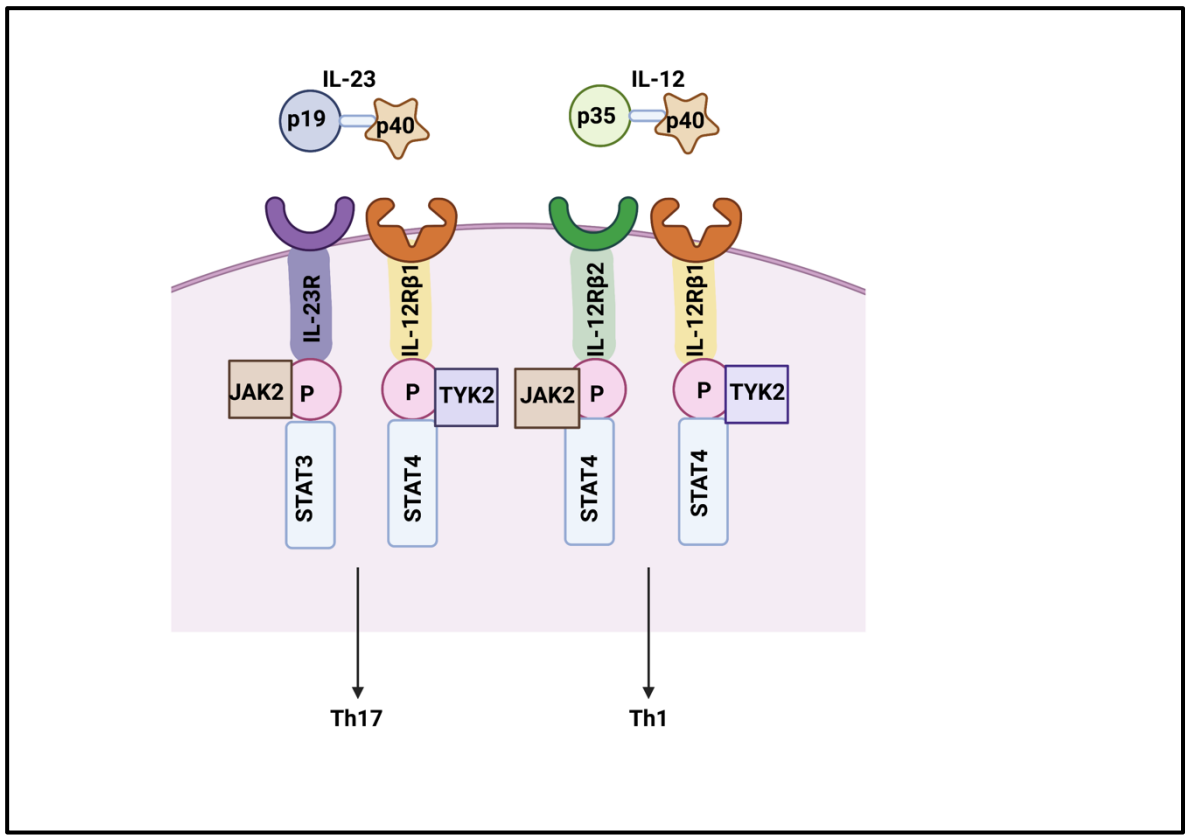

Figure 1.5 IL-23 and IL-12 signalling

IL-23 is comprised of the IL-23p19 and IL-12/23p40 subunits, whereas IL-12 is comprised of the IL-12p35 and IL-12/23p40 subunits. IL-23 signals through IL-12Rβ1 and IL-23R, and IL-12 signals through IL-12Rβ1 and IL-12Rβ2. IL-12 can stimulate JAK2 and TYK2, which subsequently leads to phosphorylation of STAT4. IL-23 triggers phosphorylation of STAT4 through TYK2 stimulation and can also stimulate JAK signalling, but primarily signals through STAT3. IL-12 is associated with activation of Th17 responses, whereas IL-12 is associated with the activation of Th1 responses. Image made on Biorender.com and adapted from Teng *et.al.*, 2015.

JAK/STAT inhibitors are small molecules that target the JAK/STAT pathway which is involved in expression of multiple inflammatory cytokines, many of which have been implicated in PsA such as the IL-12/23 and IL-17 axis. Among the several JAK inhibitors available, there are currently only two that are approved for treatment of PsA; tofacitinib and upadacitinib[128,140]. Tofacitinib is mainly offered to patients who have had an inadequate response or intolerance to DMARDs and has been shown to be effective in terms of improvement of enthesitis, dactylitis and treatment resistance[141]. Similarly to tofacitinib, upadacitinib has also proved to be more effective in reducing disease symptoms

in PsA in patients who have had an inadequate response or intolerance to at least one biologic DMARD[142].

The PDE-4 inhibitor, apremilast has shown promise in the treatment of PsA. PDE-4 is an enzyme involved in the hydrolysis of cyclic adenosine monophosphate (cAMP), which mediates a range of anti-inflammatory and pro-inflammatory mediators. Apremilast works to block PDE-4, increasing cAMP levels which, in turn, suppresses TNF-α production and subsequent pro-inflammatory activity[143,144]. Apremilast has been assessed in large-scale clinical trials and shown to be safe and effective across a range of PsA disease phenotypes. However, it is significantly more expensive than other therapies, and is likely to be a second or third treatment choice[143].

It is evident that treatment strategies in PsA are improving, however a lot more research and development needs to be done in terms of cost, side effects and reducing the amount of different treatments a patient with PsA is prescribed through better understanding of disease pathogenesis.

1.4.4 A potential for ANXA1 signalling in PsA?

As mentioned in previous sections, evidence of a role for ANXA1 in autoimmune and inflammatory disease has been widely implicated, with roles in skin and joint pathology being frequently alluded to.

Although limited, there is evidence of a role for ANXA1 in psoriatic disease. One study identified ANXA1 as an autoantibody in PsA, with serum expression levels of the protein being more than twice that of healthy controls[145]. Moreover, ANXA1 was shown to be localised to the upper layer of the psoriatic epidermis, suggesting a role for it in skin pathology. Other studies have supported this idea, suggesting that ANXA1 expression may play a role in keratinisation disorders[146,147]. Additionally, ANXA1 was shown to be involved in predicting response to anti-TNF therapy in PsA[148]. Overall, this data provides evidence of ANXA1 signalling in the inflammatory response in PsA, through a mechanism that is not yet understood.

Several studies have focused on the role of ANXA1 in the Th17-mediated inflammation that is evident in PsA. Yazid *et. al.* analysed murine models of

retinal autoimmune disease and showed that ANXA1$^{-/-}$ mice produced more Th17 related cytokines in comparison to WT mice. The group further investigated patients with uveitis and found that ANXA1 levels were low in these patients compared to healthy control patients. High levels of anti-ANXA1 antibodies were also seen in the serum of the uveitis patients[78]. This suggests an anti-inflammatory role for ANXA1 in Th17-mediated inflammation. In contrast, ANXA1$^{-/-}$ mouse models of EAE showed reduced levels of disease compared to WT mice and furthermore, ANXA1$^{-/-}$ mice exhibited a reduced Th17 profile and had reduced IL-17 production in comparison to WT mice[149]. However, it is worth noting that the majority of the data indicating a role for ANXA1 in Th17-mediated pathology in PsA is murine data and although promising, this may not directly translate to humans.

A role for ANXA1 in arthritic disease has also been suggested. CD4^{+} T cells in patients with RA have increased ANXA1 expression compared to HCs[34]. ANXA1 was also found to be released from activated RA synovial fibroblasts (RASF) and was associated with matrix metalloproteinase-1 secretion, which is known to play a key role in collagen degradation[59,79]. Contrastingly, Headland *et.al.* have suggested that ANXA1 could play a role in the protection of cartilage in arthritis patients generating data showing that ANXA1/FPR2 interactions were associated with reduced matrix degradation and inflammatory mediator production in animal models of arthritis[150].

Recent data has also suggested a role for ANXA1 in reducing pathological bone resorption and inflammation. This study additionally showed ANXA1 inhibited osteoclast differentiation through suppression of NF-κB signalling and activation of the peroxisome proliferator-activated receptor γ (PPARγ) signalling pathway[151]. Interestingly *PPARγ* plays an important role in the regulation of the skin barrier permeability by inhibiting keratinocyte proliferation and promoting terminal differentiation of the epidermis. Hence, proteins involved in the *PPAR*γ pathway have been suggested as a viable targets for treating psoriatic skin pathology[152].

The ANXA1 receptors FPR1 and FPR2 have also been implicated in psoriatic skin pathology as well as arthritic disease. Blockade of FPR1 in human neutrophils

attenuated psoriasis-like inflammation *in vivo*[153], which included a reduction in epidermal hyperplasia, neutrophil infiltration into the skin, and transepidermal water loss[153]. Moreover, addition of an FPR1 agonist in the collagen-induced arthritis (CIA) murine model of RA, suppressed Th1 and Th17 responses via IL-10 production. Together, these data suggest a more anti-inflammatory role for FPR1 in psoriatic and arthritic inflammation.

Contrastingly, Salamah *et.al* have shown FPR2 to be involved in the development of pathogenesis and platelet-mediated complications during psoriasis in mice, suggesting a more pro-inflammatory role for FPR2[154]. Interestingly, addition of an FPR2 agonist reduced osteoclastogenesis and inflammation in a mouse model of RA and was associated with anti-inflammatory effects in human joint cells[81], suggesting different roles for FPR2 in skin and joint pathology.

It is evident that the role of ANXA1 and its receptors in PsA pathology are not well defined. With most of the data discussed above being in animal models, this project aimed to identify whether expression levels of ANXA1, FPR1 and FPR2 differ in PsA human samples and if expression is linked with any disease-relevant features. These data will help improve understanding both of PsA pathogenesis but also what role, if any, ANXA1 and its receptors play in PsA.

1.5 ANXA1 signalling in cancer

1.5.1 The immune system in cancer

Cancer is initiated through a series of mutations that result in the induction of abnormal rates of processes key to survival and growth of tumour cells[155]. The ability of cancer cells to develop ways of mimicking immune tolerance mechanisms and avoid detection from the immune system is key in cancer progression. Chronic inflammation has been shown to be vital in cancer progression through stimulation of cancer cell proliferation and metastasis[59,156].

Certain inflammatory cells play more prominent roles at different stages of tumour development. For example, NK and CD8+ T cells play a more prominent role initially recognising more immunogenic cancer cells and eliminating them. These cells have widely recognised anti-tumour properties[157,158]. Contrastingly,

CD4+ T cells are involved in triggering the production of pro-inflammatory cytokines such as TNF-α to elicit protective functions from cells such as macrophages[156,159].

The role that B cells play in cancer has recently been described as multi-faceted[160]. Adoptive transfer of B cells into T and B cell deficient mice restored premalignant inflammation and angiogenesis alongside other characteristics associated with malignancy[161]. However, the presence of activated B cells in tertiary lymphoid structures (TLS) has been associated with improved outcomes and treatment response in many cancers, which suggests an anti-tumour role for B cells in cancer[160,162,163].

Innate immune cells such as neutrophils are also key drivers of cancer-associated inflammation and high numbers of these cells has been associated with poor prognosis in several forms of cancer, including melanoma[164], colorectal cancer (CRC)[165] and gastric adenocarcinoma[166,167]. In contrast, in CRC, infiltration of the tumour by tumour associated neutrophils (TANs) was correlated with enhanced prognosis associated with triggering of infiltration of CD8+ T cells[168]. Interestingly, TANs have also been thought to contribute to the initial inflammatory process present during the initiation of cancer. In a mouse adenocarcinoma model, TANs were shown to promote the growth of the tumour[156,169] .

When undetected cancer cells survive and progress to established tumours, they manipulate the immune response as they adapt. Cancer cells will recruit specific immune cells such as Tregs or pro-tumoral macrophages which can dampen or 'switch off' responses from cells that are primarily tumoricidal[156]. Tumour-associated-macrophages (TAMs) in particular are vital players in the chronic inflammatory response that drives cancer progression and have also been associated with poor prognosis and reduced survival[170]. Once activated, macrophages can be referred to as the "M1" pro-inflammatory type or the "M2" anti-inflammatory type. During the initial stages of tumorigenesis, M1 macrophages play a prominent role in the removal of cancer cells that trigger an immune response. However, as the cancer evolves, TAMs adopt the M2

phenotype[156,171]. TAMs have been shown to support tumour growth in several ways such as initiating angiogenesis, and metastasis[172,173].

It is evident that different immune cells can play certain roles at all stages of tumour progression and that inflammation can be beneficial initially in combatting cancer growth but can contribute to its progression if it becomes chronic.

1.5.2 ANXA1 and FPR signalling in cancer

There is a large amount of evidence suggesting a role for ANXA1 in cancer, however, much of the data is conflicting. ANXA1 was shown to be upregulated in several cancers such as lung, pancreatic and colorectal cancer[174–176]. Contrastingly, cancers such as larynx, prostate and esophageal cancer have been associated with a downregulation in ANXA1[177–179]. Suggested mechanisms for the variability in ANXA1 expression amongst different cancer types include mutations or deletions of or epigenetic changes to the *ANXA1* gene[59,180].

ANXA1 has been evidenced to play a wide range of roles in cancer, including in regulation of cellular proliferation, metastasis, modulation of cancer-associated signalling pathways and modulation of treatment resistance[181], with roles being drastically different between cancer types. For example, ANXA1 knockdown in a breast cancer cell line resulted in increased tumour cell proliferation and growth[182], whereas ANXA1 knockdown in human glioblastoma cells significantly reduced their tumorigenicity and was associated with inhibition of colony stimulation of the cells and leukocyte infiltration. Moreover, human glioblastoma cells were shown to overexpress FPR1, and knockdown of both FPR1/ANXA1 diminished tumour growth even further[183], suggesting a role for ANXA1/FPR1 signalling in this particular cancer type.

A role for ANXA1 in metastasis is implicated in almost all cancer types analysed, however results between studies are also contradictory. ANXA1 knockdown in invasive basal-like breast cancer cells reduced metastatic activity, and, likewise, addition of ANXA1 to these cells promoted metastasis[181,184]. This process was associated with an increase in transforming growth factor ß (TGFß) signalling, which is essential for epithelial-mesenchymal transition (EMT) in metastasis.

Contrastingly, transfection of ANXA1 into an estrogen-independent breast cancer cell line (MDA-MB-231) was associated with a reverse in the EMT phenotype and reduced metastasis, through a process that was deemed to be independent of TGFß signalling[181,185].

ANXA1 has been suggested as a biomarker in several cancer types[186–188] and has also been implicated in resistance to treatment[181], but again, the research is contradictory. In breast cancer cell lines, higher ANXA1 expression was associated with drug resistance[189], whereas, in pancreatic cancer cell lines, low ANXA1 was associated with resistance to treatment[190]. ANXA1 expression was associated with better overall survival in epithelial ovarian cancer, and it has been suggested that this could help inform treatment strategies[191].

Both FPR1 and FPR2 have been implicated in cancer pathogenesis. Most of the data available suggests a pro-tumour role for FPR1 in cancer. High FPR1 expression corresponds to poor prognosis in neuroblastoma[192] and gastric cancer[193]. Moreover, a loss of function mutation in *FPR1* had a negative impact on metastatic free survival in two breast cancer cohorts[194]. Similarly, to FPR1, FPR2 seems to play a primarily pro-tumour role in cancer. High FPR2 expression is associated with poor prognosis in colon cancer[195] and epithelial ovarian cancer[196] and, similarly to FPR1, FPR2 was associated with worse prognosis in gastric cancer. Moreover, FPR2 was shown to be functionally involved in metastasis and invasiveness in this cancer type[197]. Studies have stressed the importance of ANXA1/FPR signalling in the aggressiveness of several cancers, suggesting interactions with ANXA1 and FPR1/FPR2 in the context of several cancers, seems to be primarily pro-tumour[48].

It seems that ANXA1 and its receptors can mediate diverse pathways in several forms of cancer, however, a lot of the available data on ANXA1 is contradictory. It is evident that ANXA1 can activate a range of signalling pathways depending on the cell type[44,198], therefore, further analysis into the exact signalling mechanisms of ANXA1 and the FPRs in each cancer type will prove beneficial in understanding what role they may play in disease progression.

1.6 Multiple myeloma

1.6.1 Symptoms and pathogenesis of Multiple Myeloma

Multiple myeloma (MM) is a malignant form of cancer caused by abnormal proliferation of terminally differentiated B cells (plasma cells) and occurs throughout the bone marrow (BM). If left uncontrolled, production of MM plasma cells can ultimately lead to end-organ damage[199]. MM is the second most common haematological malignancy in Europe, with patients having one of the longest time-to-diagnosis intervals compared to other cancers; time from symptom onset to diagnosis is averaged at 99 days[200].

MM initiates as monoclonal gammopathy of undetermined significance (MGUS), progressing to smouldering multiple myeloma (SMM), both of which are asymptomatic conditions. Each of these conditions can be defined based on the levels of plasma cells and immunoglobulin in the BM, blood (MGUS and SMM) and urine (SMM). When SMM progresses to MM, the patient is usually symptomatic[201]. Clinical presentation of MM can be described using the "CRAB" acronym (hyper**c**alcemia, **r**enal insufficiency, **a**naemia, and **b**one lesions), which can be used to distinguish between active, symptomatic and asymptomatic MM[202].

Due to the numerous clinical presentations of MM, a range of symptoms are experienced. Abnormal proliferation of plasma cells can damage the bone, leading to symptoms such as pain and, occasionally, fractures. An overabundance of plasma cells in the BM minimises space for other blood cells to form, causing symptoms such as anaemia (fewer red blood cells) and increased susceptibility to infections (fewer white blood cells). Hypercalcemia occurs in MM when the bones are damaged, and calcium is released into the blood. Too much calcium in the blood can cause tiredness, nausea and drowsiness. More severe symptoms of MM include spinal cord compression and decreased kidney function. The former is due to the large amount of plasma cells in the BM, whereas the latter is due to a build-up of the light-chain immunoglobulin part of the abnormal antibodies (M proteins) produced by the MM plasma cells. The light chain immunoglobulin (termed Bence Jones protein) can damage the kidneys as

it passes through the blood into the urine and can also subsequently, be measured in the urine[203].

MM disease progression is triggered by a combination of genetic, epigenetic and biological events[204] (Figure 1.6). Initiation of MM is thought to occur in the germinal centre during B cell class switching and somatic hypermutation. Primary translocations are initiated by breaks in double stranded DNA, which leads to abnormal fusions with other breaks. Translocations that have been identified in MM involve the immunoglobulin heavy chain (IgH) gene loci, with the majority being associated with the *IgH* gene locus at chromosome 14[204,205].Translocations involving oncogenes can result in their increased expression, contributing to disease progression and resistance to therapy. For example, the t(14;4) translocation is linked with an upregulation in fibroblast growth factor receptor 3(FGFR3), which is associated with poor prognosis and resistance to certain treatments in MM[206]. Primary translocations are thought to occur early in the disease pathogenesis, followed by secondary translocations later on that contribute to disease progression, alongside other factors such as increased angiogenesis[207,208].

Somatic mutations are also common in MM, although frequencies vary amongst patients. Frequently mutated genes include *BRAF*, *FAM46C*, and *DIS3*, as well as structural variants of the *MYC* oncogene. Aberrant activity of *MYC* is associated with genomic instability and disease progression. Epigenetic changes such as aberrant DNA methylation are common in MM. Studies have reported epigenetic inhibition of tumour suppressor genes in MM, with methylation status being associated with overall survival and prognosis[209].

The BM microenvironment composition is key for MM progression. Bone marrow stromal cells (BMSCs) aid in growth of MM cells and their homing and retention in the BM. Interaction between MM cells and the BM microenvironment results in secretion of a range of cytokines (IL-6, TNF-α) and growth factors (B-cell activating factor (BAFF), vascular endothelial growth factor (VEGF), that regulate growth, proliferation, migration and treatment resistance in MM cells. Secretion of factors such as BAFF stimulates the nuclear factor kappa B (NF-κB) pathway, which is associated with promotion of survival, and proliferation of MM

cells. Additionally, interaction between MM cells with BMSCs and bone forming cells (osteoblasts) can increase the production of osteoclastic stimuli such as receptor activator of NF-κB ligand (RANKL) and increase bone resorbing cell (osteoclast) activity, contributing to MM bone disease[205,210,211].

The BM microenvironment can also mediate suppression of the immune system, particularly immune responses led by $CD8^+$ T cells and NK T cells[205]. Although MM is characterised as a plasma cell neoplasm, the role of B cells in this suppressive state is not yet fully understood. Recently, Bregs have been suggested to confer immunosuppressive roles in myeloma by production of IL-10. These Bregs were also upregulated in the BM at the time of MM diagnosis and downregulated at the time of response to therapy[212,213].Treatment outcomes in MM have improved, but the disease remains incurable and therefore, more research needs to be undertaken to identify new biomarkers and therapeutic targets[213].

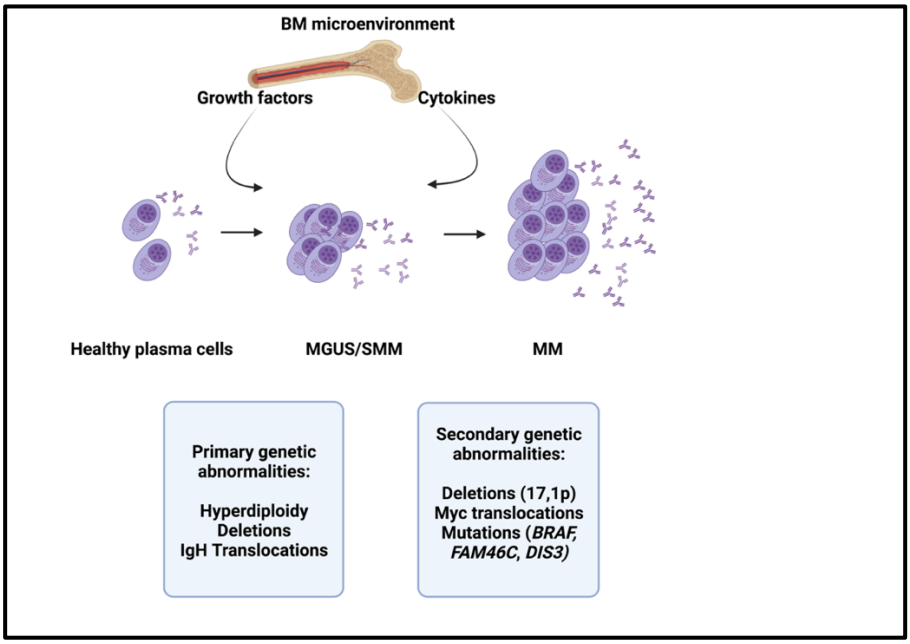

Figure 1.6 MM pathogenesis

MM initiates from healthy plasma cells, progresses to asymptomatic MGUS and SMM before progressing to symptomatic MM. Primary genetic abnormalities play key roles in the early stages of MM pathogenesis, whereas secondary genetic abnormalities are key for progression from MGUS/SMM to MM. The BM microenvironment plays key roles in promoting growth and survival of MM cells through the release of various growth factors and cytokines.

1.6.2 Current biomarkers in MM

There are currently several diagnostic and prognostic biomarkers used in MM, each measured using range of procedures (BM biopsy, urine and serum analysis, karyotyping, Fluorescent In Situ Hybridisation (FISH) and imaging). Levels of clinical markers such as serum and urine M protein and serum calcium, haemoglobin and creatinine in addition to specific cytogenetic abnormalities (translocations) are used for both staging of MM and informing treatment plans. Although informative, this method of determining prognosis can be inconsistent and non-specific. M protein is only detected in 18% of MM patients and ß2-microglobulin (high serum levels in MM) levels can be swayed by various other factors that are independent of MM pathogenesis[214]. Therefore, much research has focused on finding better, more reliable diagnostic and prognostic biomarkers for MM.

Genomic biomarkers are extensively used in determining diagnosis and prognosis in MM. Copy number variations (CNV) detected by FISH (gain or loss in chromosome arms), alongside translocations are key in MM pathogenesis. MM can be divided into two main subtypes based on chromosome copy number alterations: hyperdiploid and non-hyperdiploid.Hyperdiploidy (gains in complete chromosomes) is common in MM, and is considered a primary event in this disease, alongside translocations. Hyperdiploidy alone has a favourable prognosis in MM, whereas nonhyperdiploid events (e.g translocations and chromosome deletions) are associated with worse prognosis[215,216].

The prognostic value of MM chromosomal translocations varies. T (4;14) has been associated with poor prognosis in MM, however, treatment with protein inhibitors such has bortezomib has been shown to improve outcomes in patients with this translocation. Contrastingly, other chromosomal translocations such as t(14;20) and t(14;16) as well as loss of the small arm of chromosome 17 (17p) are associated with worse prognosis despite advances in treatments[216,217].

Gene mutations are also extremely common in MM. Results of several studies identified the MAPK pathway, which includes *KRAS*, *NRAS*, and *BRAF* genes, as the most commonly mutated in MM[216,218-220]. The prognostic impact of mutations

in this pathway are not well understood. Recent data showed that two patients with the *BRAF*-V600E mutation had achieved a sustained response to the BRAF inhibitor vemurafenib, suggesting that patients with this mutation could benefit from targeted treatment, however, more data is needed to determine this[216,221]. Mutations in other genes associated with DNA repair such as *TP53*, *ATM* and *ATR* are also associated with poor prognosis in MM, whereas mutations in genes such as *IRF4* and *EGR1*, which are associated with plasma cell differentiation, are associated with a more favourable prognosis[216,218,222,223].

Recent research has focused on the potential of other blood biopsies for MM diagnosis and prognosis. In MM, a BM biopsy is the gold standard for diagnosis, but this can be extremely painful and invasive. It also does not inform prognosis as well as other markers. Research has focused on looking at circulating tumour cells (CTCs) or circulating tumour DNA (ctDNA) in the peripheral blood of MM patients as prognostic tools. Results have shown these methods can accurately detect a range of mutations in other cancers compared to standard methods, as well as serving biomarkers of diagnosis, prognosis and treatment response markers[224,225]. More recently, higher levels of CTCs have been associated with worse survival, especially in patients with active disease relapse[226,227]. Limited studies have looked at ctDNA and have shown promising results. Genetic abnormalities were concordant between cDNA and BM samples, however, this was only assessed in 10 patients[216,228].

Assessment of predictive biomarkers in immunotherapy is also underway. Immunotherapy is common in MM and includes monoclonal antibodies that target specific antigens. Antibodies which target the immune checkpoint proteins such as programmed cell death protein 1(PDL-1) have shown promise in cancers such as Hodgkin lymphoma[229]. Moreover, PD-1 has been shown to be highly expressed in relapsed disease in MM. Bustoros *et.al.* have determined that it is unlikely that a single biomarker will be efficient in predicting treatment response in MM; rather, integration of multiple genetic, protein and transcriptomic parameters[216].

1.6.3 Current treatment strategies in MM

Treatment regimens in MM usually consist of a combination of either proteasome inhibitors, immunomodulatory agents and monoclonal antibodies with a chemotherapeutic drug and/or a corticosteroid[230].

Proteasome inhibitors work to inhibit one or more subunits of the 26S proteasome, which can result in the degradation of parts of the NF-κB signalling pathway, endoplasmic reticulum stress and modification of the BM microenvironment, reducing the survival of MM cells[231]. Bortezomib is a commonly used proteasome inhibitor and has generally improved overall survival and progression free survival in MM patients[232,233]. The proteasome inhibitor carfilzomib in combination with dexamethasone produced better response rates in refractory MM patients compared to those treated with bortezomib alone[230,234].

Immunomodulatory drugs such as thalidomide and lenalidomide work by triggering the degradation of the B cell transcription factors Ikaros (IKZF1) and Aiolos (IKZF3)[235] and have had a major impact in the treatment of MM. Lenalidomide in combination with a steroid (dexamethasone) is an approved treatment in those with newly diagnosed and relapsed or refractory MM. Moreover, continuous administration of lenalidomide and dexamethasone was shown to enhance survival outcomes in newly diagnosed MM patients compared to a fixed-term treatment[230,235].

Monoclonal antibodies have shown even further promise with regards to treatment response rates. The anti-CD38 antibody, daratumumab had an overall response rate of 93% when combined with lenalidomide and dexamethasone compared to 30% as a single agent[230,236]. Additionally, combination of pembrolizumab (targeting PD-1) with lenalidomide and dexamethasone in relapsed/refractory MM patients resulted in an overall response rate of 73%[230,236].

With high dose therapy (HDT) and autologous stem cell transplantation being the standard treatment for most newly diagnosed MM patients, much research is focusing on finding new treatments that are both less invasive and elicit fewer

side effects[230]. Moreover, overall survival data is uncertain for a number of combination therapies used in MM treatment due to a lack of long-term follow up data, which won't be available for several years. More research is needed to improve understanding of MM disease pathogenesis and treatment response, as well as identifying molecular subtypes of MM patients that are likely to benefit long-term from certain targeted therapies[237].

1.6.4 A role for ANXA1 signalling in MM?

Evidence of a role for ANXA1 and FPR1/FPR2 in MM is limited, however, there are some studies suggesting that ANXA1 is involved in modulating response to treatment, specifically to bortezomib. Knockdown of ANXA1 both *in vivo* and *in vitro* was shown to amplify the anti-tumour effects of bortezomib. Cell apoptosis was enhanced in ANXA1 knockdown MM cells treated with bortezomib compared to ANXA1 knockdown or bortezomib treated only cells. Moreover, ANXA1 downregulation was shown to enhance bortezomib-mediated anti-inflammatory actions (decreased IL-6 and IL-23) in MM cells and was also associated with a downregulation in p-STAT, a key regulator of cell survival[238]. Additionally, studies looking at the role of hypoxia-inducible factor-1α (HIF-1α) in MM disease progression showed that HIF-1α was associated with a resistance to the anti-angiogenesis effect mediated by bortezomib or lenalidomide and that silencing of HIF-1α was also associated with a downregulation in ANXA1[239]. Overall, these data suggest that ANXA1 could play a pro-inflammatory, pro-survival role in MM disease progression, which in turn, could affect responses to treatment, particularly with bortezomib.

The limited data available for FPR1 and FPR2 in MM suggests a similar role for these receptors in disease pathogenesis. Studies in mouse models engrafted with a MM cell line showed that blockade of FPR1 reduced MM tumour burden[240]. Analysis of gene interactions from a MM database showed that FPR2 was amongst the top 10 significant hub genes (indicating that it has interactions with many other genes in these samples), suggesting that FPR2 signalling is key in these MM samples[241].

Although a role for ANXA1 and FPR1/FPR2 has been implicated in several cancer processes, it is evident that the role these proteins play in MM is not well defined. Based on this, and the fact that the majority of data suggesting a role for these proteins in MM is in cell lines, this project aimed to analyse expression levels of ANXA1, FPR1 and FPR2 in MM patient samples. Furthermore, the project aimed to identify whether ANXA1, FPR1 and/or FPR2 expression is correlated with any disease-relevant features such as survival and prognosis, to improve understanding of these three proteins and their potential role in MM.

1.7 Hypothesis and Aims

ANXA1 is a key signalling protein involved in the immune response, and has an established anti-inflammatory role in innate immunity, with a less defined role in adaptive immunity. Dysregulation of ANXA1 has been implicated in a range of inflammatory diseases and cancers. Moreover, the ANXA1 receptors, FPR1 and FPR2, have been implicated in these diseases and have been suggested as markers of both survival and treatment response. Despite the wide range of diagnostic tests and therapeutics available, there are many forms of inflammatory disease and cancer in which identification of new biomarkers and therapeutic targets is essential. Two prime examples of this are the inflammatory disease, psoriatic arthritis (PsA,) and the B cell neoplasm, multiple myeloma (MM). Despite some evidence, the role of ANXA1, FPR1 and FPR2 in these two diseases remains widely unexplored. The overall hypothesis of this study was: ANXA1 signalling (via FPR1/FPR2) in distinct immune cell subsets is involved in the pathogenesis of PsA and MM. Additionally, this project was in collaboration with Medannex Limited, who have generated an anti-ANXA1 antibody, (MDX-124), which added an additional hypothesis: blockade of ANXA1 via a novel monoclonal antibody can alter its inflammatory response.

In addressing this hypothesis, aims were broadly divided into two sections: assessment of the role of ANXA1 signalling in PsA and MM and assessment of the impact of addition of MDX-124 to healthy and inflammatory cells.

To address these hypotheses, this PhD project aimed to:

- Assess if protein expression levels of ANXA1, FPR1 and FPR2 on a range of immune cell subsets and/or gene expression of these markers in PsA and MM are associated with disease pathogenesis in terms of factors such as prognosis and overall survival.

- Investigate key disease-associated signalling pathways for ANXA1, FPR1 and FPR2 involvement in PsA and MM

- Determine the effects of addition of MDX-124 to healthy and inflammatory cells.

Chapter 2 Materials and methods

2.1 Patients and controls

Peripheral blood mononuclear cells (PBMCs) were obtained from buffy coats (Scottish blood transfusion service), leukocyte cone samples (Newcastle NHS blood transfusion service) or peripheral blood from healthy volunteers (Sir Graeme Davies building, GBRC). Patient and healthy volunteer samples were collected in tubes with a lithium heparin anticoagulant. Psoriatic Arthritis (PsA) samples were obtained from Glasgow Royal Infirmary or Gartnavel General hospital clinics, and Multiple Myeloma (MM) samples were obtained from Gartnavel General hospital. All samples were taken from individuals with informed consent by a trained phlebotomist. PsA patients were clinically classified as having active disease (using DAS28 or DAPSA clinical disease scores, number of swollen joints, number of painful/tender joints, CRP & ESR levels). Appropriate ethical approval was in place.

2.2 Cell isolation, culture and treatment

2.2.1 Peripheral blood mononuclear cell isolation

Buffy coat samples were diluted 1:1 (fresh healthy control and patient sample blood was undiluted) in sterile PBS (Gibco, 14190-094) and layered using Histopaque-1077 (Sigma, H8889). This was centrifuged, for density gradient separation, at 2100rpm for 21 minutes with no break. This allows the blood to form several layers in the tube, consisting of erythrocytes at the bottom, followed by a layer of Ficoll and the peripheral blood mononuclear cell (PBMC) layer on top of the Ficoll. All centrifugation steps were conducted at room temperature, with a swingout rotor.

The final layer on top of the PBMCS is plasma, with the PBMC layer forming directly below. Using a Pasteur pipette, the plasma layer was removed to within 1cm of the PBMC layer and either discarded or frozen in 1ml aliquots at -80°C for future analysis. The buffy coat layer was removed using a Pasteur pipette and transferred into a fresh 50ml falcon tube. PBMCs were then washed twice in

sterile PBS (400g, 10 minutes). If the cell pellet was particularly red (red blood cell contamination), the pellet was resuspended in 3mls of 1X red cell lysis buffer (Stem cell, 20110) for 3 minutes at room temperature, followed by a further wash in PBS (400g, 10 minutes).

For counting, PBMCS were resuspended in 10-20mLs of PBS depending on pellet size. For dead cell exclusion, 10 µl of tryphan blue was mixed with 80µL of PBS and this was further combined with 10 µl of cells (1:10 dilution, which was adjusted depending on cell density). 10µl of this cell dilution was added to a haemocytometer and a light microscope was used to count the cells (EVOS, Thermofisher Scientific; UK). PBMCS were washed again in PBS (400g, 10 minutes) and resuspended in the appropriate buffer at an appropriate dilution for further analysis. Cells to be used for future analysis were frozen in 20% DMSO in Foetal bovine serum (FBS) and slowly frozen in the Thermo Scientific™ Mr. Frosty™ Freezing Container overnight before being transferred to corresponding boxes in the -80 °C freezer.

For myeloma patient samples, bone marrow samples did not require density separation due to the fragility of the sample. Cells were first placed in red cell lysis buffer and lysed as previously mentioned, then washed at room temperature (300g x 10 minutes) before use.

2.2.2 $CD14^+$ primary monocyte isolation

PBMCs were isolated as previously mentioned. Cells were counted, washed in PBS and resuspended in cell separation buffer (CSB, see appendix). Monocytes were extracted using CD14 positive selection beads (Miltenyi Biotec, 130-050-201), according to the manufacturer's guidelines. CD14 is the lipopolysaccharide (LPS) receptor and is preferentially expressed on monocytes and macrophages[242].

In brief, prior to isolation, cells were centrifuged at room temperature (300g for 10 minutes), the supernatant aspirated, and cells resuspended in 80 µL of CSB and 20 µl of CD14 beads per 10^7 cells. This solution was mixed and placed in the fridge for 15 minutes. Cells were washed in CSB (1−2 ml per 10^7 cells) to remove any excess beads by centrifuging at room temperature (300g for 10 minutes).

The supernatant was aspirated, and cells were resuspended in CSB (Up to 10^8 cells in 500 µl). For higher and lower cell numbers buffer volume was scaled accordingly.

For isolation of $CD14^+$ monocytes, an LS column (Miltenyi Biotec, 130-042-401) was placed in the magnetic field of a MidiMACS (Miltenyi Biotec) separator. A 15ml tube was placed below the column for collection of fluid. The LS column was rinsed with 3ml of CSB, then the cell suspension was added to the column. The column was washed a further 3 times (3mls CSB) and the negative fraction collected in a tube below. The column was removed from the magnetic field and placed on top of a 15ml tube. The plunger was pushed firmly into the column and the $CD14^+$ cells were removed into the tube below. A purity check was carried out to verify that the separation from the kit was efficient before continuing with further donors.

2.2.3 Isolation of primary monocytes by CD16 and CD14 positive selection

In order to compare the four different monocyte populations ($CD14^+CD16^+$, $CD14^+CD16^-$, $CD14^-CD16^-$.$CD14^-CD16^+$) a double isolation was carried out using both the CD14 kit mentioned above and a CD16 positive selection kit from the same manufacturer (Miltenyi Biotec,130-091-765). The CD16 positive selection was carried out first as this way was determined to work better at detecting the populations with fewer numbers ($CD16^+CD14^+$). PBMCs were isolated as mentioned previously and resuspended in CSB.

In brief, a depletion step was carried out before isolation of $CD16^+$ monocytes. This involved removal of $CD15^+$ granulocytes and $CD56^+$ NK cells as both cell types express CD16. Prior to isolation, cells were centrifuged at room temperature (300g for 10 minutes) the supernatant aspirated, and cells resuspended in 300 µL of buffer per 10^8 cells.100 µL of both FC receptor (FCR) blocking reagent and of Non-Monocyte Depletion Cocktail were added per 10^8 cells. FCR blocking reagent is used to decrease non-specific binding of beads to the monocytes and hence improves the specificity of the labelling. As previously, buffer and bead volumes were scaled up appropriately. Cells were

mixed well with the buffer and beads and incubated in the fridge for 15 minutes. Cells were washed in CSB (5−10 ml per 10^8 cells) to remove any excess beads by centrifuging at room temperature (300g for 10 minutes). The supernatant was aspirated, and cells were resuspended in CSB (Up to 1.25 10^8 cells in 500 µl. For higher and lower numbers buffer volume was scaled accordingly).

For depletion, an LD column (Miltenyi Biotec, 130-042-901) was placed in the magnetic field of a MidiMACS separator. A 15ml tube was placed below the column for collection of fluid. The LD column was rinsed with 2ml of CSB, then the cell suspension was added to the column. The column was washed a further 2 times (1ml CSB) and the negative fraction collected in a tube below. This fraction contains the unlabelled monocytes. Cells were washed in CSB at room temperature at (300g 10 minutes), supernatant aspirated and cells resuspended in 400µl of CSB.

For isolation of $CD16^+$ cells,100 µl of CD16 microbeads was added to the cells. This solution was mixed and incubated in the fridge for 15 minutes. Cells were washed in CSB (5−10 ml) to remove any excess beads by centrifuging at room temperature (300g for 10 minutes). The supernatant was aspirated, and cells were resuspended in CSB (Up to10^8 cells in 500 µl. For higher and lower numbers buffer volume was scaled accordingly). An LS column was placed in the magnetic field of a MidiMACS (Miltenyi Biotec) separator and separation was carried out as mentioned previously.

When both a CD16 positive and negative fraction were obtained, a further CD14 positive selection was carried out on each of the fractions in order to obtain the different monocyte populations. A purity check was carried out to verify that the separation from the kit was efficient before continuing with further donors.

2.2.4 LPS treatment of primary monocytes

To investigate the effects of MDX-124 on primary monocytes in an inflammatory setting, 100,000 cells from the populations isolated above were plated and incubated with or without 100ng/ml of MDX-124 overnight. The following day 10ng/ml of Lipopolysaccharide (LPS, InvivoGen, Ultrapure from *Escherichia.Coli*-K12) was added to the cells for 24 hours (hrs). LPS is widely recognized as a

potent activator of monocytes/macrophages, and its effects include an altered production of key mediators, such as inflammatory cytokines and chemokines. Following LPS incubation, supernatant was taken from the cells and centrifuged. Supernatant was aliquoted and stored at -80 until further analysis.

The duration of LPS stimulation and dosage were both optimised using $CD14^+$ monocytes only before stimulation with all of the monocyte populations isolated above.

2.2.5 Differentiation and treatment of THP-1 cell line

THP-1 cells were obtained from ATCC (ATCC® TIB-202™). These cells originate from a patient with acute monocytic leukaemia and have been used widely in the literature to investigate the function and regulation of monocytes and macrophages[243]. The cells were maintained in complete RPMI 1640 (cRPMI- see appendix) medium in a 37°C, 5% CO2 incubator. The medium was changed twice a week.

To obtain cells that mimicked macrophage biology, THP-1 cells were differentiated using 50ng/ml of 12- phorbol 13-myristate acetate (PMA) for 3 days, then rested for a further 4 days. This allowed the cells to mature into adherent, spindle-shaped, macrophage-like cells. Cells were also assessed for an upregulation in the macrophage markers CD11b and CD14.

100ng/ml of MDX-124 was added to THP-1 cells to determine any baseline effects the antibody might have on these cells. MDX-124 was added for 24,48 and 72 hours. Cells were detached from the tissue culture plate using accutase (Sigma, A6964), washed in PBS and stained for expression of macrophage markers (CD11b and CD14) at each time point. To determine if the antibody had any effect on the macrophage differentiation process, cells were stimulated with PMA as previously described, and MDX-124 was added for 3 or 7 days. Cells were assessed under the microscope for macrophage-like appearance and stained for surface expression of CD11b, CD14 and other markers of interest.

2.3 MDX-124

MDX-124 is a humanised, monoclonal, anti-ANXA1 antibody owned by the project industry collaborators, Medannex Limited. The ultimate aim of the company is to develop MDX-124 as a treatment (targeting ANXA1) for use in the clinic. Due to MDX-124 still being in development, different conditions such as buffer and storage temperature were still under optimisation between batches (various production methods were optimised by collaborating companies).

2.3.1 MDX-124 development timeline

Monoclonal antibodies can exhibit several macro and micro-heterogeneities that can affect their efficacy and safety[244]. Optimisation of MDX-124 storage and buffer conditions were optimised at Medannex. Initially MDX-124 was produced through a transient expression method in mammalian cells, which is common for small scale protein production, but can lead to heterogeneity between batches[245]. The first batch of MDX-124 (denoted as Batch 1 in results chapter 3, figure 3.3) used in the project was manufactured by Fusion antibodies. This batch was provided in phosphate buffered saline (PBS). PBS was chosen as a buffer due to it being widely available and having a wide buffering capacity at pH neutral conditions. The buffer also contains no components that would potentially interfere with biological or i*n-vivo* assays. Batch 1 was stored at 2-8°C as Medannex were unsure of the effect of freeze/thaw cycles on antibody stability.

After various stability and quality control (QC) tests were carried out (methods section 2.3.2) by Medannex, long-term storage of MDX-124 at -20°C was determined as stable (Batch 2, results chapter 3, figure 3.3).

As MDX-124 was developed, it transitioned from being produced by a transient cell line (mammalian cells), to production through more a stable expression method in Chinese hamster ovary (CHO) cells. CHO cells are widely used in therapeutic antibody production due to their ability to produce stable proteins in a cost-efficient manner[245]. Specialised stability studies (methods section 2.3.2), in which several storage conditions and buffer formulations were

assessed. Data was then analysed to identify the best combination of buffer and pH that gave the best stability profile (in this case 8% sucrose, 20mM histidine, 0.01 % polysorbate pH 6.3).

Monoclonal antibody production using stable transfection methods as this is a requirement for Good manufacturing process (GMP) manufacture. Stable cell line expression of the antibodies provides more consistency between batches, whereas transitory expression can sometimes lead to batch inconsistences[246]. This process required a specialized GMP compliant company, and hence Fuji were chosen for this. Fuji carried out a series of stability tests which required MDX-124 to be in a tailor-made formulation (8% sucrose, 20mM histidine, 0.01 % polysorbate pH 6.3). Higher concentrations (30mg/ml) of the antibody per volume were also used compared to the previous, lower concentrations (<10mg/ml) as Fuji showed this concentration in the new buffer was more suitable for the distribution of the antibody in the clinic. The new antibody batch was aliquoted and frozen at -80°C for long-term storage. With labelling, the antibody was thawed and was stored in the fridge after conjugation (batch 3, results chapter 3, figure 3.3).

2.3.2 Quality control tests carried out on MDX-124 by Medannex Limited

MDX-124 went through an extensive optimisation process (conducted by Medannex), whereby which analysis methods were optimised to ensure that results were accurate and reproducible each time the antibody material was tested.

In brief, analytical methods used included:

- Size exclusion chromatography (SEC) to measure protein purity by measuring the amount of aggregates and monomer (antibody aggregation can alter their biological activity and poses several safety concerns when used therapeutically[247]).
- ELISA binding to measure the affinity of the antibody binding to ANXA1

- Imaged capillary isoelectric focusing (icIEF), which separates proteins by charge. This was used both to identify MDX-124 and associated (lot-to lot) variants, as well as monitoring the stability of MDX-124.
- Reduced and non-reduced capillary electrophoresis for MDX-124 identification and characterization between batches
- Glycan profiling (surface glycan on antibodies can depending on the nutrients fed to the mammalian cells)
- Detection of other impurities left over from manufacturing such as mammalian host cell protein and DNA residue and residual methotrexate (used a as a cell selective agent) as well conducting as protein A affinity purification methods.

Once these tests were established, Medannex could then identify MDX-124 batch to batch differences as well as identifying any changes in MDX-124 due to degradation.

2.3.3 MDX-124 conjugation

It is essential for the antibody conjugation process to occur in a buffer free of primary and secondary amines. Notably, histidine, which is part of the MDX-124 storage buffer, is an amino acid that contains secondary amines[248], and is therefore not compatible with the conjugation process. To overcome this issue, proteins are frequently buffer-exchanged into PBS before conjugation[249].

A buffer exchange was therefore carried out on MDX-124 produced from the CHO cell line mentioned above, and the antibody was placed in PBS before labelling with AF647.The buffer exchange was carried out according to the manufacturer's instructions (ThermoFisher Scientific). In brief, Zeba™ Micro Spin Desalting Columns (ThermoFisher) were used to process the antibody through a series of centrifugation steps in which MDX-124 was transferred from the histidine-sucrose buffer formulation into PBS.

MDX-124 and isotype (Biolegend,403502) antibodies were conjugated in house using the AF647 labelling kit and protocol from Thermo Fisher[250]. In brief, a 1 M solution of sodium bicarbonate was made by adding 1ml of deionised water to the vial of sodium bicarbonate provided in the kit and mixing. Both MDX-124 and

isotype antibodies were labelled at a concentration of 1mg/ml. 10ul of the 1Molar solution of sodium bicarbonate was mixed with 100ul of MDX-124(at 1mg/ml) This mixture was then transferred to a vial of reactive AF647 dye provided, gently mixed, capped and stored at room temperature in the dark for 1 hour. The vial was gently inverted several times every 15 minutes to increase labelling efficiency.

For purification of the labelled antibody, spinning columns were prepared. Columns were placed on top of a 6ml polystyrene tube and 1ml of purification resin was added to each spin column (one per antibody). A further 500ul of purification resin was added to the column and the column (and tubes) were centrifuged at room temperature (1100g for 3 minutes). The buffer at the bottom of the polystyrene tube was discarded. After labelling was completed, labelled antibodies were added to the spinning columns and centrifuged at room temperature (1100g for 5 minutes). The labelled antibodies were then collected and stored appropriately (2-8°C).

2.3.4 Apoptosis assay

In order to ensure 100ng/ml of MDX-124 was not inducing cell death, an apoptosis assay was carried out using PBMCs obtained from buffy coat samples. The Annexin V staining kit (for flow cytometry analysis) from Invitrogen works to detect the presence of phosphatidyl serine (PS) on the surface of apoptotic cells using an anti-Annexin V protein. Annexin V is a calcium dependent phospholipid binding protein which binds PS with high affinity, allowing for detection of cells undergoing apoptosis[251]. The kit also contains propidium iodide (PI), a nuclear and chromosome counterstain. The ability of PI to bind to its target depends on the permeability of the cell membrane. Therefore, it cannot stain live or early apoptotic cells but has the ability to stain cells undergoing late apoptosis or undergoing another form of inflammatory cell death called necrosis[252](Figure 2.1).

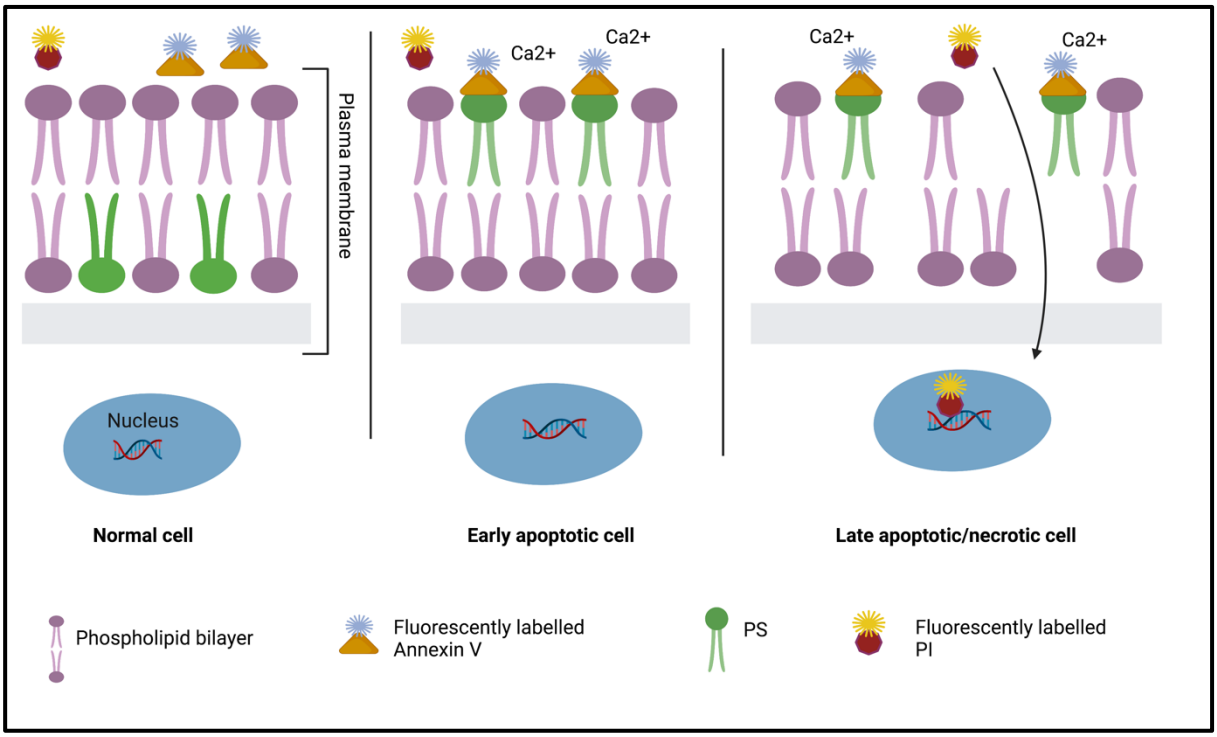

Figure 2.1 Principles of the Annexin V staining apoptosis assay.

In a normal (non-apoptotic, non-necrotic) cell, PS remains unexposed within the phospholipid bilayer of the cell, Annexin v does not bind to it and there is no fluorescent signal. During early apoptosis, PS is exposed at the surface of the cell membrane, allowing fluorescently labelled Annexin V to bind to it (in the presence of calcium) producing fluorescent staining. At this stage, the cell membrane is still impermeable to fluorescently labelled PI. During late apoptosis or necrosis, the cell membrane becomes more permeable and allows fluorescently labelled PI to enter the cell and bind to its nuclear target, causing fluorescent staining. Image made using Biorender.com.

PBMCs were isolated as previously mentioned, diluted to 1 million cells per ml, and plated onto a 24 well tissue culture plate. For optimisation of the assay (before addition of MDX-124), cells were stimulated with either 50ng/ml or 100ng/ml of phorbol 12-myristate 13-acetate (PMA) and incubated at 37°C either overnight or for 4 hours to determine the best conditions to induce apoptosis. The overnight stimulation with 50ng/mL of PMA resulted in a consistent increase in both early and late apoptotic cells compared the other conditions. This condition was therefore used for subsequent experiments.

Once the assay was optimised, 100ng/ml of MDX-124 was added to PBMCs treated with 50ng/ml of PMA and incubated overnight. PBMCs were transferred from the tissue culture plate into flow cytometry tubes and staining was carried out according to the protocol from Invitrogen[253]

In brief, PBMCs were transferred to 6ml polystyrene tubes and washed (400g for 5 minutes) once in PBS followed by another wash in 1X annexin binding buffer (Invitrogen, V13246). For staining, PBMCs were resuspended in 1X annexin binding buffer at $1x10^6$ per ml. 5µl of Annexin V (FITC) antibody was added to the respective tubes. Anti-CD3 (AF700), anti-CD4 (V500) and anti-CD8 (APC Cy7) antibodies (3µl per well) antibodies were added to detect T cells. Unstained PBMCs were used as controls for the staining and PBMCs were heat killed at 65°C for 5 minutes as a control for necrosis. PBMCs were vortexed and incubated with the antibodies at room temperature (15 minutes in the dark). The cells were washed again in 1X annexin binding buffer. 5µl of PI stain was added to the PBMCs directly prior to analysis on the BD Bioscience LSRII flow cytometer. Data was then analysed using FlowJo (v10.6.1) Software.

2.3.5 Seahorse metabolomics assay

In order to determine if MDX-124 was affecting the metabolic profile of cells a metabolic stress assay was conducted on the Seahorse machine at the Beatson institute. PBMCs were isolated as previously stated. Initially all PBMCs were used but due to variation in results because of the different cell populations present, solely monocytes were used for future experiments. Monocytes were isolated by other members of the Goodyear group using the CD14 negative selection kit from Stem cell technologies[254].

The day before the PBMC/monocyte isolation, cell Tak solution was prepared at a concentration of 1.21mg/ml for binding of the cells to the seahorse plate. The solution was pH'd between 6-8 and 25 µl of it was added per well of the seahorse plate. The plate was then incubated at room temperature for 30 minutes, washed twice with water and left overnight to dry (room temperature). On the day of isolation, the drug cartridge for the Seahorse machine was hydrated by adding 200µl of Seahorse calibrant per well. This was wrapped in parafilm and left to incubate overnight at 37°C in a CO_2 free incubator. Isolated monocytes were plated at 1×10^5 100µl in the seahorse (96 well) plate. The plate was then centrifuged (200g no brake for 2 minutes) and this was repeated in the reverse orientation. The cells were then left overnight in the 37°C incubator (in their own media).

The day of the Seahorse analysis, (serum free) seahorse media was prepared with 1% glutamine, glucose and growth factors. The media was adjusted to a pH of 7.4. MDX-124 was added to the cells for 4 hrs. Different doses of MDX-124 were assessed, the working concentration of 100ng/ml and also 1000ng/ml

The plate was sealed transported on ice to the Beatson Institute where the media was then aspirated and replaced with 175μl of Seahorse media. The cells were then incubated for 45 minutes in the 37°C CO2 free incubator. During this period the drug cartridge for the seahorse analysis was prepared by making up the necessary dilutions of the seahorse drugs and adding 25μL of each drug (Oligomycin, CCCP, Rotenone & Antimycin) to the corresponding ports on the drug cartridge. The drug cartridge was then incubated for 15 minutes in the 37°C CO2 free incubator. Once the seahorse plate and cartridge were ready, the mito-stress assay was conducted on the Seahorse machine.

The mito-stress assay is carried out using various modulators of respiration and the Seahorse machine (Agilent technologies) produces measurements of mitochondrial respiration using the oxygen consumption rate (OCR) and glycolysis using the extracellular acidification rate (ECAR) in live cells[255]. Different parameters are also calculated from the OCR graphs produced, giving information on mitochondrial function. An example of the OCR graph produced is shown on the Agilent website[256]. Parameters calculated from this graph are:

1. Basal respiration rate (energy demands of the cell at baseline)
2. ATP production
3. H+ Proton leak (respiration not coupled to ATP production- can be associated with mitochondrial damage)
4. Maximum respiration that the cell can achieve
5. Spare respiratory capacity (capability of the cell to respond to energetic demands)
6. Non-mitochondrial oxygen consumption (helps to accurately calculate mitochondrial respiration.

By measuring each of these parameters, the ability of MDX-124 to impact mitochondrial function (as well as cellular glycolysis) can be assessed.

2.4 Cell surface staining using flow cytometry

2.4.1 Staining protocol

The surface expression of ANXA1 alongside various markers were analysed across a range experiments following the same staining protocol. For staining, a maximum of 1 x 10^6 cells were transferred into a 6ml polystyrene tube and topped up to 50ml with Flow Cytometry Staining Buffer (eBioscience™,00-4222-26). Tubes were then centrifuged at 400g for 5 minutes. Supernatant was removed, FCR block added (Miltenyi Biotec, 2µl per 1 million cells) and appropriate antibodies added. A range of antibodies were used for different experiments (see Table 2.1). Cells were incubated for 20 minutes on ice (to reduce non-specific antibody binding) and protected from light (fluorophore-conjugated antibodies were used). Tubes were topped up to 50ml with Flow Cytometry Staining Buffer and centrifuged at 400g for 5 minutes to remove excess antibody. Supernatant was removed and cells resuspended in 300µl of Flow Cytometry Staining Buffer for instant analysis or in 1X CellFix buffer (BD, 340181). Samples to be fixed were incubated for 20 minutes at room temperature, washed in Flow Cytometry Staining Buffer (400g, 5 mins) and resuspended in 300µl of Flow Cytometry Staining Buffer.

Fixed samples were stored at 4°C and analysed the following day on either the Fortessa, LSRII (BD Biosciences) or attune (ThermoFisher) depending on availability. All data was analysed using FlowJo (v10.6.1) software.

2.4.2 Characterisation of ANXA1 surface expression on tissues from different species

An aim in the study was to determine whether MDX-124 could bind to tissues in animal models of interest for the ongoing pre-clinical development programmes at Medannex, particularly rat and Golden Syrian hamster models. Hence, binding of MDX-124 to these models was assessed.

Rat spleen and lymph node tissue was received from the University of Glasgow Central Research Facility and used under licenses issued by the UK Home Office. Tissues were cut into smaller pieces using a sterile scalpel. Each tissue was then filtered through a 70μM filter into a 50ml falcon tube. For the spleen, red blood cell lysis was carried out. Cells were washed washed in Flow Cytometry Staining Buffer (400g, 5 mins) before staining with live/dead (ef506, eBioscience) and then AF647-labelled MDX-124 (each on ice for 20 minutes). Cells were fixed and analysed on the ThermoFisher attune flow cytometer.

Golden Syrian hamster tissue samples received from Viroclinics were as follows; spleen, left lung, right lung after lung lavage with MACS solution, lung lavage (lung was washed with 1ml of MACS solution) and whole blood in an EDTA tube. Spleen was processed as previously mentioned for the rat tissue. Lung tissue was digested in Liberase solution (Roche, 5401020001) in a 37°C shaking incubator for 2 hours. After digestion, red cell lysis was carried out, followed by a wash in Flow Cytometry Staining Buffer (400g, 5 mins). PBMCs were isolated from whole blood as previously mentioned, although numbers were low as the blood had haemolysed upon arrival. All isolated cells and lung lavage were washed in Flow Cytometry Staining Buffer (400g, 5 mins) prior to staining. Staining was carried out as mentioned previously. Cells were fixed and analysed on the ThermoFisher attune flow cytometer.

Table 2.1 Antibodies for flow cytometric analysis

Specificity	Fluorescent Label	Clone	Concentration (µg/ml)	Supplier	Catalogue Number	µl/sample
Annexin-A1	AF647	N/A	1000	Medannex	N/A	1-2
Human IgG1	AF647	QA16A12	1000	BioLegend	403502	1-2
FPR1	FITC	W15086B	N/A	BioLegend	391604	5
FPR2	PE	304405	N/A	R&D Systems	FAB3479P	5
CD16	PerCP/Cyanine5.5	3G8	N/A	BioLegend	302028	2
CD16	PE/Cyanine7	3G8	N/A	BioLegend	302016	1
CD16	BV421	3G8	N/A		302038	
CD14	BV605	M5E2	N/A	BioLegend	301834	2
CD14	APC/Cyanine7					1
CD11b	PE/Cyanine7	ICRF44	N/A	BioLegend	301322	2
CD11C	AF700					3
HLA-DR	BUV395	G46-6	N/A	BD Biosciences	564040	5
HLA-DR	PE/Cyanine7	G46-6	N/A	BD Biosciences	560651	2
CD303	PerCP/Cyanine5.5	201A	N/A	BioLegend	354210	5
CD56	BV510	5.1H11	N/A	BioLegend	362534	1
CD19	PeDazzle	HIB19	N/A	BioLegend	302552	1
CD19	AF700	HIB19	500	BioLegend	302226	2
CD19	BV510	HIB19	N/A	BioLegend	302242	1
CD20	V450	L27	N/A	BD Biosciences	561164	2
CD3	AF700	UCHT1	500	BioLegend	300424	2
CD3	BV510	UCHT1	N/A	BioLegend	300448	1
CD38	PE/Cyanine7	HB7	N/A	BioLegend	356608	2
CD138	BV421	MI15	N/A	BioLegend	356516	3
CD24	BV711	ML5	N/A	BioLegend	311136	2

CD27	V500	M-T271	N/A	BD Biosciences	561222	2
CD43	BV605	IG10	N/A	BD Biosciences	563378	2
IgM	PerCP/Cyanine5.5	G20-127	N/A	BD Biosciences	561285	5
IgD	APC-H7	IA6-2	N/A	BD Biosciences	561305	5
CD69	BV421	FN50	N/A	BioLegend	310930	2
CD10	BV786	HI10a	N/A	BD Biosciences	564960	2
CD5	PE eFluor 610	L17F12	N/A	ThermoFisher Scientific	61-0058-42	1
CD8a	APC-eFluor 780	RPA-T8	N/A	ThermoFisher Scientific	47-0088-42	2
CD4	V500	L200	N/A	BD Biosciences	560768	1
CCR6	BV711	G034E3	N/A	BioLegend	353436	5
CD161	PE-eFluor 610	HP-3G10	N/A	ThermoFisher Scientific	61-1619-42	1
TCR gamma delta	BV650	B1	200	BD Biosciences	564156	2
CXCR3	PE/Cyanine 7	CEW33D	N/A	ThermoFisher Scientific	25-1839-42	2
CCR4	BV605	L291H4	N/A	BioLegend	359418	5
CCR10	PerCP/Cyanine5.5	IB5	200	BD Biosciences	564772	2
CCR7	BV785	G043H7	N/A	BioLegend	353436	5
CD45RA	V450	HI100	N/A	BD Biosciences	560362	1
Fixable Viability Dye	eFluor 506	N/A	N/A	ThermoFisher Scientific	65-0866-14	1
Fixable Viability Dye	eFluor 780	N/A	N/A	ThermoFisher Scientific	65-0865-14	1

2.5 Functional assays with MDX-124

2.5.1 Analysis of single cytokine production via ELISA

Either cell culture supernatants or human plasma samples were used for analysis. Cell culture supernatants were collected and centrifuged at 600g for 5 minutes (mins) to remove any cells or debris into a pellet. The supernatants and plasma samples were stored at -80°C until needed. A few samples were initially run neat to check if dilutions were required. If required, samples were diluted appropriately in assay buffer for subsequent experiments. ELISAs were carried out according to the manufacturer's (Invivogen) instructions, which varied depending on the lot number.

In brief, For ELISAs with cell culture supernatants, ELISA plates (corning) were coated with appropriate dilutions of either an anti-IL-6 or anti-TNFα capture antibody and incubated at 2-8°C overnight. The next day, the wells were aspirated, washed with ELISA wash buffer (see appendix) and tapped try on absorbent paper. Plates were then blocked with ELISA assay buffer (see appendix) at room temperature for 1 hour. Plates were aspirated and standards (appropriate dilutions were made in assay buffer) and samples were loaded into the appropriate cells. Directly after this, the detection antibody (at the appropriate dilution for the kit) was added to all the wells and plates were incubated for 2 hours at room temperature with shaking. Plates were then aspirated and washed with ELISA wash buffer 5 times. The streptavidin-HRP (at the appropriate working dilution) was added to the wells and plates were incubated at room temperature for 30 minutes with shaking. Plates were washed with ELISA wash buffer 5 times and the TMB substrate was added to the wells for a maximum of 30 minutes at room temperature (covered in metallic foil to protect it from the light) whilst shaking. Stop solution (2N H_2SO_4) was added and absorbance was measured at 450nm within 30 minutes of adding the stop solution using a Tecan Sunrise Absorbance reader. Cytokine concentrations were determined within the range of the standard curve (Figure 2.2)

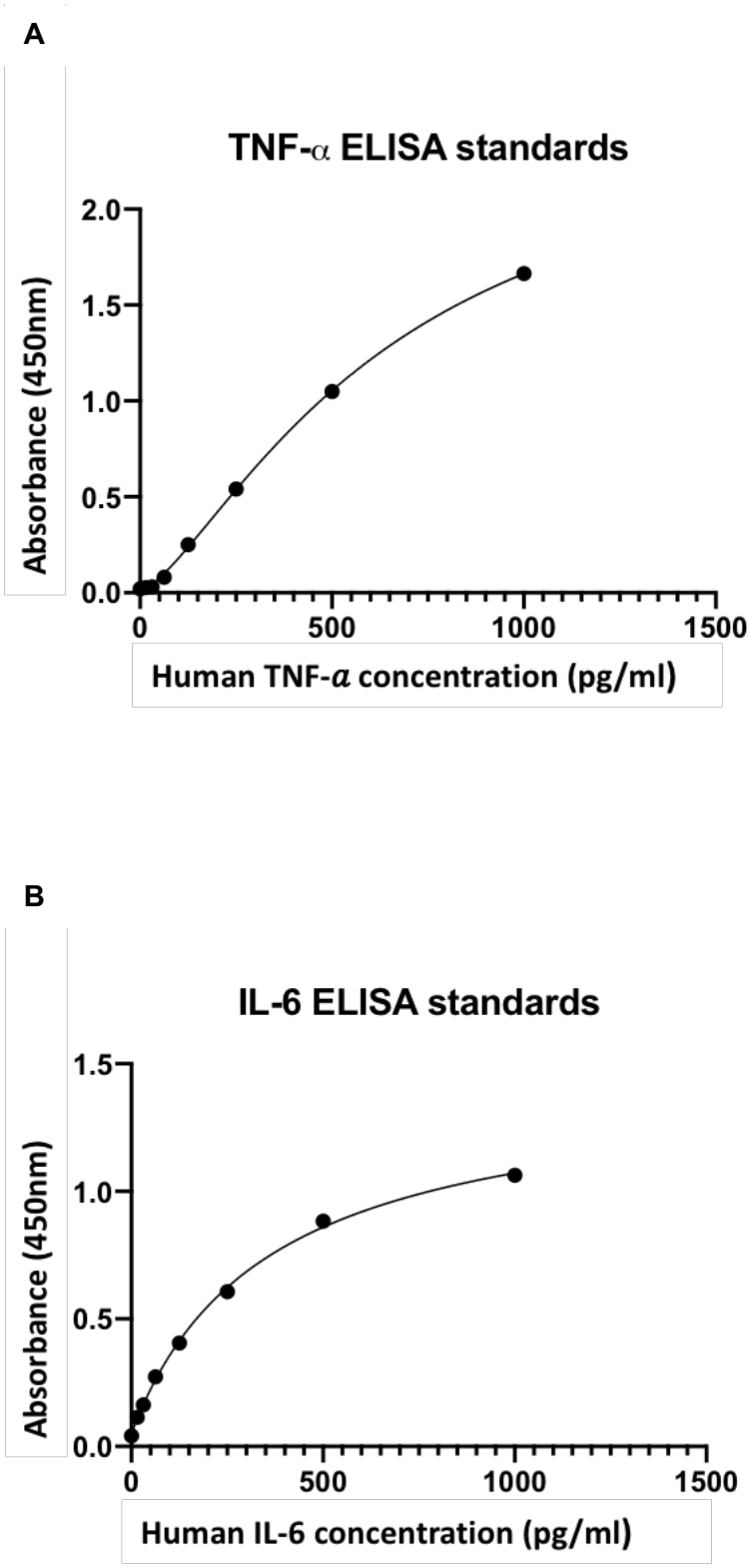

Figure 2.2 IL-6 and TNF-α ELISA standard curves

Standard curves for the (A) IL-6 ELISA and (B) TNF- α ELISA assays. For each assay, a standard vial was reconstituted in assay diluent (see appendix) to a concentration of 10,000ng/ml. A dilution series was then carried out using assay diluent to produce a range of standards within the assay detection limits (15.6-1000pg/ml). Assay diluent served as the zero standard (0pg/ml). Absorbance of each standard was read at 450nm on the Tecan Sunrise Absorbance reader. A standard curve was produced using concentration and absorbance values on GraphPad Prism 9 software and used to calculate the concentration of IL-6 and TNF-α in PsA and HC supernatants.

ANXA1 levels in plasma samples were assessed using the kit protocol from Invivogen[257].In brief, plates already came pre-coated with an anti-ANXA1 antibody. Samples and standards were added to the plate (at appropriate dilutions in assay diluent) and the plate was incubated at room temperature for 2.5 hours whilst shaking. Wells were aspirated and washed 4 times as previously described. A biotin conjugate was added to the wells and the plate was incubated 1 hour at room temperature whilst shaking. The wells were aspirated and washed 4 times. Streptavidin HRP solution was added to the wells and the plate was incubated for 45 minutes at room temperature whilst shaking. The wells were aspirated and washed 4 times as and TMB substrate and stop solutions were added as previously mentioned. Absorbance was read at 450nm using a Tecan Sunrise Absorbance reader. Cytokine concentrations were determined within the range of the standard curve (Figure 2.3)

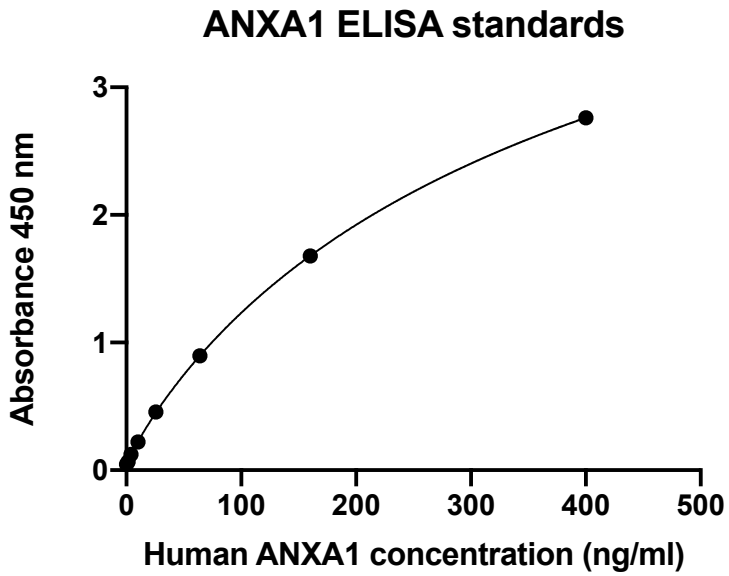

Figure 2.3 ANXA1 ELISA standard curve

The standard vial was reconstituted in assay diluent C (provided in the kit) to a concentration of 400ng/ml. A dilution series was then carried out using assay diluent C to produce a range of standards within the assay detection limits (1.64-400ng/ml). Assay diluent C served as the zero standard (0ng/ml). Absorbance of each standard was read at 450nm on the Tecan Sunrise Absorbance reader. A standard curve was produced using concentration and absorbance values on GraphPad Prism 9 software and used to calculate the concentration of ANXA1 PsA and HC plasma samples.

2.5.2 Proteome profiler for kinase and multi cytokine analysis

2.5.2.1 Sample preparation

Analysis was carried out to assess the impact of addition of MDX-124 to differentiated THP-1s. THP-1 cells were differentiated with and without 100ng/ml of MDX-124 as mentioned previously. Cell supernatant was collected at day 7 and analysed for cytokine production using the R&D systems Proteome Profiler Human XL Cytokine Array Kit (ARY022B).

For obtainment of lysates, at day 7, cells were placed in serum-free medium (serum starved) for 24 hours. Serum starvation is a commonly used method for synchronisation of mammalian cells[258], and it was crucial that both experimental groups were synchronised before addition any further stimulants. This ensured removal of the impact of the cell cycle on the response of each of the groups to cell stimulation. Cells were stimulated with cell stimulation cocktail (see appendix for components and volumes) for 5 minutes and cell lysates were obtained and frozen at -80 °C until analysis using the Proteome Profiler Human Phospho-Kinase Array Kit (R&D Systems, ARY003C).

The amount of protein in the lysates was quantified using the Pierce BCA protein Assay kit from ThermoFisher BCA assay[259], which involved incubating set standards and samples with the kit's working reagent for 30 minutes and quantifying protein values based on a standard curve read at 570nm (Figure 2.4).

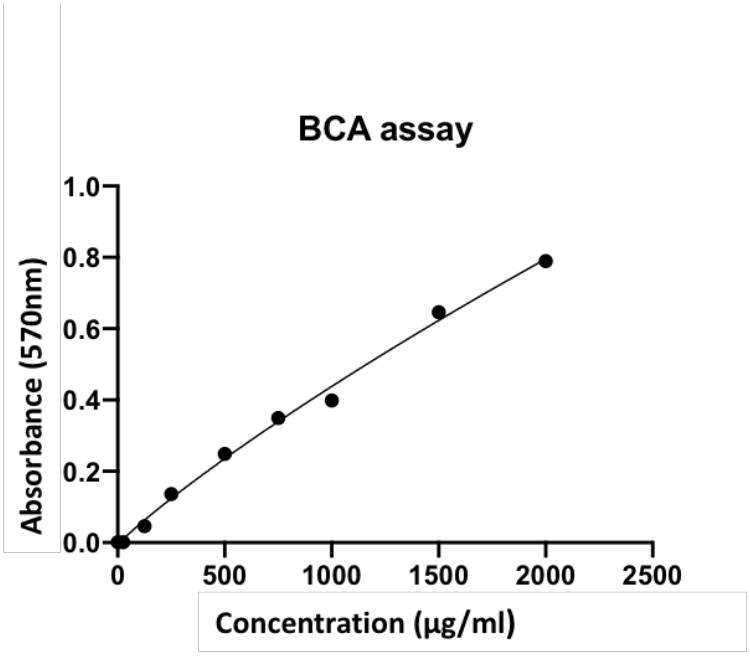

Figure 2.4 BCA assay standard curve

25 µl of the standards provided and samples were added to a 96 well plate. 200 µl of working reagent (provided in the kit) was added and the plate was at 37°C for 30 minutes. The plate was cooled to RT and absorbance of each standard was read at 570nm on the Tecan Sunrise Absorbance reader. A standard curve was produced using concentration and absorbance values on GraphPad Prism 9 software and used to calculate the concentration of protein in each sample.

2.5.2.2 Human XL Cytokine Array kit protocol

The assay was carried out in accordance with the manufacturer's protocol. One membrane per sample was used. A four well multi-dish was provided for incubation of each membrane with reagents required for each step of the assay.

In brief, 2mls of blocking buffer was added to each of the wells and each membrane was placed in a separate well facing upwards. Dishes were covered and incubated at room temperature for 1 hour on a rocking platform shaker. The blocking buffer was aspirated from the wells and 1.5mls of sample was added to each membrane and incubated on a rocking platform shaker at 2-8°C overnight (samples were prepared to a total volume of 1.5ml by diluting with blocking buffer).

The next day, membranes were transferred into separate containers and washed using the wash buffer provided (diluted to 1X in deionised water) for 10 minutes on a rocking platform shaker. This was repeated a further two times. Membranes were transferred back into the multi-dish and 1.5ml of detection antibody (at

the specified dilution) was added. Membranes were incubated at room temperature for 1hr on a rocking platform shaker. Membranes were removed and washed as previously mentioned and transferred back into the multi-dish. 2ml of streptavidin-HRP was added per well and membranes were incubated at room temperature for 30 minutes on a rocking platform shaker, before washing as previously mentioned. Membranes were removed from the wash container and blotted on absorbent paper to remove excess wash buffer, then placed onto the bottom sheet of a plastic sheet protector with the identification number facing upwards. 1ml of Chemi Reagent Mix was added per membrane and each membrane was covered with the plastic sheet protector. Membranes were placed with identification numbers facing upwards into an auto-radiography cassette and exposed to X-ray film for 1-10 minutes. The exposure time that produced the most optimal image was used for analysis.

2.5.2.3 Phosphokinase Array kit protocol

Two membranes (part A and part B) per sample were used. Membranes were blocked using 1ml of blocking buffer per well in an 8-well multi-dish container at room temperature for 1 hour on a rocking platform shaker. Blocking buffer was aspirated and 1ml of sample was added to membrane A and membrane B (samples were diluted to a final volume of 2.0ml using an array buffer provided). Dishes were covered and incubated on a rocking platform shaker at 2-8°C overnight.

The next day, membranes were removed and washed three times as previously described in the cytokine XL assay (both membrane A and B were washed in the same container, 10mL of wash buffer per membrane- 20mls in total per wash). Membranes were then removed and placed back in respective wells in the multi-dish container. 1mL of detection antibody was added per well (for membrane A, 20μl of reconstituted detection antibody A was added to 1.0mL of array buffer provided and for membrane B. 20μl of reconstituted detection antibody B was added to 1ml of array buffer provided). Membranes were incubated in the multi-dish at room temperature for 2 hours on a rocking platform shaker and washed as previously described (20ml per container).1ml of Streptavidin-HRP was added

per membrane and the rest of the assay was carried out as for the Cytokine XL assay.

2.5.2.4 Image analysis

Pixel densities for each proteome profiler assay were obtained using the recommended Quick Spots image analysis software from Western Vision[260]. This software works to create a template (using information on where each analyte is positioned on the membrane) to analyse pixel density (average pixel density was calculated, and average background signal was subtracted from this using negative control spots). Graphs of average pixel density of MDX-124-treated groups relative to control groups were produced using GraphPad Prism (version 9) software.

2.6 Analysis of RNA sequencing data

2.6.1 Database analysis

PsA gene expression data (alongside limited clinical data) was provided in normalised read counts from Hanna Johnsson from the School of Infection and Immunity, University of Glasgow. Normalisation was conducted by Hanna using the Bioconductor DESeq2[261] package. To normalise for sequencing depth and RNA composition, DESEQ2 uses a median of ratio's method to divide counts by sample-specific size factors determined by median ratio of gene counts relative to geometric mean per gene[262,263]. The raw and processed PsA sequencing data is available on the Gene Expression Omnibus (GEO), under accession GSE205748.

Multiple myeloma (MM) gene expression data was obtained upon being granted access to the CoMMpass database[264] and was provided as normalised transcripts per million (normalisation software details were not provided) which is the number of counts per length (kb) of transcript per million reads mapped. This method takes into account differences in sequencing depth and gene length[262].

Differential gene expression analysis was done on R studio using the Bioconductor DESeq2 package using normalised gene count data. Limited clinical data was also available from the CoMMpass database.

Results from differential gene expression analysis from both datasets were used to carry out pathway analysis using the Bioconductor clusterProfiler package[265] and correlation analysis using the Stats package[266]. Several plots and graphs were also made with each dataset using the ggplot2[267] package.

2.7 Statistical analysis

Statistical analysis was performed either using GraphPad Prism (v9) software or using R studio. When applicable, data was tested for normal distribution (D'Agostino & Pearson test) to determine which statistical tests to use. For sample sizes bigger than 30 normality was assumed. Data which followed a normal (Gaussian) distribution was assessed using parametric tests. If data was not normally distributed (or insufficient data was available to assess normality), non-parametric tests were used. In general, when comparing two groups a student's paired or unpaired t-test was used for normally distributed data and the non-parametric equivalents (Wilcoxon and Mann Whitney U test) were used for data that was not normally distributed. When comparing multiple groups to a control group a non-parametric Friedmann's test was used (data was not normally distributed). A P value of < 0.05 was considered significant. Information on which statistical analysis was carried out on each set of data can be found in the figure legends.

Chapter 3 Assessment of a novel antibody against Annexin A1

3.1 Introduction

Annexin A1 (ANXA1) has been shown to play key roles in immunity, including that of an anti-inflammatory mediator in innate immunity[27]. During homeostasis, ANXA1 is primarily expressed in the cytoplasm of granulocytes and monocytes. When inflammation occurs, ANXA1 can be transported to the cell membrane and secreted into the circulation to mediate its signalling through receptors on target cells[56,71]. ANXA1 signals through the formyl peptide family of receptors, of which there are three in humans; FPR1, FPR2 and FPR3. Most of the of the available data suggests this signalling is mediated mainly through FPR1 and FPR2 in disease settings. [23,28,29] FPRs bind a wide range of ligands to mediate processes such as chemotaxis and phagocytosis[268].

ANXA1 has been associated with a range of inflammatory diseases [78,80] and cancers [269,270]. Moreover, there is evidence that ANXA1 is expressed at higher amounts on the T cells of people with autoimmune disease[34].

Psoriatic arthritis (PsA) is an inflammatory disease of the musculoskeletal system associated with cutaneous psoriasis (PsO) in the form of scaly psoriatic plaques[271]. The pathogenesis of PsA is far from understood. However, much research has indicated that the disease process in PsA could be driven by autoreactive T cells, in particular IL-17 producing T helper cells (Th17), which have been implicated in driving the inflammatory response in psoriatic plaques[90,98].

There is no diagnostic test for PsA, resulting in a delay in diagnosis and hence in many cases worsening of disease pathogenesis[111]. Moreover, although treatments have definitely improved over the past few years, there is still no way to predict which treatments are going to give optimal outcomes in each patient and side effects from therapeutic drugs are still plentiful[272]. Thus, there is a need for better biomarkers, treatments and improved ways of predicting response to therapy in PsA.

With the majority of data indicating a role for ANXA1 in inflammatory diseases such as PsA coming from murine studies [73,78,273], it was considered key in the current study to investigate the potential role of this protein and its receptors in PsA using human samples. Changes in expression of ANXA1 and its receptors (FPR1/2) on immune cells from PsA patients were assessed and compared to healthy control cells to identify any potential ANXA1-mediated signalling pathways in PsA. Furthermore, the effects of adding a novel humanised, anti-ANXA1 monoclonal antibody (Mab), MDX-124, (obtained from Medannex Limited) to the identified cell types of interest were explored in terms of modulation of the inflammatory response. This antibody is currently under development as a potential therapeutic and notably, this work will support the development of the antibody.

Given the proprietary nature of the Medannex antibody, it was essential that initial studies were undertaken to investigate its use in the various experimental setups to be employed in the study. Furthermore, in pilot experiments prior to this studentship (unpublished data obtained outside of this project within the Goodyear lab), antibody concentrations were determined, and an observation was made (change in media colour) that suggested that the 100ng/ml working dose of the antibody was potentially affecting cell viability or alternatively, cellular metabolism. Thus, it was important to investigate this observation in further detail and ensure the antibody was not impacting cell viability or key metabolic processes within the cells. The working dose of MDX-124 had been previously optimised as 100 ng/ml during earlier studies within the Goodyear lab, and hence was used in all following experiments.

The research presented in this chapter sought to determine:

1. Characterisation of surface ANXA1 expression levels on immune cells, including:

    - Checking for consistent staining between batches of MDX-124
    - Characterisation of ANXA1 and FPR1/2 surface expression on human immune cell subsets

2. Whether the working (100 ng/ml) dosage of MDX-124 could be affecting key cellular processes including:

    - Cell death
    - Cell metabolomics

3.2 Results

3.2.1 MDX-124 surface staining in animal tissue

To determine the full experimental scope of MDX-124, it was questioned whether this antibody could be used in an alternative setting (i.e., animal models of disease). Focus was placed on determining whether MDX-124 could bind to tissues in animal models of interest for the ongoing pre-clinical development programmes at Medannex, particularly rat and Golden Syrian hamster models.

In the first instance, rat spleen and lymph nodes samples were obtained, and single cell suspensions stained with AF647 fluorochrome labelled MDX-124. An AF647- labelled isotype control antibody was used to define background staining; technical triplicates were also undertaken. The gating strategy is shown in figure 3.1A. Flow cytometric analysis revealed that MDX-124 was able to bind to rat cells (Figure 3.1). In general, spleen single cell suspension preparations stained had an increased level of ANXA1 positive cells (~2% of cells, Figure 3.1B), compared to lymph node single cell suspension preparations (~1%, Figure 3.1C).

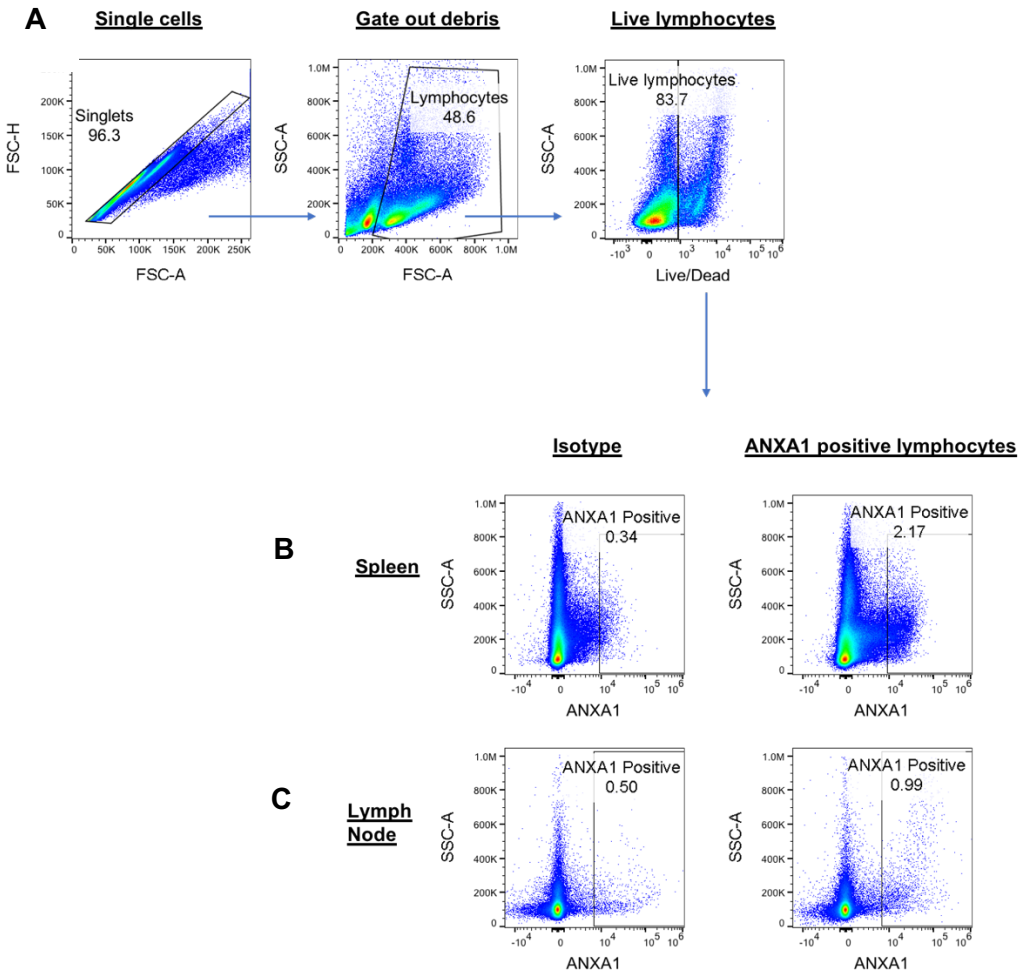

Figure 3.1 MDX-124 binds to rat lymph node and spleen cells

Cells were extracted from a rat spleen and lymph node sample and stained with either an AF647-labelled isotype antibody or AF647- labelled MDX-124 and washed in FACS buffer before running on the BD Attune flow cytometer. (A)Single cells were first gated, debris was gated out (to gate lymphocytes) and then live cells. From live cells, ANXA1 positive spleen and lymph node cells were gated. Representative flow cytometry plots showing ANXA1 positive populations are shown for (B) spleen and (C) lymph node samples. FACS plots were produced using FlowJo software (v10.6.1).

Given the current interest in COVID-related studies and respiratory models of disease, single cell suspension from Golden Syrian hamster tissue (obtained from Viroclinics), was also evaluated. Viroclinics provided spleen, left lung tissue, right lung tissue after lavage with MACs tissue solution as well as lung lavage fluid (bronchoalveolar lavage or BAL) and whole blood in an EDTA tube. An AF647- labelled isotype control antibody was used to define background staining; technical triplicates were also undertaken. The gating strategy is shown in Figure 3.2A. Flow cytometric analysis revealed that MDX-124 was able to bind to CHO cells (Figure 3.2). In general, spleen, lung and washed lung single single cell suspension preparations had a similar % of ANXA1 positive cells (<2%, Figure 3.2B-Figure 3.2D). BAL and whole blood samples had negligible levels of ANXA1 positive cells (<1%).

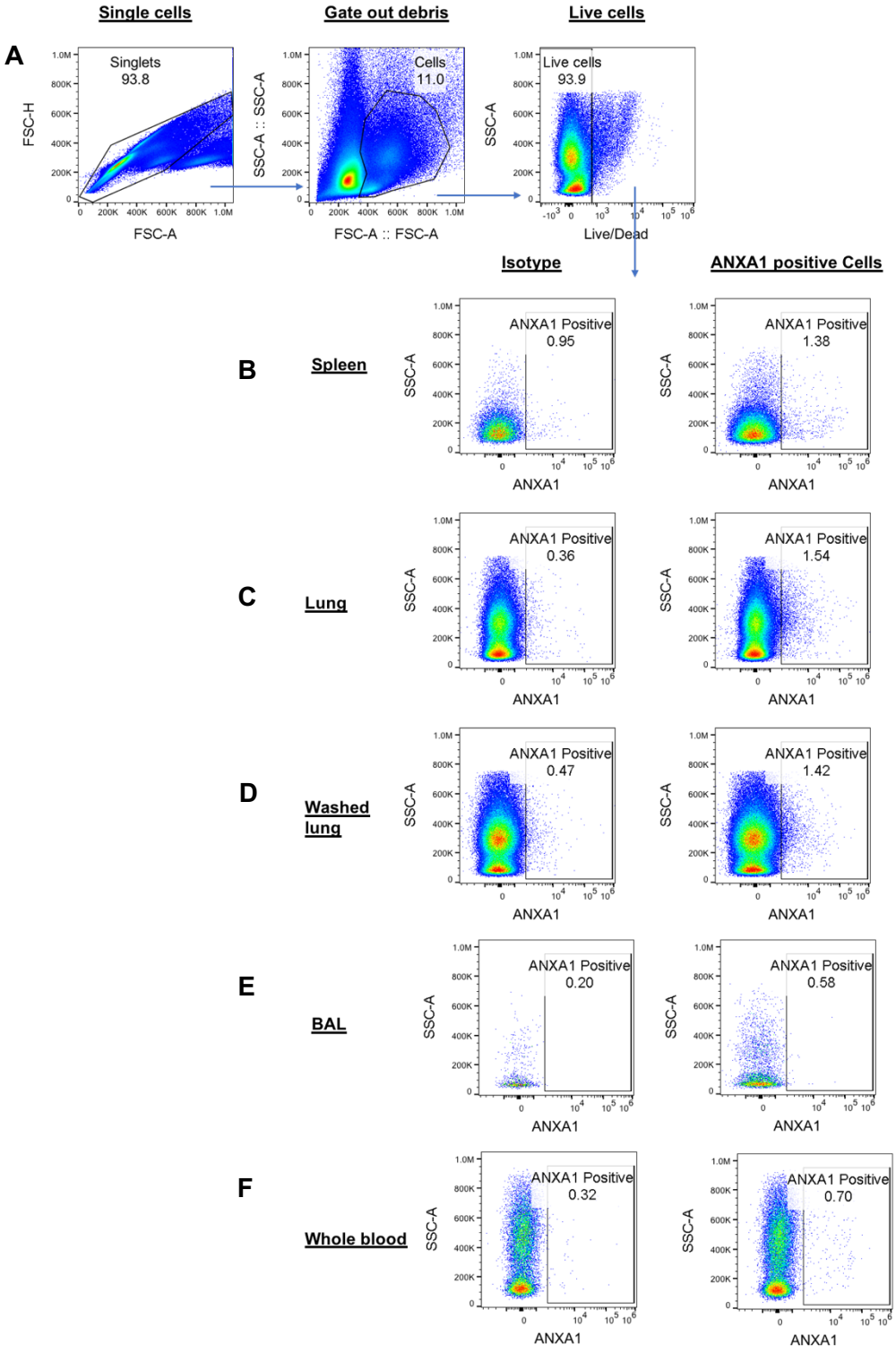

Figure 3.2 MDX-124 binds to Golden Syrian hamster cells

Cells were extracted from a Golden Syrian hamster Lung and spleen samples. PBMCs were isolated from whole blood and stained and BAL was stained as is. Cells were stained with either an AF647- labelled isotype antibody or AF647- labelled MDX-124 and washed in FACS buffer before running on the BD Attune flow cytometer. (A)Single cells were first gated, debris was gated out (to gate lymphocytes) and then live cells. From live cells, ANXA1 positive (B)spleen, (C)Lung (D) Washed lung (E) BAL and (F) PBMCs from whole blood were gated. Representative flow cytometry plots showing ANXA1 positive populations are shown for each of the samples tested. FACS plots were produced using FlowJo software (v10.6.1)

These preliminary results indicated the potential of MDX-124 to bind to rat and CHO tissue cells, however, future experiments are needed to determine if the staining profile in rats is similar to that seen in humans. This would include adding various markers for immune cell subsets (monocytes, T cells, B cells etc). As this was not a main objective of the project, these experiments were not conducted in this study.

3.2.2 MDX-124 batch comparisons

Due to MDX-124 still being in development, conditions such as antibody storage and buffer composition were still being optimised by Medannex (see materials and methods section 2.3 for details on MDX-124 development) and it was important to ensure this did not impact the consistency of results obtained in this study. Moreover, MDX-124 batches were self-conjugated (see materials and methods section 2.3.3), thus, it was vital to ensure staining from separately conjugated batches was consistent.

Initial batches of MDX-124 (Batch 1 and Batch 2) obtained from Medannex were provided in phosphate buffered saline (PBS) and stored at 2-8°C as there was no available data regarding the stability of the antibody during freeze/thaw cycles. These batches were both produced from transient cell lines; however, Batch 1 was stored at 2-8°C and Batch 2 was stored at -20°C long term and at 2-8 °C after conjugation. A third batch (Batch 3) was produced from a stable cell line and was stored at -80°C long term and at 2-8°C after conjugation. Additionally, this batch was stored in a histidine-sucrose buffer rather than PBS and buffer exchange into PBS was required before conjugation of his batch could be carried out. All of these differences in storage conditions made it essential to check comparability of surface staining between batches.

To compare surface binding between MDX-124 batches, PBMCs were stained for ANXA1 expression, alongside CD14 as a monocyte marker. The gating strategy is shown below (Figure 3.3A). Monocytes were used for comparisons based on previous data showing these cells express high amounts of surface ANXA1

compared to other cell types[29], and thus, this would allow for identification of any changes in staining more easily

An initial experiment was performed to evaluate the cell binding activity of MDX-124 from Batch 1. Positive staining was determined in comparison to an appropriate isotype control (Figure 3.3B). MDX-124 from Batch 1 interacted with 99.5% of monocytes. A subsequent experiment evaluated the cell binding activity of MDX-124 from Batch 2 and 3. This enabled the direct comparison of the two batches. This experiment revealed that both batches where able to substantially bind to human monocytes (batch 2 - 99.8% and batch 3 – 98.2% of cells). These data suggested that storage setting did not substantially alter the binding properties of the antibody formulation.

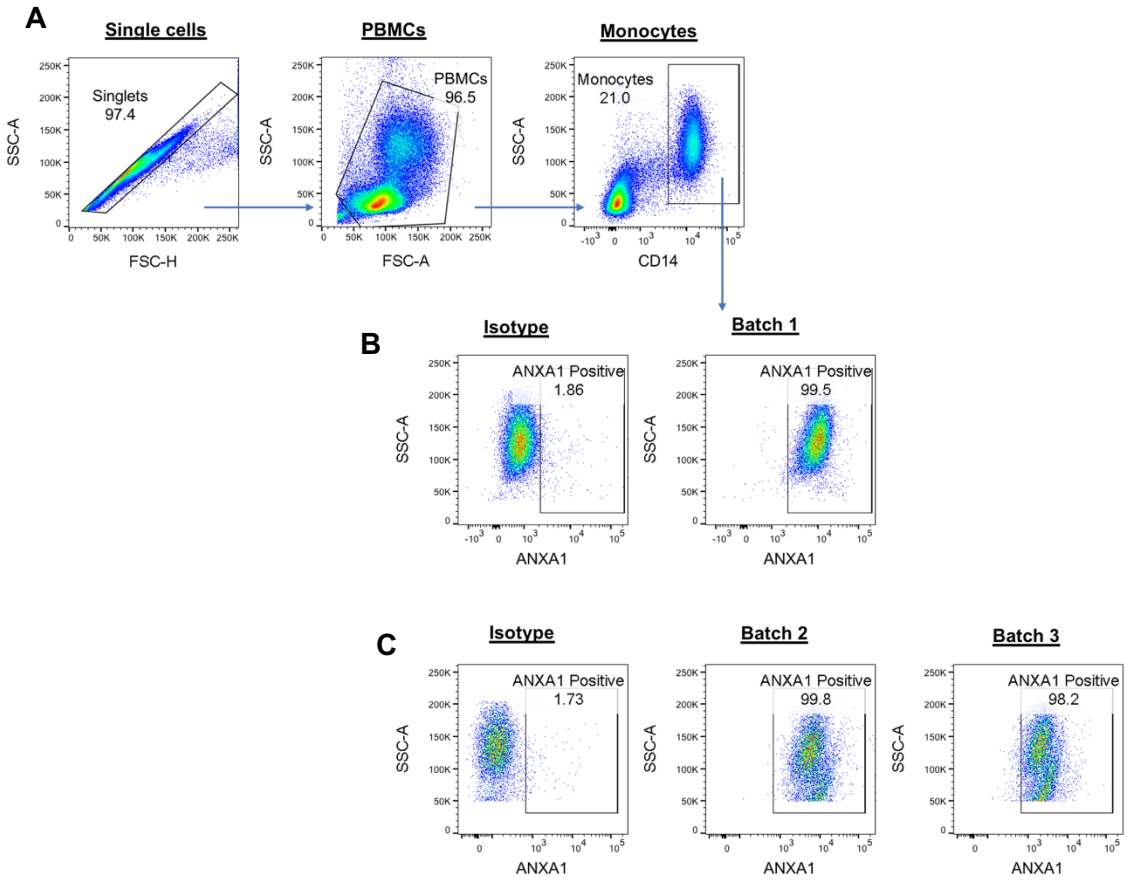

Figure 3.3 MDX-124 batch comparisons

PBMCs were extracted from peripheral blood and stained with anti-CD14 as well as an AF647 labelled MDX-124 or an AF647-labelled isotype control. Cells were washed in FACS buffer before running on the BD Attune flow cytometer. (A) Single cells were first gated followed by PBMCs and then monocytes. MDX-124 surface binding was assessed using (B) Batch 1, (C) Batch 2 and Batch 3. Appropriate isotype controls were used for each experiment. Representative flow cytometry plots showing ANXA1 positive populations are shown for each of the batches tested. FACs plots were produced using FlowJo (v10.6.1) software.

3.2.3 MDX-124 surface staining of healthy human PBMCs

Prior to undertaking a large multiparameter flow cytometric study in patient samples, an initial analysis was performed to characterise MDX-124 and FPR binding to healthy control blood samples. Staining was carried out using fresh blood from two healthy donors. PBMCs were isolated and stained with antibodies against markers of monocyte, B cell and T cell populations alongside MDX-124, anti-FPR1 and anti-FPR2 antibodies. Prior studies have shown that surface ANXA1 expression increases upon activation of cells[29], therefore, staining was assessed in both stimulated (cell stimulation cocktail (80nM PMA and 1.34μM ionomycin per ml), ThermoFisher) and unstimulated cells, to allow better characterisation of ANXA1 expression.

Representative gating strategies for each cell type are shown in Figures 3.4A-D. Expression of ANXA1, FPR1 and FPR2 was evaluated in 2 healthy donors, which showed consistent results. Consistent with the literature[29], the majority of ANXA1 positive cells were monocytes, particularly upon stimulation (Figure 3.4E). The proportion of ANXA1+ $CD14^+CD16^+$ monocytes in particular increased substantially upon stimulation (~6% to ~91%), and the same was evident with $CD16^+CD14^-$ monocytes (~1% to ~65). In general, ANXA1 expression didn't change much upon stimulation of $CD14^+CD16^-$(~5% to ~7%), and $CD14^-CD16^-$ monocytes (<1% to ~2%). FPR1 was abundant on both $CD14^+CD16^+$ and $CD14^+CD16^-$ monocytes. This expression remained the same upon stimulation of $CD14^+CD16^+$(~90% in both groups) and decreased to negligible levels upon stimulation of $CD14^+CD16^-$ monocytes (~86% to <1%). Additionally, the proportion of $CD14^-CD16^+$ $FPR1^+$ and $CD14^-CD16^-$ $FPR1^+$ monocytes was negligible. FPR2 expression was generally low on all monocyte populations assessed, however, increased slightly upon stimulation in $CD14^+CD16^+$(<1% to ~1%), $CD14^+CD16^-$(<1% to ~3%) and $CD14^-CD16^+$(<1% to ~1%), monocytes, with similar expression being evident in $CD14^-CD16^-$(<1%) monocytes in unstimulated and stimulated groups.

The proportion of $CD4^+CD8^+$ $ANXA1^+$ T cells was higher than any of the other T cell populations assessed, which increased substantially upon stimulation (~25% to ~84%) (Figure 3.4F). Likewise, the proportion of ANXA1+ cells increased upon simulation in all of the other T cell subsets assessed.

The proportion of FPR1$^+$ T cells was generally much lower than for ANXA1, however, similarly, the proportion of CD4$^+$CD8$^+$ FPR1$^+$ T cells was higher than any of the other T cell populations assessed, and also increased upon stimulation (~10% to ~15%). FPR2 expression was negligible between unstimulated and stimulated groups on most T cell subsets assessed (Figure 3.4G). CD4$^+$CD8$^+$ T cells expressed more FPR2 than any of the other T cell populations, however this was not evident after stimulation (~1% to 0).

B cell expression of ANXA1, FPR1 and FPR2 was generally low (<3%), however, expression of all proteins increased upon stimulation (Figure 3.4D).

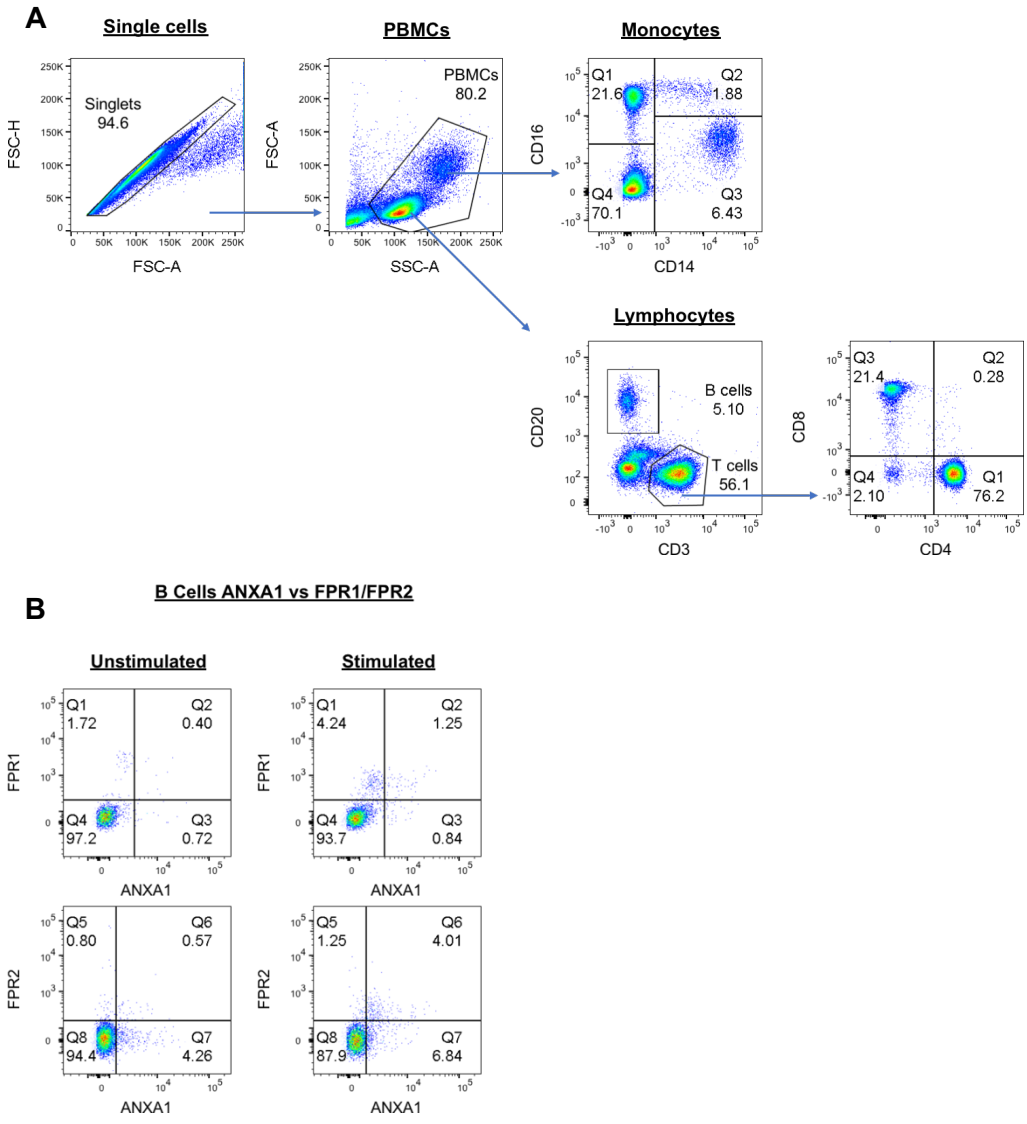

C

CD14+CD16+ monocytes ANXA1 vs FPR1/FPR2

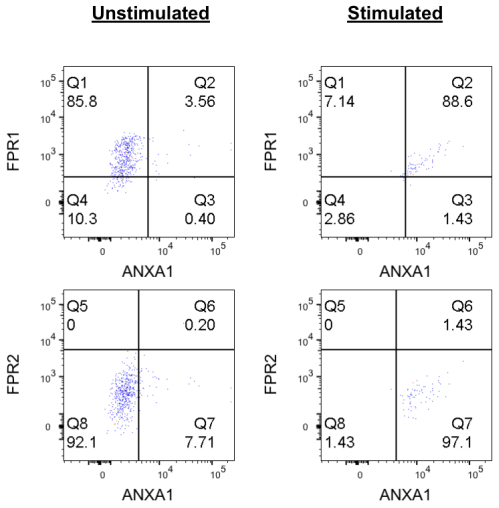

CD14+CD16- monocytes ANXA1 vs FPR1/FPR2

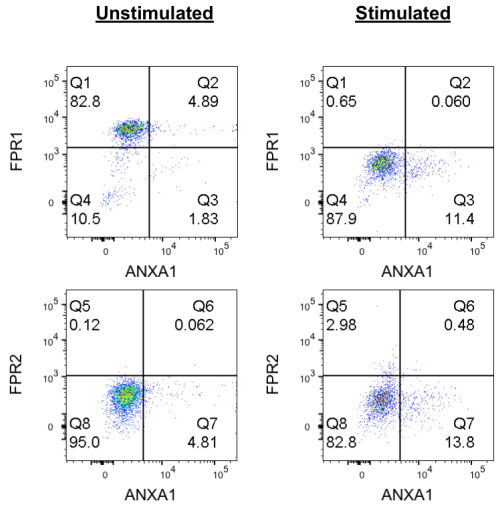

CD14-CD16+ monocytes ANXA1 vs FPR1/FPR2

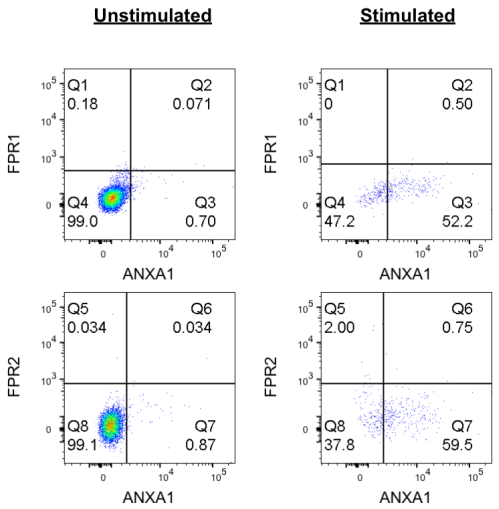

CD14-CD16- monocytes ANXA1 vs FPR1/FPR2

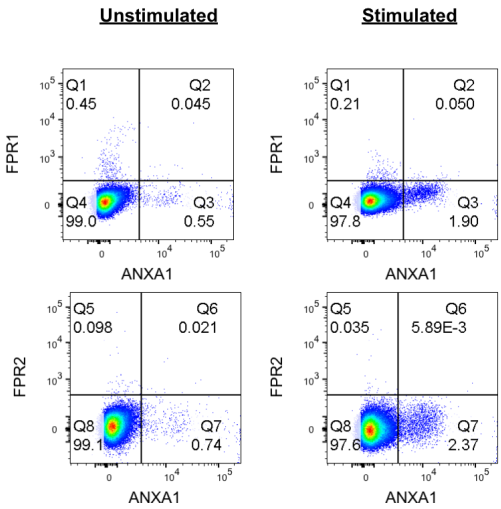

D

CD4+CD8+ T cells ANXA1 vs FPR1/FPR2

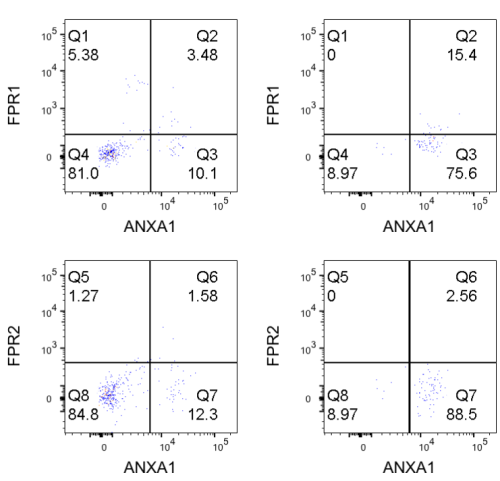

CD4+CD8- T cells ANXA1 vs FPR1/FPR2

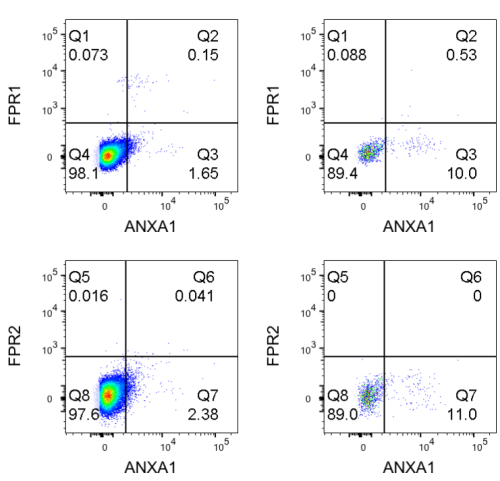

CD4-CD8+ T cells ANXA1 vs FPR1/FPR2

Unstimulated **Stimulated**

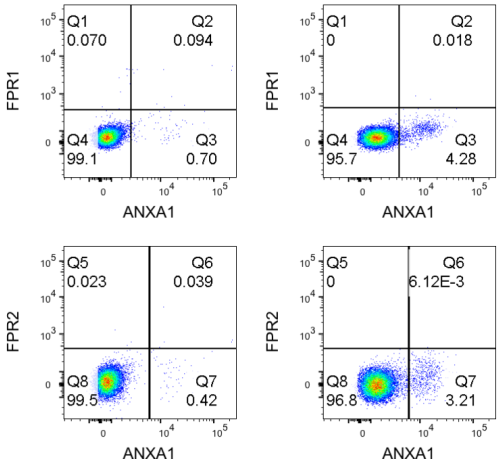

CD4-CD8--T cells ANXA1 vs FPR1/FPR2

Unstimulated **Stimulated**

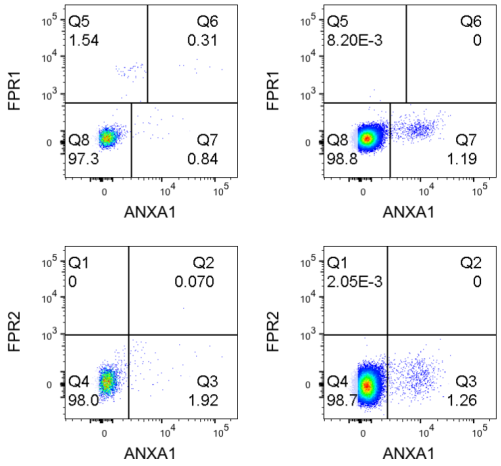

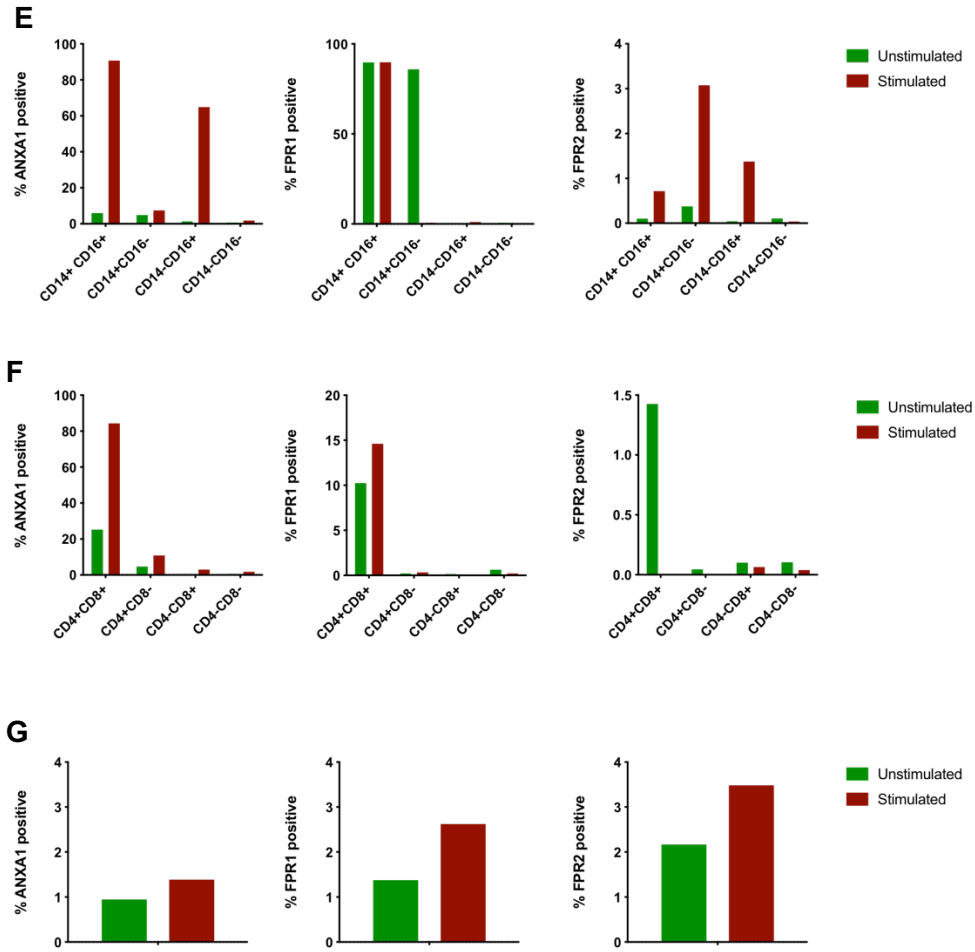

Figure 3.4 Characterisation of ANXA1, FPR1 and FPR2 surface expression in healthy PBMCs

PBMCs were isolated from fresh healthy blood samples and either left unstimulated or stimulated with cell stimulation cocktail (ThermoFisher) for 4 hrs. Cells were stained with antibodies against B cell (CD20), T cell (CD3,CD4,CD8) and monocyte markers(CD14,CD16), alongside MDX-124, anti-FPR1 and anti-FPR2 antibodies. (A) A representative FACs plot showing the gating strategy used. Singlets were first gated followed by PBMCs, then monocytes and lymphocytes(T cells, B cells). Monocytes were further characterised based on their CD14 and CD16 expression, and T cells were further characterised based on their CD4 and CD8 expression. ANXA1, FPR1 and FPR2 expression was characterised between unstimulated and stimulated groups for(B) B cell, (C) monocyte and (D) T cell populations assessed. FACS plots were produced using FlowJo (v 10.6.1) software. Graphs were then produced assessing the mean proportion of ANXA1+, FPR1+ and FPR2+ (E) monocytes, (F) T cells and (G) B cells. N=2 healthy donors. Graphs were produced using GraphPad Prism (v9) software. Statistical analysis was not conducted due to the low N number.

3.2.4 Refinement of PsA flow cytometry panel

Preliminary flow cytometric data on ANXA1 surface expression in PsA was obtained prior to the initiation of the work in this thesis. This study (carried out by Dr Aysin Tulunay-Virlan) involved 6 healthy control and 6 PsA samples and used a previous formulation of MDX-124. Notably, the study did not assess the expression of FPR1 or FPR2. However, there was sufficient data to enable an informed approach for further studies aimed at characterising the expression of ANXA1, FPR1 and FPR2 in PsA (results chapter 4). To achieve this, the previously defined mean fluorescent intensity (MFI) values for ANXA1 expression in monocyte and dendritic cell (DC), B cell and NK cell/T cell and populations were re-interrogated.

MDX-124 was fluorescently labelled in-house by Dr Tulunay Virlan, and so the effects of non-specific binding of the antibody and autofluorescence were taken into account by using an isotype control antibody labelled at the same time, using the same fluorophore (AF647). An isotype control is an antibody of the same isotype as the primary antibody (MDX-124) than is non-specific to the antigen of interest (ANXA1). Delta (Δ) MFI values for each population were then calculated by subtracting the isotype control stains from the ANXA1 stain, to account for non-specific background staining. Heatmaps were produced of the Δ MFI values between healthy control (HC) and PsA samples to allow characterisation of ANXA1 expression in the PsA samples and provide information on which specific cell populations to focus on for further analysis.

Re-analysis revealed that monocyte populations were high expressors of ANXA1 in both PsA and HC samples (Figure 3.5A). In particular, $CD14^{dim}CD16^{+}$ monocytes expressed more ANXA1 in PsA samples (HC mean ΔMFI=15027, PsA mean ΔMFI=19186). Moreover, it was also apparent in the B cell panel that unswitched memory B cells were the highest expressors of ANXA1 (Figure 3.5B), which once again was consistent across both HC and PsA patients (HC mean ΔMFI=893, PsA mean ΔMFI=1350). Evaluation of the T cell panel revealed that $CD4^{+}$ TEMRA and expressed high ANXA1 in HC samples compared to PsA samples (HC mean ΔMFI=36051, PsA mean ΔMFI=8374)

Additionally, Gamma delta (GD) T cells expressed high ANXA1 in HC samples (mean ΔMFI=26317) and moderate levels in PsA samples (mean ΔMFI=6488) (Figure 3.5C).

To further visualise the specific differences in ANXA1 expression in each of monocyte, DC, B cell and T cell populations, individual populations with significant differences between HC and PsA patients were investigated. Notably only T cell populations expressed significantly different ANXA1 in PsA (Figures 3.5D-3.5I). In particular, $CD4^+$ T cell subsets ($CXCR3^-CCR4^+$, T helper (Th)22, Th2 and Th17) and $CD8^+$IL-22 producing T cells (Tc22) from PsA samples expressed significantly less surface ANXA1.

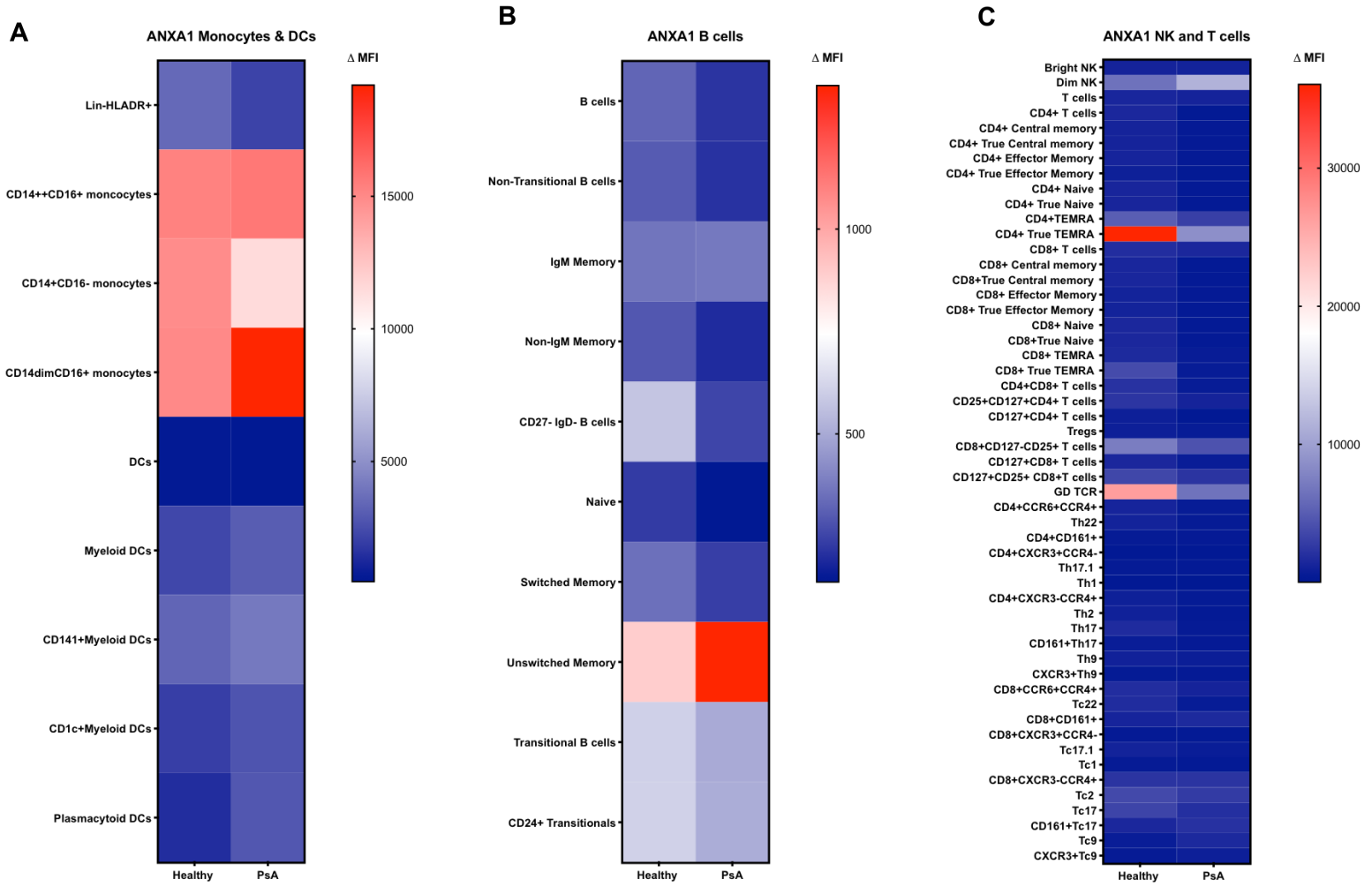
A
ANXA1 Monocytes & DCs
Δ MFI
15000
10000
5000
Lin-HLADR+
CD14++CD16+ moncocytes
CD14+CD16- monocytes
CD14dimCD16+ monocytes
DCs
Myeloid DCs
CD141+Myeloid DCs
CD1c+Myeloid DCs
Plasmacytoid DCs
Healthy
PsA
B
ANXA1 B cells
Δ MFI
1000
500
B cells
Non-Transitional B cells
IgM Memory
Non-IgM Memory
CD27- IgD- B cells
Naive
Switched Memory
Unswitched Memory
Transitional B cells
CD24+ Transitionals
Healthy
PsA
C
ANXA1 NK and T cells
Δ MFI
30000
20000
10000
Bright NK
Dim NK
T cells
CD4+ T cells
CD4+ Central memory
CD4+ True Central memory
CD4+ Effector Memory
CD4+ True Effector Memory
CD4+ Naive
CD4+ True Naive
CD4+TEMRA
CD4+ True TEMRA
CD8+ T cells
CD8+ Central memory
CD8+True Central memory
CD8+ Effector Memory
CD8+ True Effector Memory
CD8+ Naive
CD8+True Naive
CD8+ TEMRA
CD8+ True TEMRA
CD4+CD8+ T cells
CD25+CD127+CD4+ T cells
CD127+CD4+ T cells
Tregs
CD8+CD127-CD25+ T cells
CD127+CD8+ T cells
CD127+CD25+ CD8+T cells
GD TCR
CD4+CCR6+CCR4+
Th22
CD4+CD161+
CD4+CXCR3+CCR4-
Th17.1
Th1
CD4+CXCR3-CCR4+
Th2
Th17
CD161+Th17
Th9
CXCR3+Th9
CD8+CCR6+CCR4+
Tc22
CD8+CD161+
CD8+CXCR3+CCR4-
Tc17.1
Tc1
CD8+CXCR3-CCR4+
Tc2
Tc17
CD161+Tc17
Tc9
CXCR3+Tc9
Healthy
PsA

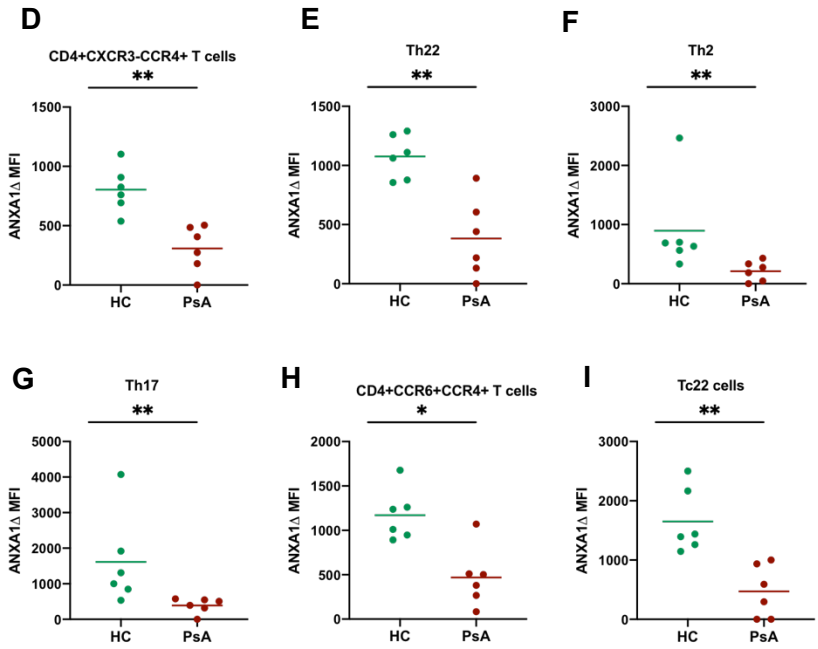

Figure 3.5 Characterisation of ANXA1 surface expression in PsA and HC immune cell populations

ΔMFI data was obtained from Aysin Tulunay Virlan and heatmaps were generated of mean ANXA1 ΔMFIs between HC and PsA samples from (A) monocyte and DCs (B) B cells and (C) NK and T cells. (D-I). Graphs were produced of populations with significantly different ANXA1 expression in PsA compared to HCs. The non-parametric Mann Whitney U test was used to determine significance (appropriate normality tests were carried out to determine which statistical tests to use). Graphs were produced and statistical tests were carried out using GraphPad Prism (v9) software HC N=6,PsA N=6. * $p<0.05$, **$p<0.01$,***$p<0.001$

Based on results indicating that particularly monocytes were high expressors of ANXA1 in both HC and PsA samples, it was decided to continue with markers against these populations in future flow cytometric analysis to further characterise FPR1 and FPR2 expression in PsA. Moreover, differences in expression were evident in both B cell and T cell populations in PsA, therefore it was of interest to keep these populations in future flow cytometry panels. Considering the T cell panel used by Dr.Tulunay-Virlan was an extensive, multi-parameter panel with a considerable amount of markers in it, careful consideration was needed as to which markers to use for future analysis alongside anti-FPR1 and anti-FPR2 antibodies. As differences in ANXA1 expression had primarily been evident Helper ($CD4^+$) and cytotoxic ($CD8^+$) T cell populations, it was decided that focus would be placed on using markers against these populations in future flow cytometric analysis, thus, NK and Treg markers were excluded from future panels (Results chapter 4).

3.2.5 MDX-124 does not induce apoptosis in healthy cells

Preliminary data obtained prior to this project revealed that addition of 100ng/ml MDX-124 to differentiating T helper 17 (Th17) cells was associated with a colour change in the cell media. To ensure that this effect was not due to MDX-124 impacting cell viability, the effects of MDX-124 on cell apoptosis were explored.

An apoptosis assay was conducted using the Annexin V Apoptosis Detection kit (for flow cytometric analysis) (ThermoFisher Scientific). Peripheral blood mononuclear cells (PBMCs) were extracted (see materials and methods section 2.2.1) from healthy control samples and stimulated with phorbol 12-myristate 13-acetate (PMA) to induce apoptosis. Cells were heat killed at 65ºC as positive control for necrosis. As preliminary experiments showing colour changes in the media of MDX-124-exposed cells used T cells, the level of apoptosis in these cells was assessed alongside PBMCs. PBMCs were fluorescently stained for T cell markers (CD3, CD4 and CD8) alongside Annexin V, as a marker of apoptosis and propidium iodide (PI), as a marker of necrosis (the functional significance of these markers is explained in materials and methods section 2.3.4). Initial gating strategies focused on including all cellular debris/dead cells to pick up all of the cells undergoing apoptosis and necrosis (Figure 3.6A), however, this resulted in inconsistent data between experimental replicates (data not shown). To compensate for this confounding factor, the cellular debris was excluded (Figure 3.6B).

The apoptosis assay was first optimised with PBMCs to determine the best dosage and incubation time with PMA to induce the greatest difference in apoptosis/necrosis between unstimulated and stimulated controls. Different dosages (100ng/ml and 50ng/ml) of PMA were trialled alongside different incubation times (4 hours (hrs) or overnight). Compared to the other conditions trialled, an overnight stimulation with 50ng/ml of PMA resulted in the greatest increase in both early and late apoptotic cells in the stimulated samples compared to unstimulated controls (Figure 3.6C). This condition was therefore used for subsequent experiments.

Analysis of data from 6 healthy donors indicated no significant difference in the % of cells in early apoptosis, late apoptosis and necrosis between MDX-124 treated and untreated cells, amongst each of the cell populations analysed. In general, $CD8^+$ T cells and $CD4^-$ $CD8^-$ double negative (DN) T cells exhibited great survival compared to $CD4^+$ and $CD4^+CD8^+$ double positive (DP) T cells, independent of MDX-124 addition (Figure 3.6D). All in all, this data suggested MDX-124 was not impacting cell viability, thus, it was decided that further investigations were needed into the cause of MDX-124-associated colour changes in cell media in preliminary studies.

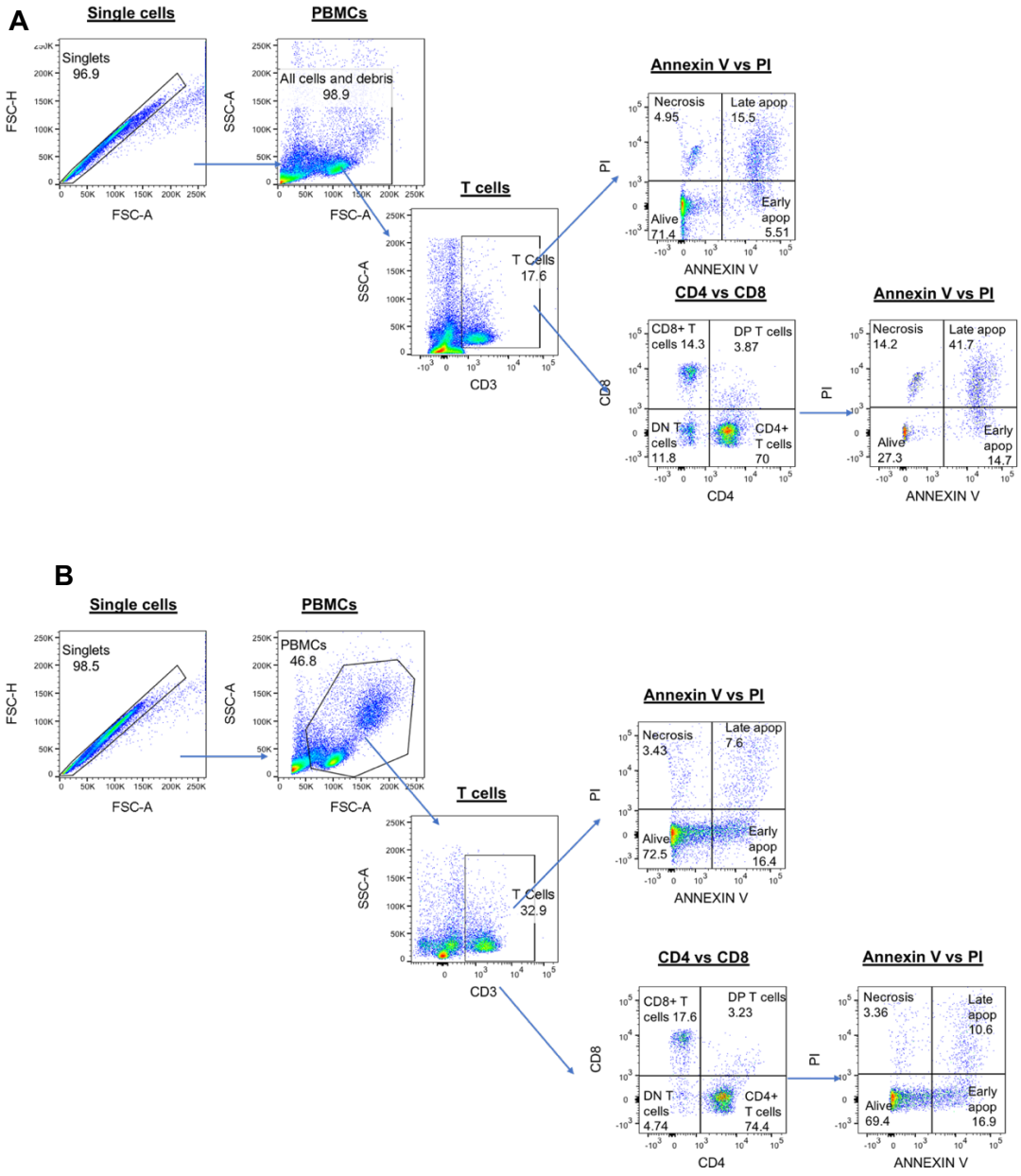

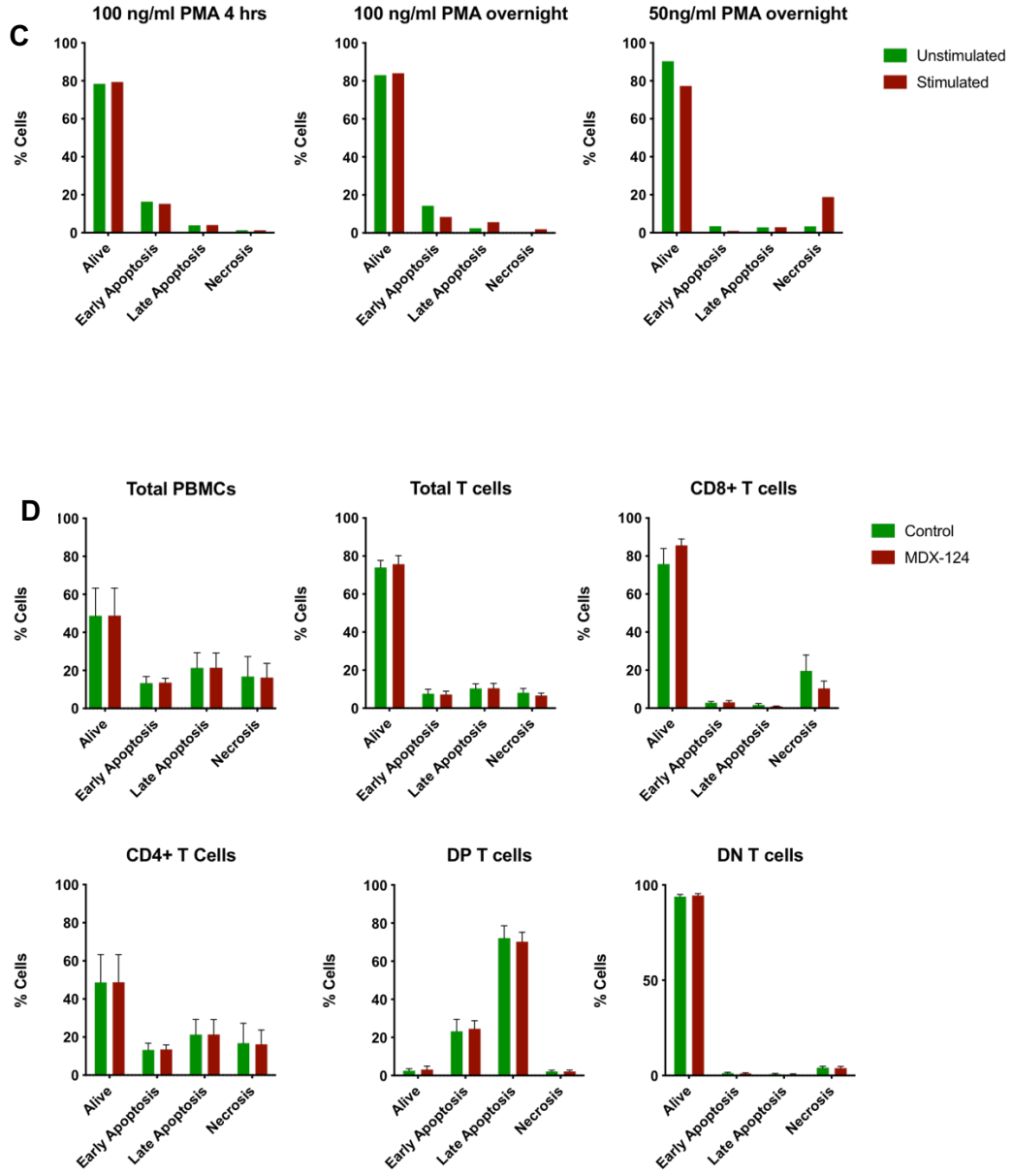

Figure 3.6 Apoptosis assay

Cells were stimulated with PMA to induce apoptosis and stained for T cell markers (CD3, CD4 and CD8) alongside Annexin V as a maker of apoptosis and PI as a marker of necrosis. Appropriate FMO controls were used for gating. (A)Initially all cells and debris were gated but this resulted in inconsistent data between experimental replicates. (B) Debris were excluded from the gating strategy, which included gating single cells, whole PMBCs, T cells and CD4/CD8 T cell populations. Total PBMCs, total T cells and each individual T cell population were gated for Annexin V and PI. FACs plots were produced using FlowJo (v 10.6.1) software. (C)During optimisation of the assay cells were stimulated with 100ng/ml PMA for 4 hrs, 100ng/ml PMA overnight or 50ng/ml PMA overnight. 50ng/ml of PMA overnight was selected as the optimal condition for future experiments. (D) Total PBMCS, total T cells, CD8+ T cells, CD4+ T cells, DP T cells and DN T cells were assessed for levels of apoptosis and necrosis. Cells were heat killed at 65ºC as positive control for necrosis. N=6 buffy coat donors. Statistical tests and graphs were produced using GraphPad Prism (v9) software. A non-parametric Multiple Wilcoxon test was used to determine significance (appropriate normality test were used to determine which statistical test to use).

3.2.6 Assessment of the effects of MDX-124 on cellular metabolism

Another theory for the media colour change in T cells incubated with MDX-124 was that this antibody could be affecting cellular metabolism. Indeed, manipulation of ANXA1 expression has been shown to effect the metabolome in tumour cells[274]. To investigate this, a mito-stress assay was carried out. Initial experiments were carried out on purified monocytes due to known increased expression of ANXA1[29].

The mito-stress assay is performed using various modulators of respiration and is interpreted based on measurements of mitochondrial respiration using the oxygen consumption rate (OCR) and glycolysis using the extracellular acidification rate (ECAR) in live cells provided by the Seahorse XF Analyzer (Agilent) [255].Different parameters are also calculated from the OCR graphs produced, giving information on mitochondrial function. By measuring each of these parameters, the ability of MDX-124 to impact mitochondrial function (as well as cellular glycolysis) was assessed (see methods and materials section 2.3.5 for more information on interpretations of different parameters).

An initial experiment was conducted assessing the effect of MDX-124 on cell metabolism when run at two different concentrations (the working concentration of 100ng/ml and 1000ng/ml). The same volumes of the antibody diluent (PBS) as antibody were added for each concentration and used as vehicle controls. Unstimulated control cells were also used. Unfortunately, in the initial experiment, because different volumes of PBS had to be added to control for the amount of antibody stock added to the assay, this revealed that a 10-fold increase in PBS had a dramatic impact on OCR values. Furthermore, it should be noted that the addition of any volume of PBS (i.e., 1µl) was sufficient to modulate OCR profiles compared to unstimulated cells (Figure 3.7A).

Due to the controls showing differing results, OCR-defined parameters were not calculated compared to unstimulated or between the antibody concentration. A subsequent mito-stress assay was carried out that used dilutions that were optimised to add the same volumes of antibody and PBS to the wells for both 100ng/ml and 1000ng/ml of MDX-124(1µl). The OCAR and ECAR graphs are shown

in Figure 3.7B. To investigate whether comparison of appropriate vehicle to antibody concentration revealed anything, a limited analysis for OCR-define parameters was conducted. This revealed that in both instances' addition of MDX-124 resulted in an increase in all of the OCR parameters calculated, however, 100ng/ml of MDX-124 was associated with a more substantial increase compared to PBS controls (Figures 3.7D-H). This experiment was run on one biological sample and unfortunately due to the COVID-19 pandemic, no additional repeats were obtained for statistical analysis to determine if the results are significant between donors. however, statistical tests were conducted between technical replicates ran for each OCR measurement. Analysis of technical replicates revealed that 100ng/ml of MDX-124 was associated with a significant increase in both basal and maximal respiration and spare respiratory capacity compared to PBS controls. This suggests that MDX-124 could be affecting cellular respiration, however, this is only data from one donor, and conclusions cannot be drawn until sufficient repeats are acquired.

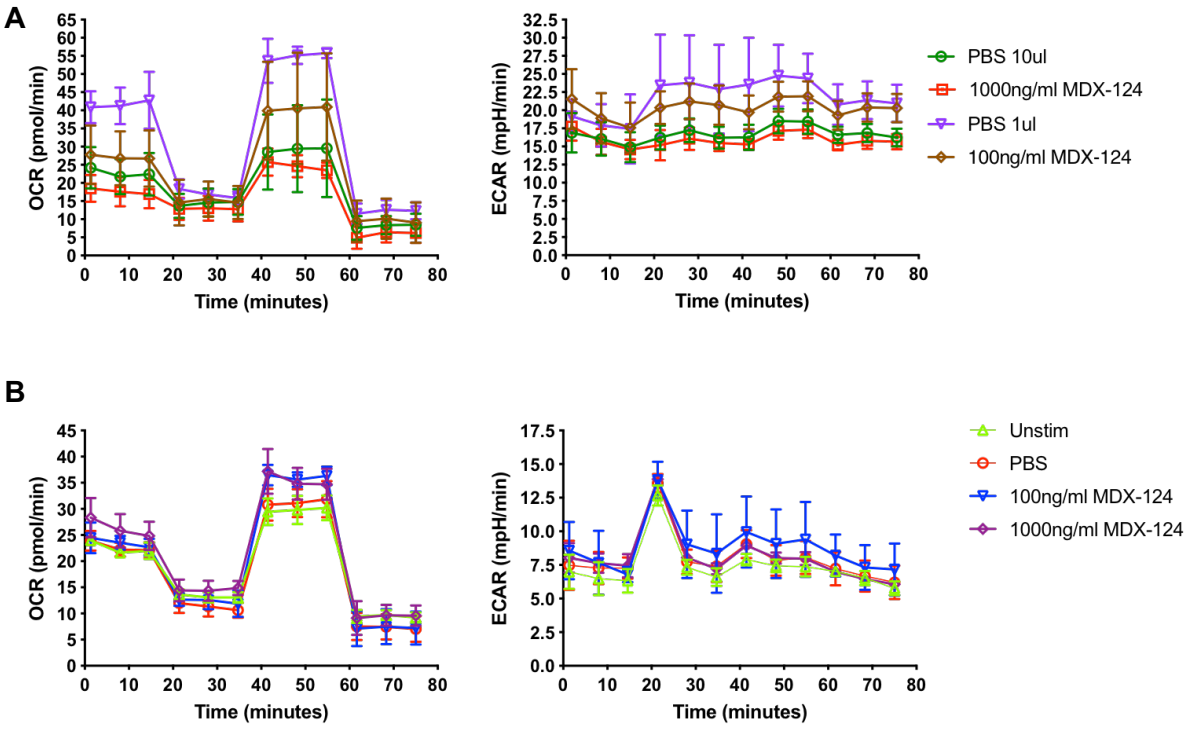

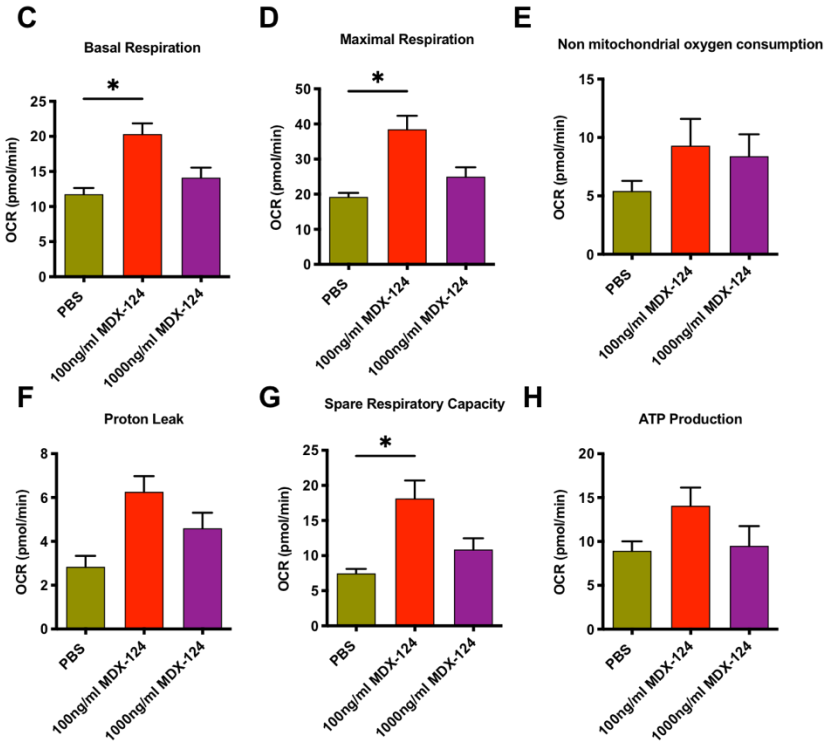

Figure 3.7 100ng/ml MDX-124 may affect cellular respiration

PBMCs were isolated from whole blood, followed by isolation of monocytes. Monocytes were plated and incubated overnight at 37°C. Cells were then treated with 100ng/ml or 1000ng/ml of MDX-124 for 4 hours the next day, prior to analysis with the seahorse machine. Initial experiments used the same volume of PBS as MDX-124 (1µl for 100ng/ml and 10µl for 1000ng/ml). Different volumes of PBS had a substantial effect on OCAR values. (B)PBS control and antibody volumes were standardised so that the same volume of each dilution was added to the respective wells. Graphs showing (A) OCR (B) ECAR (C) basal respiration rate (D) maximal respiration, (E) non-mitochondrial oxygen consumption rate, (F) proton leak, (G) spare respiratory capacity and (H) ATP production data calculated from OCAR values is shown. N=1 donor represented with 4 technical repeats. * $p<0.05$, ** $p<0.01$, *** $p<0.001$ compared to PBS control samples. Statistical significance was determined using a non-parametric Friedman's test. Graphs were produced using GraphPad Prism (v9) software.

3.3 Discussion

MDX-124 is currently being developed as a therapeutic antibody in diseases in which ANXA1 is implicated in the pathogenesis, particularly in autoimmunity and cancer. Therefore, MDX-124 needed to go through all of the optimisation stages required for therapeutic antibody production.

When optimising a therapeutic antibody for use there are several factors that need to be considered in terms of storage. The antibody needs to be stored in the correct buffer, at the correct temperature and in the correct conditions to allow for maximum stability and immunogenicity[275]. Medannex selected PBS as a storage buffer for their humanised MDX-124, primarily because it is widely available and frequently used as a buffer for therapeutic antibodies due to its neutral pH and compatibility with a range of methods[249,276]. Long-term storage of therapeutic antibodies between -20 and -80°C is common, due to improved stability and reduced microbial contamination, however, with certain antibodies protein aggregation and destabilisation can occur[277]. Therefore, initial batches of MDX-124 were also store at 2-8°C, until the stability of MDX-124 at lower temperatures was determined (batch 1, figure 3.3).

Initially MDX-124 was produced through a transient expression method in mammalian cells. This method is common for small scale production of antibodies during initial screening checks. However, due to the nature of mammalian cells, this can lead to heterogeneity between batches[245]. Long-term storage of this batch at -20°C was determined as stable (batch 2, figure 3.3) through various quality control (QC) assays carried by Medannex (see material and methods section 2.3.2 for details).

As MDX-124 was developed, it transitioned from being produced by a transient cell line (mammalian cells), to more a stable expression method in Chinese hamster ovary (CHO) cells. CHO cells are widely used for the production of therapeutic antibodies due to their ability to produce correctly folded, stable proteins in a cost-efficient manner, with minimal heterogeneity between batches[245]. In order to produce MDX-124 in these CHO cells, Medannex had to carry out specialised stability studies, which required the antibody to be stored

in a histidine-sucrose buffer. The concentration of the antibody was also raised to a higher concentration than previously used (from 10mg/ml for initial batches to 30mg/ml) as studies carried out by Medannex showed that storage at this concentration was more suited to the clinic and also to distribution. This batch of MDX-124 was stored at -80°C long-term (see materials and methods section 2.3.2 for details on stability studies).

All batches of MDX-124 were stored in the fridge after conjugation. It is typically essential for the antibody conjugation process to occur in a buffer free of primary and secondary amines. Notably, histidine, which is part of the MDX-124 storage buffer, is an amino acid that contains secondary amines[248], and is therefore not compatible with the conjugation process. To overcome this issue, proteins are frequently buffer-exchanged into PBS before conjugation[249]. A buffer exchange was therefore carried out on MDX-124 produced from the CHO cell line mentioned above, and the antibody was placed in PBS before labelling with AF647 (Batch 3, figure 3.3).

Antibody-based therapeutics have the ability to trigger strong, sometimes unwanted, immune responses in human recipients. This can sometimes be due to off-target binding[278]. It is therefore vital that results remain consistent throughout the antibody testing process, as well as throughout preliminary studies, both for safety and efficacy purposes[249]. As storage conditions of antibodies and conjugated proteins can impact the results of biological assays, the comparability of binding of different MDX-124 batches was assessed. Surface staining showed no difference in the percentage of ANXA1 detected using the different batches of MDX-124, indicating that results of flow cytometry staining experiments between different MDX-124 batches could be comparable in these preliminary studies (Figure 3.3).

Previous research on ANXA1 has shown that under resting conditions, ANXA1 is primarily expressed intracellularly in innate immune cells such as monocytes and neutrophils, with lymphocytes expressing it at lower levels. Research has also shown that ANXA1 translocates to the cell membrane upon cellular activation, where it can mediate its biological effects though the FPRs.[29]. Reproducibility of scientific data is fundamental for conducting successful scientific research.

Initial staining experiments were carried out with MDX-124 to characterise ANXA1 expression on immune cells and see if we could reproduce what has been shown in the literature, both for comparability but also to give us some preliminary data for deciding on future flow cytometric panels. Consistent with previous research, we showed that ANXA1 surface expression increased upon cellular activation, with activated monocytes showing generally higher ANXA1 surface expression compared to other cell types (Figure 3.4). This indicated that MDX-124 was binding appropriately and detecting the expected proportions of ANXA1 in the assessed cell types under resting and stimulated conditions.

Flow cytometric analysis has provided vital in the detection of PsA specific cell types, and more recently, in profiling immune cells to discriminate between PsA and PsO patients[279]. I wanted to use flow cytometric techniques to profile immune cells in PsA in terms of both their ANXA1 and FPR expression to see if I could identify any differences compared to HC cells. Flow cytometric analysis requires careful interpretation and selection of specific cellular markers to focus on. In order to narrow down which cell types to focus on in PsA as well as narrow down the amount of antibodies used in the panel due to cost constraints, analysis of previous flow cytometric data from PsA samples was carried out. Analysis of previously obtained data identified cell populations including monocytes, unswitched memory B cell and GD T cells as high expressors of ANXA1 in both HC and PsA samples and showed significantly reduced expression of ANXA1 in several T cell populations (Figure 3.5). This provided valuable information on which cell types to focus on and therefore, which antibodies to include in future flow cytometry panels (Results chapter 4).

Therapeutic antibodies can affect a range of biological processes, from apoptosis, to cell metabolism[280,281]. Colour changes had been observed in the cell media upon addition of MDX-124 to healthy cells (previous data in the Goodyear group). And although, this could have been due to the effects of MDX-124 on various cellular processes, we wanted to ensure that this was not due to the antibody killing healthy cells. Results from the apoptosis assay indicated that 100ng of MDX-124 did not appear to be inducing apoptosis in healthy PBMCs and provided reassurance that the antibody was not impacting cell viability (Figure 3.6).

Results from the apoptosis assay prompted further exploration into what effects MDX-124 could be having on cellular function. Changes to pH can cause colour changes in cellular media[282], and additionally, changes in cellular metabolism can induce changes in pH[283]. Therefore, we decided to explore if MDX-124 could induce any changes to cellular metabolism. Data from this project suggested that 100ng of MDX-124 could impact cellular metabolism through enhancement of mitochondrial respiration (Figure 3.7). Mitochondrial respiration is the most prominent source of cellular energy in the form of adenosine triphosphate (ATP)[284]. This is also reflected in our data showing increased ATP production in MDX-124-treated cells. One explanation could be that MDX-124 could somehow enhance the proliferation in these monocytes, therefore increasing their energy demand and ATP production, as is seen in rapidly proliferating cells in diseases such as cancer [285]. Moreover, studies have shown that ANXA1 can play a role in reducing cellular proliferation through interaction with the ERK signalling pathway. Therefore, it is not entirely surprising that manipulating the activity of ANXA1 with MDX-124 could enhance proliferation[286]. It is important to note that only one donor was assessed for metabolic changes, therefore, no conclusions can be drawn from this data, but preliminary results do prompt further investigation into effects of MDX-124 on cellular metabolism.

It is worth highlighting that a limitation of the project was that we were unable to assess batch comparability of MDX-124 with every single assay conducted in the project to ensure results through the PhD project were entirely comparable. This was due to project time constraints that were only made worse by the COVID-19 pandemic. Furthermore, prior experiments conducted by Dr Tulunay-Virlan used a different batch of MDX-124 than used in any of the experiments in this study, which doesn't necessarily mean that experiments with future batches will produce the same results.

Other limitations are that, as is the case with many therapeutics, we are not entirely certain how MDX-124 works, which means that it could be triggering certain pathways we are unaware of, leading to unwanted (potentially detrimental effects). Based on experimental data both from Medannex and from this project (Chapter 4), it is believed that MDX-124 works by blocking

extracellular ANXA1 and preventing it from carrying out its function via the FPRs. However, further analysis is needed to confirm this.

In summation, data presented in this chapter has provided valuable information on the consistency and range of MDX-124 binding and provided some information on what metabolic pathways MDX-124 could be inducing in healthy cells. Furthermore, surface staining experiments with MDX-124 allowed characterisation of ANXA1 and FPR expression in several immune cell types. This has in turn, shaped the focus of subsequent studies in this project by highlighting which immune cell subsets to focus on for analysis of the role of ANXA1 and the FPRs in PsA.

Chapter 4 Annexin A1 and the Formyl peptide receptors in inflammatory disease

4.1 Introduction

Inflammation is a normal defence mechanism of the immune system and can be triggered by a variety of factors, including pathogens, toxins and damaged cells[287]. Under normal circumstances, once the stimulant is cleared, the inflammatory response arrests. However, in the case of inflammatory disease, the inflammation persists, which can lead to multi tissue and organ damage[288].In the case of autoimmune inflammation, the target is the body's own cells; the immune system begins to attack healthy tissues. Autoimmune diseases can be systemic (e.g systemic lupus erythematosus, SLE) or tissue specific (e.g multiple sclerosis, MS).

The exact cause of the autoimmune process is unknown, however, suggested triggers include genetics and environmental factors such as UV radiation, stress and diet[289,290]. The pathogenesis of several autoimmune diseases has been linked with dysregulated activity of key signalling proteins, one of which is the immunomodulatory protein, Annexin A1 (ANXA1). ANXA1 is a glucocorticoid (GC) induced protein and has been associated with innate[67] and adaptive[70,149] immune cell dysregulation in several inflammatory diseases. Moreover, the FPR receptors through which ANXA1 signals have also been implicated in inflammatory disease[70,72].

On the cellular level, adaptive immune cells such as T cells and B cells are thought to be key players in the autoimmune process. In particular, uncontrolled activation of IL-17 producing T helper (Th17) cells have been implicated in several autoimmune and inflammatory diseases[74,273,291]. It is suggested that IL-17 triggers an upregulation in expression of several inflammatory genes through the activation of transcription factors such as NF-κB and hence causes prolonging of the inflammatory process[292]. To illustrate a role for ANXA1 in this process, studies have shown that ANXA1$^{-/-}$murine models of experimental autoimmune encephalomyelitis (EAE), had a reduced Th17 profile compared to wild type mice[149]. Moreover, ANXA1-overexpressing transgenic mice had increased inflammation and accumulated Th17 cells in inflamed tissues compared to wild

type mice[293]. Additionally, B cells can enhance the autoimmune process through several cellular processes such as secretion of self-reactive (auto) antibodies, autoantigen presentation and secretion of inflammatory cytokines[294]. Increased levels of ANXA1 autoantibodies are evident in patients with inflammatory bowel disease (IBD) and SLE, suggesting a potential role for ANXA1 in B cell-mediated inflammation.

PsA is an immune mediated, chronic, inflammatory form of arthritis, associated with cutaneous psoriasis (PsO)[295]. Psoriasis pathogenesis is believed to be mediated through interactions between T cells, dendritic cells and keratinocytes in the lesional skin[98]. Increased numbers of activated macrophages have also been observed in the PsO lesional skin[296]. Moreover, the PsA synovial fluid (SF) has been shown to be dominated by activated macrophages and monocytes, particularly intermediate ($CD14^+CD16^+$) monocytes[297].

The initiation and perpetuation of the inflammatory response in the skin to the inflammation in the joints in PsA is not very well understood. Initial theories have suggested monocyte-derived TNF-α as the link between PsO and PsA, but more recently, focus has been on IL-17 and its associated pathways in combination with this TNF-α activation[298–300].

Despite advances in PsA therapeutics , there is still no clear method to predict treatment outcomes, and side effects can be plentiful [272], Moreover, there are no approved diagnostic tests for PsA, which can drastically impact prognosis[111].Therefore, better diagnostic and prognostic biomarkers as well as therapeutic targets, are needed for PsA. To tackle this, a better understanding of what is happening with the immune system activation and regulation in PsA is required.

As PsA is a disease associated with dysregulated inflammation, and ANXA1 has been implicated in similar diseases, it was key to understand if ANXA1 (and its receptors) could also play a role in PsA. Moreover, with most of the evidence of a role for ANXA1 in inflammatory disease being from mouse models[73,78,273], the primary focus of this work was on human samples to provide a further understanding of ANXA1 in PsA.

The research presented in this chapter sought to determine:

1. Whether expression levels of ANXA1 and its receptors (FPR1/FPR2) are altered in PSA compared to HC samples, including:
    - Analysis of gene expression using RNA sequencing data
    - Cell surface expression analysis via flow cytometry
    - Plasma protein analysis via ELISA

2. The effects of blocking ANXA1 expression using a novel anti-ANXA1 monoclonal antibody (MDX-124) on the inflammatory response in both cell lines and primary cells, including:
    - Cell surface expression analysis via flow cytometry
    - Analysis of inflammatory cytokines in supernatants via ELISA

4.2 Results

4.2.1 RNA sequencing analysis of ANXA1 and FPRs in PsA skin

PsA is a heterozygous disease, occurring in around 30% of psoriasis patients[301], but the relationship between skin and joint pathology in this disease is far from understood. The focus of this project was to understand whether ANXA1 or any of its receptors could play a role in the skin pathology in PsA. RNA sequencing data was obtained from samples taken from healthy control (HC) skin, PsA lesional skin (PsA L) and PsA uninvolved skin (PsA U). This data was obtained from another researcher within the School of Infection and immunity, Hanna Johnsson (see materials and methods section 2.6.1 for normalisation details). The raw and processed sequencing data is available on the Gene Expression Omnibus (GEO), under accession GSE205748.

Reanalysis of RNA sequencing data showed that there were no significant changes in expression of the *ANXA1* gene in PsA skin biopsies compared to HCs (Figure 4.1A). However, gene expression of the ANXA1 receptors, *FPR1* and *FPR2* was increased in the PsA L skin compared to HC skin (Figures 4.1B and 4.1C). There were no significant differences in expression of these receptors between the PsA U group and any of the other groups. One PsA L sample expressed significantly more *FPR1* and *FPR2* than the rest of the samples and was identified as a potential outlier. Removal of this sample did not impact the significance of the results shown in figure 4.1 but did skew future correlation analysis in a potentially unreliable way. Taking this into account, the sample was removed from analysis.

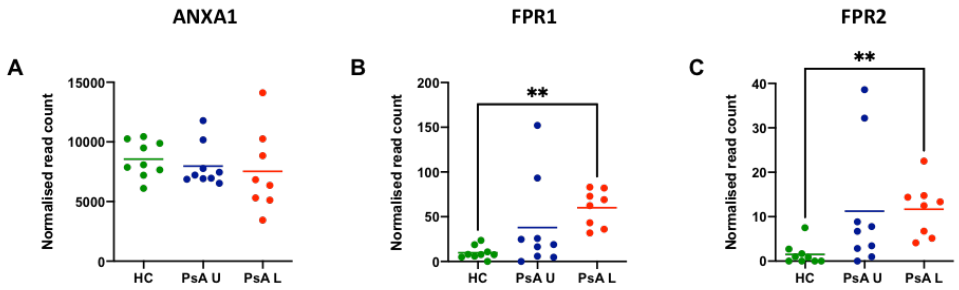

Figure 4.1 FPR1 and FPR2 genes are expressed at significantly higher levels in PsA lesional skin

Graphs showing normalised read counts of (A) *ANXA1*, (B) *FPR1* and (C) *FPR2* gene expression data from HC, PsA U and PsA L groups. Mean expression values and individual sample values are shown. Graphs were produced using GraphPad prism (v9) software. The non-parametric Kruskal-Wallis test was performed to determine statistical significance of the data (appropriate normality tests were carried out to determine if a non-parametric test should be used). HC, PSA U N=9, PsAL=8.

Having observed that FPR1 and FPR2 were upregulated in the PsA lesional skin, it was important to define the overall transcriptional profile of these samples and how this might correlate with the increased FPR1 and FPR2 levels. Differential gene expression analysis was conducted by Hanna Johnsson and a series of significance values and respective fold changes were provided for analysis. In total, there were 2151 significantly upregulated (log10p<0.05 and log2fold >1) and 4094 significantly downregulated (log10p<0.05 and log2fold <-1) genes in the PsA L skin compared to HC skin (Figure 4.2A). Significantly upregulated and downregulated genes are summarised in the volcano plot in figure 4.2B. Highlighted are the top 5 upregulated and downregulated genes (with the lowest adjusted P value).

To identify biological pathways that are enriched within the group of differentially expressed genes identified in the PsA L skin, gene enrichment analysis was conducted using the ClusterProfiler programme on R studio. Dot plots were produced of enriched biological pathways involving upregulated (Figure 4.2C) and downregulated (Figure 4.2D) genes in the PsA L skin.

Genes that were significantly upregulated in the PsA L skin were enriched in key pathways relevant to PsA pathogenesis, including lymphocyte activation and adaptive immunity (Figure 4.2C). Significantly downregulated genes were involved in pathways related to muscle regulation and contraction (Figure 4.2D). This supports previous research suggesting a role for these pathways in PsA pathogenesis which showed that pathways involving muscle contraction were

enriched in PsA peripheral blood samples[302]. A list of enriched genes in each pathway in figure 4.2C and 4.2D is shown in supplementary tables 1 and 2 (see appendix).

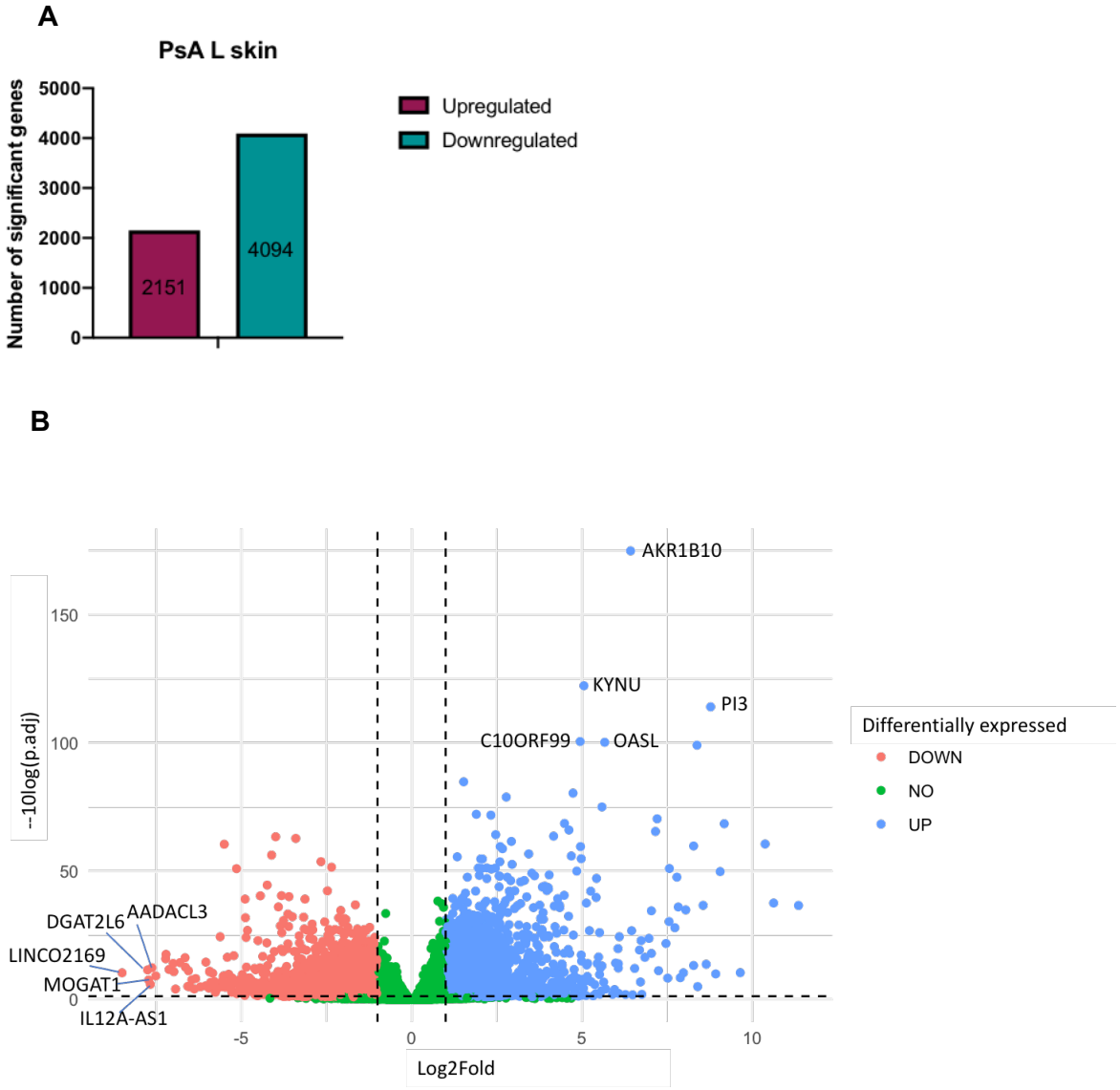

C

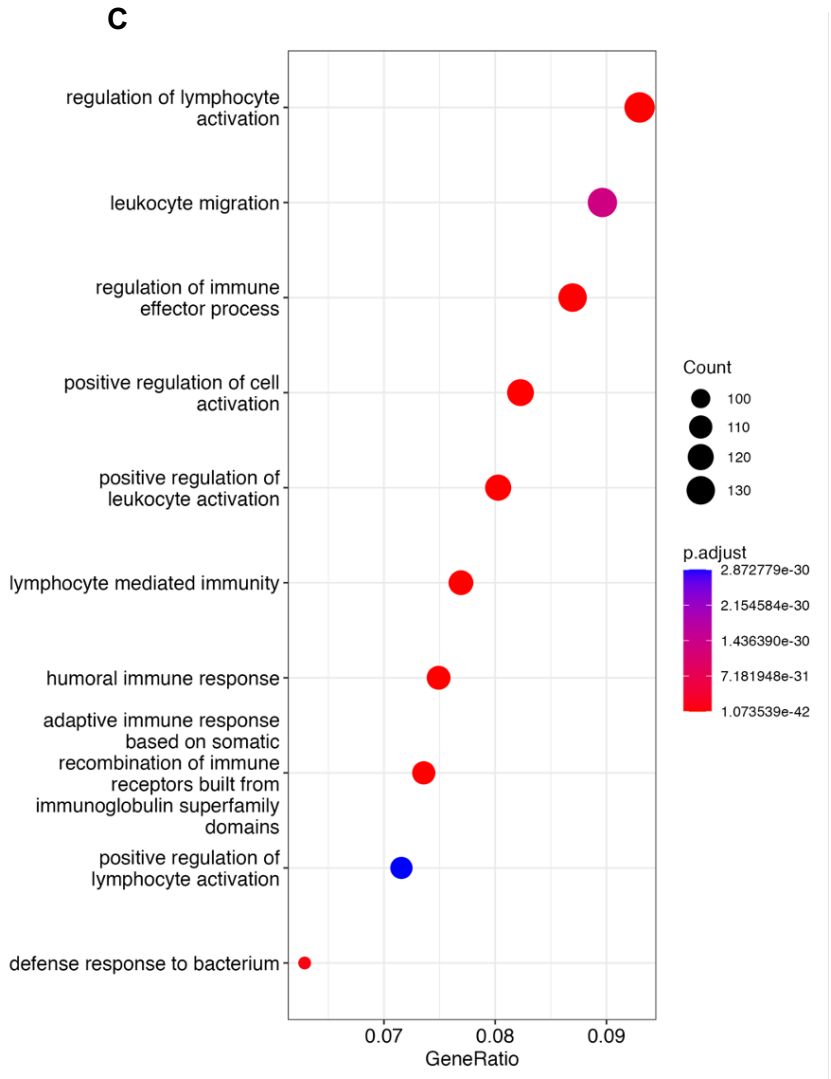
regulation of lymphocyte activation
leukocyte migration
regulation of immune effector process
positive regulation of cell activation
positive regulation of leukocyte activation
lymphocyte mediated immunity
humoral immune response
adaptive immune response based on somatic recombination of immune receptors built from immunoglobulin superfamily domains
positive regulation of lymphocyte activation
defense response to bacterium
0.07
0.08
0.09
GeneRatio
Count
100
110
120
130
p.adjust
2.872779e-30
2.154584e-30
1.436390e-30
7.181948e-31
1.073539e-42

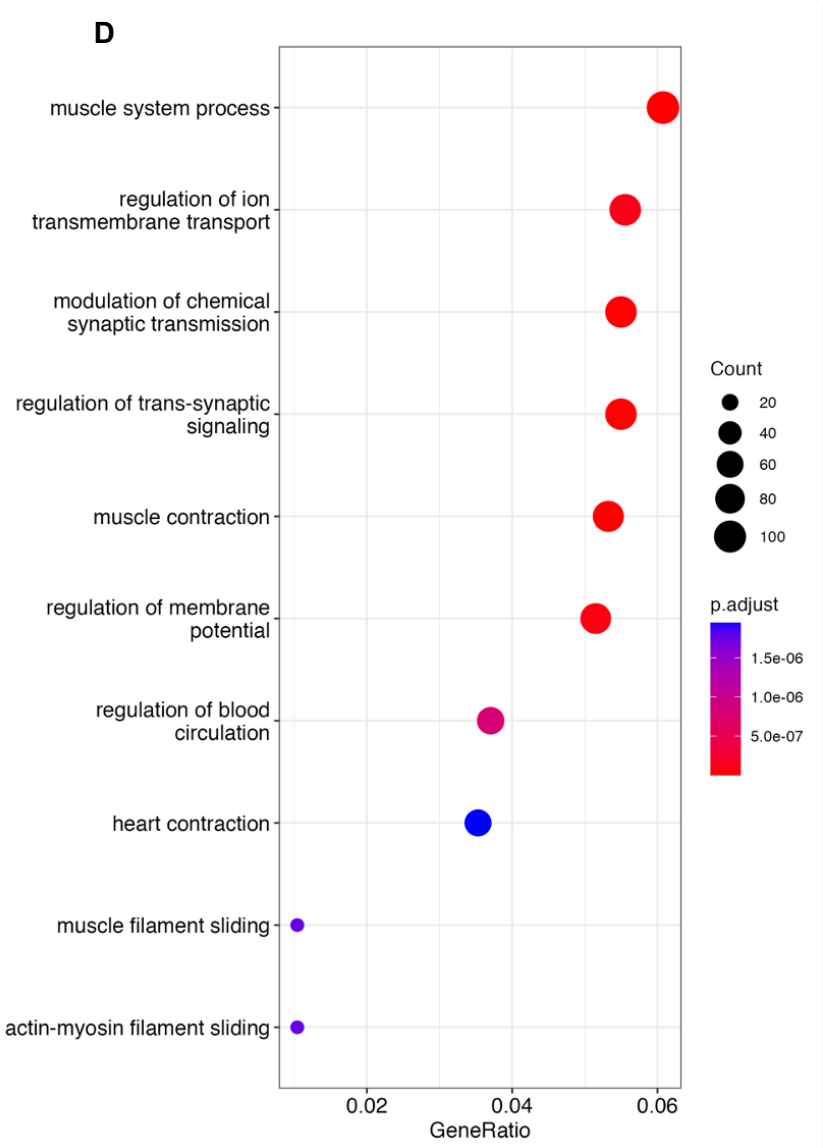

Figure 4.2 Multiple signalling pathways are upregulated in the PsA L skin

(A) Bar graph showing a total of 2151 significantly upregulated and 4094 significantly downregulated genes in the PsAL skin compared to HC skin. (B) Volcano plot showing fold change and significance of differences in genes in the PsaL skin compared to HC skin. (C) Pathway analysis showing the top 10 signalling pathways involving genes that are significantly upregulated in the PsA L skin. (D) Pathway analysis showing the top 10 signalling pathways involving genes that are significantly downregulated in the PsA L skin. Number of genes is denoted by the size of the circle (the bigger the circle, the more genes) and significance is denoted by the colour of the circle (more significant= stronger red colour).

To investigate the relationship of these changes in the PsA L skin to *FPR1* and *FPR2* expression, correlation analysis was performed on R studio. To achieve this, and to potentially identify any genes linked to *FPR1* and *FPR2* expression, the top differentially expressed genes with a significant positive and negative correlation with *FPR1* and *FPR2* were identified. Due to the large number of genes significantly correlating with *FPR1* and *FPR2*, (> 40 with a Spearman's correlation co-efficient of 0.9) and the potential influence of a small sample size on correlation analysis, stringent cut-offs for the correlation co-efficient were

used. A positive correlation was determined as a Spearman's correlation co-efficient (R value) of ≥ 0.95, and a negative correlation was determined as an R value of ≤ -0.95. P values of < 0.05 were used to determine significance.

A total of 9 genes had a significant positive correlation with *FPR1* (Figure 4.3A). Descriptions of each gene, known functions and associated diseases can be found in supplementary table 3(see appendix). Information on gene and protein function was obtained from The Human Protein Atlas[303] and the GeneCards Human gene database[304]. 4/9 (PRAL, AL355304.1, AC090229.1 and AC025181.2) of these genes were long-non-coding RNAs (LncRNAs), which have recently been implicated in the pathogenesis of several inflammatory diseases[305]. Although the function of some LncRAs is starting to be unveiled, a lot of the newly discovered transcripts have unknown functions. 2/9 of the positively correlating genes were pseudogenes, which have also been associated with inflammatory signalling[306]. The function these two pseudogenes (SLC6A10P and RPL5P34) has not been defined. Other genes that positively correlated with *FPR1* expression in the PsA L skin included those encoding proteins involved in protein synthesis (RPL38[307]) and transport (TOMM7[308]). Proteins involved in both these functions have been shown to be aberrantly expressed in PsO skin lesions[309,310]. Relevant to the function of *FPR1*, the *RGS2* gene which encodes for the Regulator of G-protein signalling 2 protein[311] also had a significant positive correlation with *FPR1* gene. Considering *FPR1* is a G protein coupled receptor[39], it is not surprising to see the *FPR1* gene correlating with a gene associated with regulation of its activity.

A total of 5 genes had a significant negative correlation with *FPR1* (Figure 4.3B) in the PsA L skin. Descriptions of each gene, known functions and associated diseases can be found in supplementary table 4(see appendix). Two pseudogenes (*SUDS3P1 and UBE2SP1)* and one LcnRNA (*AL137003.1*), negatively correlated with *FPR1* expression in the PsA L skin, and although genes of this nature have been linked with inflammation, functions of these specific genes remain undefined. *TRIM46* and *SCG2* also negatively correlated with FPR1 expression in the PsA lesional skin, however, roles for these genes in *FPR1* signalling and PsA pathogenesis are not apparent from current research.

On the basis that increased *FPR2* expression was observed in PsA L skin biopsies, the same analysis was applied to *FPR2* to investigate whether there were any correlations between this gene and any genes associated with PsA pathogenesis. A total of 14 genes positively correlated with *FPR2* in the PsA L skin (Figure 4.3C). Descriptions of each gene, known functions and associated diseases can be found in supplementary table 5(see appendix). 6/14 genes that positively correlated with *FPR2* expression in PsA L skin were LncRNAs, again, with undefined functions. Genes positively correlating with *FPR2* that could potentially be relevant to PsA pathogenesis were those encoding proteins involved in cellular proliferation (*DYNAP*) and reduced Nicotinamide adenine dinucleotide (NADH) metabolism (*MDH1).* Keratinocyte proliferation is enhanced in psoriatic skin lesions through a process which requires NADH-dependent oxidative phosphorylation[312]

A total of 13 genes negatively correlated with *FPR2* expression in the PsA L skin (Figure 4.3D). Descriptions of each gene, known functions and associated diseases can be found in supplementary table 6 (see appendix). 9/13 genes were relatively new transcripts with undefined functions, and hence, whether they interact with FPR2 associated pathways is unknown. Genes that negatively correlated with *FPR2* in the PsA L skin and that could be relevant to FPR2 function were *RPTOR* and *SLCO3A*. RPTOR encodes the Regulatory associated protein of MTOR complex 1 protein (MTORC1) which has been shown to be inhibited by FPR2[313]. *SLCO3A* encodes the Solute Carrier Organic Anion Transporter Family Member 3A1, which is known to play roles in NF-κB signalling, which, similarly has been shown to be inhibited by FPR2[314].

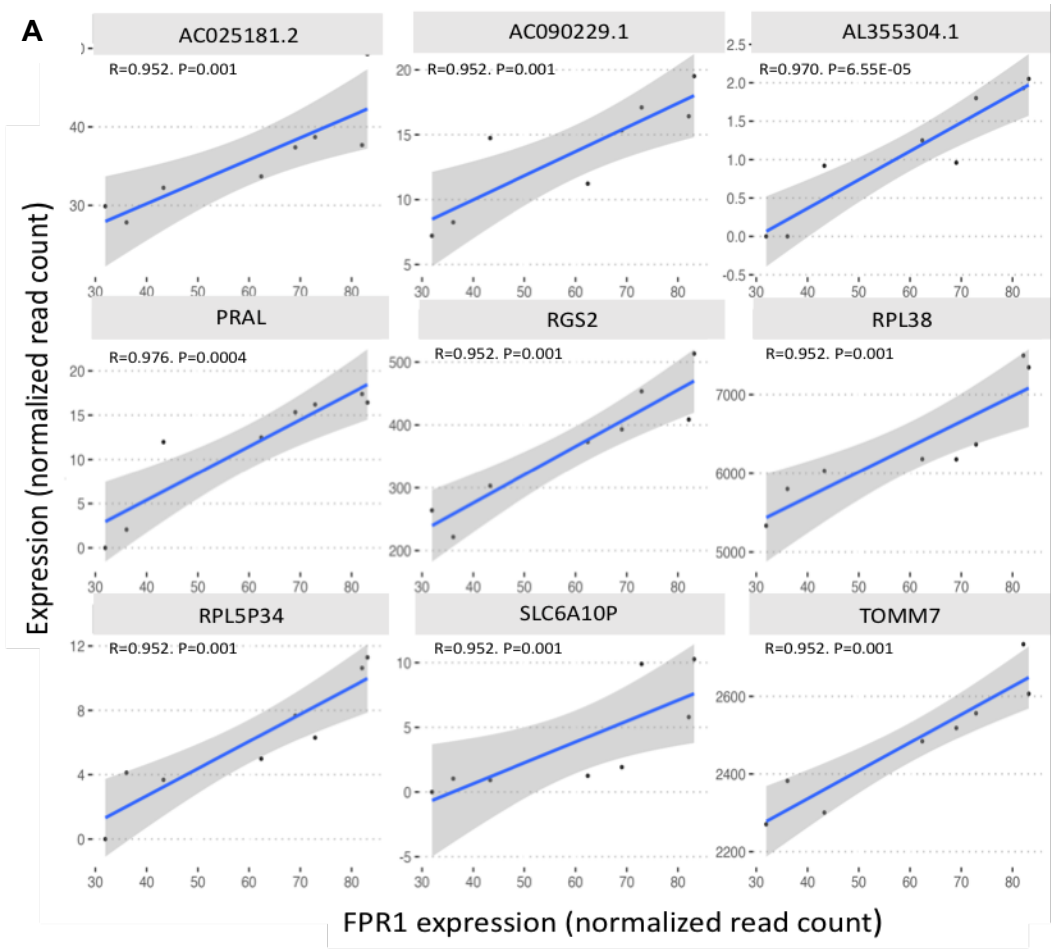
A
AC025181.2
R=0.952. P=0.001
AC090229.1
R=0.952. P=0.001
AL355304.1
R=0.970. P=6.55E-05
PRAL
R=0.976. P=0.0004
RGS2
R=0.952. P=0.001
RPL38
R=0.952. P=0.001
RPL5P34
R=0.952. P=0.001
SLC6A10P
R=0.952. P=0.001
TOMM7
R=0.952. P=0.001
Expression (normalized read count)
FPR1 expression (normalized read count)

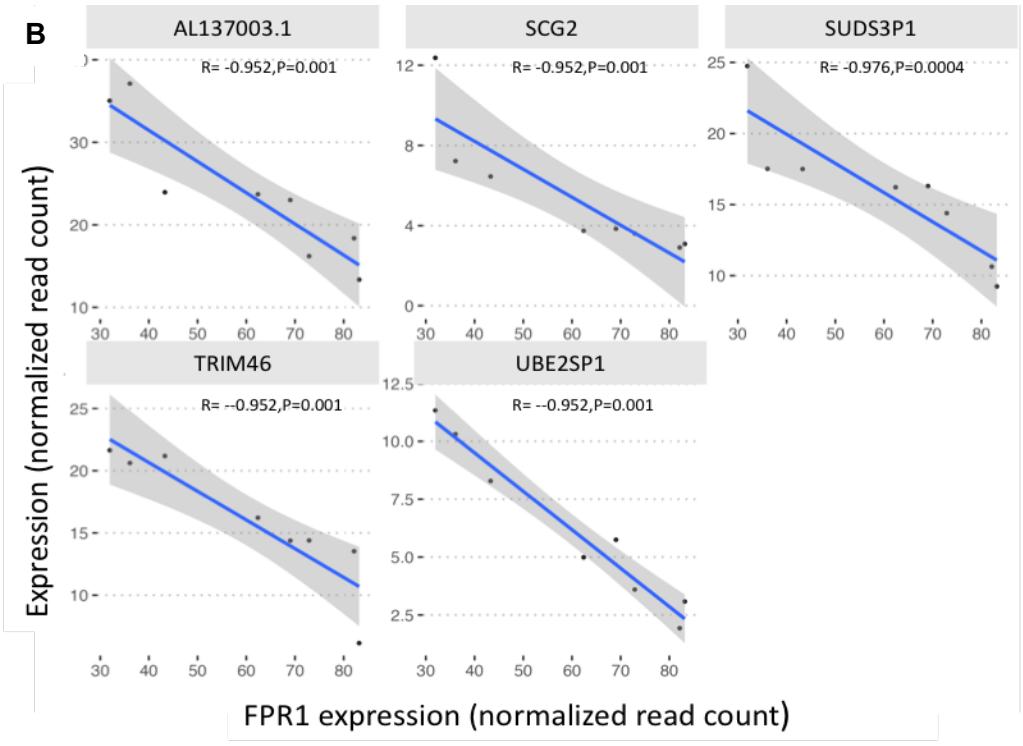
B
AL137003.1
R= -0.952,P=0.001
SCG2
R= -0.952,P=0.001
SUDS3P1
R= -0.976,P=0.0004
TRIM46
R= --0.952,P=0.001
UBE2SP1
R= --0.952,P=0.001
Expression (normalized read count)
FPR1 expression (normalized read count)

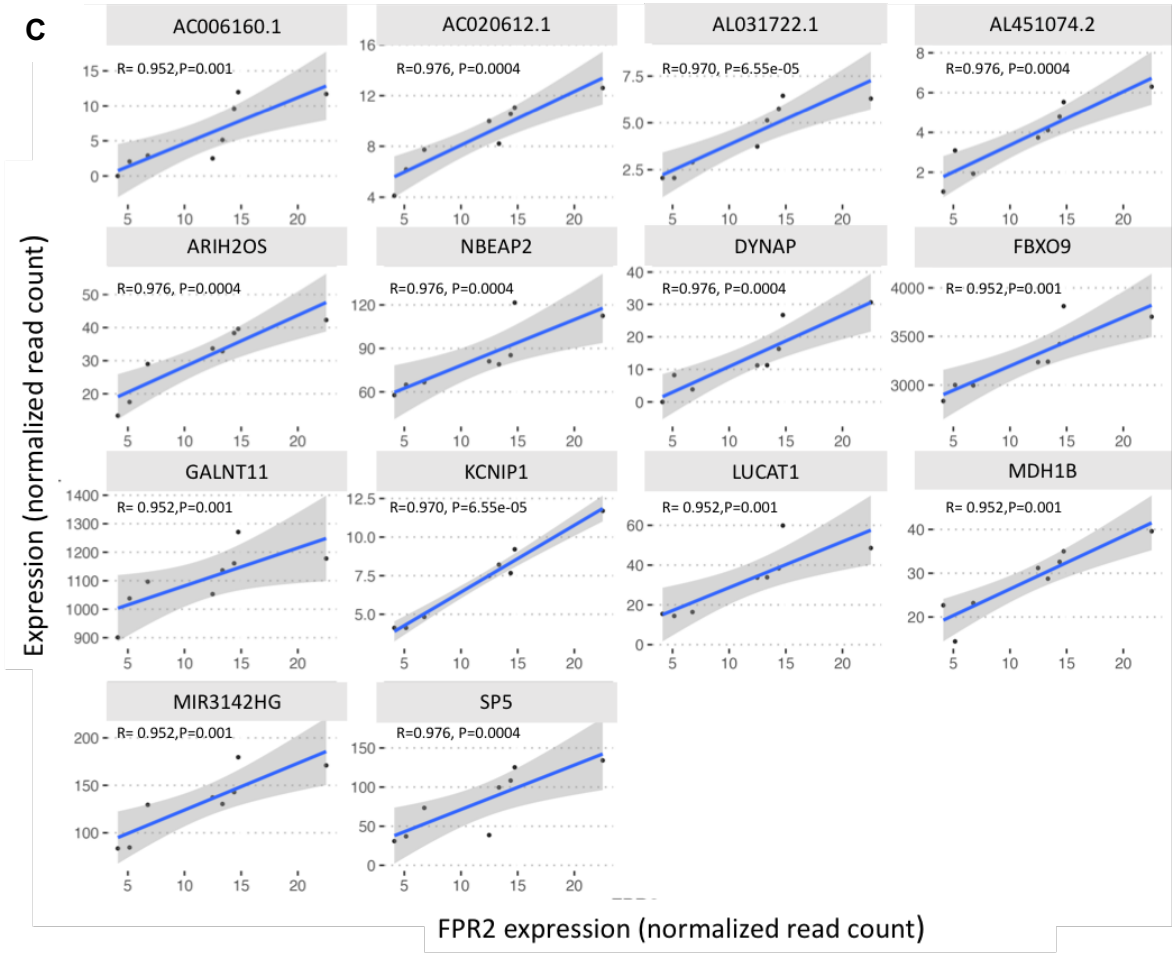
C
AC006160.1
R= 0.952,P=0.001
AC020612.1
R=0.976, P=0.0004
AL031722.1
R=0.970, P=6.55e-05
AL451074.2
R=0.976, P=0.0004
ARIH2OS
R=0.976, P=0.0004
NBEAP2
R=0.976, P=0.0004
DYNAP
R=0.976, P=0.0004
FBXO9
R= 0.952,P=0.001
GALNT11
R= 0.952,P=0.001
KCNIP1
R=0.970, P=6.55e-05
LUCAT1
R= 0.952,P=0.001
MDH1B
R= 0.952,P=0.001
MIR3142HG
R= 0.952,P=0.001
SP5
R=0.976, P=0.0004
Expression (normalized read count)
FPR2 expression (normalized read count)

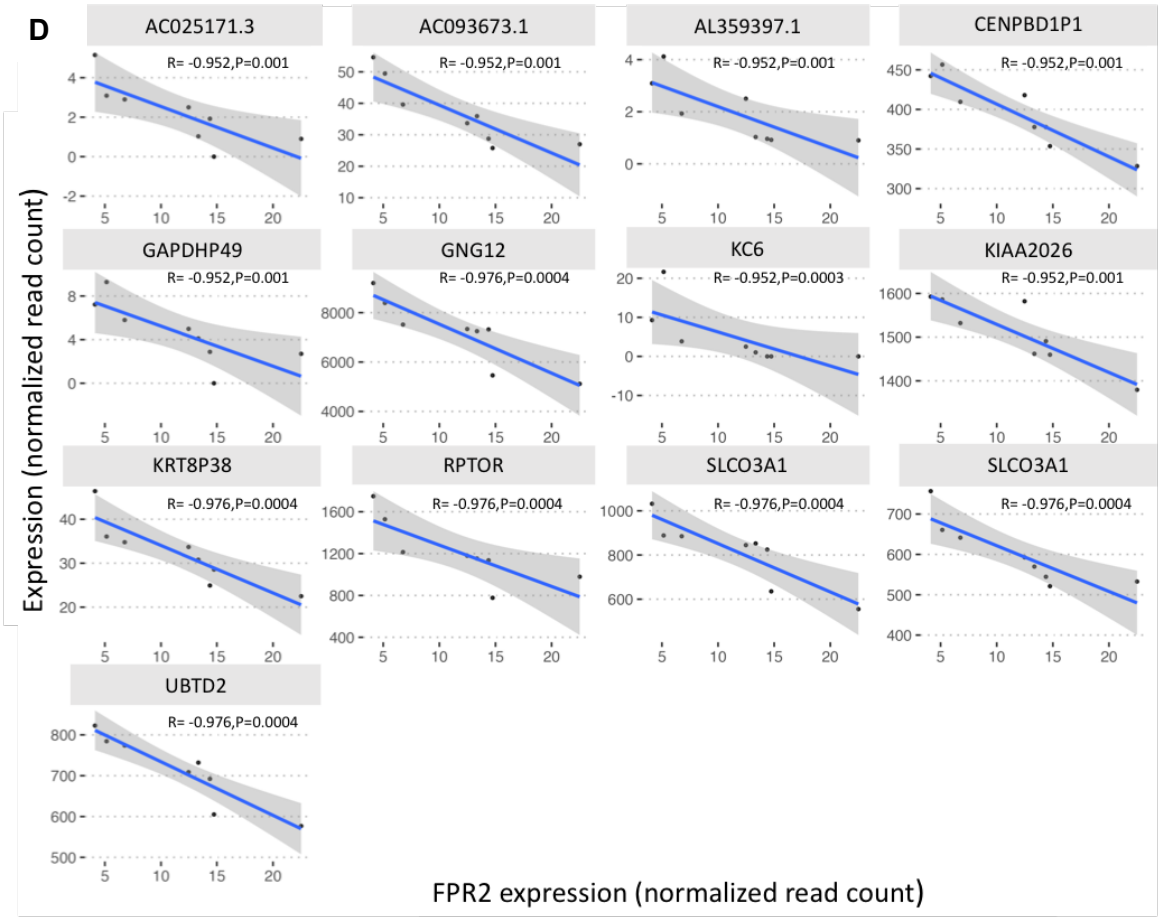

Figure 4.3 Genes in the PsA L skin with the top correlations with FPR1 and FPR2

Graphs showing genes in the PsA L skin with the top (A) positive and (B) negative correlations with FPR1 and the top (C) positive and (D) negative correlations with *FPR2.* Spearman's correlation coefficients (R values) are shown. An R value of ≥ 0.95 was determined as a positive correlation and an R value of ≤ -0.95 was determined as a positive correlation. P values of < 0.05 were used to determine significance. Graphs were produced and correlation analysis was conducted on R studio. N=8.

Overall, this preliminary data has highlighted several genes that correlate with *FPR1* and *FPR2* in PsA skin lesions that have an association with *FPR1*/*FPR2* signalling (e.g *RGS2*) or pathways relevant to PsA pathogenesis (e.g *MDH1*). However, as the N number in this study is relatively low (N=8), these findings need to be confirmed in a larger, independent cohort. Additionally, power calculations are needed to determine the ideal sample size needed for this experiment.

4.2.2 Enriched signalling pathways in the PsA L skin involving FPR1 and FPR2

Analysis was conducted using the PathfindR[315] programme on R studio to identify ernriched pathways in the PsA L skin involving FPR1 and/or FPR2 activity. PathfindR used the entire gene list from the PsA L skin samples and identified active subnetworks of protein-protein interactions and subsequent enriched pathways using the KEGG[316] database. Three pathways came up as enriched from the KEGG database involving *FPR1* and *FPR2*; those involved in neutrophil extracellular trap (NET) formation (FPR1 and FPR2), Staphylococcus aureus (*S. aureus*) infection (FPR1 and FPR2) and the Rap1 signalling pathway (FPR1). Figures 4.4A-4.4C show the three KEGG pathways mentioned and highlight interactions with *FPR1* and *FPR2*.

It is not entirely surprising that the *S. aureus* infection pathway (Figure 4.4A) is enriched in this dataset as previous studies have shown *S. aureus* to be present on the skin of people with psoriatic lesions[317]. In the *S. aureus* infection pathway, FPR1 and FPR2 (denoted FPRL1 in Figure 4.4A) were shown to primarily be involved in neutrophil inhibition of chemotaxis and phagocyte activation through interaction with proteins on the surface of the *S. aureus* bacterium. The *S.aureus* protein, chemotaxis inhibitory protein of *S. aureus* (CHIPS) is able to inhibit chemotaxis in the neutrophil through inhibition of FPR1. Interestingly the *S. aureus* bacterium has been shown to produce an FPR2-specific protein, FPRL1 inhibitory protein (FLIPr), that inhibits its actions in the neutrophil. This has also been shown experimentally[318].

In the NET formation pathway FPR1 and FPR2 (denoted FPR in Figure 4.4B) can both interact with N-Formyl-methionyl-leucyl-phenylalanine (fMLP), a potent chemotactic factor. fMLP can then go on to activate calcium signalling, PI3K-Akt signalling, NADPH Oxidase signalling and autophagy regulation pathways via FPR1 and FPR2 (Figure 4.4B). NET formation is also extremely relevant in the context of PsA as NET formation was found to be increased in the blood and lesional skin of PsA patients, which also correlated with disease severity[319].

Rap1 is a small guanine nucleotide triphosphatase (GTPase) that controls several signalling processes, including mitogen-activated protein (MAP) kinases as well

as playing a role in cell adhesion[320]. More relevantly, a role for Rap1 in T cell-mediated autoimmune disease has been suggested[321]. In Figure 4.4C, FPR1 is shown to play a role in this pathway through activation of the second messengers calcium, cyclic AMP (cAMP) and diacylglycerol (DAG). These indirectly activate Rap1 which, in turn, indirectly regulates several biological processes including adhesion and migration as well as regulation of MAP kinases and PI3 kinase-Akt signalling. Additionally, a role for MAP kinases in the development of psoriasis has been implicated[322].

A

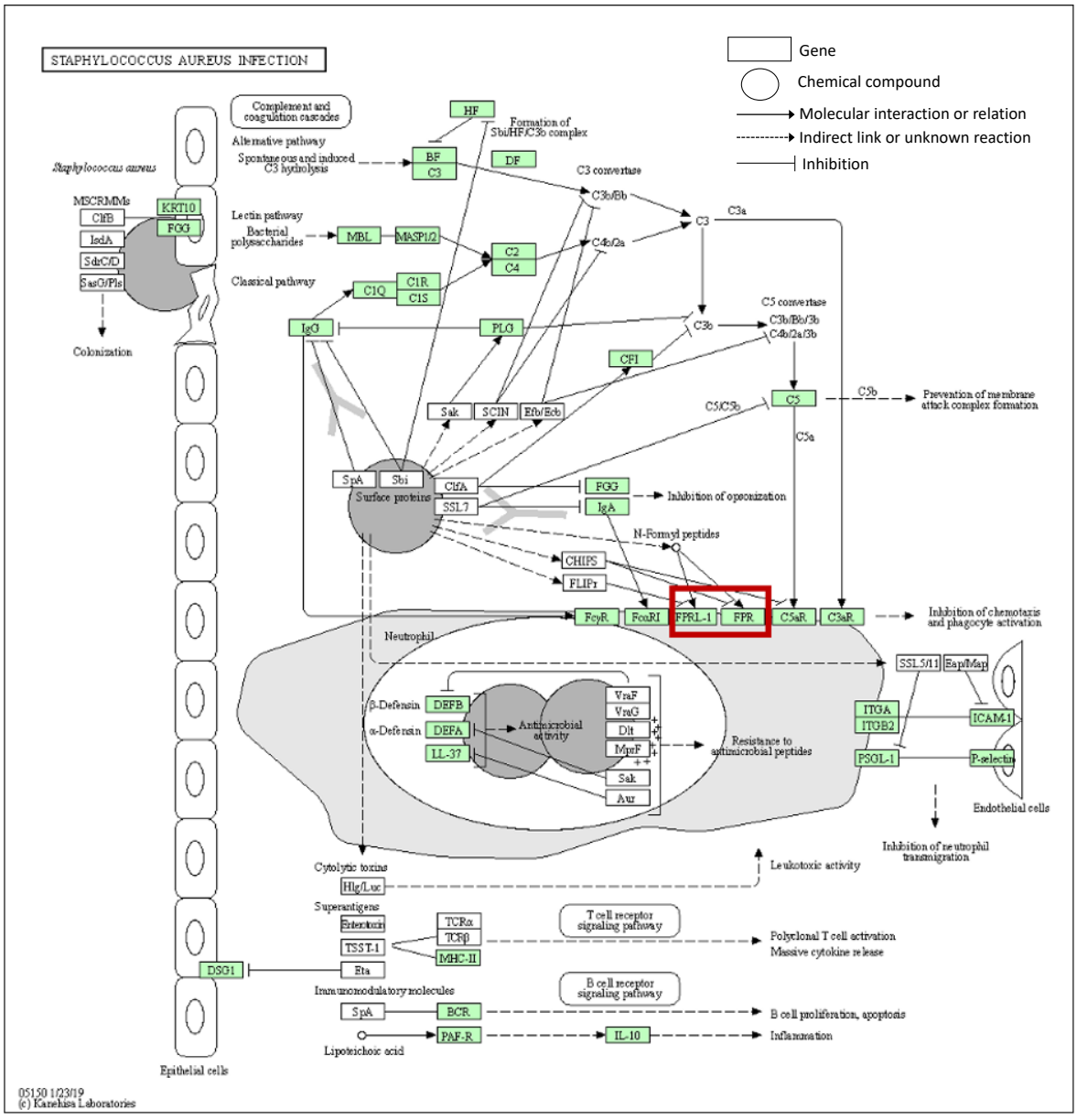

B

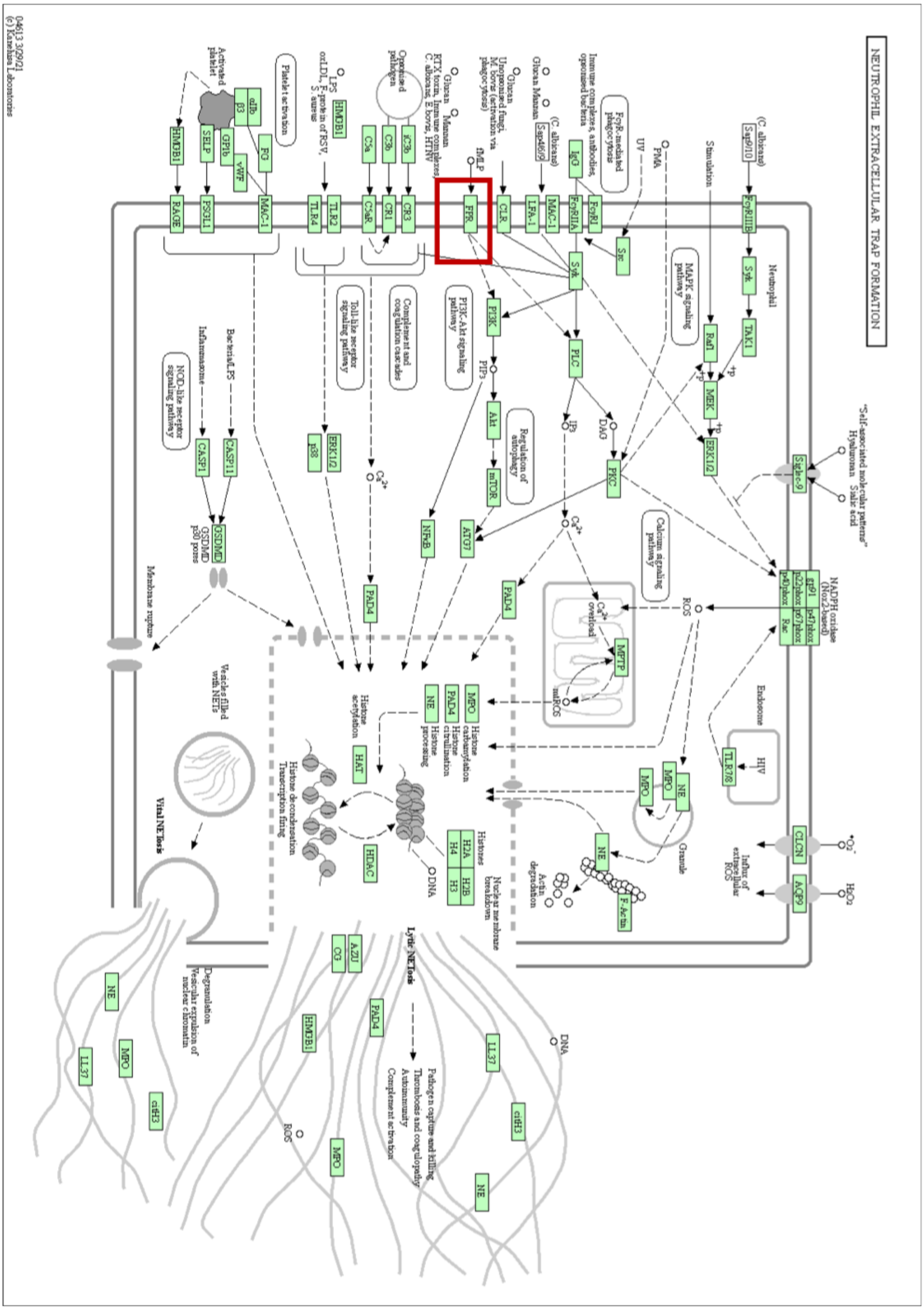
NEUTROPHIL EXTRACELLULAR TRAP FORMATION
Neutrophil
Lytic NETosis
Vital NETosis
04613 3/29/21
(c) Kanehisa Laboratories

C

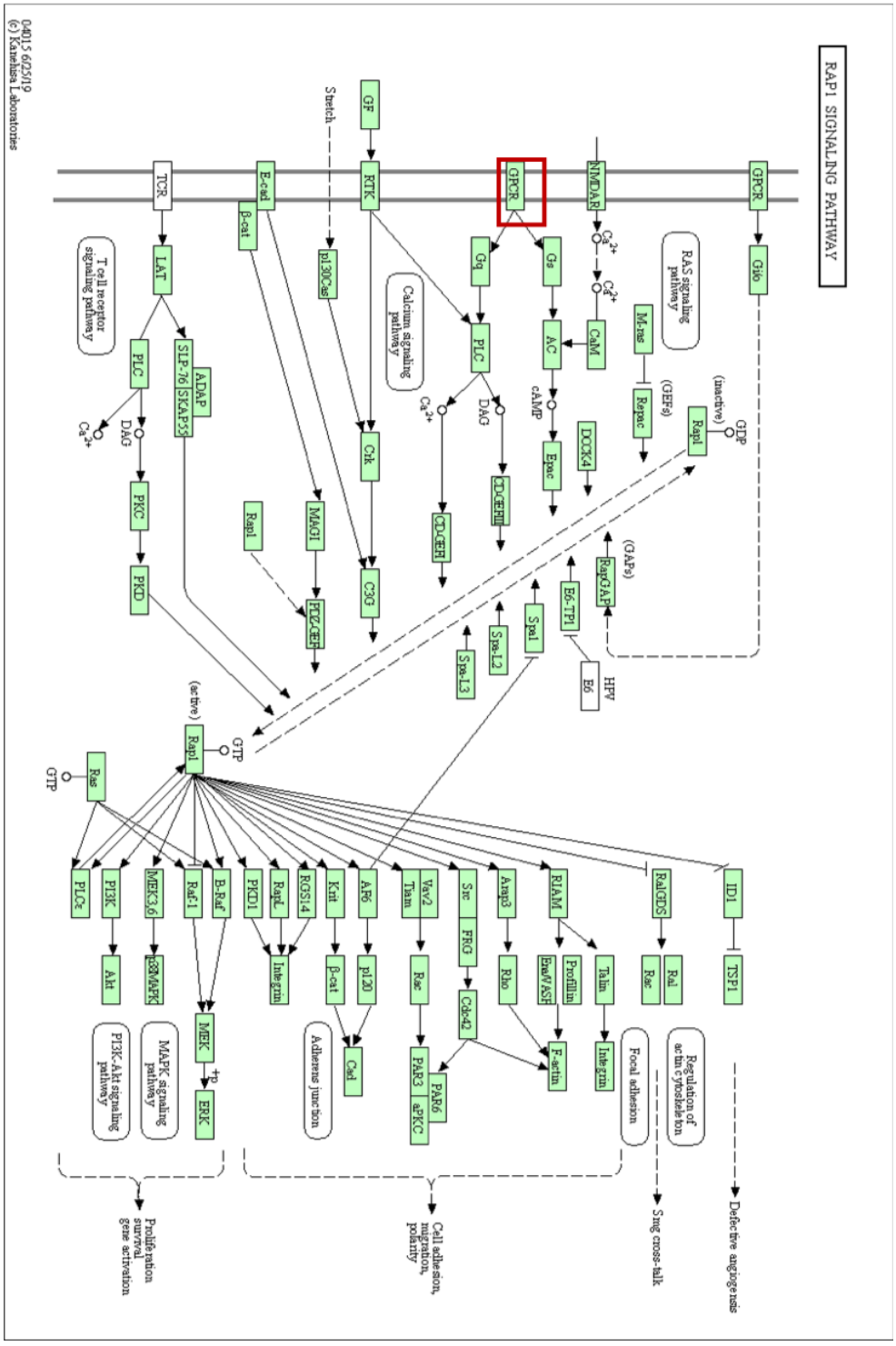

Figure 4.4 FPR1 and FPR2 are involved in key signalling pathways in the PsA L skin

Diagrams taken from the KEGG database showing the key signalling pathways enriched in the PsA L skin where FPR1 and FPR2 are upregulated. Diagrams show the role of FPR1 and FPR2 in (A) *S.aureus* infection pathways (KEGG entry hsa0510) and (B) NET formation pathways(KEGG entry hsa04613). FPR1 is also shown to play a role in (C) the Rap1 signalling pathway (KEGG entry hsa04015). Green boxes Red boxes highlight FPR involvement within the pathway. A key for symbols shown in the diagrams has been added to 4.3A. Green boxes are used by the KEGG database for hyperlinking to genes (not relevant to this analysis).

In summation, this analysis has identified three pathways associated with FPR1 activity and two pathways involving FPR2 activity in PsA L skin samples. Moreover, each of these pathways are associated with functions that could be relevant to PsA pathology in terms of bacterial responses in the psoriatic lesions (*S. aureus* infection pathway), disease severity (NET formation) and development (Rap1 pathway).

4.2.3 Analysis of ANXA1, FPR1 and FPR2 surface protein expression in PsA

ANXA1 is primarily expressed in the subcellular granules or cytoplasm of the cells that express it. ANXA1 can be transported to the cell surface upon cellular activation during an inflammatory response or through glucocorticoid stimulation[27]. ANXA1 is then free to trigger any relevant signalling, which is evidenced to be mediated via the FPRs, primarily FPR1 and FPR2 in the context of disease[23,28,29]. PsA is a disease that is certainly associated with an overactivation of immune cells and a chronic inflammatory response[90,98].

Therefore, it was of interest to investigate surface expression levels of ANXA1 and its receptors on immune cells from PsA patients to determine if expression was significantly different on any particular subsets of cells compared to healthy controls. It was also key to identify if there were any immune cell subsets associated with PsA disease pathogenesis that had significantly altered ANXA1, FPR1 and/or FPR2 expression. Three separate flow cytometry panels were designed to assess monocyte and DC, B cell and T cell populations for ANXA1 and FPR1/2 expression (details of antibodies and fluorophores can be found in materials and methods section 2.4.2). These panels were used to assess 9 PsA and 6 HC samples. Out of the 6 HC samples, only three were able to be age matched.

Positive staining for FPR1 and FPR2 was defined as a higher fluorescence detection than the fluorescence minus one control staining (FMO) and positive staining for ANXA1 was determined as higher fluorescence detection than the isotype control stain. An FMO control consists cells from the same population stained with all of the fluorescent markers in the panel apart from a specific marker of interest. FMO controls are essential in multicolour flow cytometry

panels as they take into account background staining coming from other fluorophores which may contribute to detection of the fluorophore of interest[323]. As MDX-124 is a novel antibody and was labelled in- house (see details in methods section 2.3.3), the effects of non-specific binding of the antibody and autofluorescence were taken into account by using an isotype control antibody labelled at the same time, using the same fluorophore (AF647). An isotype control is an antibody of the same isotype as the primary antibody (MDX-124) than is non-specific to the antigen of interest (ANXA1).

Gating strategies for the monocyte and DC panel (Figure 4.5A), the B cell panel (Figure 4.5B) and the T cell panel (Figure 4.5C) are shown below.

A **Monocyte and DC panel**

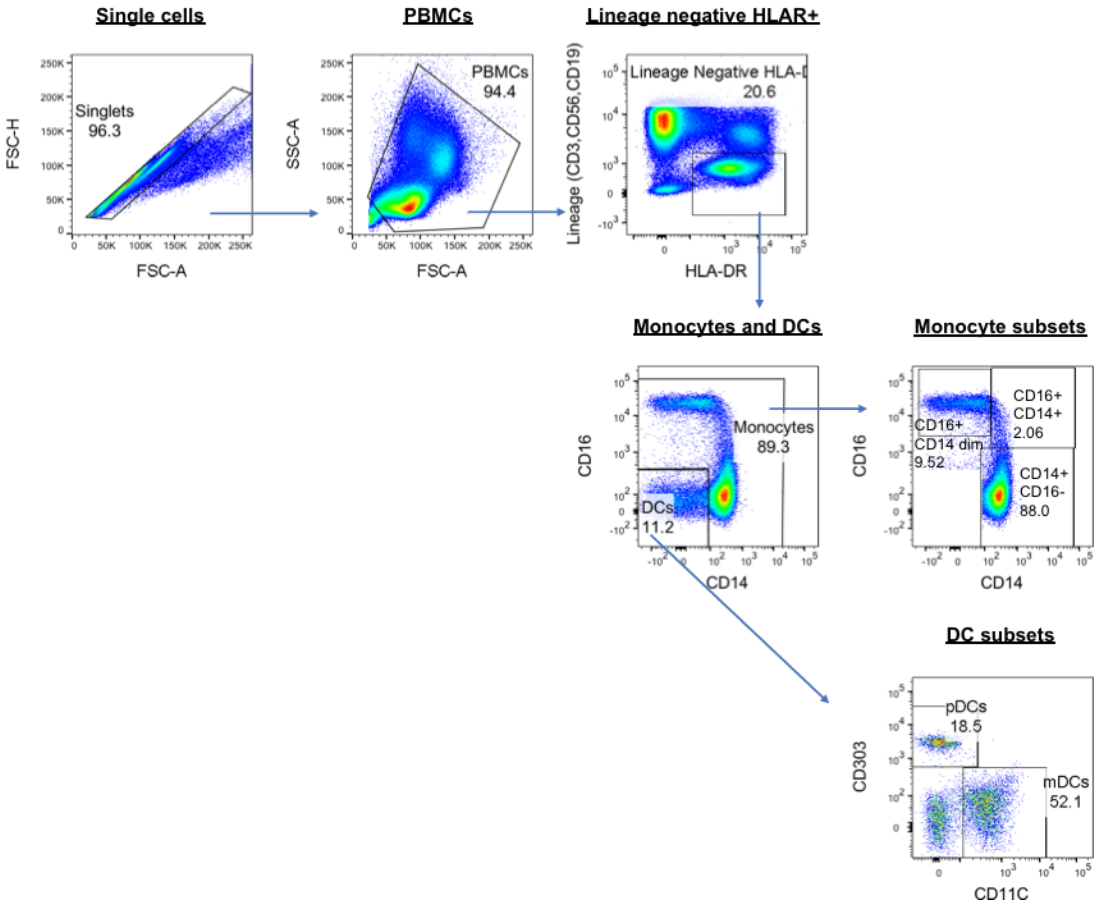

B

B cell panel

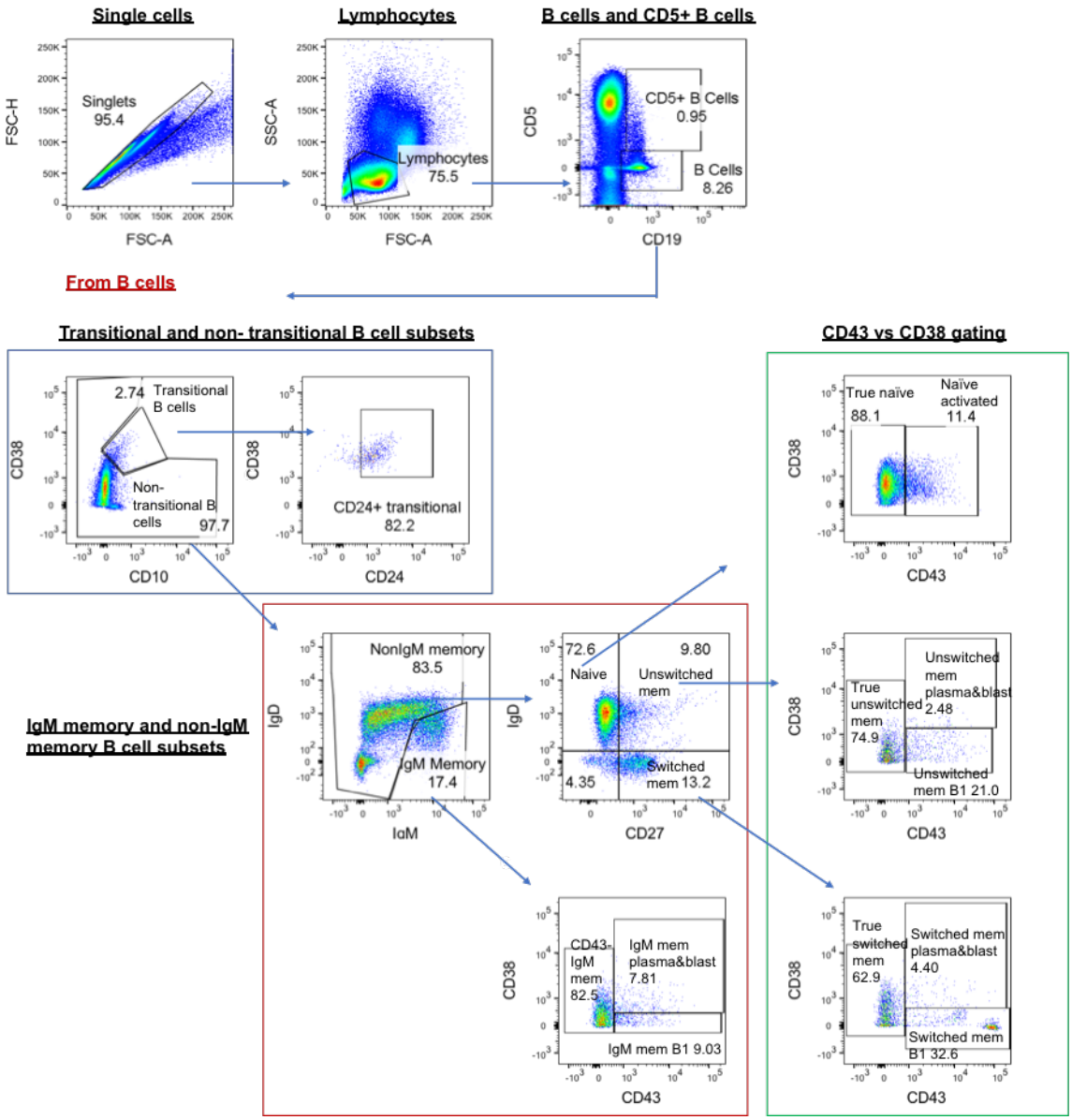

C

T cell panel

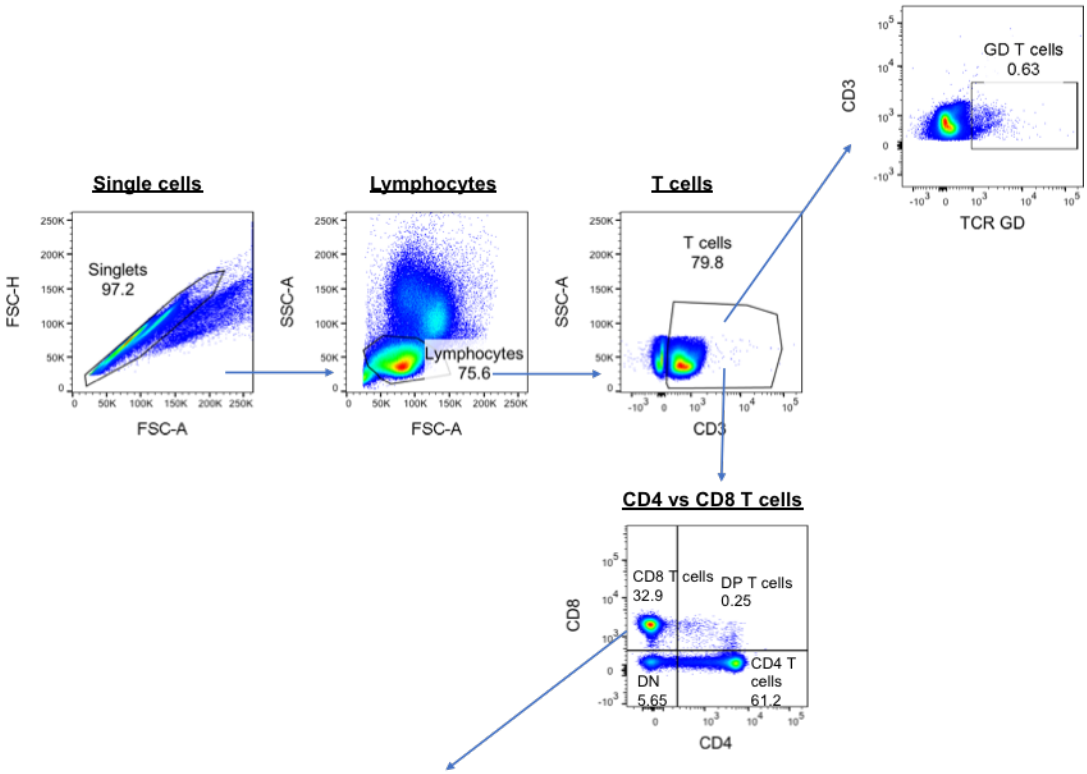

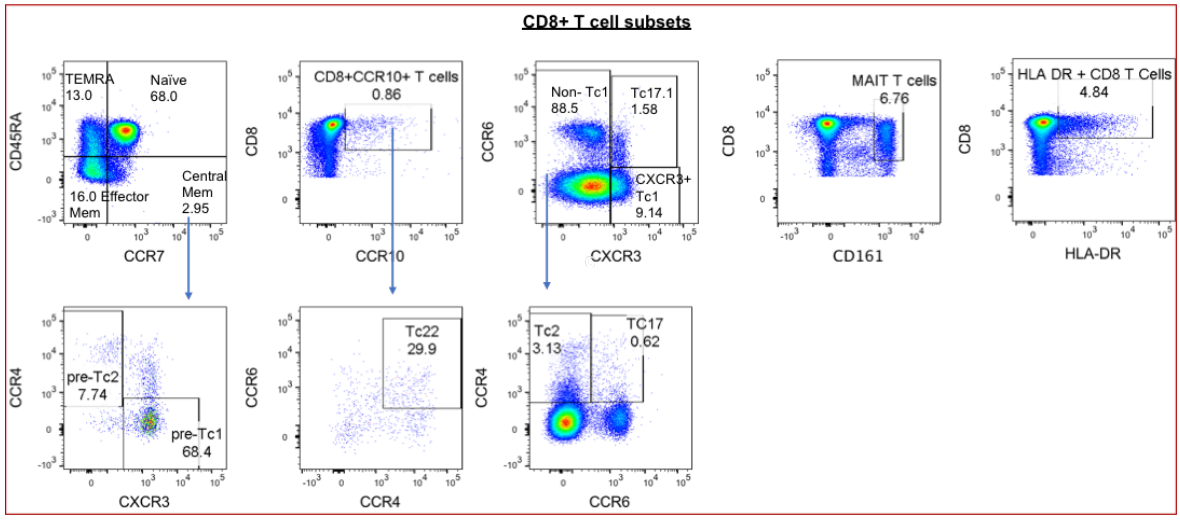

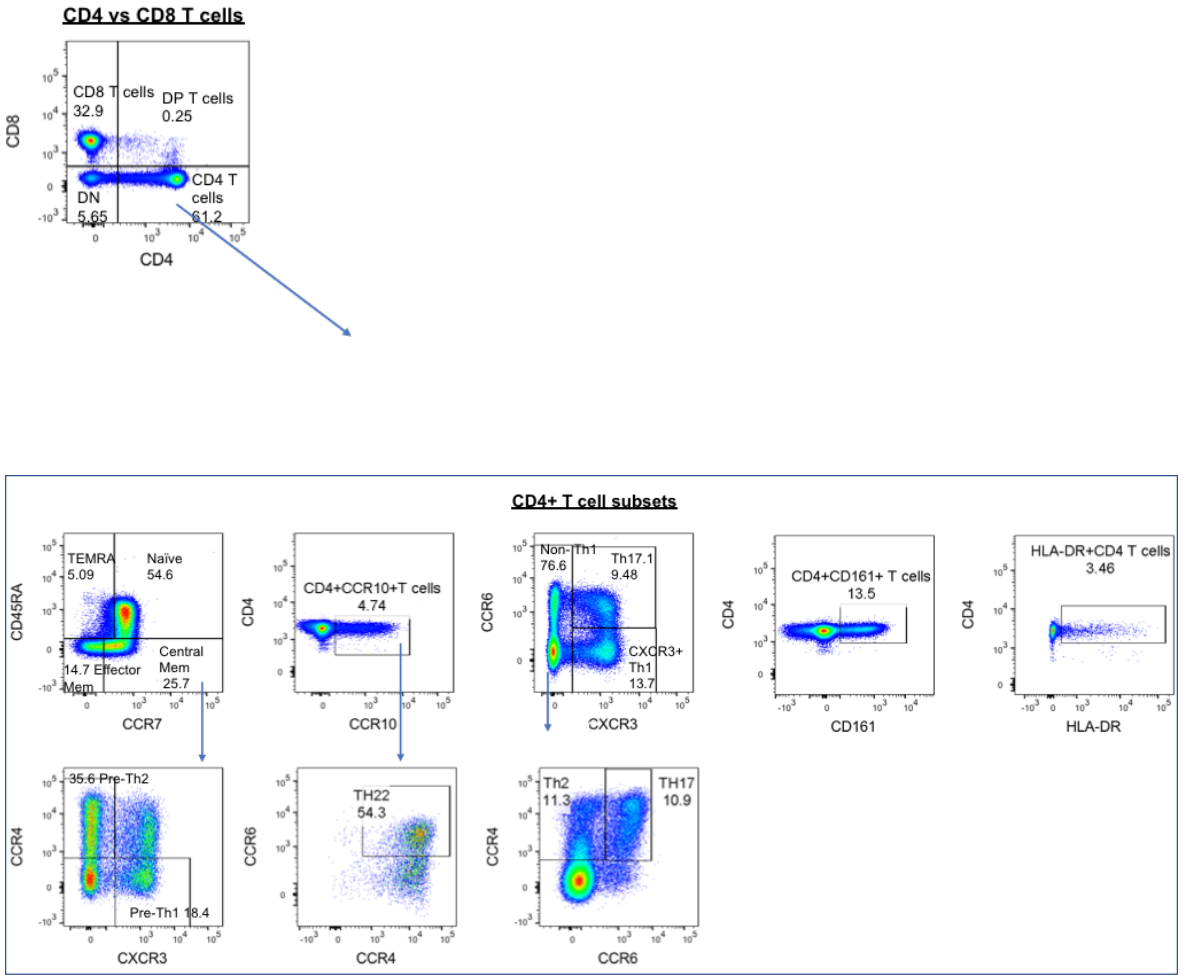

Figure 4.5 Gating strategy for flow cytometry analysis of Monocyte/DC, B cell and T cell panels

(A) For the monocyte panel, single cells were first gated, followed by PBMCs. Cells that were lineage CD3, CD19 and CD56) negative and HLA-DR positive were selected. Monocytes were then gated based on their expression of CD16 and CD14 and DCs were gated based on their negative expression of CD16 and CD14. DC subpopulations were gated based on their expression of CD11c (myeloid or mDCs) and CD303 (plasmacytoid or pDCs).

(B) For the B cell panel, single cells and lymphocytes were first gated, followed by B cells based on their CD19 expression. A subpopulation of $CD5^+$ B cells was also gated. Non-transitional and transitional B cells were gated based on their CD38 and CD10 expression and $CD24^+$ cells were further gated from transitional B cells. IgM memory and non-IgM memory B cell subsets were gated from non- transitional B cells based on their IgM and IgD expression. Subpopulations of IgM memory B cells were then gated based on their CD27 expression. Further subpopulations were gated from IgM memory and (non-IgM memory) unswitched memory B cells based on CD43 and CD38 expression.

(C) For the T cell panel, single cells and lymphocytes were gated, followed by $CD3^+$ T cells. T cells were further gated for their expression of the Gamma delta (GD) T cell receptor (TCR) and CD4/CD8 expression. Subpopulations of CD4 and CD8 T cells were then individually gated based on HLA-DR, CCR10, both CXCR3 and CCR6 and both CD45RA and CCR7 expression. Subpopulations of these cells were gated based on their CCR4 and CCR6 and CXCR3 expression.

FACS plots were produced using FlowJo (v 10.6.1) software.

Analysis was conducted on FlowJo (v10.6.1) software to obtain the geometric mean expression of ANXA1, FPR1 and FPR2 on the cell populations of interest. Delta (Δ) MFI values for each population were then calculated by subtracting the (FMO and isotype) control stains from the FPR1, FPR2 and ANXA1 stains, to account for non-specific background staining. Mean ΔMFI values were used to produce heatmaps to simultaneously look at the expression of ANXA1(Figure 4.6A), FPR1(Figure 4.6B), and FPR2 (Figure 4.6C) in all of the cell subsets gated.

Consistent with the literature[29], monocytes were high expressors of ANXA1 in both HC and PsA samples (Figure 4.6A). $CD16^{+}CD14^{dim}$ monocytes were the highest ANXA1 expressors within the monocyte panel and expressed higher ANXA1 in PsA (HC mean ΔMFI=2547, PsA mean ΔMFI=2738). In the B cell panel, unswitched memory plasma and blast cell populations were high ANXA1 expressors in both HC (mean ΔMFI=1442) and PsA, with higher expression being apparent in the PsA samples (mean ΔMFI=2449). Gamma delta (GD) T cell populations expressed higher ANXA1 in PsA (HC mean ΔMFI=127, PsA mean ΔMFI=473). The same was evident with Type 1 cytotoxic T cell (TC1) populations, particularly $CXCR3^{+}$Tc1 (HC mean ΔMFI=22, PsA mean ΔMFI=500) and $CXCR3^{+}CCR6^{+}$Tc17.1 populations (HC mean ΔMFI=173, PsA mean ΔMFI=472). In contrast ($CXCR3^{-}$)Tc17 populations expressed higher ANXA1 in HC samples (HC mean ΔMFI=438, PsA mean ΔMFI=5).

A similar pattern was seen in the FPR1 expression heatmap (Figure 4.6B). Monocytes were amongst the highest expressors of FPR1 in both PsA and HC samples. $CD16^{+}CD14^{+}$ monocytes in particular expressed the highest FPR1 in PsA (HC mean ΔMFI=1875, PsA mean ΔMFI=2644). Both switched memory (HC mean ΔMFI=93, PsA mean ΔMFI=417) and unswitched memory (HC mean ΔMFI=235, PsA mean ΔMFI=383) plasma and blast cells expressed higher FPR1 in PsA, as well as unswitched memory B1 cells (HC mean ΔMFI=148, PsA mean ΔMFI=372). As with ANXA1, ($CXCR3^{+}CCR6^{+}$) Tc17.1 populations expressed more FPR1 in PsA (HC ΔMFI=23, PsA ΔMFI=111). The same was seen with Tc17(HC mean ΔMFI=33, PsA mean ΔMFI=71) and GD T cell (HC mean ΔMFI=34, PsA mean ΔMFI=69) populations, although expression of FPR1 in general was lower in T cells compared to monocyte, DC and B cell populations, which could result in small changes in expression appearing more substantial in the heatmap.

Monocytes were amongst the highest expressors of FPR2, with higher expression in PsA being evident on $CD14^{+}CD16^{-}$ monocytes (HC mean ΔMFI=10, PsA mean ΔMFI=16) and $CD14^{+}CD16^{+}$ monocytes (HC mean ΔMFI=7, PsA mean ΔMFI=18). However, as mentioned above, when interpreting this data, it is worth noting that FPR2 expression on monocytes was substantially lower than for ANXA1 and FPR1, meaning small changes in expression could appear more substantial in the heatmap. Unswitched plasma and blast cells were amongst the top expressors of FPR2 in PsA in the B cell panel, with higher expression than in HC samples (HC mean ΔMFI=37, PsA mean ΔMFI=48). Contrastingly, $CD5^{+}$ B cells expressed more FPR2 in HC samples (HC mean ΔMFI=59, PsA mean ΔMFI=32). Relevantly, these cells have recently been implicated in the negative regulation of TCR signalling and have been suggested as protective in autoimmunity[324]. As shown with FPR1 and ANXA1, $CXCR3^{+}CCR6^{+}$ Tc17.1 population expressed more FPR2 in PsA (HC ΔMFI=25, PsA ΔMFI=111), as well as Tc17(HC mean ΔMFI=3, PsA mean ΔMFI=71) and GD T cell (HC mean ΔMFI=16, PsA mean ΔMFI=69) populations.

A

ANXA1 surface expression

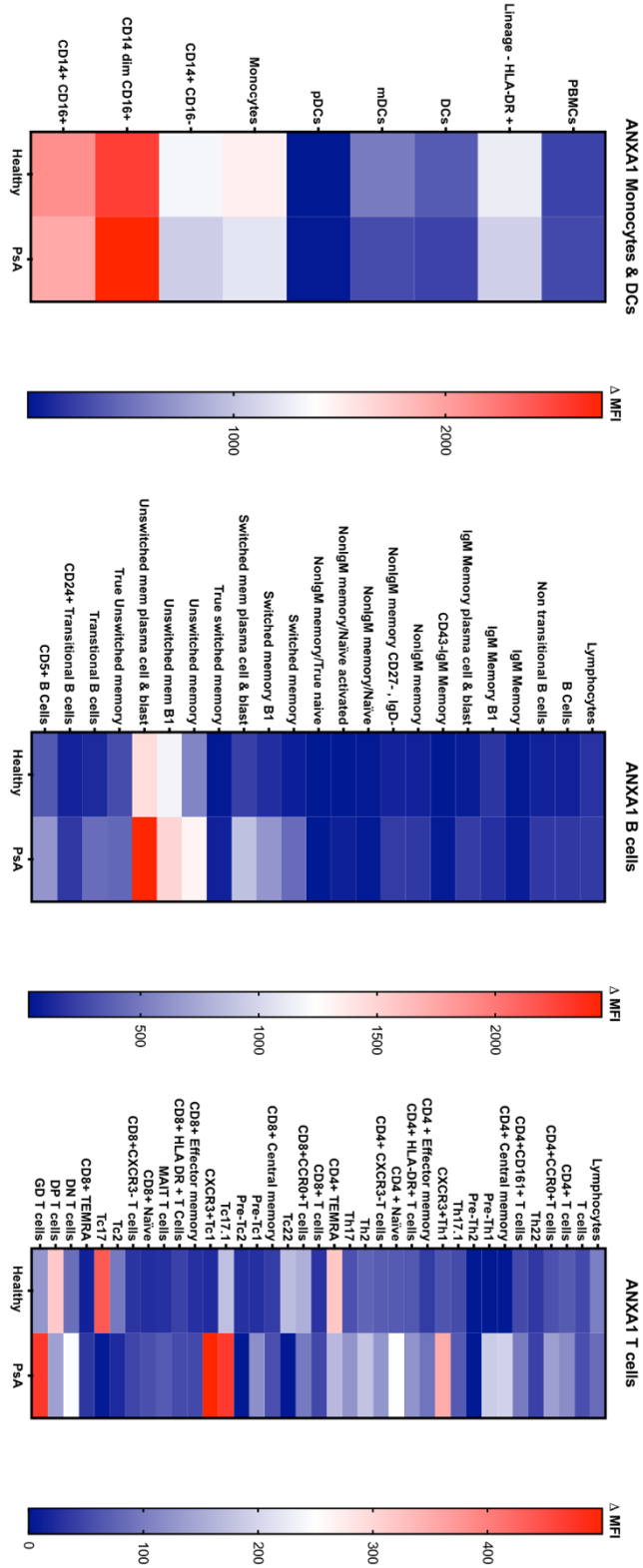

B

FPR1 surface expression

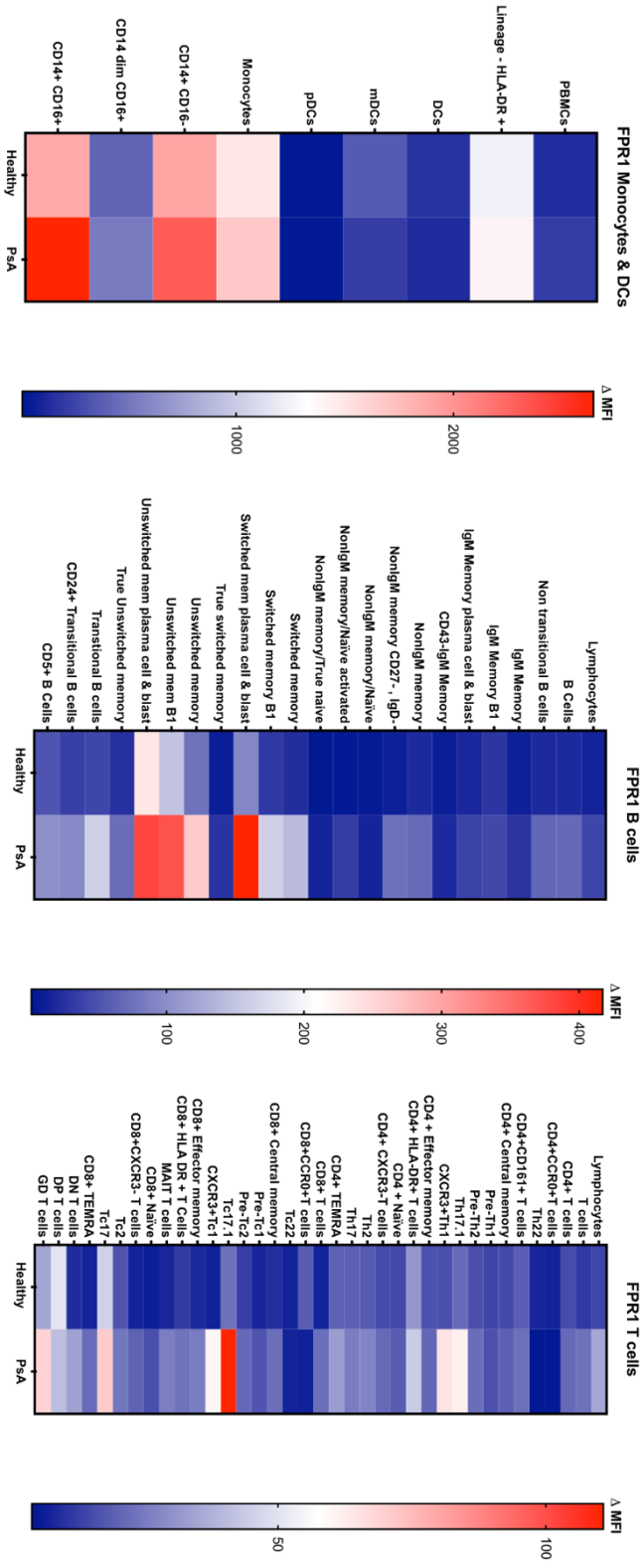

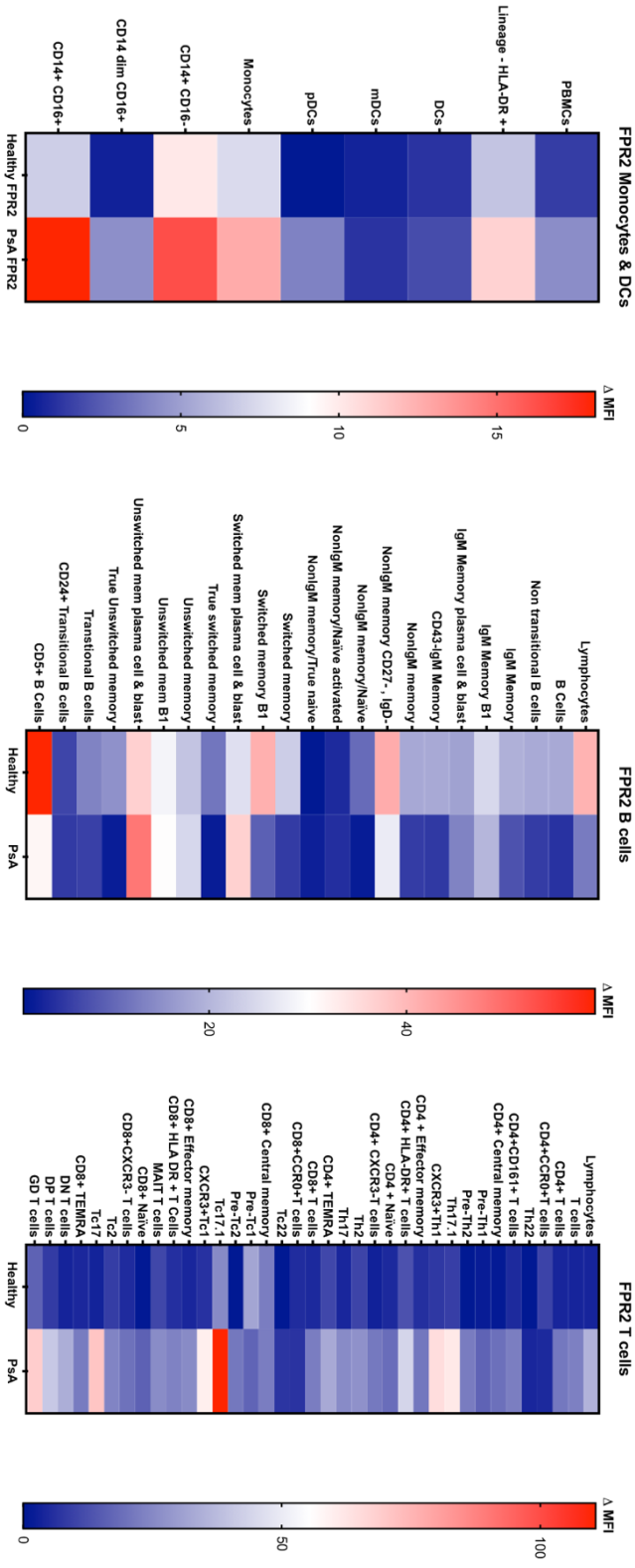

Figure 4.6 Expression profiles of ANXA1, FPR1 and FPR2 on peripheral blood immune cell subsets.

PBMCs were extracted from peripheral blood and stained for several monocyte, B cell and T cell markers as well as surface expression of ANXA1, FPR1 and FPR2. Δ MFIs were calculated using appropriate controls (stained sample minus FMO or isotype control) and heatmaps were produced of mean Δ MFIs for (A) ANXA1, (B) FPR1 and (C) FPR2 surface expression on monocyte and DC populations, B cell populations and T cell populations. Heatmaps were produced using GraphPad prism v9 software. HC N=6, PSA N=9

Having investigated the global shifts in ANXA1, FPR1 and FPR2 surface expression on different immune cell subsets, it was key to look at the sample specific data across the controls and patient samples to determine if there were any significant differences in expression between the groups.

Three cell populations expressed significantly different ANXA1 in PsA compared to HC samples (Figure 4.7A). In the monocyte and DC panel, myeloid (m)DCs expressed significantly less ANXA1 in PsA patient samples. Switched memory B1 cells ($CD38^{-}CD43^{+}$ switched memory B cells) expressed significantly more ANXA1 in PsA. Additionally, a subset of IL-17 secreting $CD8^{+}$ cytotoxic T cells (Tc17) expressed significantly less surface ANXA1 in PsA samples (Figure 4.7A).

Fifteen cell populations expressed significantly different FPR1 in PsA compared to HC samples (Figure 4.7B). $CD16^{+}CD14^{+}$ monocytes expressed significantly more FPR1 on their cell surface in PsA. Naïve B cell populations (true naïve and activated) switched memory B cell populations (B1 and plasma cell and blast), unswitched memory B cells and transitional B cells all expressed significantly more surface FPR1 in PsA samples. Significantly more FPR1 was also expressed on the surface of $CD8^{+}$ cell populations, including the autoimmune- associated[325] Mucosal-associated invariant T (MAIT) cells, Tc17.1 cells, CXCR3 Tc1 cells, $CXCR3^{-}$ cells, TEMRA, effector memory, naïve and central memory cells.

Twenty-three cell populations had significantly different FPR2 surface expression in PsA samples compared to HC samples, (Figure 4.7C). $CD43^{-}$ IgM and true unswitched memory B cell populations expressed significantly more surface FPR2 in HC samples. In contrast, most T cell populations expressed significantly more surface FPR2 in PsA. These differences did not appear to be $CD8^{+}$ T cell specific, as seen with FPR1 expression. Both $CD4^{+}$ and $CD8^{+}$ TEMRA, naïve, effector memory and central memory populations expressed significantly more FPR2 in PsA, as well as ($CD4^{+}$ and $CD8^{+}$) HLA-DR^{+} cells, $CD161^{+}$cells and $CXCR3^{+}$Tc1 cells. Additionally, several Il-17 producing T cells (Th17, Tc17, Th17.1, Tc17.1) as well fully differentiated ($CCR7^{-}$) Th2 and Tc2 cells and pre-th2 and Tc2 cells expressed significantly more FPR2 in PsA. The greatest statistical difference between PsA and HC sample was observed in $CD8^{+}$ central memory, naïve and Tc2 cells ($P<0.0001$).

A

ANXA1 surface Expression

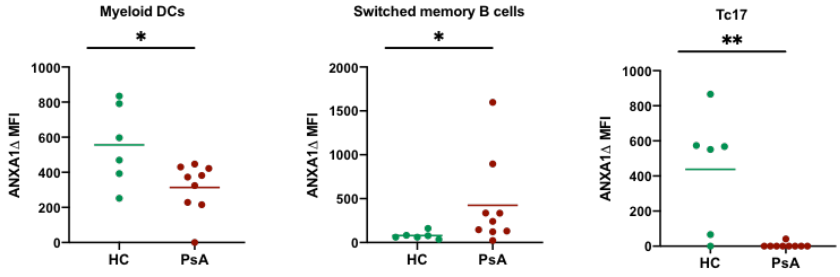

B

FPR1 surface Expression

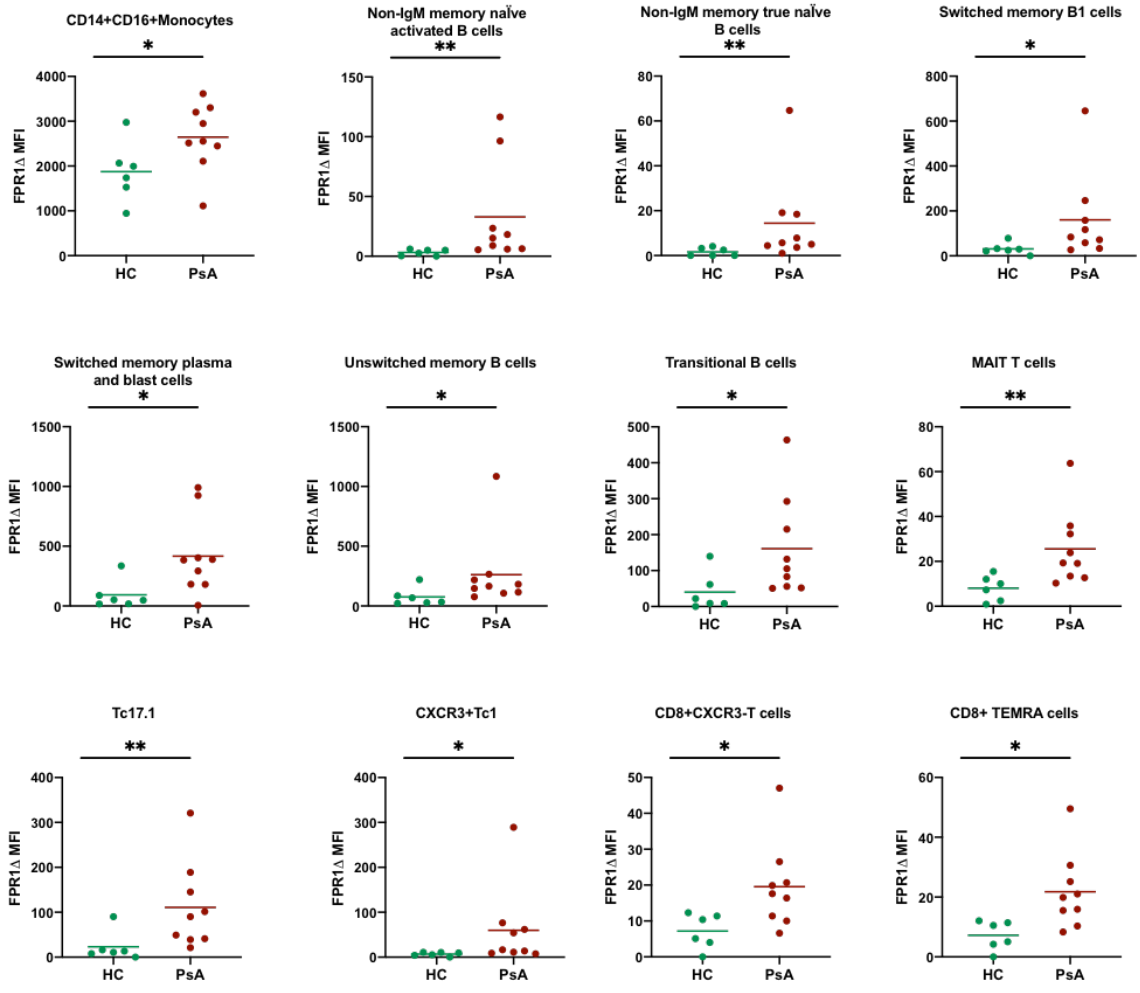

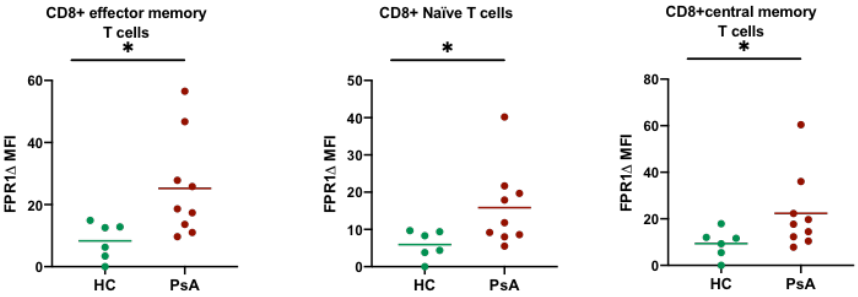

C

FPR2 surface Expression

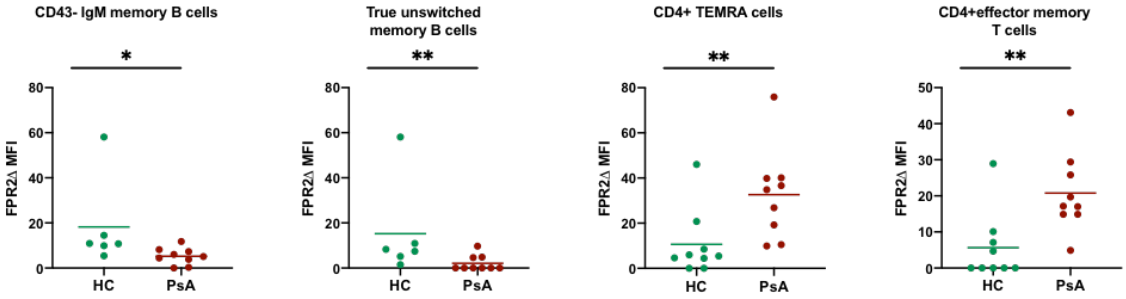

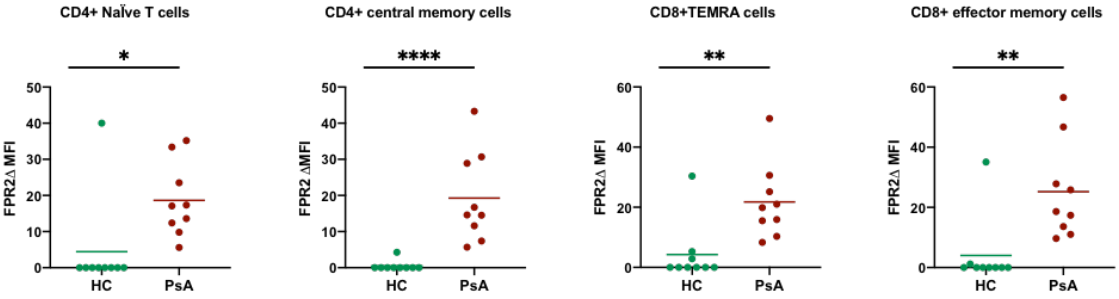

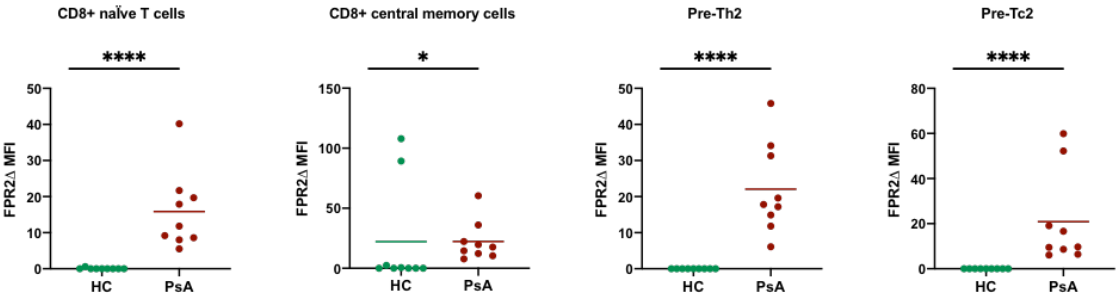

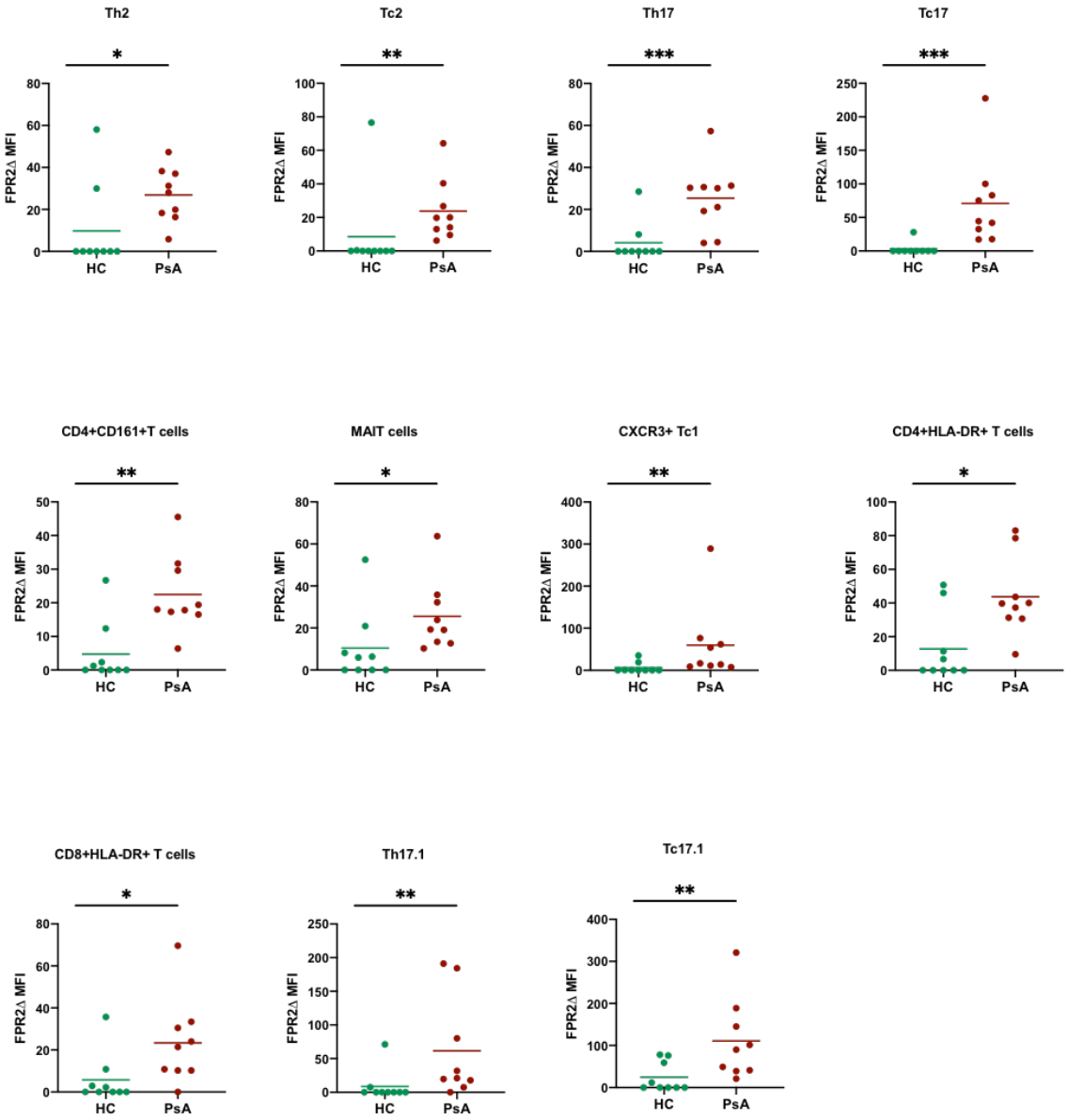

Figure 4.7 Surface expression of ANXA1 and its receptors is altered in a cell-specific manner in PsA

Graphs showing differences in **Δ** MFIs for (A) ANXA1 (B) FPR1 and (C) FPR2 between healthy control and PsA patient samples. The non-parametric Mann Whitney U test was used to determine significance (appropriate normality tests were carried out to determine which statistical tests to use). Graphs were produced and statistical tests were carried out using GraphPad Prism (v9) software. HC N=6,PsA N=9. * $p<0.05$, **$p<0.01$,***$p<0.001$

Recent evidence has emerged suggesting that levels of circulating ANXA1 could be a useful biomarker in several inflammatory diseases, such sepsis and chronic obstructive pulmonary disease (COPD)[326-328]. Based on this, the levels of ANXA1 in HC and PsA plasma samples were analysed to see if there were any significant differences in ANXA1 expression between the groups. Plasma samples collected from the same PsA patients (with the exception of HC1 and PsA5) as used for flow cytometry analysis in results section 4.5 and 4.6, alongside 3 extra (age-matched) healthy control samples were analysed. Two HC and one PsA sample were outside of the detectable limits of the assay and could not be re-tested due to low sample availability (see materials and methods section 2.5.1 for information on standards and assay range). Concentrations of ANXA1 ranged from 8-401 ng/ml in HC samples and from 6-1976 ng/ml in PsA samples, with substantial variation between donors. There was no significant difference in plasma ANXA1 expression between HC and PsA samples (Figure 4.8). Further analysis with more age-matched controls will prove useful in confirming this result (in some instances, small sample sizes can increase the chance of important biological differences being missed).

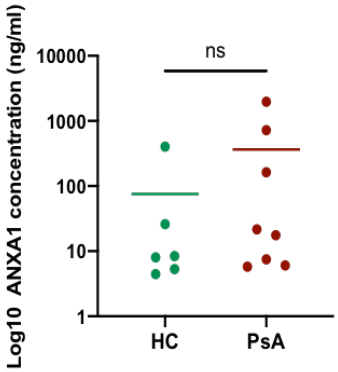

Figure 4.8 No significant difference in plasma ANXA1 expression between PsA and HC samples

Graph showing the concentration of ANXA1 (ng/ml) in the plasma of HC and PsA samples. Samples producing signals greater than that of the highest standard were diluted and reanalysed if enough sample was available (HC5 and HC6 values were out of the detectable range of the ELISA (>400ng/ml) and could not be repeated due to low sample availability. A non-parametric Mann-Whitney U test was performed to determine statistical significance. HC N=6, PsA N=8. Graphs were produced and statistical tests conducted using GraphPad Prism (v9) software.

In summary, this data has identified nuances in ANXA1, FPR1 and FPR2 surface protein expression in PsA that appear to be cell type specific. FPR1 appears to be upregulated on specific adaptive immune cell types in PsA samples, whereas whether ANXA1 and FPR2 are up or downregulated in PsA is dependent on the innate or adaptive immune cell type they are expressed on. Additional studies investigating FPR1/FPR2-ANXA1 signalling mechanisms would prove useful for understanding these nuances in expression. Differences in circulating ANXA1 expression are not apparent in PsA compared to HCs, however further samples are needed to confirm this result. Additionally, power calculations are needed to determine the ideal sample size needed to for optimal significance testing of this experiment.

4.2.4 Assessment of the correlative relationship between ANXA1, FPR1 and FPR2 expression and clinical markers of disease activity

The Disease Activity Index for Psoriatic Arthritis (DAPSA) is a routine measurement of disease activity in PsA. It takes into account the number of swollen (out of 66) and tender (out of 68) joints, the level of pain (in the form of a visual analogue scale or VAS) and serum markers of inflammation (CRP and ESR) [115] (see table 1.1 in introduction section 1.32 for a summary of disease scores and interpretations). Having identified altered FPR1 and FPR2 gene and protein expression in PsA, as well as altered ANXA1 protein expression, (Figures 4.1 and 4.7), it was important to assess the correlative relationship between ANXA1, FPR1 and FPR2 gene and protein expression and DAPSA scores.

For the patients used for the (PsA L) RNA sequencing data, information on ESR, CRP and swollen joint count (SJC) and tender joint count (TJC) was assessed as DAPSA scores were not available. It is worth noting that not all the clinical features were available for all the patients (e.g some CRP values were missing and some ESR values were missing).There was no significant correlation between ANXA1, FPR1 or FPR2 gene expression and ESR, CRP, or the number of swollen or tender joints (Figure 4.9A-4.9C). However, it is important to note that this data is only preliminary; due to the small sample size, the spearman's correlation coefficient (R) is easily swayed by outliers, therefore, this data needs to be confirmed in a larger, independent cohort.

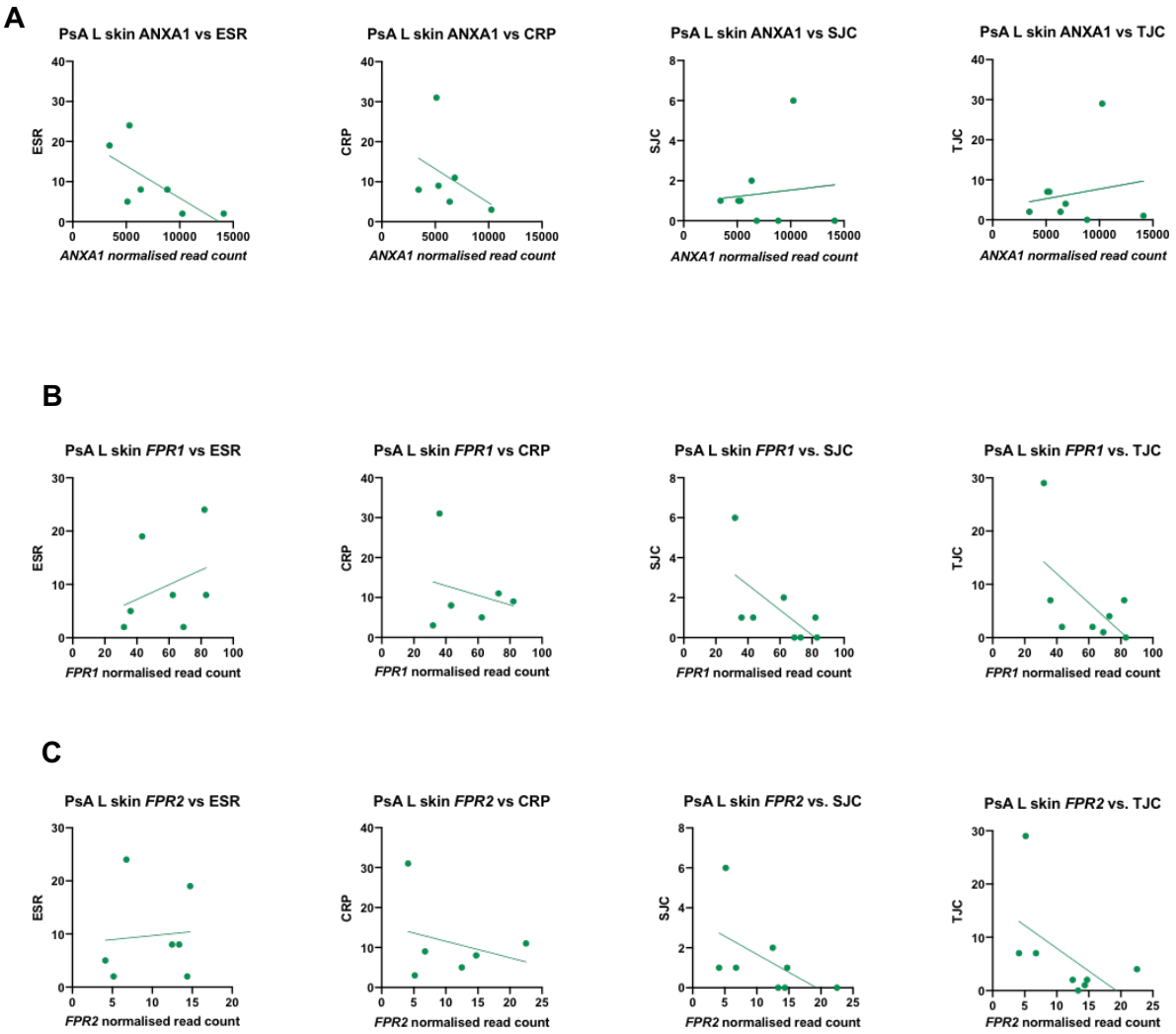

Figure 4.9 ANXA1, FPR1 and FPR2 gene expression in PsA L skin do not correlate with clinical markers of disease activity

ESR, CRP, SJC and TJC were plotted against gene expression of (A) ANXA1, (B) *FPR1* and (C) *FPR2.* A Spearman's rank correlation coefficient was calculated(R), and the linear regression of the data was plotted. PsA samples N=9, however ESR and CRP scores were not available for all of the PsA patients. Graphs were produced and correlation analysis was conducted using GraphPad Prism (v9) software.

It was then decided to assess whether there were any significant correlations between ANXA1, FPR1 and FPR2 surface protein expression and disease activity. For a more focused approach, the cell populations were limited to those which had shown significant changes in these proteins in PsA (Figure 4.7). The correlative relationships of ANXA1, FPR1 and FPR2 surface expression and DAPSA were assessed (Figure 4.10).

There was no correlation between DAPSA and ANXA1 or FPR2 expression on any of the cell populations assessed (Figures 4.10A and 4.10C). FPR1 surface expression positively correlated significantly with DAPSA on activated switched memory B1 cells, and transitional B cells (Figures 4.10B). However, it is worth noting that this is preliminary analysis; due to the low sample size and the probability that outliers are skewing the correlation analysis, these results need to be confirmed in a larger, independent cohort. Additionally, power calculations are needed to determine the ideal sample size needed to for optimal significance testing of this experiment.

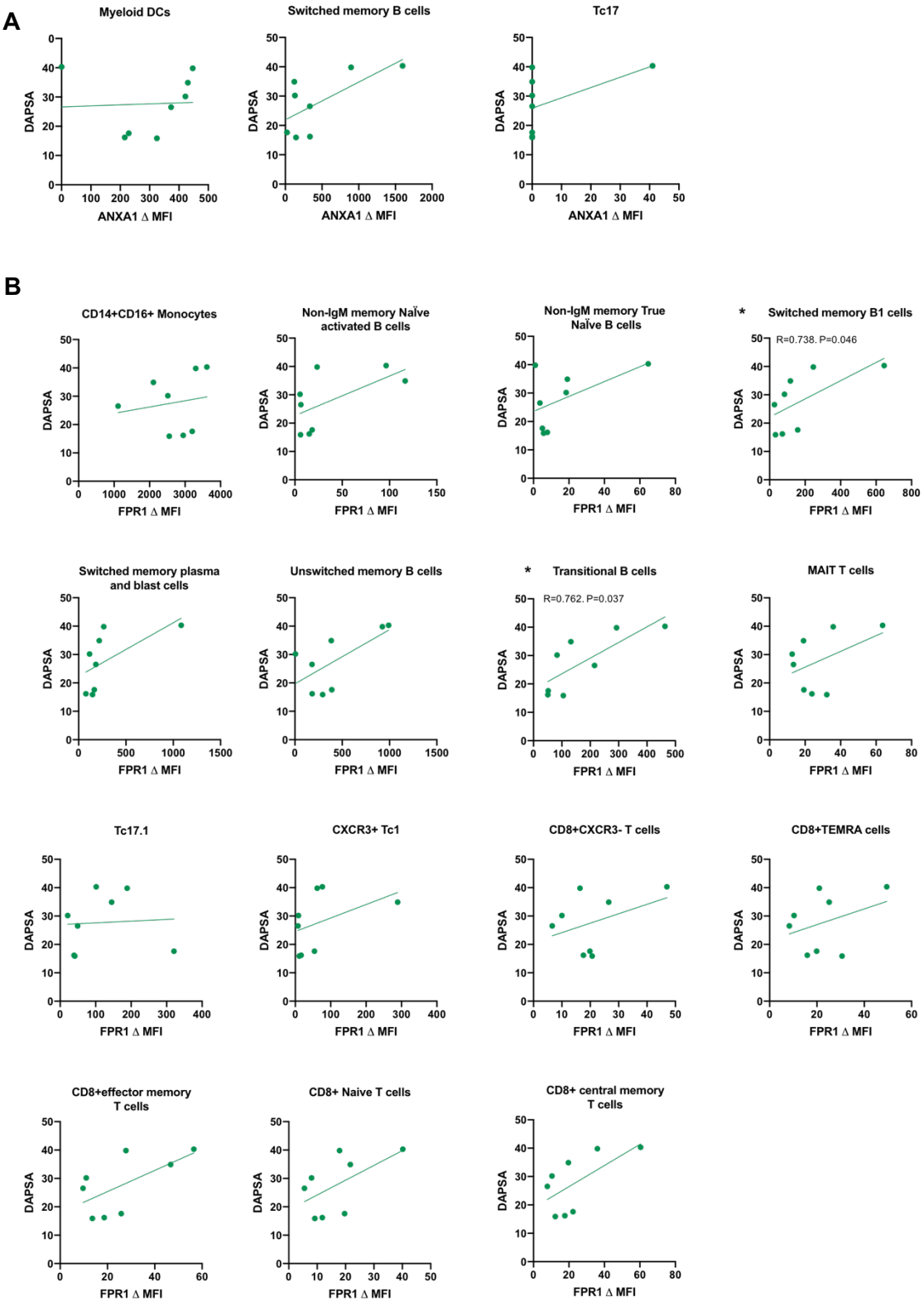

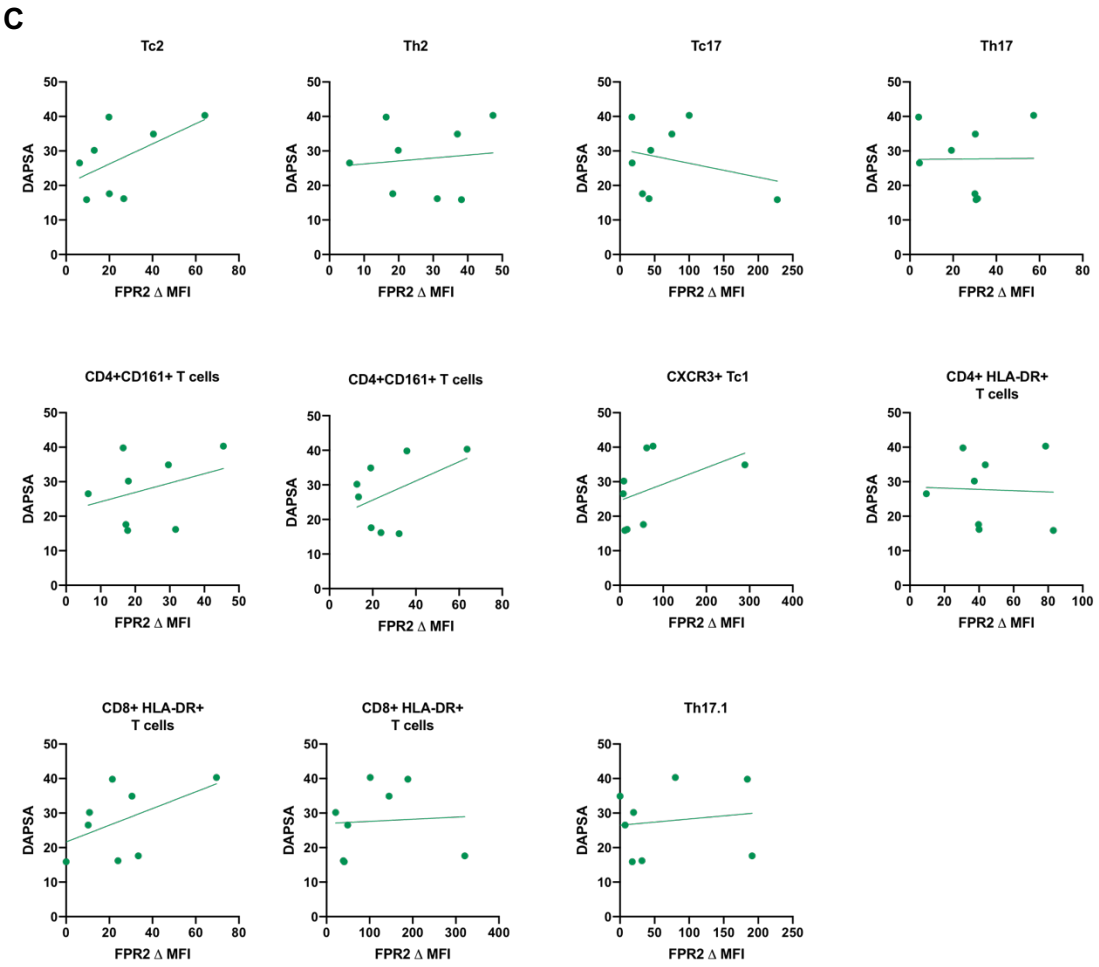

Figure 4.10 FPR1 surface expression on certain B cell subsets correlates with DAPSA

The Δ MFI of (A) ANXA1, (B) FPR1 and (C) FPR2 expression in cell populations identified in figure 4.7 was plotted against the PsA disease activity index, DAPSA. Spearman's rank correlation coefficient was calculated(R), and the linear regression of the data was plotted. Cell populations in which surface expression was identified as having a significant correlation with DAPSA are marked with an asterisk and P and R values shown. PsA N=8 (DAPSA score was not available for one patient). Graphs were produced and correlation analysis was conducted using GraphPad Prism (v9) software.

4.2.5 Investigation of FPR1 signalling in the THP-1 cell line

Based on surface expression data (Figure 4.6) showing that monocytes are high expressors of ANXA1, experiments were conducted to assess the effects of the anti-ANXA1 antibody, MDX-124, on the THP-1 monocytic cell line. These cells originate from a patient with acute monocytic leukaemia and have been used widely in the field to investigate the function and regulation of monocytes and macrophages[243].

A common method of differentiating THP-1 cells into macrophage-like cells is to stimulate with phorbol-12-myristate-13-acetate (PMA). After differentiation with PMA, THP-1 cells change from rounded non-adherent monocyte-like cells to adherent, spindle-shaped macrophage-like cells (Figure 4.11A). Additionally, upregulation of CD11b and CD14 has been shown to occur upon differentiation of THP-1 cells with PMA[329]. To confirm this, THP-1 cells were evaluated for CD11b and CD14 expression before and after differentiation. Results showed an upregulation in the percentage of CD11b (~11% to ~99%) and CD14 (~1% to ~23%) positive cells after differentiation (Figure 4.11B). In addition, THP-1 cells were assessed for their expression of FPR1 and FPR2 during the differentiation process (Figure 4.11C). In general, the frequency of FPR1 and FPR2 positive (undifferentiated) THP-1s was low (<1%). The frequency of FPR1 positive cells increased throughout the differentiation process from day 3 (~2%) to day 7 (~9%), whereas the frequency of FPR2 positive cells remained low on days 3 and 7 (<1%).

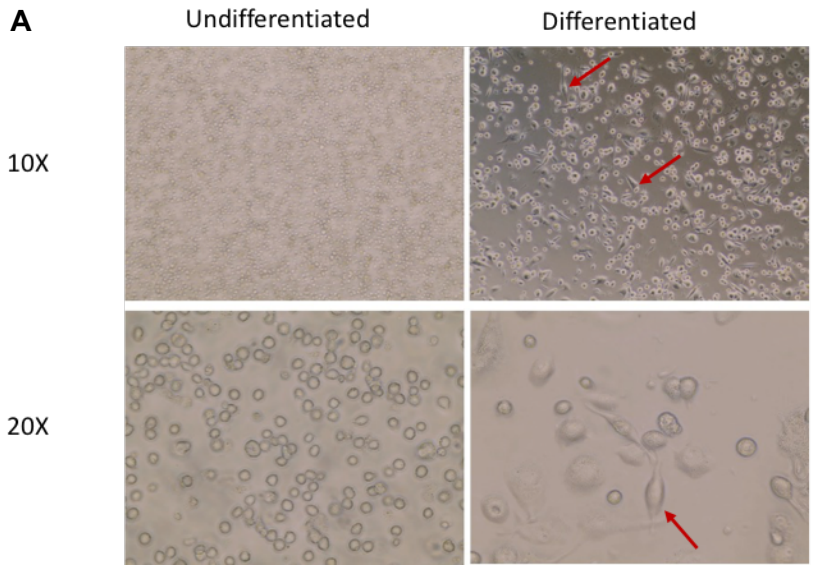

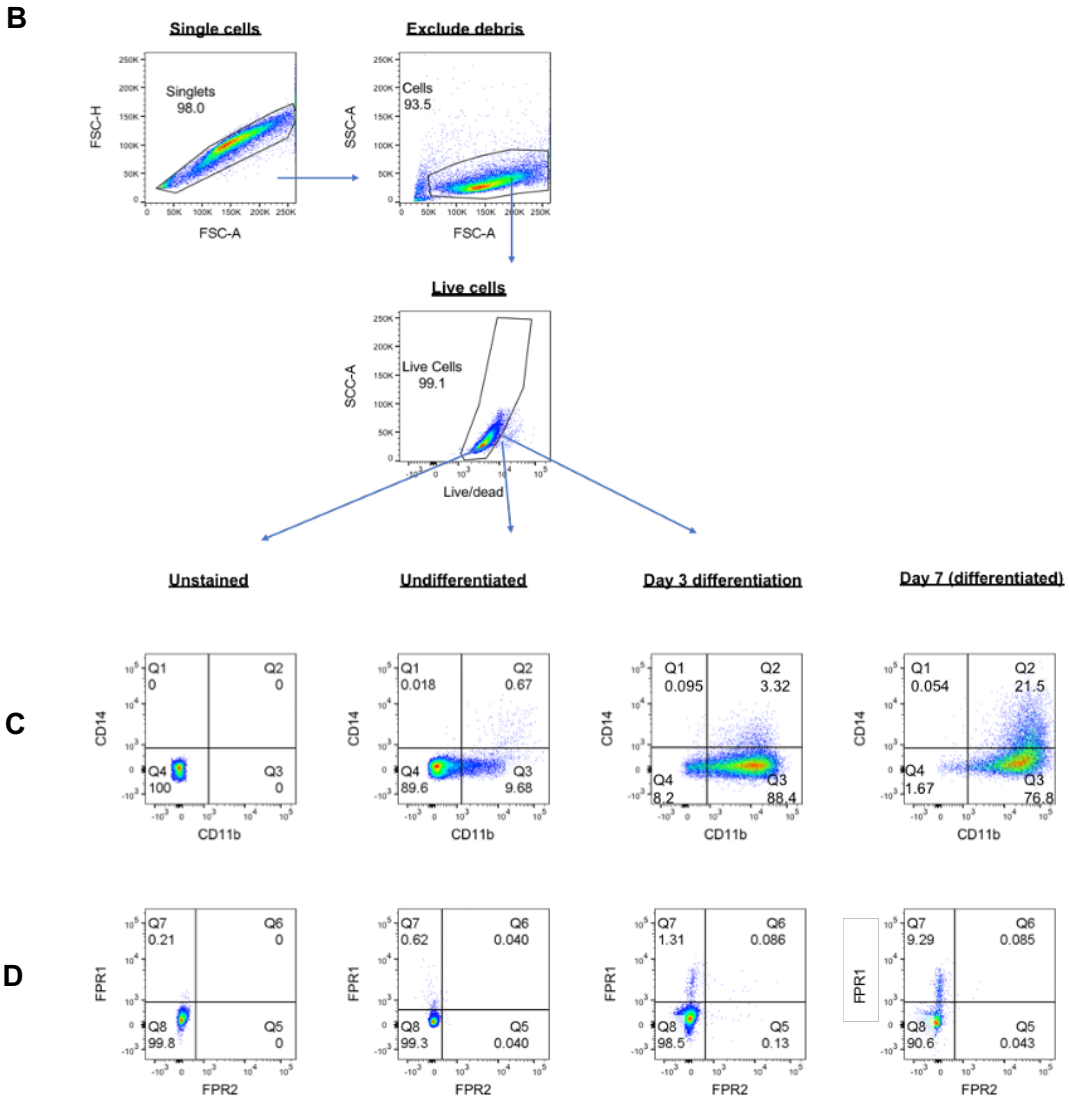

Figure 4.11 Differentiation of THP-1s into macrophage-like cells

(A) Undifferentiated THP-1s are round, non-adherent, monocyte-like cells.THP-1s were differentiated with 50ng/ml of PMA for 3 days and rested for 7 days to form adherent, spindle-shaped cells (B)Cells were stained with anti-CD11b, anti-CD14, anti-FPR1 and anti-FPR2 antibodies and washed in FACS buffer before running on the LSR II flow cytometer. The gating strategy used identified single cells, excluded debris from these cells and then gated the live cells from this. (C) Live cells were then gated for CD11b and CD14 expression as well as (D) FPR1 and FPR2 expression. Representative plots of staining from undifferentiated THP-1s and THP-1s from day 3 and day 7 (fully differentiated) of the differentiation process are shown. Unstained control plots for each stain are shown. N=1 representative data of N= 3 technical replicates. FACS plots were produced using FlowJo (v 10.6.1) software.

Before assessing the effects of MDX-124 on differentiation of THP-1 cells, initially, the effect of adding MDX-124 to undifferentiated THP-1 cells was assessed. Firstly, an initial staining experiment was carried out to ensure THP-1 cells expressed ANXA1 on their surface. The gating strategy showing ANXA1^{+} THP-1s is shown below (Figure 4.12A). Surface expression on unstimulated THP-1s was low (1.36%), however this was similar expression to that seen on unstimulated primary monocyte populations (Chapter 3, Figure 3.14).

MDX-124 was added to THP-1 cells for 24, 48 and 72 hours(hrs). The cells were then assessed for any changes in CD11b and CD14 surface expression as well as expression of the ANXA1 receptors FPR1 and FPR2, compared to control samples (without MDX-124). Addition of MDX-124 to THP-1 cells was not associated with any apparent difference in surface expression of CD11b, CD14, FPR1 or FPR2 at any of the timepoints assessed (Figure 4.12B-D).

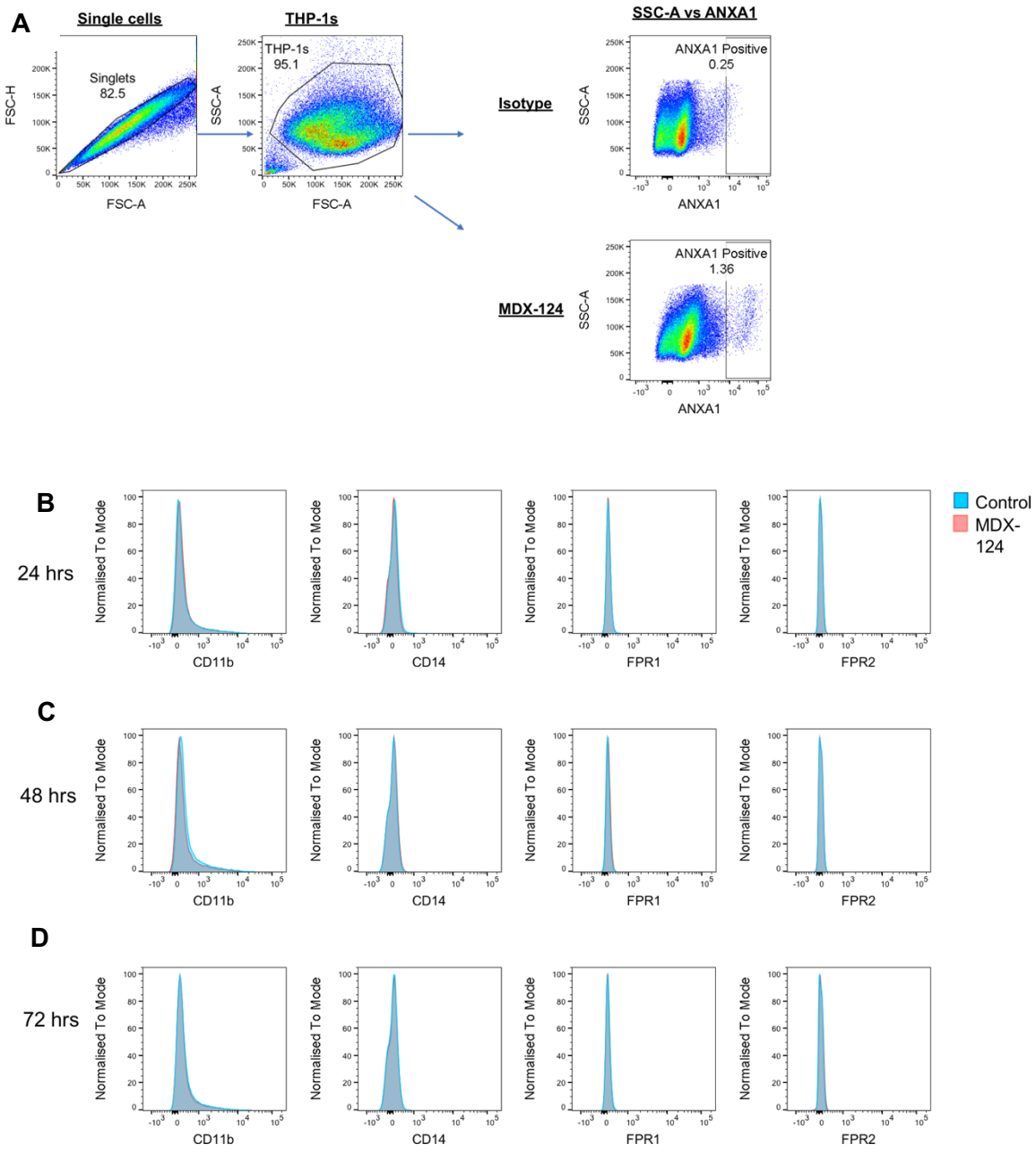

Figure 4.12 MDX-124 has no effect on undifferentiated THP-1 cells

(A) Gating strategy showing THP-1 cells express ANXA1 on their surface. Single cells were gated followed by THP-1 cells and ANXA1 positive cells. Isotype control staining is also shown. THP-1 cells were exposed to 100ng/ml of MDX-124 for (B) 24, (C) 48 and (D) 72 hrs with unexposed THP-1 cells used as controls. Cells were stained with anti-CD11b, anti-CD14, anti-FPR1 and anti-FPR2 antibodies and washed in FACS buffer before running on the LSR II flow cytometer. Three technical repeats were carried out for every condition apart from the 24 hr controls and the FPR1 staining at 72 hours, where only 2 technical repeats were carried out. Histograms were produced using FlowJo (v 10.6.1) software.

Next, the effect of MDX-124 on the differentiation of THP-1 cells was assessed on days 3 and 7. Representative histograms of CD11b, CD14, FPR1 and FPR2 frequency are shown for day 3 (Figure 4.13A) and day 7 (Figure 4.13B). Analysis revealed no change in the frequency of CD11b (Figures 4.13C and 4.13G), CD14 (Figures 4.13D and 4.13H), and FPR2 (Figures 4.13F and 4.13J) positive cells on days 3 and 7. Additionally, there was no change in the frequency of FPR1 positive cells on day 3 (Figure 4.1E), however, a decrease in FPR1 positive cells is seen when the THP-1s were differentiated with MDX-124 on day 7 compared to controls(Figure 4.13I). This shift in FPR1 expression is also evident in the histogram in Figure 4.13B.

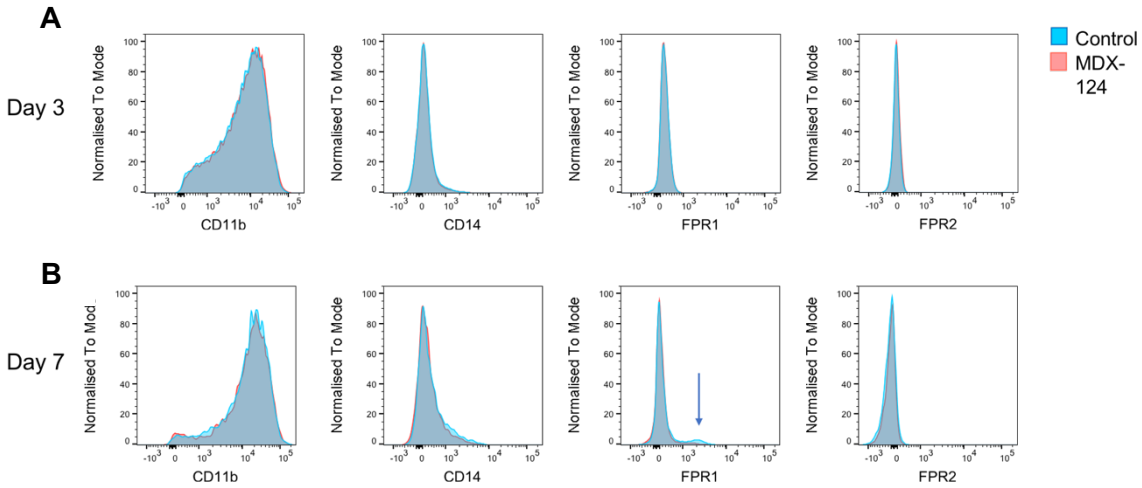

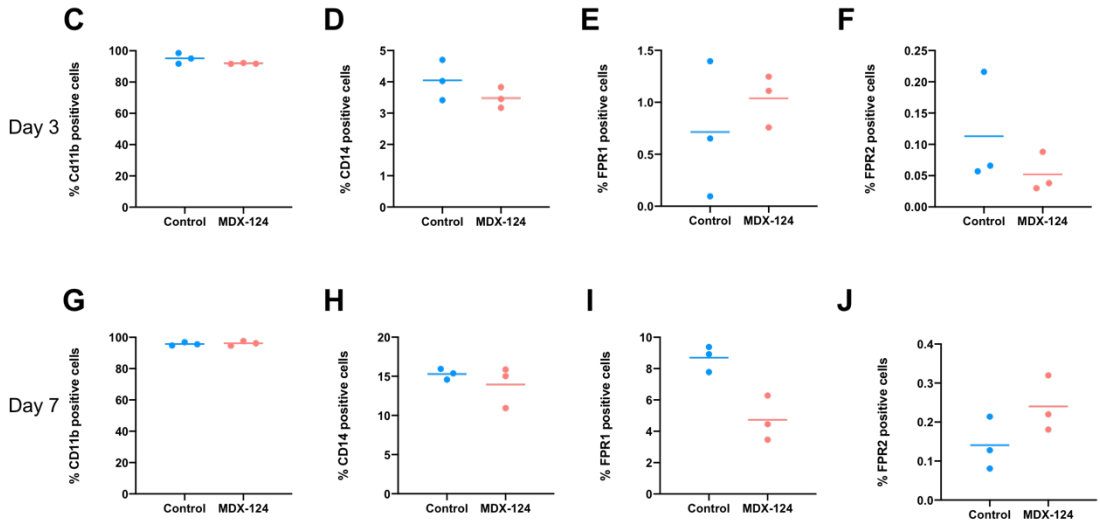

Figure 4.13 Treatment with MDX-124 during the differentiation of THP-1 cells is associated with a downregulation in surface FPR1

THP-1 cells with and without addition of 100ng/ml of MDX-124 were differentiated with 50 ng/ml of PMA for 3 days and rested for a further 4 days to allow them to develop into fully differentiated macrophage-like cells. Cells were stained with anti-CD11b, anti-CD14, anti-FPR1 and anti-FPR2 antibodies and washed in FACS buffer before running on the LSR II flow cytometer. Representative histograms of staining at (A) day 3 and (B) day 7 are shown. Arrow highlights the FPR1 positive population at day 7. (C-J) Graphs plotting % positive staining for each of the technical replicates carried out are shown (N=3) alongside the mean % positive staining. Histograms were produced on FlowJo (v 10.6.1) software and graphs were produced on GraphPad Prism (V9) software.

After identifying that addition of MDX-124 to THP-1 cells was associated with a decrease in the percentage of FPR1 positive cells on day 7, it was key to investigate any potential signalling that MDX-124 could be inducing in these cells which might be associated with downregulation of FPR1. A common way to identify differences in cell signalling is to measure the level or activity of protein kinases. Protein kinases are enzymes involved in the phosphorylation and hence modulation of proteins involved in several biological signalling pathways, from growth to apoptosis[330].

Phosphorylated (and hence activated) protein kinase levels were assessed in lysates from day 7 THP-1 cells differentiated with MDX-124 (100ng/ml) and compared to lysates from control (unexposed) cells using the R&D Systems Proteome Profiler™ human phospho-kinase array kit[331]. The location and position of each of the analytes assessed as well as MDX-124-treated and control blot images are shown in Figures 4.14A and 4.14B. Differences between MDX-124 exposed and control groups were expressed in terms of fold change in signal detected from the assay (Mean pixel density). Similar to methods used in other

research groups with this assay[332], fold changes of greater than 1.5 were considered upregulated.

Amongst all of the phosphokinases assessed, the highest expressed phosphokinases in both MDX-124-treated and control cells were Signal Transducer and Activator of Transcription (STAT)a/b and p38α mitogen activated protein (MAP) kinase (Figure 4.14C), both of which have been implicated in the regulation of inflammation[333,334]. Analysis of fold change revealed that a total of 11/34 phosphokinases assessed were upregulated in THP-1 cells differentiated with MDX-124 compared to control cells (Figure 4.14D). The greatest fold increase in MDX-124 treated cells was in Chk-2, which is a key component of the DNA damage response[335]. MDX-124-treated THP-1s were associated with increases in phosphokinases associated with cell survival (p70 S6 Kinase[336]), growth (AKT 1/2/3[337]) and regulation of inflammation (GSK-3α/β[338] and STAT2[338]) as well as cell proliferation and apoptosis (JNK1/2/3, c-Jun, p53[339]). Additionally, increased ERK/1/2 expression was observed in MDX-124 treated cells. The ERK1/2 pathway is involved in many of the processes mentioned above, including survival, proliferation and differentiation[340].

This data is reflective of other studies showing that downregulation of FPR1 in cell lines subjected to inflammatory stimuli was associated with decreased apoptosis and improved survival, through regulation of the MAP kinase pathway.[341] Additionally, ANXA1 has been shown to regulate inflammation through modulation of MAP kinase signalling[56]. This allows for speculation that MDX-124 binding to ANXA1 could somehow be preventing ANXA1-FPR1-mediated regulation of the pro-inflammatory and pro-apoptotic functions of the MAP Kinase pathway, through a mechanism not yet understood.

A

A	1&2	3&4	5&6	7&8	9&10	B	11&12	13&14	15&16	17&18
A	Reference Spot						Akt 1/2/3	Akt 1/2/3		Reference Spot
B		CREB	EGF R	eNOS	ERK1/2		Chk-2	c-Jun		
C		Fgr	GSK-3α/β	GSK-3β	HSP27		p53	p53	p53	
D		JNK 1/2/3	Lck	Lyn	MSK1/2		p70 S6 Kinase	p70 S6 Kinase	PRAS40	
E		p38α	PDGF Rβ	PLC-γ1	Src		PYK2	RSK1/2	RSK1/2/3	
F		STAT2	STAT5a/b	WNK1	Yes		STAT1	STAT3	STAT3	
G	Reference Spot	β-Catenin			Negative control		STAT6	HSP60		Negative control

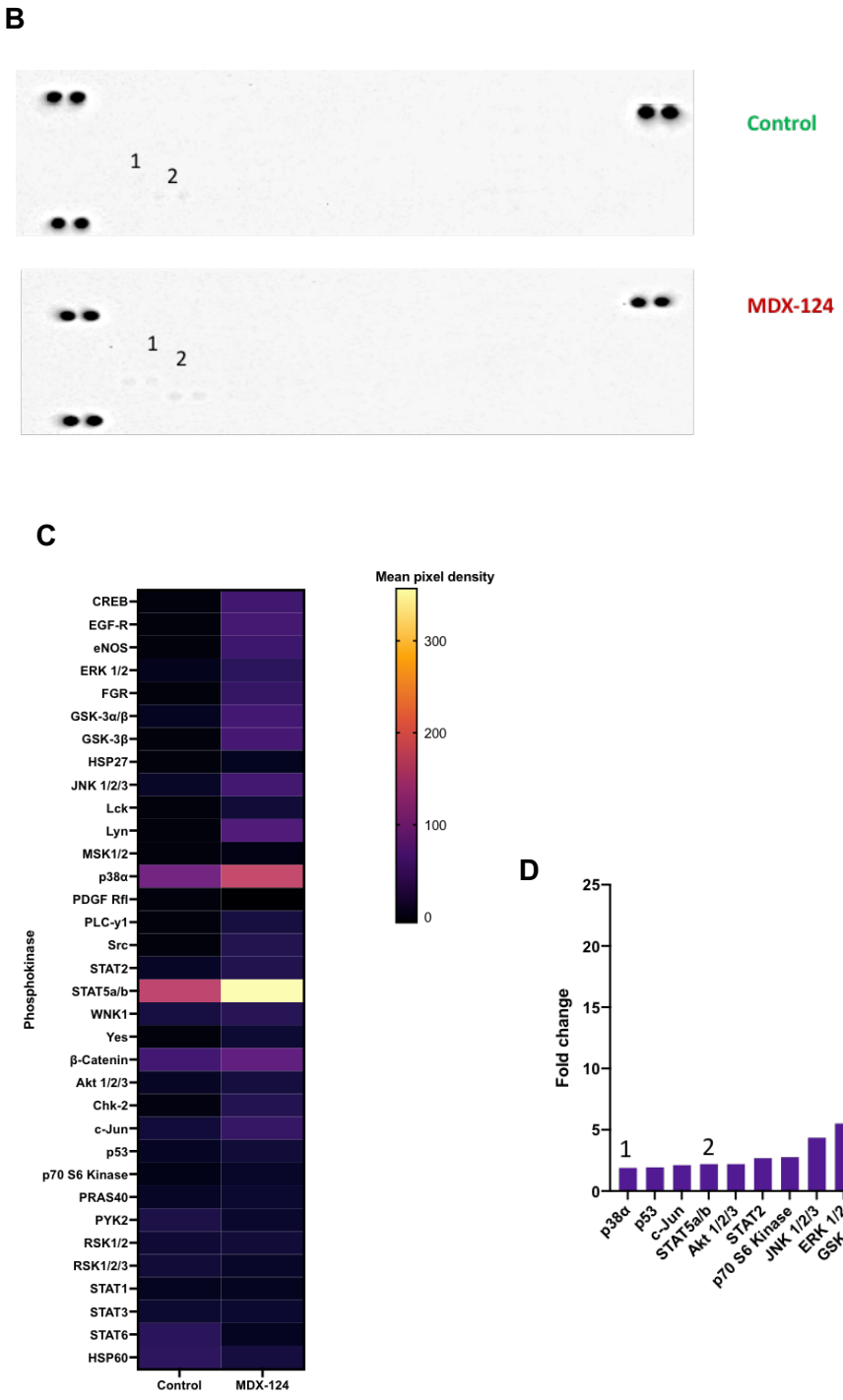

Figure 4.14 Treatment with MDX-124 during the differentiation of THP-1 cells is associated with increased production of several phosphokinases

THP-1 cells were differentiated with 50 ng/ml of PMA and for 3 days and rested for a further 4 days to allow them to develop into fully differentiated macrophage-like cells.100ng/ml of MDX-124 was added for the duration of the differentiation process (7 days). Cells that were unexposed to MDX-124 were used as controls. Cells were serum starved for 24 hrs before stimulation with cell stimulation cocktail for 5 minutes to induce phosphokinase production. Lysates were collected and analysed for phosphokinase production. Protein in the lysates was quantified using BCA assay. (A) shows the location and well numbers of the 34 analytes assessed over the two membranes (A and B) for each condition as well as positive control reference spots and negative control spots. Upregulated=red (B) shows images of the MDX-124- treated and control blots and highlights top expressed analytes (1=p38 and 2=STATa/b).(C) Heatmap showing mean pixel densities of the 34 phosphokinases assessed in MDX-124-treated and control groups (D) fold changes in 11 phosphokinases identified as upregulated (>1.5) in MDX-124-treated cells. 1 and 2 correspond to the highlighted analytes in (B). Image analysis of blots was conducted using Quick Spots software from Western Vision and graphs were produced using GraphPad Prism (v9) software.

In order to investigate whether MDX-124 had any impact on extracellular signalling in addition to intracellular signalling, the supernatant of MDX-124-treated cells was collected on day 7 and assessed for production of several cytokines, chemokines, growth factors and acute phase proteins simultaneously, and compared to supernatant from control cells.

A total of 32/102 cytokines assessed were upregulated (fold change >1 .5) in the THP-1 cells exposed to MDX-124. Upregulated analytes and their corresponding positions are recapitulated in Figure 4.15A. Analytes were grouped into 'cytokine and chemokines', 'growth factors' and 'other soluble proteins, receptors and enzymes' to allow better categorisation of the effects of addition of MDX-124 to THP-1 cells during differentiation. Images of the individual blots of control and MDX-124-treated cells can be seen in Figure 4.15B. The majority (46.9%) of upregulated proteins produced by MDX-124-treated cells were in the cytokine and chemokine group, followed by other soluble proteins, receptors and enzymes (31.2%) and growth factors (21.9%) (Figure 4.15C).

MDX-124 treatment of THP-1s was associated with an increase in several cytokines associated with monocyte function (Figure 4.15D). The monocyte-derived cytokine, resistin, exhibited the highest signal in the MDX-124-treated group. This cytokine is recognised as an important meditator of chronic inflammation in monocytes and macrophages, and has interestingly been shown to be induced by leptin, another differentially expressed protein in MDX-124-treated cells[342,343]. Furthermore, interleukin (IL)-34, a cytokine involved in monocyte and macrophage survival and differentiation[344], had the highest fold increase in in MDX-124-treated cells compared to controls. This supports the data in Figure 4.14 showing an increase in intracellular (phosphokinase) signalling associated with survival and mediation of inflammation.

MDX-124- treatment was also associated with an increased production in several growth factors related to both monocyte differentiation and proliferation (GM-CSF[345]) and proliferation of cancer cells (fibroblast growth factor (FGF)-7[346]) (Figure 4.15E). Additionally, increased production of several soluble proteins related to cancer signalling was evident in MDX-124-treated cells. This included Kallikrein-3, also known as prostate specific antigen, which is frequently

associated with several cancers including those of the breast, ovary and skin[347] and trefoil factor 3 (TFF3), which is implicated in several pro-cancer processes, including the promotion of growth and invasiveness of cancer cells[348].

A

	1&2	3&4	5&6	7&8	9&10	11&12	13&14	15&16	17&18	19&20	21&22	23&24
A	Reference Spot	Adiponectin	Apolipoprotein A-I	Angiogenin	Angiopoietin-1	Angiopoietin-2	BAFF	BDNF	C5/C5a	CD14	CD30	Reference spot
B		CD40 ligand	Chitinase 3-like 1	Complement Factor D	C-Reactive Protein	Cripto-1	Cystatin	Dkk-1	DPPIV	EGF	EMMPRIN	
C		ENA-78	Endoglin	Fas Ligand	FGF basic	FGF-7	FGF-19	Flt-3 Ligand	G-CSF	GDF-15	GM-CSF	
D	GROα	Growth Hormone	HGF	ICAM-1	IFN-γ	IGFBP-2	IGFBP-3	IL-1α	IL-1β	IL-1ra	IL-2	IL-3
E	IL-4	IL-5	IL-6	IL-8	IL-10	IL-11	IL-12 p7	IL-13	IL-15	IL-16	IL-17A	IL-18 Bpa
F	IL-19	IL-22	IL-23	IL-24	IL-27	IL-31	IL-32	IL-33	IL-34	IP-10	I-TAC	Kallikrein 3
G	Leptin	LIF	Lipocalin-2	MCP-1	MCP-3	M-CSF	MIF	MIG	MIP-1α/MIP-1β	MIP-3α	MIP-3β	MMP-9
H	Myeloperoxidase	Osteopontin	PDGF-AA	PDGF-AB/BB	Pentraxin 3	PF4	RAGE	RANTES	RBP-4	Relaxin-2	Resistin	SDF-1α
I	Serpin E1	SHBG	ST2	TARC	TFF3	TfR	TGF-α	Thrombospondin-1	TNF-α	uPAR	VEGF	
J	Reference Spot		Vitamin D BP	CD31	TIM-3	VCAM-1						Negative Control

B

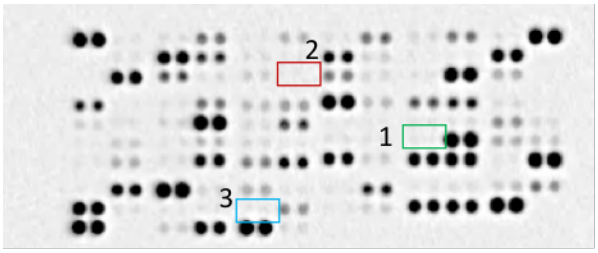

Control

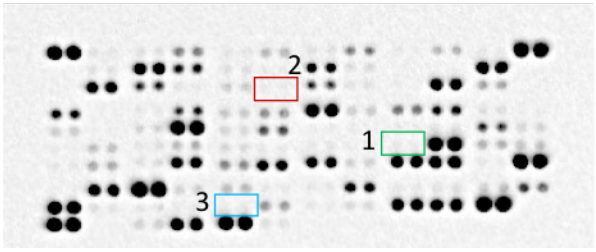

MDX-124

C

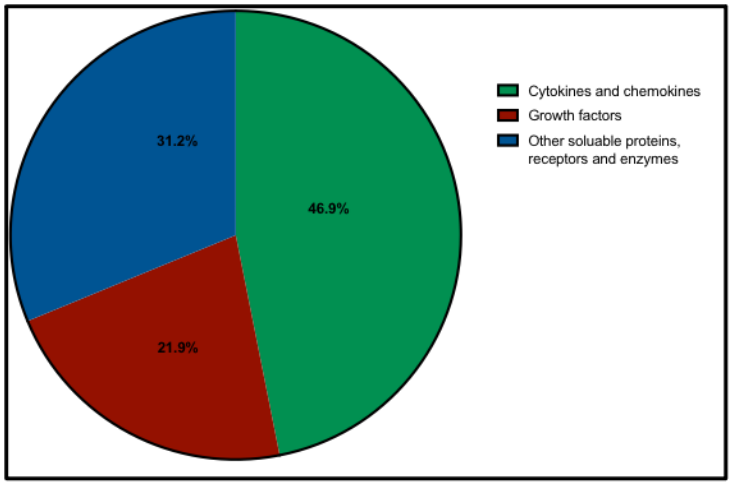

D

Cytokines and chemokines

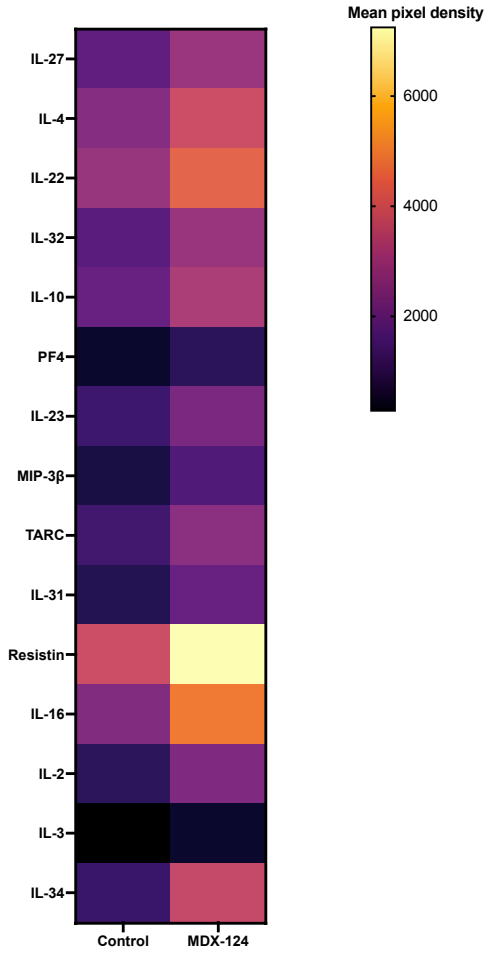

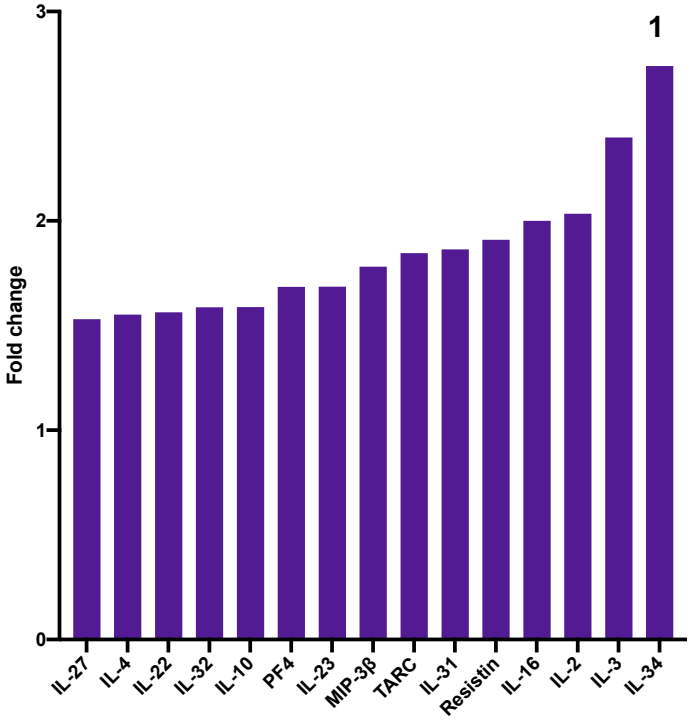

E

Growth factors

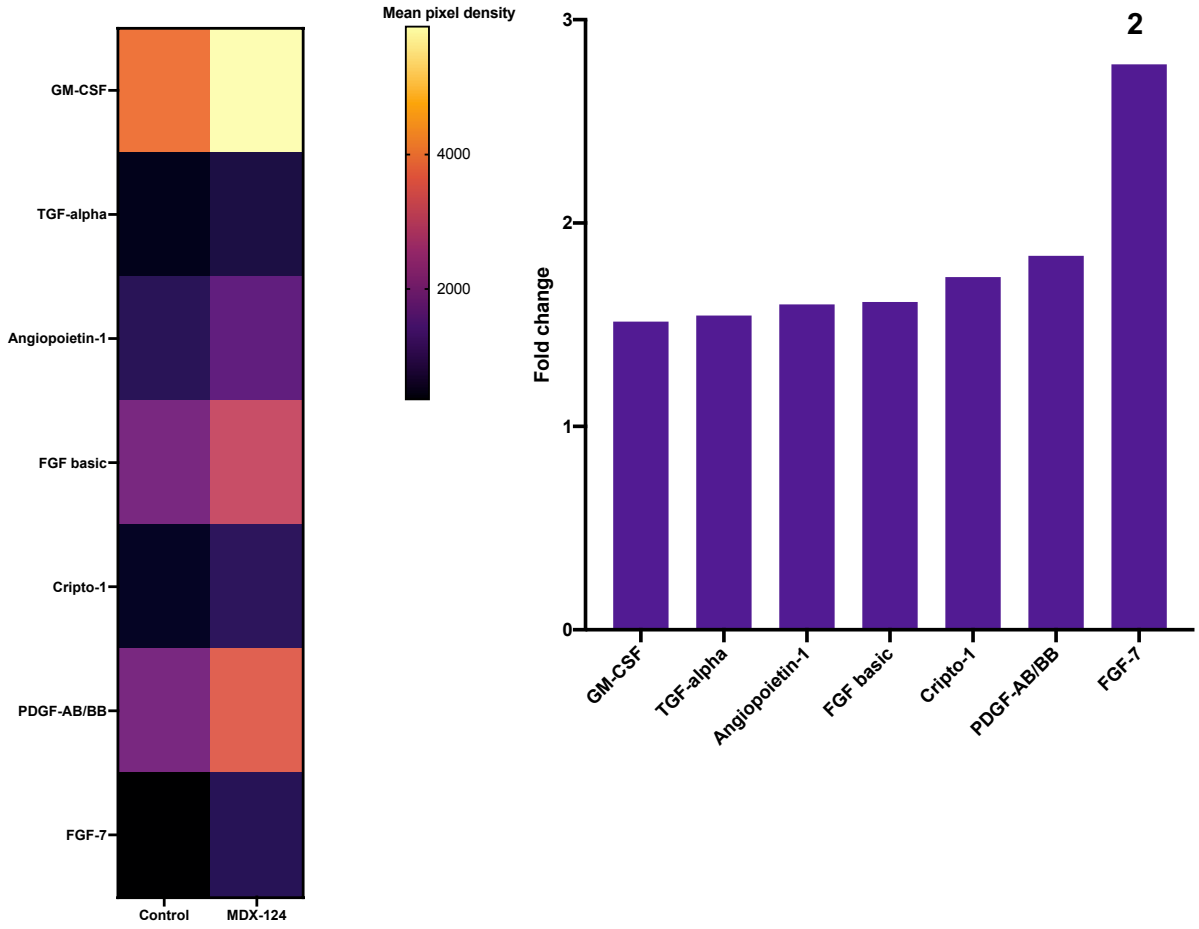

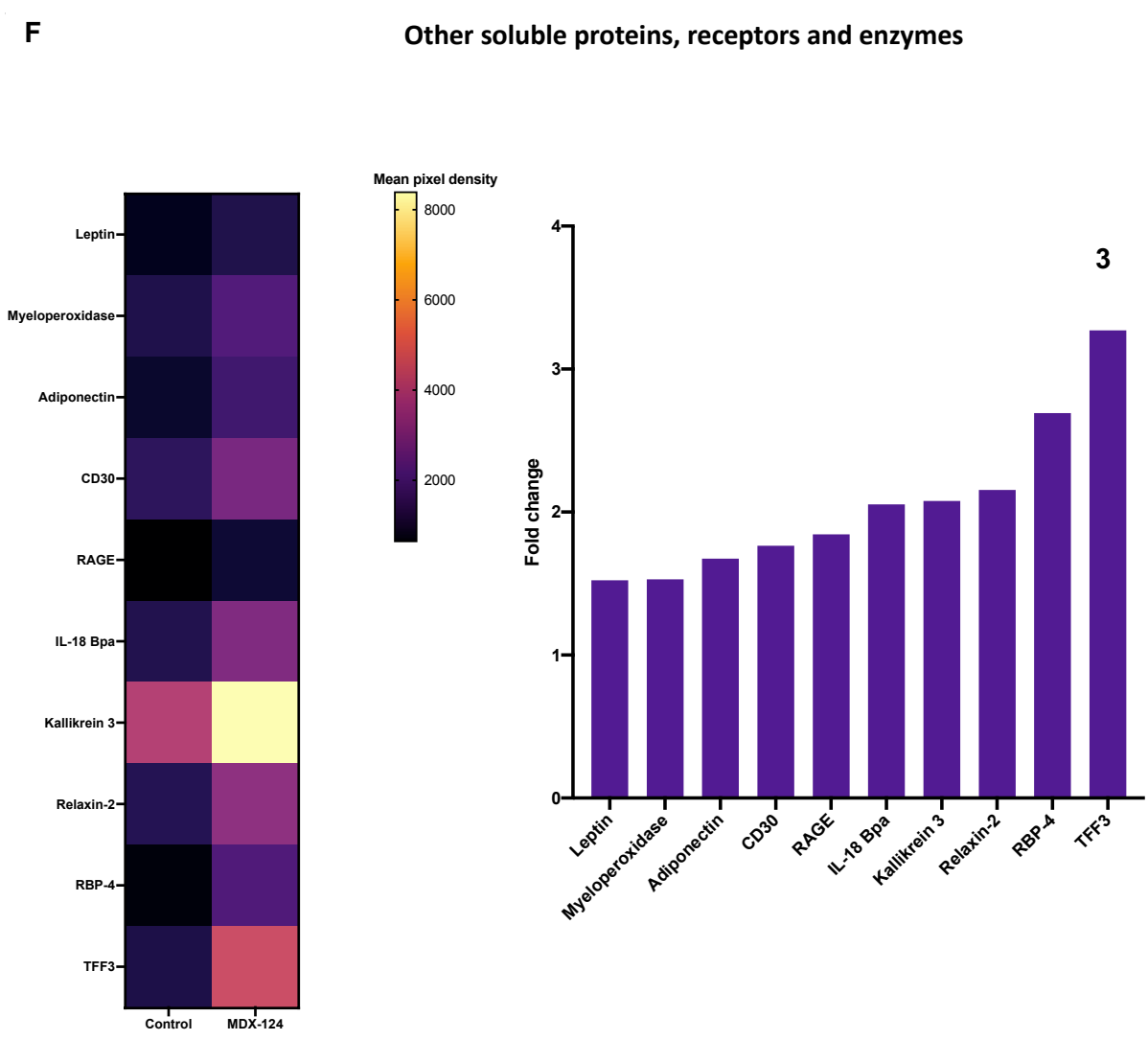

Figure 4.15 Treatment with MDX-124 during the differentiation of THP-1 cells is associated with increased production of cytokines, growth factors and other soluble proteins associated with survival and inflammation

THP-1 cells were differentiated with 50 ng/ml of PMA and for 3 days and rested for a further 4 days to allow them to develop into fully differentiated macrophage-like cells.100ng/ml of MDX-124 was added for the duration of the differentiation process (7 days). Cells that were unexposed to MDX-124 were used as controls. Supernatant was collected on day 7 and analysed for production of 102 analytes using the R&D systems Human Cytokine XL array kit. (A) shows the location and well numbers of the 102 analytes assessed for each condition as well as positive control reference spots and negative control spots. Upregulated=red (B) shows images of the MDX-124-treated and control blots and highlights analytes with the highest fold change in each of the 3 subgroups (1=IL-34,2=FGF-7, 3=TFF3). (C) Pie chart showing the proportion of upregulated proteins in each of the three subgroups. Heatmaps show mean pixel densities and fold changes for upregulated (>1.5-fold change) proteins in the (D)cytokine and chemokine group, (E)growth factor group and (F) other soluble proteins, receptors and enzymes group. Analytes highlighted in (B) are also highlighted in the fold change graphs. Image analysis of blots was conducted using Quick Spots software from Western Vision and graphs were produced using GraphPad Prism (v9) software.

Taken together, this data reflects both the nature of THP-1s as cells of monocytic origin, but also their origin from acute monocytic leukemic cancer cells[349].The signalling that encompasses both the function of THP-1s as monocytic and cancerous cells seems to be enhanced through an MDX-124-asscociated upregulation of intracellular phosphokinases and extracellular signalling proteins associated with cell survival, proliferation, and regulation of inflammation and differentiation. Additionally, addition of MDX-124 during THP-1 cell differentiation is associated with a downregulation in FPR1, through a mechanism that is not understood, but could be related to the enhancement of THP-1 cell survival through kinases such as those involved in the MAP kinase pathway.

An important thing to consider when interpreting this data is that THP-1s, being a homozygous cell line, do not reflect the complex heterogenous nature of primary monocytes, and hence, responses to MDX-124 might not be the same in primary monocytes. Therefore, this data can only be used to inform future experiments in primary monocytes rather than concluding anything about the impact of MDX-124 on their function.

4.2.6 MDX-124 treatment of primary monocytes

To transition the findings in THP-1s back to primary cells, the impact of MDX-124 to primary monocytes in terms of their inflammatory cytokine output was investigated. Of particular interest was the effects of MDX-124 addition to $CD16^{+}CD14^{+}$ monocytes as increased expression of FPR1 had been detected on these cells in PsA samples (Figure 4.7).

With no access to PsA patient samples, an inflammatory setting was mimicked by exposing healthy monocytes to bacterial lipopolysaccharide (LPS). LPS is widely recognised as an activator of monocytes and macrophages and has been used in a range of studies investigating inflammation. This is mostly due to its ability to activate inflammatory cytokines such as TNF-α and IL-6[350].

LPS dosage and exposure time was first optimised with 10ng/ml of LPS for 24 hrs determined as optimal for cytokine production (data not shown). A double

monocyte isolation was carried out; first with a CD16 positive isolation kit (Miltenyi Biotec), then with a CD14 positive isolation kit to obtain $CD16^+$ $CD14^+$ monocytes from PBMCs and allow comparison with the three other main monocyte populations ($CD16^-CD14^-$, $CD16^+CD14^-$, $CD16^-CD14^+$). Cells were primed with 100 ng/ml of MDX-124 overnight and then stimulated with 10 ng/ml of LPS for 24 hrs. Cell supernatant was collected and analysed for production of the inflammatory cytokines IL-6 and TNF-α (see materials and methods section 2.5.1 for information on standards and assay range). Cytokine levels were assessed upon addition of LPS alone, MDX-124 antibody (AB) treated alone and MDX-124 in combination with LPS compared to an unstimulated control.

Consistent with other studies showing that IL-6 production in primary cells is enhanced in response to LPS[351], $CD14^+$ $CD16^+$ monocytes treated with LPS alone produced significantly more IL-6 compared to unstimulated controls (Figure 4.16A). However, this increase more than doubled upon addition of MDX-124 (From~10pg/ml in unstimulated controls to~80pg/ml with LPS alone to ~209pg/ml in LPS and MDX-124 treated cells). This significant increase in IL-6 production is induced with LPS (7pg/ml) in $CD14^-$ $CD16^-$ monocytes but not with addition of MDX-124(50pg/ml) (Figure 4.16B). No significant changes in IL-6 production are evident in any of the conditions tested in $CD14^-$ $CD16^+$ monocytes (Figure 4.16C). In general, $CD14^+CD16^-$ monocytes produced more IL-6 than any of the other monocyte populations assessed (Figure 4.16D). $CD14^+CD16^-$ monocytes treated with LPS alone (595pg/ml) and in combination with MDX-124 (574pg/ml) produced significantly more IL-6 compared to addition of MDX-124 alone(7pg/ml), whereas only LPS in combination with MDX-124 was associated with a significant increase in IL-6 production compared to unstimulated controls(24pg/ml).

Consistent with other studies showing that TNF- α production in primary cells is enhanced in response to LPS[352], $CD14^+CD16^+$ monocytes produced significantly more TNF-α than unstimulated controls (11pg/ml) when exposed to LPS(27pg/ml), however, this increase was enhanced with addition of MDX-124(210pg/ml) (Figure 4.16E). $CD14^-CD16^-$ monocytes expressed significantly more TNF-α in LPS treated groups(16pg/ml) compared to MDX-124 alone treated groups(4pg/ml), which was also enhanced slightly upon addition of MDX-124 to

LPS (17pg/ml) (Figure 4.16F). Similar to IL-6, no significant changes in IL-6 production are evident in any of the conditions tested in $CD14^{-}$ $CD16^{+}$ monocytes (Figure 4.16G). $CD14^{+}CD16^{-}$ monocytes expressed significantly more TNF-α when treated with LPS (132pg/ml) and LPS in combination with MDX-124(103pg/ml) compared to cells treated with MDX-124 alone(3pg/ml), an effect that seems to be mediated by LPS rather than MDX-124 (Figure 4.16H).

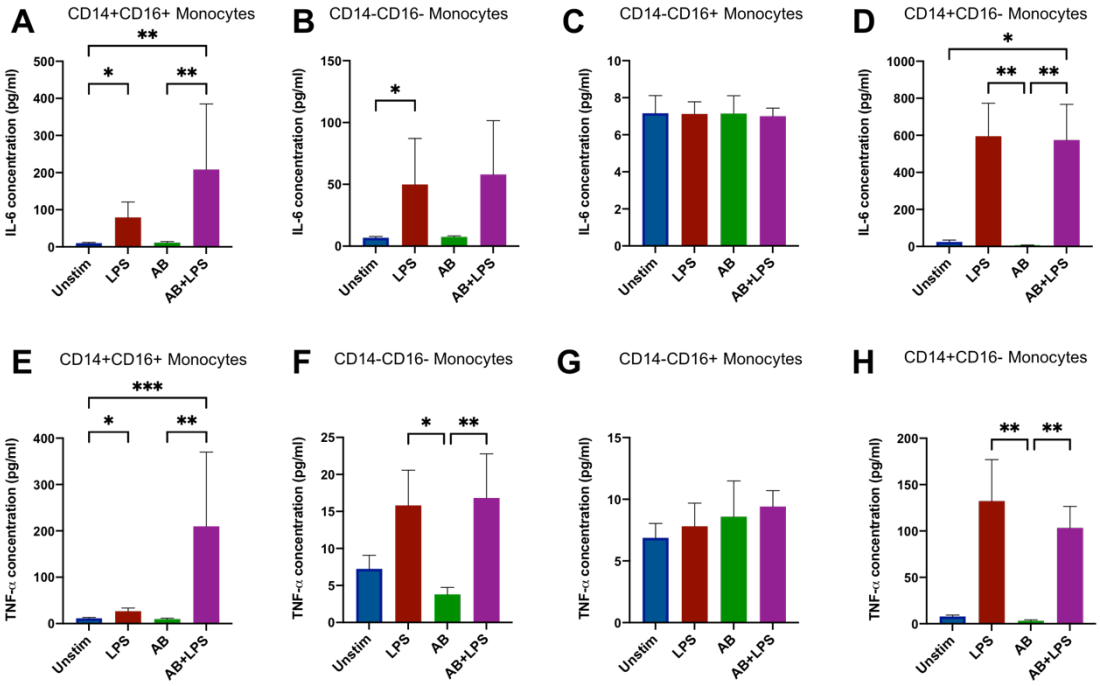

Figure 4.16 Figure 4.16 MDX-124 treatment enhances LPS-associated pro-inflammatory cytokine production in $CD14^{+}$monocyte populations

$CD16^{+}CD14^{-}$, $CD16^{-}CD14^{-}$, $CD16^{+}CD14^{-}$ and $CD16^{-}CD14^{-}$ monocytes were isolated using positive selection kits (Miltenyi Biotec). Cells were primed with 100ng/ml of MDX-124 overnight and then stimulated with 10 ng/ml of LPS for 24 hrs before supernatant was collected for analysis. Graphs show expression levels of in (A-D) IL-6 and (E-H) TNF-α production upon addition of LPS, MDX-124 and LPS in combination with MDX-124 in each of the monocyte cell populations compared to unstimulated controls. All data represent mean ± SEM, n= 5, * $p<0.05$, ** $p<0.01$,*** $p<0.001$. Statistical significance was determined using a non-parametric Friedman's test.

In summation, this data suggests that MDX-124 in combination with LPS can enhance inflammatory cytokine (TNF- α and IL-6) production in primary monocytes compared to treatment with MDX-124 alone. This is evident particularly in $CD14^{+}CD16^{+}$ monocytes, where LPS was shown to enhance MDX-124-associated TNF-α and IL-6 production. This coincides with data in THP-1 cells presented in Figure 4.15, showing an upregulation in inflammatory cytokine production upon addition of MDX-124 to PMA-differentiated THP-1s and suggests addition of MDX-124 to stimulated monocytic cells is associated with an enhanced inflammatory response. Importantly, due to the low sample size

analysed in this set of experiments, conclusions cannot be drawn until these results are confirmed in a larger, independent cohort. Additionally, power calculations are needed to determine the ideal sample size needed to for optimal significance testing of this experiment.

4.3 Discussion

Psoriatic arthritis (PsA) is an extremely heterogenous disease, associated with chronic inflammation and dysregulation of several immune cell subsets[92]. Research has implicated aberrant activity of both innate immune cells such as monocytes and macrophages and adaptive immune cells such as T cells and B cells in Psoriasis (PsO) and PsA pathogenesis, which is associated with uncontrolled production of several pro-inflammatory cytokines such as IL-17 and IL-23[104,108,109,353]. Although substantial research has revealed these key aspects of disease pathogenesis, there is an unmet need for better diagnostic and prognostic biomarkers in PsA and hence, a better understanding of disease initiation and progression is needed.

Annexin-A1 (ANXA1) is a glucocorticoid-induced signalling protein implicated in a wide range of biological pathways, many of which are dysregulated in inflammatory disease. Research has indicated that ANXA1 primarily signals through the formyl peptide receptors (FPR), FPR1 and FPR2, particularly in disease[23–25]. Based on previous studies implicating a role for ANXA1 and FPR1/FPR2 signalling chronic inflammation[49,67,81], research presented in this chapter focused on exploring the ANXA1-FPR signalling pathway in PsA. The aim of this chapter was to understand if this pathway was associated with factors relevant to PsA disease pathogenesis and identify which disease-relevant cells were responsible for ANXA1-FPR1 signalling in PsA.

Although the exact trigger for PsA is unknown, evidence has indicated that disease-associated inflammation is triggered by a series of environmental and genetic events[354]. Over the past several years, there have been many large-scale genomic studies which have identified a range of PsA-associated genetic variants, however understanding the biological function of these variants and translating them to potential treatment targets has been challenging[355].

Altered expression of certain genes, particularly inflammatory genes, can be seen in both PsA and PsO, however, there is a clear difference in the molecular pathways that are activated between the two diseases. What triggers progression from PsO to PsA is far from understood[356]. Moreover, what links the

skin and joint pathology within PsA subsets is still unclear[357]. Analysis of PsA lesional (PsA L) skin samples in this study revealed 2151 significantly upregulated genes in the PsA L skin. These genes were mainly involved in processes such as lymphocyte activation and adaptive immunity, reflecting the mounting evidence that overactivation of adaptive immune cells, particularly T cells can drive PsA pathogenesis[358,359](Figure 4.2).

This study also showed that FPR1 and FPR2 were amongst the significantly upregulated genes in the PsA L skin (Figure 4.1). Moreover, FPR1 had a significant positive correlation with genes encoding the RPL38 and TOMM7 proteins, both of which have been shown to be aberrantly expressed in psoriatic skin lesions [34,35]. Additionally, FPR2 significantly correlated with *MDH1* in the PsA L skin, a gene that encodes the malate dehydrogenase 1 enzyme. This enzyme is associated with reduced Nicotinamide adenine dinucleotide (NADH) metabolism. This is also relevant to PsA disease pathogenesis as keratinocyte proliferation is enhanced in psoriatic skin lesions through a process which requires NADH-dependent oxidative phosphorylation[38].This preliminary analysis of PsA L skin genetic data provided some insight into what genes FPR1 and FPR2 could be interacting with in PsA skin lesions, however, future work is required to understand the relevance of these interactions in the context of PsA disease pathogenesis. In an attempt to understand the role of FPR1 and FPR2 signalling in PsA skin lesions, further analysis in this chapter focused on identifying key pathways associated with FPR1 and FPR2 activity in the psoriatic skin lesions.

Dysregulation of the skin microbiome and immune response in the skin has been shown to sustain the psoriasis [360,361]. Moreover, particular bacteria such as Staphylococcus aureus (*S. aureus*) are shown to be more abundant in those with psoriasis than rheumatoid arthritis (RA)[317]. Data in this study identified an upregulation of the (*S. aureus*) infection pathway in PsA L skin samples assessed compared to HC skin. Interestingly, this pathway is known to involve both FPR1 and FPR2 signalling, highlighting a potential pathway that could involve dysregulated signalling these two receptors in PsA skin lesions.

This study also identified an upregulation in pathways involved in neutrophil extracellular trap (NET) formation in the PsA L skin compared to HCs. NET

formation is part of the neutrophil's response to infection. These extracellular structures are composed of enzymes and proteins that help to encapsulate and destroy invading microbes[362]. Interestingly, NET formation was found to be increased in the blood and lesional skin of PsA patients, which also correlated with disease severity[319]. It could be speculated that this pathway is heightened in the PsA L skin in response to the overabundance of bacteria such as *S. aureus*, thus linking both FPR1 and FPR2 activity to the (dysregulated) response to infection in PsA. Future studies on how alterations these pathways affect disease activity and/or treatment response will prove vital in understanding the role of FPR1 and FPR2 signalling in PsA.

In order to translate the data that we obtained in the PsA L to peripheral blood, analysis in this study focused on profiling the expression levels of ANXA1, FPR1 and FPR2 on different immune cell subsets in PsA. Flow cytometric analysis presented in this chapter identified differences in ANXA1, FPR1 and FPR2 surface expression in PsA that appeared to be cell type specific (Figure 4.7). In particular, analysis of FPR2 expression in PsA revealed increased expression of this receptor in 21 T cell populations (Figure 4.7). T cells are the most frequent type of inflammatory cell in the skin and joints of PsA patients[92]and are associated with hyperproliferation of keratinocytes and production of key pro-inflammatory cytokines linked with PsA pathogenesis such as IL-17[96,97].

The abundance of FPR2 expression on a range of PsA T cell subsets analysed allows for speculation that this receptor could be involved somehow in T-cell signalling in PsA. FPR2 is the most versatile of the formyl peptide receptors and can bind a variety of pro and anti-inflammatory ligands. Additionally, studies have shown the anti-inflammatory signalling mediated through FPR2 to be initiated through interactions with ANXA1[29,363]. Considering data in this chapter also identified reduced ANXA1 on IL-17 producing $CD8^+$ T cells (Tc17) in PsA, it could be speculated that there is reduced ANXA1-FPR2 binding in PsA, thus freeing more FPR2 to be detected flow cytometrically in these samples. This reduced ANXA1-binding could also contribute to the hyper-inflamed state evident in PsA through lack of FPR2-mediated anti-inflammatory signalling on these T cells. In experiments in collagen-induced arthritis and contact hypersensitivity mouse models, deficiency of ANXA1 was associated with

enhanced T cell-dependent inflammation, supporting this idea of an anti-inflammatory role for ANXA1 in these cells[58].

In addition to this, several other T cell subsets associated with IL-17 production had altered FPR1 and FPR2 expression in PsA samples. An upregulation in FPR2 (Tc17 and Tc17.1) and FPR1(Tc17.1, MAIT cells) was evident in IL-17-producing cells. $CD8^{+}CD161^{+}$ MAIT cells in particular have been recently implicated in PsA, mostly due to their uncontrolled production of IL17-A in the PsA synovial fluid[325]. Data from this chapter indicates that there could be a dysregulation in ANXA1-FPR signalling in these IL-17 producing cells in PsA, which could potentially contribute to the uncontrolled inflammatory response in this disease. However, power calculations to determine how many samples are needed to validate this result are needed.

The presence of antibodies that react to self-antigens (autoantibodies) is a key feature of many inflammatory diseases and have been used to inform the diagnosis of diseases such as rheumatoid arthritis (RA)[364]. Recently, novel autoantibodies have been detected in patients with PsA against proteins associated disease pathogenesis (e.g IL-37 which is upregulated in psoriatic lesions)[365]. Moreover, production of autoantibodies in inflammatory disease has been widely attributed to dysregulation of B cells[366]. Data in this chapter identified altered expression of ANXA1, FPR1 and FPR2 in several B cell subsets in PsA. Switched memory B cell populations in particular expressed significantly more ANXA1 and FPR1, and contrastingly significantly less FPR2 in PsA samples compared to HCs.

Although there is no clear evidence of a role for these cells in PsA, increased frequencies of switched memory B cells have been observed in chronic inflammatory diseases such as pulmonary fibrosis and Diffuse Cutaneous Systemic Sclerosis, which are also associated with autoantibody production[366]. Interestingly, research has suggested that ANXA1 could function as an antigen triggering production of destructive autoantibodies[44]. It could therefore be speculated that ANXA1 signalling in PsA could be associated with B cell-mediated autoantibody production. A process that appears to be mediated more so through FPR1 than FPR2.

More evidence is presented in this chapter for dysregulated FPR1 signalling in PsA B cells through results showing increased FPR1 expression in unswitched memory and transitional B cell populations in PsA, both of which have been shown to be dysregulated in autoimmune disease[367,368]. Additionally, transitional B cells express higher amounts of the type 1 interferon (IFN) receptor and respond more powerfully to type 1 IFNs. Overactivation of this pathway has been implicated in these cells in patients with autoimmune systemic lupus erythematosus (SLE)[369]. Preliminary analysis of clinical data from PsA patients in this study allows further speculation for dysregulated FPR1/B cell signalling in PsA with results showing expression of FPR1 on both PsA switched memory and transitional B cells correlated with the PsA disease activity index, DAPSA (Figure 4.10).

Monocytes have been shown to be key players in PsA disease progression. Increased aggregation of monocytes in the peripheral blood is evident in psoriasis patients[110]. Additionally, the bone erosion in PsA is known to be mediated by an overabundance of osteoclasts, which arise from osteoclast precursors (OCPs) or circulating $CD14^+$ monocytes. Higher than normal levels of both OCPs and $CD14^+$ monocytes have been found in the peripheral blood of PsA patients, in particular $CD14^+CD16^+$ monocytes[108,109]. Data in this chapter identified increased surface expression of FPR1 in PsA in this particular $CD14^+CD16^+$ monocytic population, suggesting that FPR1 signalling could be dysregulated in these cells. It could be speculated that FPR1 signalling could be involved in the differentiation of these cells to disease-driving osteoclasts. Indeed, a role for FPR1 in osteoclast formation has been previously suggested in studies showing that FPR1 was upregulated in mice in response to receptor activator of nuclear factor κB ligand (RANKL), which is recognised as a key factor in osteoclast formation[370].

As a whole, this expression data highlights the complex, dual role ANXA1 signalling could play in inflammation, depending on the innate or adaptive immune cell it is associated with. This supports studies showing ANXA1 signalling had opposing effects in innate (neutrophil apoptosis) and adaptive (T cell proliferation) immune cells[44,59,371]. It could be that overall, the balance of

ANXA1 signalling is off in PsA. Reduced ANXA1 signalling in monocytes could minimise their pro-inflammatory actions, whereas increased signalling in T cells could enhance their activation. Additionally, this all seems to be dependent on which FPR receptor ANXA1 interacts with.

Monoclonal antibodies are a frequently used treatment in the management of PsA, primarily due to their high specificity and ability to target distinct biological pathways associated with disease pathogenesis. Moreover, due to their specificity, monoclonal antibodies are often associated with more favourable side effects compared to drugs such as TNF- α inhibitors which have warnings for serious infection and malignancy[372,373]. PsA is a heterogenous disease and therefore, presents with different characteristics and responses to treatment. Initiation of the right treatment strategy for each patient as soon as possible is vital to prevent irreversible joint and bone damage as a result of PsA disease progression. There is therefore a need for more targeted therapies in PsA, especially for those who don't respond to other treatments. Moreover, a better understanding of what biological pathways could be involved in disease progression and treatment response is essential. Considering all of these points, and the strong implications of dysregulated activity of ANXA1 in inflammatory disease[43], studies were done to assess the impact of a novel anti-ANXA1 antibody (MDX-124) on the PsA- associated inflammatory response.

Consistent with the literature[29], data in this project identified monocytes has high expressors of ANXA1 (Figure 4.6). Therefore, it was decided that monocytic cells were the most appropriate cells to conduct preliminary functional studies with MDX-124. Initially the monocytic, THP-1 cell line was chosen for this analysis. This cell line has been used widely to investigate monocyte biology but can also be differentiated into macrophage-like cells for analysis of their behaviour. A common method for this differentiation is with PMA, inducing a spindle shaped, adherent macrophage-like phenotype in these cells. Moreover, differentiation is associated within increased surface expression of CD14 and CD11b, thus increased levels of these markers can be used to confirm differentiation into a macrophage-like phenotype[374] .

THP-1 cells were differentiated for a total of 7 days and results from preliminary experiments indicated that addition of MDX-124 during this process did not appear to alter surface expression of CD11b and CD14 compared to THP-1 cells differentiated without MDX-124. Thus, suggesting that MDX-124 did not impact the differentiation of THP-1s into a macrophage-like phenotype. However, interestingly, addition of MDX-124 was associated with a downregulation in FPR1 in fully differentiated (day 7) THP-1s, indicating that MDX-124 could have an effect on FPR1-associated signalling in these THP-1 cells (Figure 4.13).

Further investigation into potential signalling pathways induced by MDX-124 revealed that MDX-124-treatment during THP-1 differentiation was associated with an upregulation of intracellular phosphokinases and extracellular signalling proteins associated with cell survival, proliferation, differentiation and inflammation (Figure 4.13 and Figure 4.14). Notably, MDX-124 treatment (and hence FPR1 downregulation) was associated with an upregulation in the MAP Kinase, p38a, which plays a central role in the pro-inflammatory response[333]. Previous studies in a chondrogenic cell line reflect these results and have indicated that FPR1 downregulates in response to inflammatory stimuli (LPS) which is associated with a pro-survival state through mediation of the MAP kinase pathway[341]. Additionally, ANXA1 is known to modulate the inflammatory response through regulation of MAP kinase signalling[56].

Although the potential mechanism FPR1 downregulation and heightening of pro-survival, pro-inflammatory pathways in the THP-1s is not understood, considering what is known about ANXA1-FPR1 signalling, a proposed mechanism has been suggested (Figure 4.17). During an inflammatory response, ANXA1 is released from the surface of activated cells into the circulation, where it can bind to its receptors in a juxtracrine or paracrine manner[59]. Additionally, ANXA1 has a well- defined anti-inflammatory role on innate immune cells such as monocytes[29]. Considering this, it could be speculated that MDX-124 binds this circulating ANXA1 in the THP-1 supernatant and prevents it from binding to FPR1 to modulate its anti-inflammatory effects in the THP-1 cells. This would in turn, explain the increased levels of pro-inflammatory intracellular and extracellular proteins produced in MDX-124 exposed THP-1s. In response to the dysregulated inflammation (due to lack of ANXA1 signalling), FPR1 downregulates to modulate

pathways (such as the MAP kinase pathway) involved in apoptosis and enhanced survival (as seen in other cell line studies). Ultimately, the mechanism by which MDX-124 regulates FPR1 and hence signalling protein expression in the THP-1s needs to be investigated further, and the MAP kinase pathway is a candidate pathway for future investigations. Studies that re-expose THP-1s to ANXA1 and investigate both FPR1 expression levels and whether the inflammatory and hence pro-survival responses in these cells are reduced would prove useful for understanding whether this is a response triggered by reduced ANXA1 binding to FPR1. Overall, data supports studies indicating an anti-inflammatory role for ANXA1 on innate immune cells[375]. Replicating these studies in adaptive immune cell lines would be important for determining whether this role is reversed or mimicked in adaptive immunity. Moreover, these studies would prove extremely useful for understanding if dysregulated ANXA1 signalling could have opposite effects in innate and adaptive immune cells in PsA.

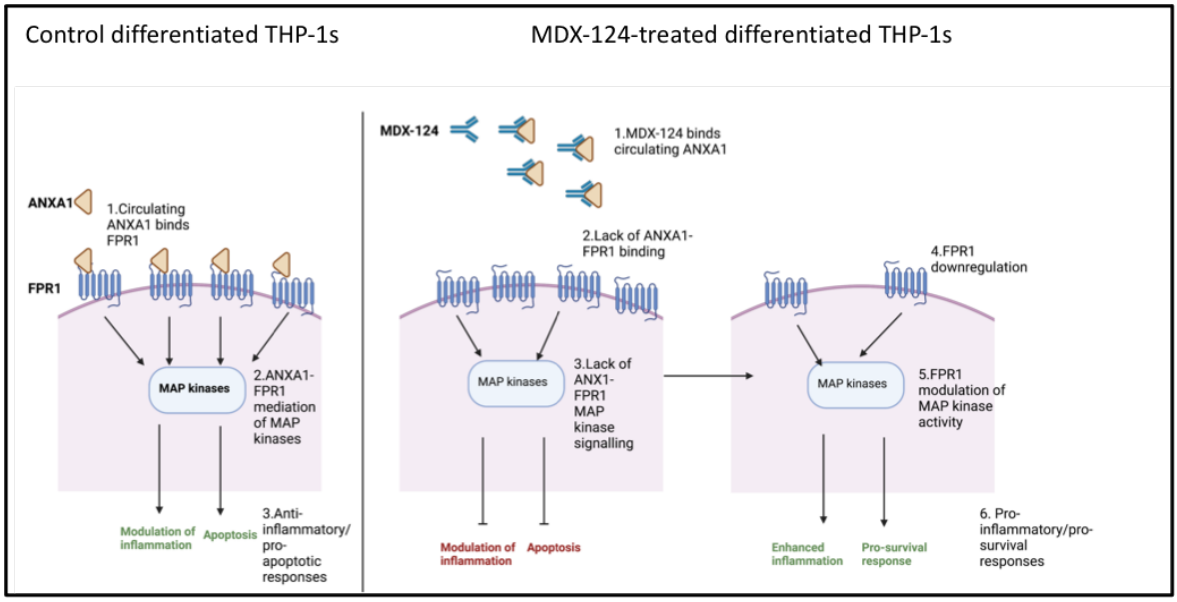

Figure 4.17 Proposed mechanism of action of MDX-124 during THP-1 differentiation

In control differentiated THP-1s, it is proposed that circulating ANXA1 binds to FPR1 on the cell surface and mediated anti-inflammatory/pro-apoptotic functions through interactions with signalling proteins such as MAP kinases. In MDX-124- treated THP-1s, a proposed mechanism is that MDX-124 binds circulating ANXA1 and prevents it from interacting with FPR1. This, in turn, reduces ANXA1-FPR1 mediated anti-inflammatory/apoptotic signalling. This increase in inflammation then triggers a downregulation in FPR1, which, in turn modulates signalling through pathways such as the MAP kinase pathway to produce a more inflammatory/pro-survival phenotype.

THP-1 cells have several limitations that need to be considered when interpreting results obtained from using them. The genetic background of THP-1s is homogenous, which, although is beneficial for minimising genetic variability between experiments, does not reflect the heterogenous biology of primary monocytes and macrophages[376,377]. Moreover, there are three main subtypes of primary monocytes ($CD14^+CD16^+$, $CD14^+CD16^-$ and $CD14^{dim}$ $CD16^+$), each exhibiting different biological responses in homeostasis and disease[377].These individual responses cannot be mimicked using the homogenous THP-1 cell line.

Another major difference between THP-1s and primary monocytes is that THP-1 cells are an immortalised cell line, that can survive in vitro for up to 3 months without changes in activity or sensitivity, a characteristic not shared with primary monocytes[376,378]. Additionally, recent data has suggested that differentiation of THP-1 cells to macrophage-like cells induces transcriptional changes not evident after differentiation of primary monocytes and has suggested this change could occur as a result or prolonged culturing of the THP-1s[379]. This highlights the importance of confirming the results obtained from THP-1 experiments in this study in primary cells before conclusions can be made.

Considering the limitations of the use of THP-1 cells, experiments were translated to primary monocytes to assess the effects of MDX-124 on their inflammatory activity. Addition of MDX-124 to primary monocytes exposed to inflammatory stimuli (LPS) was associated with an enhanced production of the pro-inflammatory cytokines TNF- α and IL-6. This indicated that MDX-124-targetting of ANXA1 is associated with an enhanced inflammatory response in monocytes, which could perhaps be through the same mechanism suggested in figure 4.17. Additionally, this MDX-124-associated pro-inflammatory effect was particularly evident in $CD14^+CD16^+$ monocytes, which were also shown to express more FPR1 in PsA (Figure 4.7). Moreover, $CD14^+CD16^+$ monocytes in particular are considered to play predominantly pro-inflammatory roles in inflammation. Taken together these data indicate a role for ANXA1 signalling primarily with FPR1 on inflammatory monocytes during inflammation and support the anti-inflammatory role of ANXA1 on monocytic cells suggested in the literature. Future studies investigating the effects of MDX-124-targeting of ANXA1 on other

cells (e.g., T cells and B cells) would prove useful in determining whether these effects are monocyte specific.

It could be speculated that a particular dosage of MDX-124 is needed to strike a fine balance between modulating the pro-inflammatory effects of dysregulated ANXA1 on some cell types (e.g., T cells) and avoid blocking the protective anti-inflammatory effects of ANXA1 on other cell types (e.g monocytes) in PsA. Further studies assessing the effects of MDX-124 dosage on different immune cell types from PsA primary samples would prove useful for understanding this.

In summary this chapter has supports the idea of the complex nature of ANXA1 and FPR signalling in inflammation and its potential dysregulation in PsA. Bioinformatic analysis has highlighted candidate pathways for further investigation that involve FPR1 and FPR1 activity and are enriched in the PsA skin lesions. Moreover, this analysis correlated expression of these receptors in the PsA skin lesions with genes relevant to PsA disease pathogenesis. This chapter also identified altered surface expression of both ANXA1 and the FPRs on PsA peripheral blood cells that appeared to be cell-type specific. This led to the hypothesis that ANXA1 could play a dual role in PsA- associated inflammation that could be dependent on both the cell type and FPR receptor involved. Analysis of more PsA and HC samples from both the skin and peripheral blood are essential for confirming these findings.

Flow cytometric analysis identified inflammatory monocytes as a candidate for further investigation into the role of ANXA1 in the inflammatory response, based on their high expression of ANXA1 and also increased expression of FPR1 in PsA. MDX-124-targeting of ANXA1 signalling both on THP-1s and primary monocytes was associated with an enhanced inflammatory response and indicated that ANXA1 was associated with an anti-inflammatory role in monocytic cells during inflammation. This response was also associated predominantly with alterations in FPR1 expression through an undefined mechanism. ANXA1/FPR1 manipulation of the MAP kinase pathway was suggested as a candidate mechanism for this, based on findings both in this study and the literature showing that alteration in FPR signalling was associated with alterations in MAP kinase proteins during inflammation. Future functional experiments investigating both FPR1 and ANXA1

activity in these cells and other cell types during an inflammatory response would prove useful for understanding the complex role of ANXA1 signalling in inflammation.

Chapter 5 Annexin A1 and the formyl peptide receptors in cancer

5.1 Introduction

Cancer is a result of several mutations leading to uncontrolled growth and division of cells[155,380]. Chronic inflammation has been shown to play a prominent role in the progression of this process, contributing to genomic instability, and key pathways involved in cancer cell proliferation and angiogenesis[156], providing evidence for a link between the immune system and cancer.

There is substantial evidence for a role for ANXA1 and the FPRs in several forms of cancer, including lung cancer[174], pancreatic cancer[175], and prostate cancer[178]. Moreover, ANXA1-FPR interactions have been shown to activate signalling pathways implicated in several cancer types[198,381](see introduction section 1.5)

Multiple myeloma (MM) is malignant form of immune cell-mediated cancer caused by abnormal proliferation of terminally differentiated B cells (plasma cells) and occurs throughout the bone marrow. Clinical presentation of MM is commonly described via "CRAB" symptoms (hyper**c**alcemia, **r**enal insufficiency, **a**naemia, and **b**one lesions). This type of cancer is usually slow to progress and consists of chromosomal translocations involving oncogenes. It is proposed that primary translocations occur early in the disease pathogenesis, followed by secondary translocations later on that contribute to disease progression. Other factors such as increased angiogenesis and growth factors are also associated with disease progression[207,208]. The availability of new drugs and also high-dose therapy has improved treatment outcomes, but the disease remains incurable and therefore, more research needs to be undertaken[213].

Although the evidence for a role for ANXA1 in MM is limited, one study has shown that knockdown of ANXA1 both *in vivo* and *in vitro* enhanced the anti-tumour effects of the commonly used MM treatment, Bortezomib, suggesting a pro-tumour role for ANXA1 in this cancer[238]. Thus, the aim of the work in this chapter was to gain further insights into the contribution and/or role of ANXA1 (and potentially the FPRs) in MM.

The research presented in this chapter sought to determine:

2. Whether expression levels of ANXA1 and the FPRs are altered in MM compared to HC samples, including:
    - Cell surface expression analysis via flow cytometry
    - RNA sequencing data analysis

2. Whether expression of ANXA1 and the FPRs in MM is associated with any disease-relevant factors including
    - Survival outcome
    - Prognosis
    - Clinical and genetic markers of disease

5.2 Results

5.2.1 Characterisation of ANXA1 and FPR1/2 surface expression in multiple myeloma

To initially evaluate whether ANXA1 and the FPRs were expressed and could potentially contribute to pathology in MM, blood and bone marrow samples from a MM patient were assessed for surface expression of ANXA1 and FPR1/2. Flow cytometric analysis was restricted to the B cell and plasma cell compartment (Figure 5.1). This involved gating on single cells, followed by peripheral blood B cells ($CD45^+CD19^+$) and MM plasma cells ($CD45^-CD138^+CD38^+$). Notably, MM plasma cells were only resent in the bone marrow (Figure 5.1A and 5.1B). Having define the cellular populations, ANXA1, FPR1 and FPR2 expression was assessed and compared to HC B cells (Figures 5.1C-5.1E).

Analysis of ANXA1 and its receptors in the MM patient's circulating B cells revealed that a substantial proportion of $CD19^+$ B cells expressed not only ANXA1 (~66%) but also FPR1 (~34%) (Figure 5.1D). In comparison, although ANXA1 was detectable on healthy control B cells it was on substantially less cells (~5-7%) (Figure 5.1C). Moreover, FPR1 was undetectable on healthy B cells. Bone marrow samples were not available from healthy controls and thus no comparison to MM could be undertaken. However, evaluation of the BM compartment in MM revealed that ANXA1 was on a proportion of MM cells (~5%) whilst FPR1 and FPR2 were not expressed (Figure 5.1E).

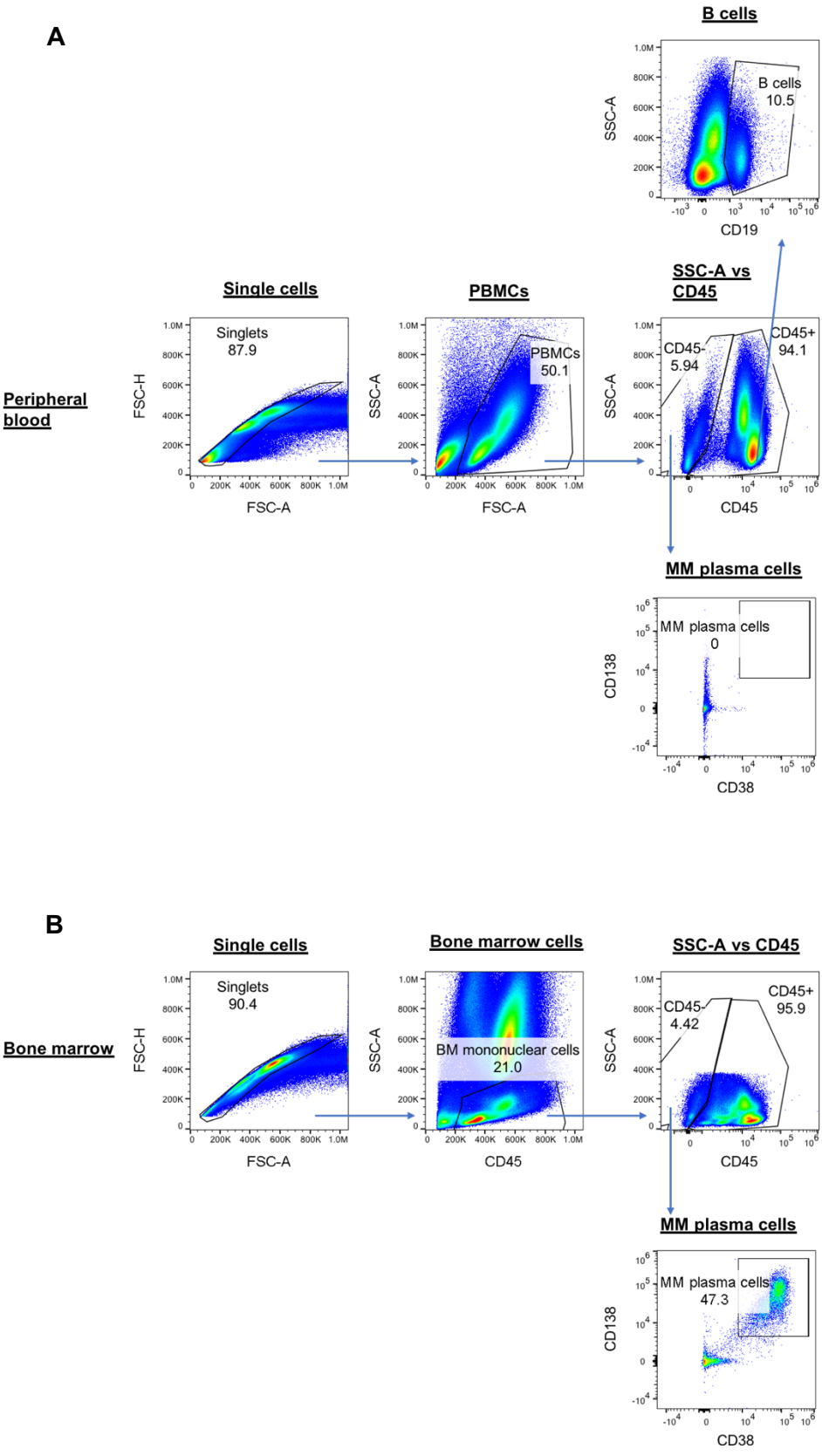
A
B cells
B cells
10.5
SSC-A
CD19
Single cells
PBMCs
SSC-A vs CD45
Peripheral blood
Singlets
87.9
FSC-H
FSC-A
PBMCs
50.1
SSC-A
CD45-
5.94
CD45+
94.1
CD45
MM plasma cells
MM plasma cells
0
CD138
CD38
B
Single cells
Bone marrow cells
SSC-A vs CD45
Bone marrow
Singlets
90.4
BM mononuclear cells
21.0
CD45-
4.42
CD45+
95.9
MM plasma cells
MM plasma cells
47.3

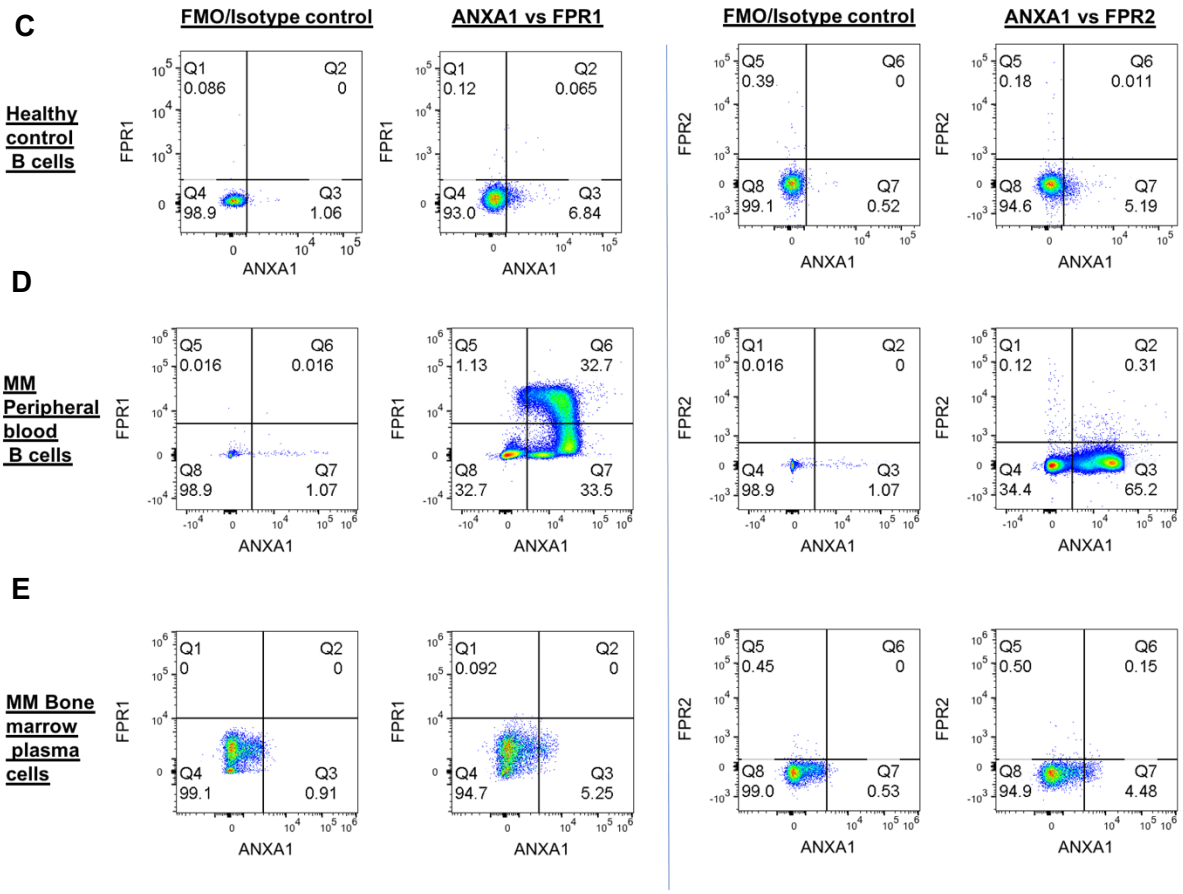

Figure 5.1 ANXA1 and FPR1 surface expression is increased on peripheral blood B cells in a MM patient

PBMCs were isolated from whole blood and BM cells were placed in red blood cell lysis buffer (stem cell) prior to staining. Cells were incubated with anti-CD45, anti-CD19, anti-CD138, anti-CD38, anti-FPR1, anti-FPR2 and MDX-124 to detect ANXA1. Cells were washed in FACs buffer prior to analysis on the BD Attune flow cytometer (MM patient) or BD LSR II flow cytometer (HC sample). The FACs plot shows the gating strategy for (A) peripheral blood and (B) bone marrow samples. Singlets were gated, followed by peripheral blood and bone marrow mononuclear cells. CD45- and CD45+ cells were then gated. From CD45- cells bone marrow MM plasma cells were gated. CD19+ B cells were gated from CD45+ cells. ANXA1 and FPR1/FPR2 surface expression was analysed on (C) healthy control B cells, (D) MM peripheral blood B cells and (E) MM bone marrow B cells. Cells were gated using appropriate FMO controls for the FPR1/2 which also contained an isotype control for ANXA1. Flow cytometry plots were produced using FlowJo (v10.6.1) software.

To confirm these initial findings, two more samples were acquired and interrogated with a more comprehensive antibody panel. This included monocyte and T cell markers as well as B cell markers. The gating strategy for this panel is shown in Figure 5.2A. Each cell population gated was assessed for ANXA1, FPR1 and FPR2 surface expression. Only peripheral blood samples were obtained for these patients and MM samples were compared with three healthy control samples.

Positive staining for FPR1 and FPR2 was defined as a higher fluorescence detection than the fluorescence minus one control staining (FMO) and positive staining for ANXA1 was determined as higher fluorescence detection than the isotype control stain. Analysis was conducted on FlowJo (v10.6.1) software to obtain the geometric mean expression of ANXA1, FPR1 and FPR2 on the cell populations of interest. Delta (Δ) MFI values for each population were then calculated by subtracting the (FMO and isotype) control stains from the FPR1, FPR2 and ANXA1 stains, to account for non-specific background staining.

In comparison to the initial MM patient, increased ANXA1 or FPR1 was not observed on peripheral blood B cells of the additional patient samples. FPR2 expression was higher in healthy peripheral blood B cells than in MM samples (Figure 5.2B).

ANXA1 Expression data was inconsistent between samples for all T cell populations apart from CD4+CD8- T cells where there was negligible expression in both HC and MM samples. FPR1 and FPR1 expression data was also inconsistent between samples for all T cell populations, with no obvious difference between HC and MM (Figure 5.2C- Figure 5.2E).

Similarly, ANXA1 and FPR2 surface expression data was inconsistent for all monocyte populations, with no visible difference between HC and MM. However, FPR1 expression was consistently higher in MM samples in all of the monocyte populations assessed (Figure 5.2F- Figure 5.2H).

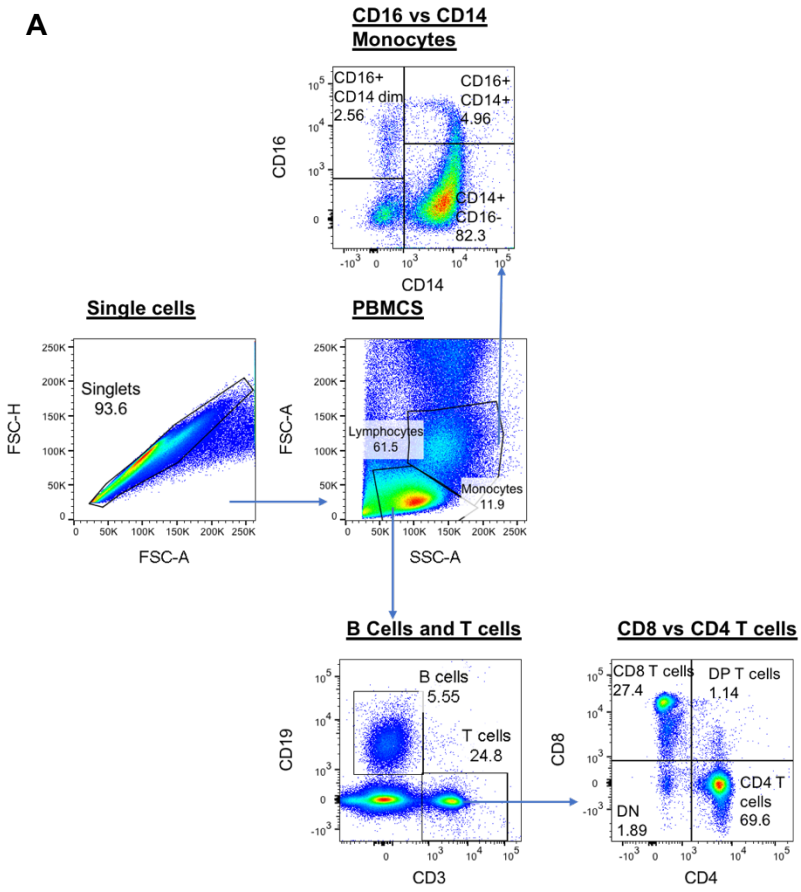
A
CD16 vs CD14
Monocytes
CD16+
CD14 dim
2.56
CD16+
CD14+
4.96
CD14+
CD16-
82.3
CD16
CD14
Single cells
Singlets
93.6
FSC-H
FSC-A
PBMCS
Lymphocytes
61.5
Monocytes
11.9
FSC-A
SSC-A
B Cells and T cells
B cells
5.55
T cells
24.8
CD19
CD3
CD8 vs CD4 T cells
CD8 T cells
27.4
DP T cells
1.14
CD4 T
cells
69.6
DN
1.89
CD8
CD4

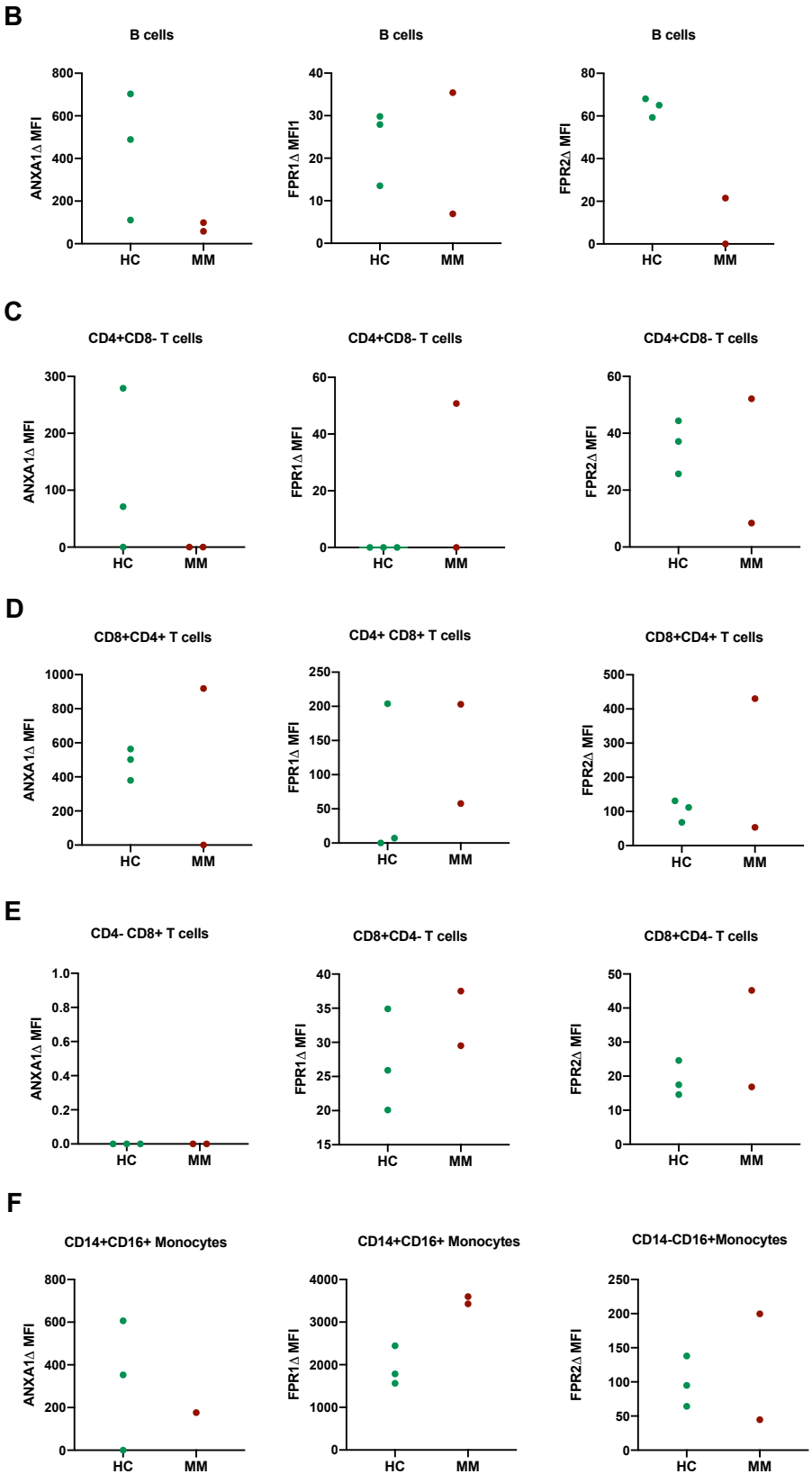
B
B cells
ANXA1Δ MFI
FPR1Δ MFI1
FPR2Δ MFI
HC
MM
C
CD4+CD8- T cells
ANXA1Δ MFI
FPR1Δ MFI
FPR2Δ MFI
D
CD8+CD4+ T cells
CD4+ CD8+ T cells
E
CD4- CD8+ T cells
CD8+CD4- T cells
F
CD14+CD16+ Monocytes
CD14-CD16+Monocytes

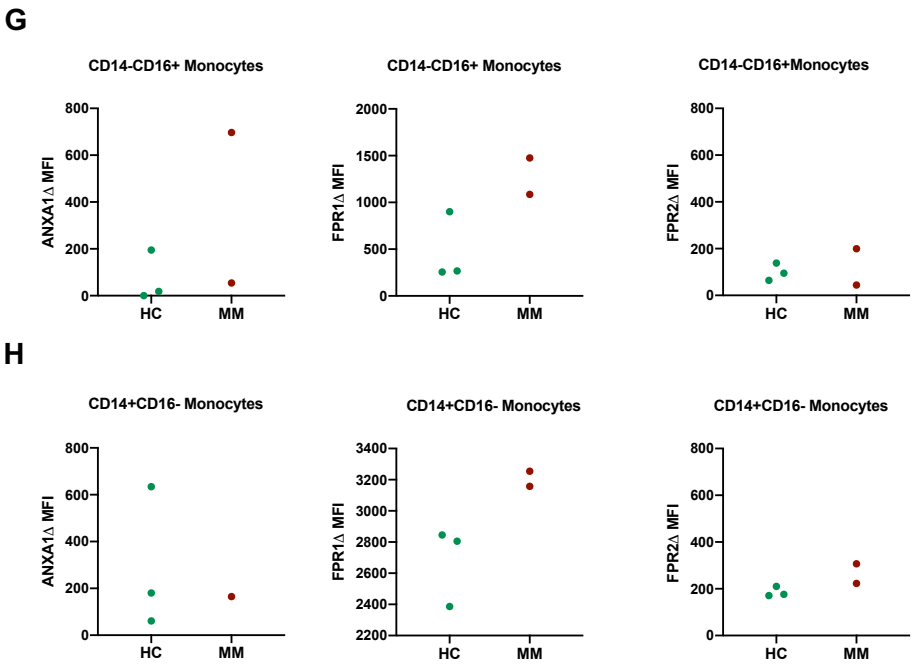

Figure 5.2 FPR1 expression is higher on peripheral blood monocytes in MM samples

PBMCs were isolated from whole blood prior to staining. Cells were incubated with, anti-CD19, anti-CD14, anti-CD3, anti-CD4, anti-CD8, anti-FPR1, anti-FPR2 and MDX-124 to detect ANXA1. Cells were washed in FACs buffer prior to analysis on the BD Attune flow cytometer (MM patient) or BD LSR II flow cytometer (HC sample). The FACs plot shows the gating strategy for (A) peripheral blood. Singlets were gated, followed by lymphocytes and monocytes. Lymphocytes were gated for B cells and T cells and T cells were further gated for CD4 and CD8 expression. Monocytes were further gated for CD14 and CD16 expression. Each population was then assessed for ANXA1, FPR1 and FPR2 surface expression. Δ MFIs for ANXA1, FPR1 and FPR2 expression were calculated using appropriate controls (stained sample minus FMO or isotype control) for 2 MM and 3 HC samples and graphs were produced for (B) B cell populations, (C-E) T cell populations and (F-H) monocyte populations. Flow cytometry plots were produced using FlowJo (v10.6.1) software and graphs were produced using GraphPad Prism (v9) software.

In summation, these experiments provided some preliminary data into which cell types express more surface ANXA1 and FPR1 in MM, particularly in the peripheral blood. However, due to the small sample size (and inconsistency of results) more samples need to be tested before any conclusions can be drawn from this data.

5.2.2 Analysis of genomic data from multiple myeloma patients using the CoMMpass database

Due to data in figure 4.1 indicating potential changes in ANXA1 and FPR1 in MM and also the fact that access to primary MM samples were restricted due to the Covid-19 pandemic, the project took a more data-driven approach to analysing expression of ANXA1 and the FPRs in MM using a publicly available MM database, the CoMMpass database[264], which contains a range of genomic and clinical data. Notably, only baseline gene expression data was available and not all patient samples had corresponding clinical data (N=550/921) (Figure 5.3A). Furthermore, aspects of the data were limited (e.g., due to study termination). For instance, survival outcomes were measured as censored overall survival, i.e., clinical information was not available for all the patients in the database and the outcome was predicted based on all other available information about the patient[382].

To initially interrogate the CoMMPass data, the transcriptional expression of baseline *ANXA1* and *FPR1* was assessed and compared to clinical outcomes. This analysis revealed that the level of *ANXA1* transcripts were higher in a subgroup of patients who had worse survival outcomes (i.e., death) **(**Figure 5.3B**)**. In comparison, expression of the *FPR1* transcript was not associated with survival outcomes (Figure 5.3C).

Given the association of ANXA1 with survival outcomes the decision was made to group MM patients based on high vs low ANXA1 expression. This analysis was conducted on R studio, and the data was grouped into quadrants. The top 25% of the data was considered high baseline ANXA1 expression and the bottom 25% of the data was considered low baseline ANXA1 expression. From these groups, differential gene expression analysis identified 3571 significantly upregulated and 228 significantly downregulated genes in patients that expressed high ANXA1 compared to those with lower ANXA1 expression (bottom 25% of the data). (Figure 5.3D). The top 5 genes with the highest positive fold change were *FGFR*3, *S100A8, S100A12, S100A9* and *TCN1* (Figure 5.3E). Of particular interest from these results was that the greatest fold change was in the Fibroblast growth factor receptor 3 (FGFR3) gene. Aberrant expression of this growth factor has been implicated in myeloma and has been associated with worst prognosis[206].

The top 5 genes with the highest negative fold change were *HMX2*, *HAPLN1*, *NF1P5*, *TEX47* and *PPP6R2*. Interestingly, hyaluronan and proteoglycan link protein 1 encoded by the *HAPLN1* gene has been implicated in drug resistance in MM[383] and the *PPP6R2* miRNA has been associated with promotion of proliferation and migration in MM[384].

The top 10 pathways involving genes that were upregulated in the high (baseline) *ANXA1* expressors (compared to low expressors in the bottom 25% of the data) were cancer-relevant pathways such as cell/leukocyte migration, angiogenesis and cell/leukocyte chemotaxis pathways[385,386]. Moreover, further analysis of the genes associated with these pathways implicated ANXA1 activity in them (supplementary Table 7). Other pathways involving genes that were upregulated in the high *ANXA1* expressors included those involved in cell matrix/structure organisation, complement activation, the humoral immune response and the immune response to bacterium (Figure 5.3F).

Genes that were significantly downregulated in MM patients that express high baseline ANXA1 were predominantly involved in pathways associated with synaptic transmission, particularly glutamatergic synapses which are abundant in the central nervous system (CNS)[387](Figure 5.3G). Pathway analysis also showed *ANXA1* was a gene associated with these pathways (Supplementary table 8). Although rare, the CNS involvement has been shown in several MM cases and correlates with very poor prognosis[388], which reflects the data in Figure 5.3B showing that this subgroup of patients have worse overall survival outcomes

A list of significance values and genes involved in each of the up and downregulated pathways (from ClusterProfiler pathways) can be seen in supplementary tables 7 and 8.

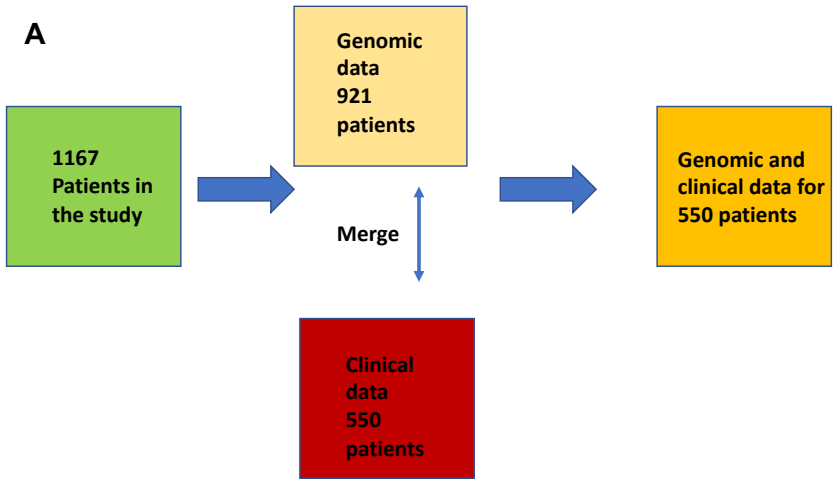
A
1167 Patients in the study
Genomic data 921 patients
Merge
Clinical data 550 patients
Genomic and clinical data for 550 patients

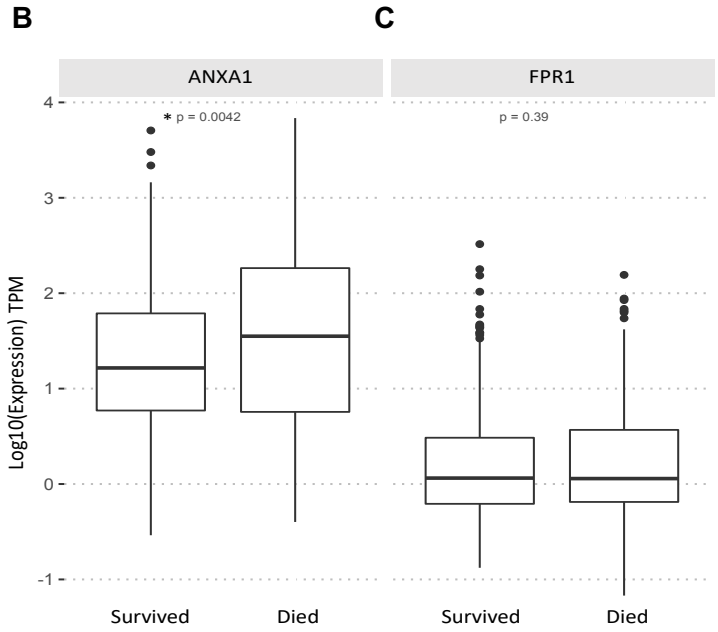
B
C
ANXA1
FPR1
* p = 0.0042
p = 0.39
Log10(Expression) TPM
4
3
2
1
0
-1
Survived
Died
Survived
Died

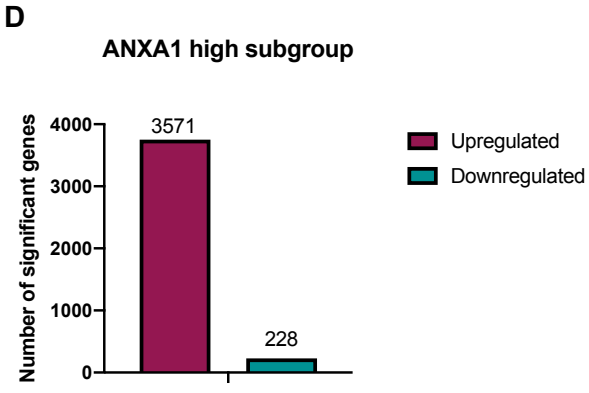
D
ANXA1 high subgroup
Number of significant genes
4000
3000
2000
1000
0
3571
228
Upregulated
Downregulated

E

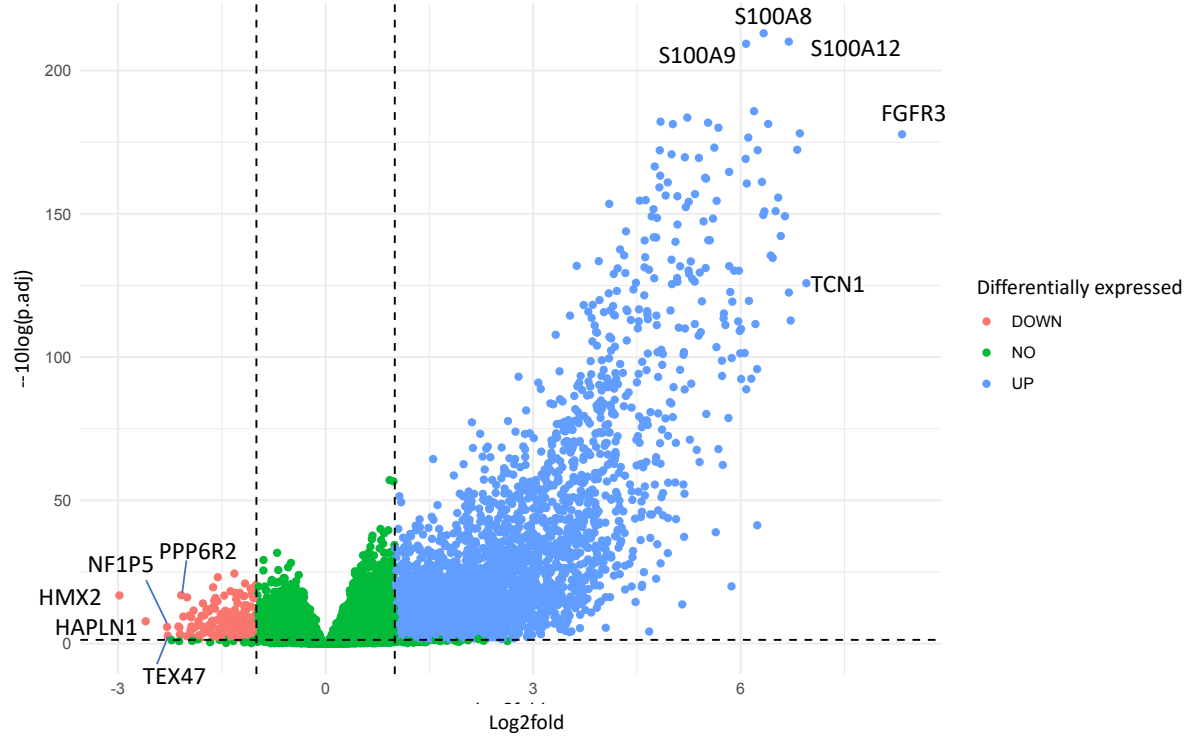
S100A8
S100A9
S100A12
FGFR3
TCN1
NF1P5
PPP6R2
HMX2
HAPLN1
TEX47
200
150
100
50
0
-3
0
3
6
--10log(p.adj)
Log2fold
Differentially expressed
DOWN
NO
UP

F

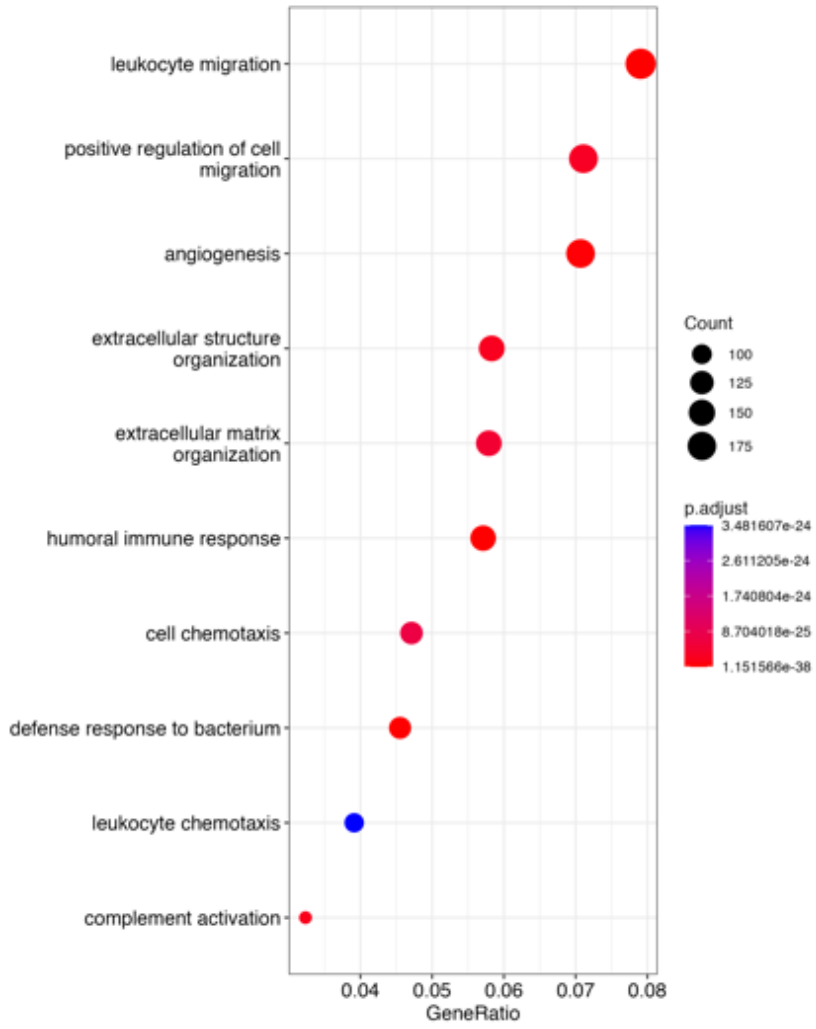
leukocyte migration
positive regulation of cell migration
angiogenesis
extracellular structure organization
extracellular matrix organization
humoral immune response
cell chemotaxis
defense response to bacterium
leukocyte chemotaxis
complement activation
0.04
0.05
0.06
0.07
0.08
GeneRatio
Count
100
125
150
175
p.adjust
3.481607e-24
2.611205e-24
1.740804e-24
8.704018e-25
1.151568e-38

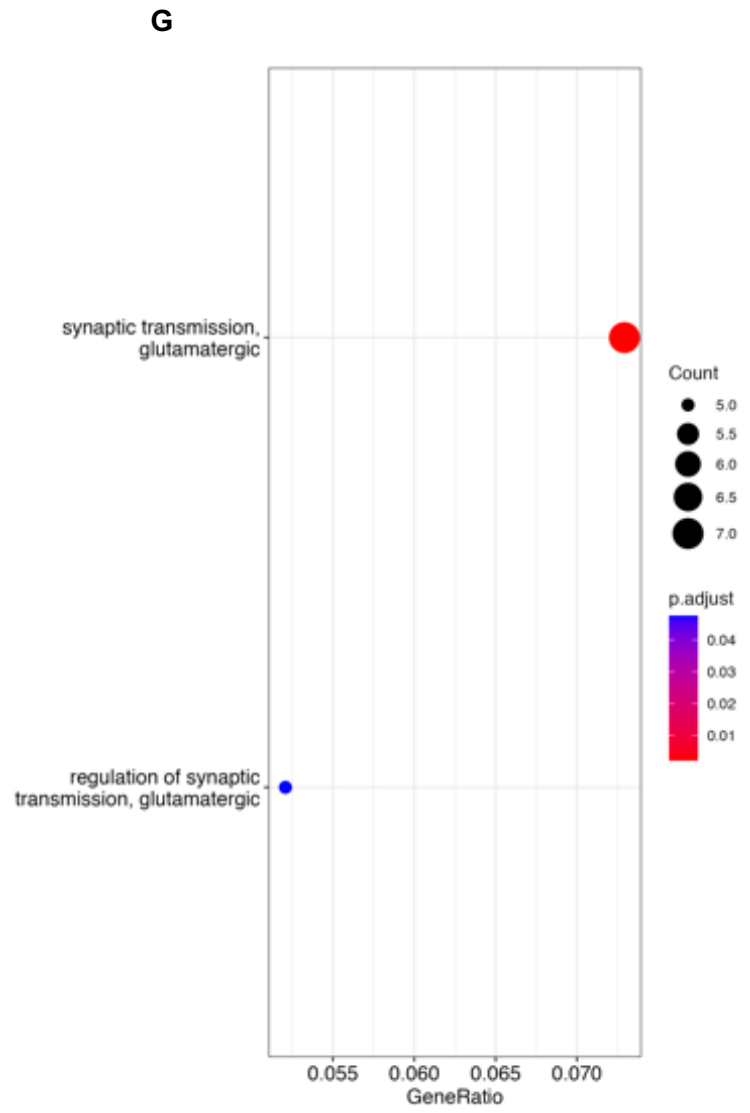

Figure 5.3 Higher ANXA1 gene expression at baseline is associated with worst survival outcomes and an upregulation in pro-cancer pathways

Gene expression data was merged with clinical data for analysis of a total of 550 patients. Boxplots were made on R studio to assess if there was a relationship between overall survival and baseline (B) *ANXA1* or (C) *FPR1* gene expression. A student's T-test was conducted, and P value of < 0.05 was considered significant. Gene expression data was provided as normalised transcripts per million (TPM). (D) Graph produced on GraphPad Prism (v9) showing the total number of upregulated and downregulated genes in MM patients with higher baseline *ANXA1* expression compared to those with lower baseline *ANXA1* expression. (E) A volcano plot showing fold change and significance of changes in MM patients with higher baseline *ANXA1* expression compared to those with lower baseline *ANXA1* expression. The top 5 genes with the highest positive and negative fold change are labelled. Pathway analysis was conducted using ClusterProfiler on R studio to reveal the top 10 pathways that the (F) significantly upregulated genes and (G) significantly downregulated genes from (C) and (D) are involved in. Gene ratio is the proportion of differentially expressed genes involved in each pathway, the number of genes in each pathway is determined by the size of the circle (count) and the adjusted P value is denoted by the colour of the circle (more red= smaller adjusted P value). MM patient N=921. All statistical tests and data parsing were conducted on R studio.

To narrow down the analysis and identify genes that are associated with higher baseline *ANXA1* expression, correlation analysis was done. Due to the large number of genes correlating with ANXA1, a positive correlation was determined as a spearman's correlation co-efficient (R value) of ≥ 0.5 and an R value of ≤ -0.5 was determined as a negative correlation. A P value of < 0.05 was determined as significant.

A total of 28 genes had a significant positive correlation with *ANXA1*(Figure 4.4A), and no genes had a significant negative correlation with *ANXA1*. The gene encoding for another Annexin family protein, Annexin A3 (*ANXA3*), which has been associated with worst prognosis in several cancers, as well as MM progression[389,390], correlated the most with *ANXA1*(R=0.61. Additionally, 22/28 of the positively correlating genes have been implicated in a form of cancer and of those 22 genes, 8 have been also implicated in MM (Figure 4.4B). Positively correlating genes also included those associated with *ANXA1* signalling (*PIK3R5*[391], *FPR1*[29], *CLEC7A*[392]). The only gene that was implicated in cancers including MM[393] and also in *ANXA1* signalling was the *FPR1* gene. In terms of function, the majority of the genes that correlate with ANXA1 expression encoded proteins involved in cell motility and structural organisation or the immune response (data shown in supplementary table 9), which links with pathway analysis in figure 4.3E showing an upregulation in these pathways in high *ANXA1* expressors.

A

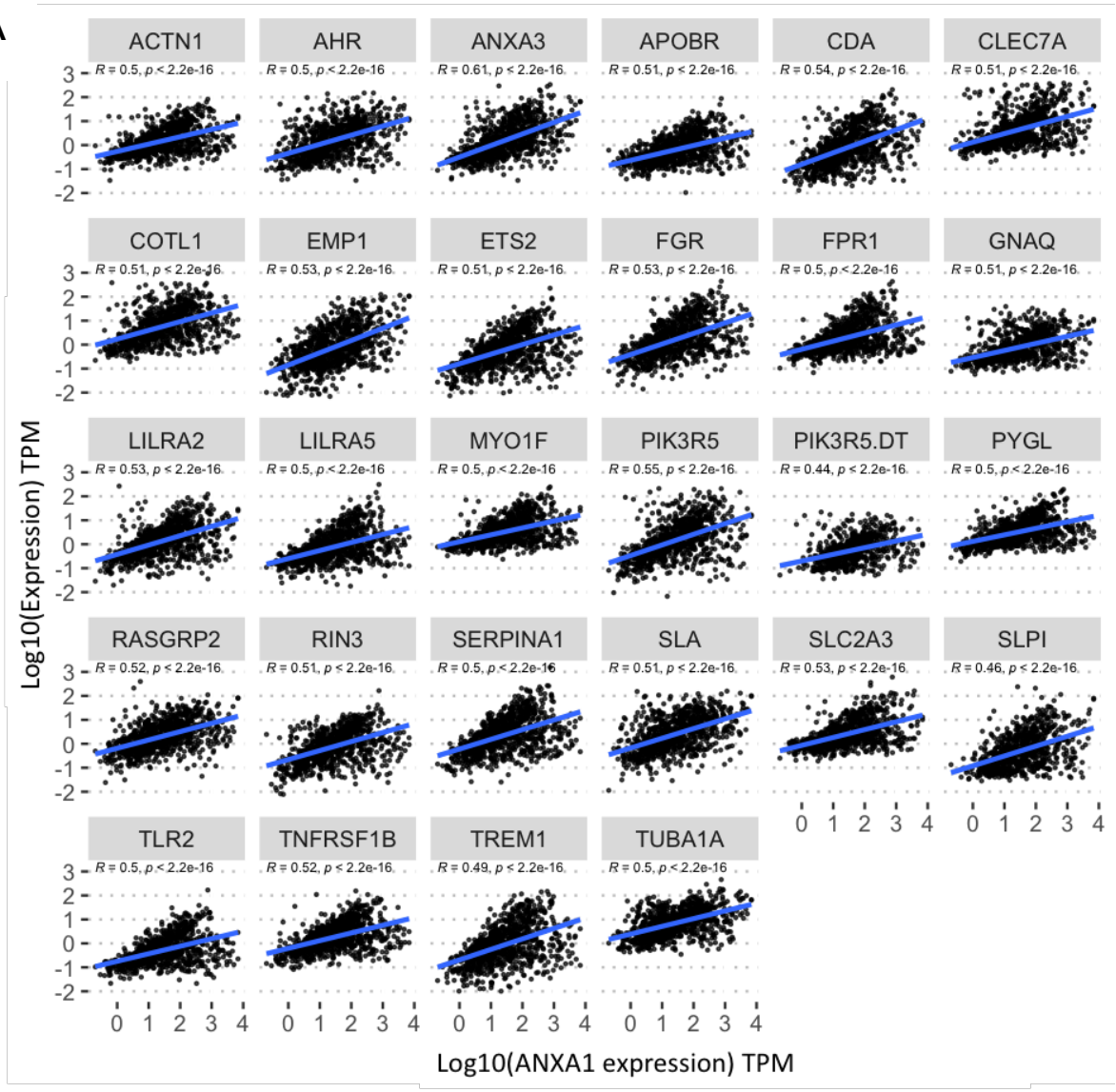
ACTN1
AHR
ANXA3
APOBR
CDA
CLEC7A
COTL1
EMP1
ETS2
FGR
FPR1
GNAQ
LILRA2
LILRA5
MYO1F
PIK3R5
PIK3R5.DT
PYGL
RASGRP2
RIN3
SERPINA1
SLA
SLC2A3
SLPI
TLR2
TNFRSF1B
TREM1
TUBA1A
Log10(Expression) TPM
Log10(ANXA1 expression) TPM

B

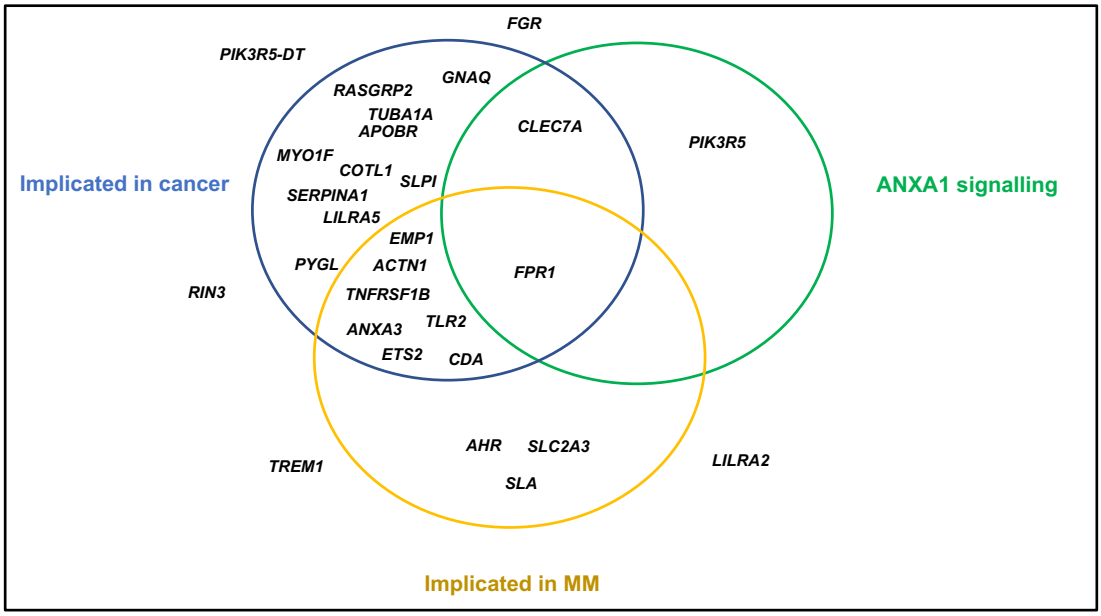

Figure 5.4 ANXA1 expression in MM cohort correlates with several cancer-associated genes

(A) *ANXA1* positively correlates with 28 genes in the MM CoMMpass cohort. Spearman's correlation values (R) are shown alongside significance values (P). (B) Venn diagram showing genes that are implicated in cancer in general, specifically in MM and/or in ANXA1 signalling. Information on gene function was obtained from the Human Protein Atlas[303] and the Genecards human gene database[304] and information on whether a gene had an association with MM was obtained from the CTD Gene-Disease Associations dataset[394]. Correlation analysis and statistical analysis was carried out on R studio. MM patient N=921.

As the CoMMpass database only had information on baseline gene expression, analysis could not be done to track *ANXA1* expression alongside treatment response over time. Moreover, treatment response data was only available as categorical data (progressive disease, stable disease, partial response, very good partial response, complete response, stringent complete response) and a lot of the data was missing for patients on the trial. Instead, alternative analysis looking at information that was available on genetic markers of worst disease prognosis and treatment response was done.

Disease progression in MM is highly associated with abnormalities at the chromosome level, that can be broadly grouped into primary cytogenetic abnormalities and secondary cytogenetic abnormalities, each of which has different effects on prognosis depending on disease stage. Primary cytogenetic abnormalities include translocations (most commonly t(11;14),t

(4;14),t(6;14),t(14;16),t(14;20)) and trisomies. Secondary cytogenetic abnormalities include amplification of the long arm of chromosome 21 (1q21 amplification), deletion of the small arm of chromosome (1p21 deletion) and deletion of chromosome 17 (del 17)[395]. All of the above abnormalities (apart from trisomies due to limited data available) were assessed alongside *ANXA1* expression and analysis showed that MM patients with the 1q21 amplification, which is associated with worst prognosis in MM, had a higher baseline *ANXA1* expression (Figure 4.5A) [396]. Moreover, the majority of genes encoding the S100 proteins are present at the 1q21 locus[397], some of which are upregulated (*S100A8*, *S100A9* and *S100A12*) in high *ANXA1* expressors from figure 4.3D. This is supportive of other data showing that amplification of the 1q21 gene was associated with an upregulation of genes located at its locus[396] (which is not always the case with gene amplifications[398]).

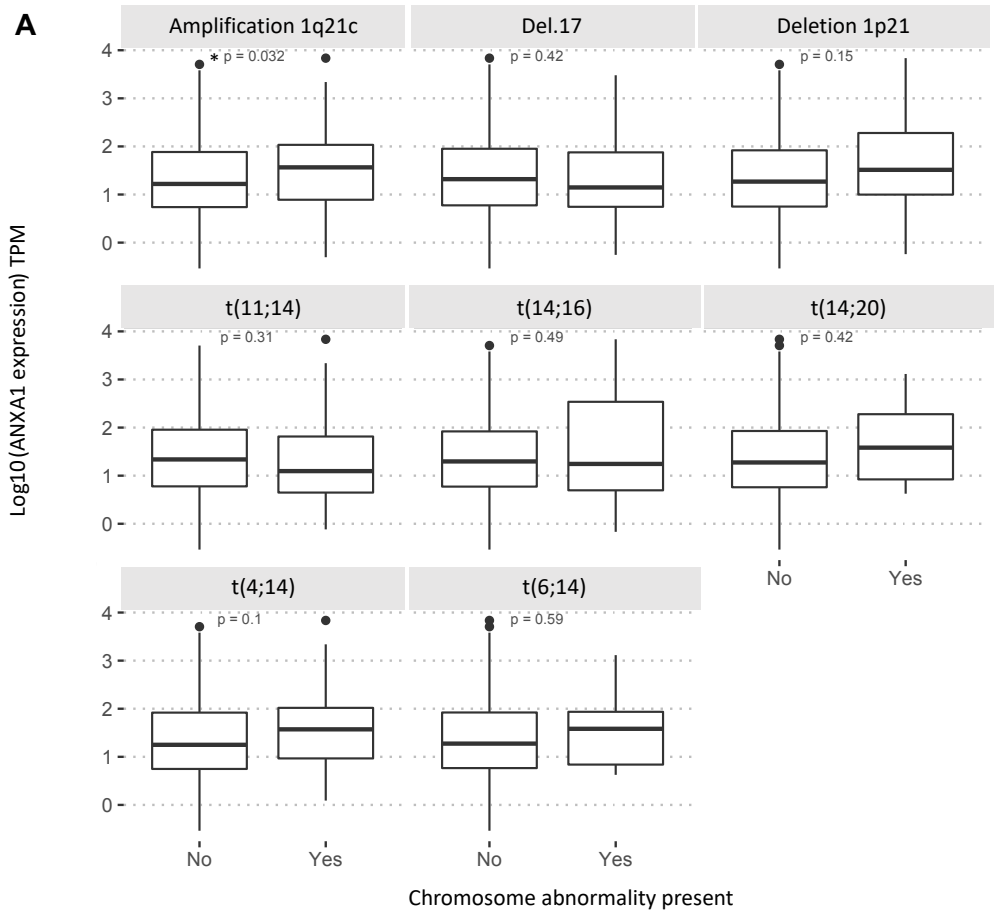

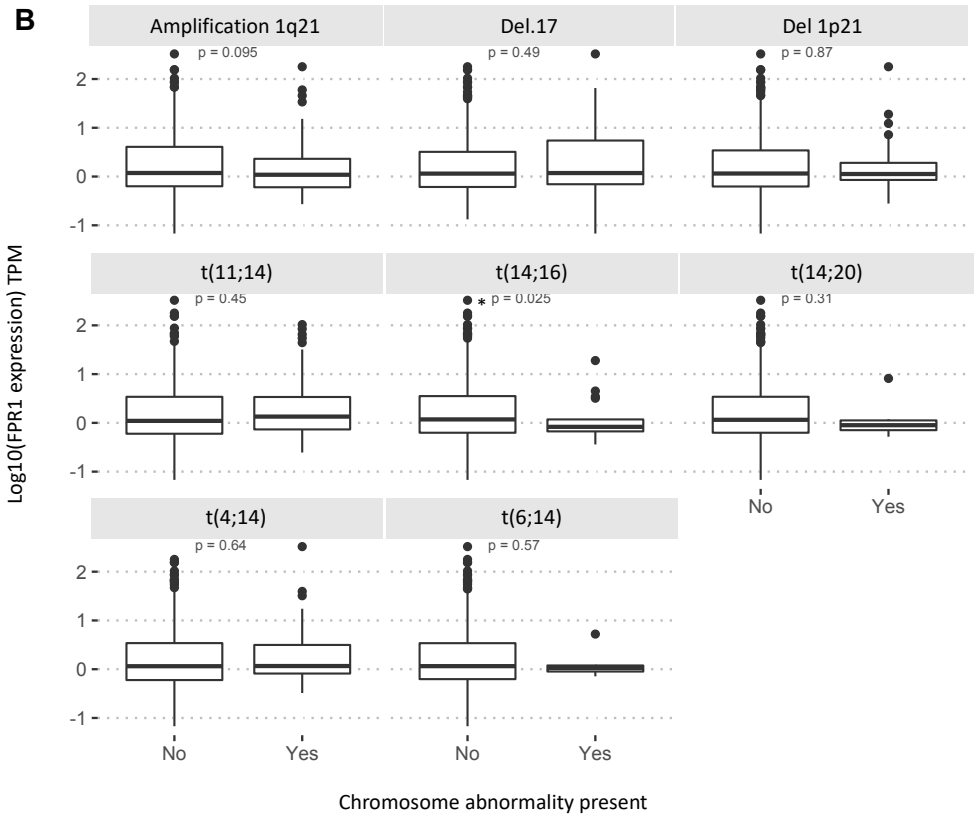

Figure 5.5 Expression of ANXA1 and FPR1 at baseline is associated with chromosomal markers of unfavourable disease prognosis

(A) Boxplots produced on R studio showing *ANXA1* expression vs the presence (Yes) or absence (NO) of a MM associated chromosomal abnormality. (B) Boxplots produced on R studio showing *FPR1* expression vs the presence (Yes) or absence (NO) of a MM associated chromosomal abnormality. A student's T-test was conducted on R studio and a P value of <0.05 was determined as significant. N=550 MM patients.

In summation, this data has shown that an increased baseline *ANXA1* is associated with worst survival outcomes in a cohort of MM patients and is also correlated with genes and gene abnormalities associated with MM pathogenesis as well as worst prognosis. Confirmation of these findings in an independent cohort would be useful for characterising the role of ANXA1 in MM its potential use as a marker of prognosis.

5.3 Discussion

Multiple Myeloma (MM) is a malignant neoplasm, characterised by abnormal proliferation of mature B cells (plasma cells) in the bone marrow (BM)[201]. Symptoms include bone damage, fatigue, renal problems and impaired immunity to name a few[399].

Myeloma pathogenesis initiates as monoclonal gammopathy of undetermined significance (MGUS), progressing to smouldering myeloma. Both of these conditions are pre-malignant (asymptomatic), involving myeloma cell growth without the bone destruction and organ involvement seen in MM[400].

Similar to in arthritic disease, MM progression relies on a tip in the balance between bone formation by osteoblasts and bone degradation by osteoclasts, favouring bone loss. Moreover, progression of MM relies heavily on involvement and composition of the bone marrow microenvironment, which contains a range of inflammatory mediators, reactive oxygen species (ROS) and reactive nitrogen intermediates (RNI). MM is also associated with a range of chromosomal and genetic abnormalities, making it a complex disease to treat[201]

Treatments for MM have improved significantly, however, the disease remains largely incurable, and treatment relapse is common. Frequently used treatments include a combination of proteosome inhibitors (to promote apoptosis in MM cells) and immunomodulatory drugs, which have shown promise in some patients. More recently, drugs have been developed to directly target the MM cells and the BM microenvironment[201]. A better understanding of the initiation of MM (through better disease models and biomarkers) and its pathogenesis is vital for improving treatment efficacy and minimising relapse.

There are several biomarkers currently used in MM diagnosis and prognosis such as the measurement of the abnormal immunoglobulin produced by MM cells (M protein) and ß2-microglobulin levels (associated with poor prognosis) amongst other factors such as serum creatinine, haemoglobin and calcium levels. However, use of these biomarkers can sometimes be problematic; for example, M protein cannot be detected in around 18% of MM cases using current testing

measures and ß2-microglobulin levels can be altered in other diseases such as kidney and liver disease. This reinforces the need for better biomarkers in the detection and staging of MM[214,401].

A major challenge in diagnosis and treatment of MM is determining the exact origin of the B cell neoplasms. Reports on the numbers and impact of circulating B cells in MM vary, although some studies have shown circulating CD19+ B cells contain genetic rearrangements identical to those expressed in BM plasma cells[402,403]. Data acquired in this project identified a substantial upregulation in the expression of ANXA1 and FPR1 surface protein expression on circulating B cells in MM patients compared to healthy cells in just 1/3 samples analysed (Figure 5.1 and 5.2). It could be speculated that there are differences in ANXA1 expression between MM patients, however as this is just preliminary data (with a low sample size), conclusions cannot be drawn. Acquisition of flow cytometric data from more MM patients would allow for a more robust result. Moreover, conducting analysis to determine if differences in surface ANXA1 and or FPR1 expression correlate with clinical parameters (i.e., survival, treatment response, disease activity) would prove useful at understanding if the difference in expression shown in this study is meaningful.

The preliminary flow cytometric data in this study, alongside the vast amount of evidence for a role of ANXA1 and FPR1 in cancer pathogenesis[193,404], led to the question as to whether ANXA1 and/or FPR1 could be used as biomarkers in MM initiation or prognosis and warranted further investigation.

MM is associated with a range of genetic factors, including gene mutations, chromosomal translocations and epigenetic changes. It is believed that MM disease progression is dependent on a combination of these genetic factors, impacting several pathways that effect the normal functioning of the plasma cell[405]. In this chapter, analysis of a cohort of MM patients showed that patients with worst survival outcomes had significantly higher baseline expression of the *ANXA1* gene. Genes associated with pathways relevant to cancer progression (such as angiogenesis and cell migration) were also upregulated in these patients. Moreover, genes specific to MM progression were

upregulated in patients expressing high *ANXA1*, namely *FGFR3,* which had the highest fold increase (Figure 5.3).

Aberrant expression of and mutations in *FGFR3* are frequently associated with worst prognosis in MM. More specifically, an upregulation of *FGFR3* is associated with the t(4;14) translocation, and patients with this translocation tend to have an overall poor prognosis[206,406]. Research has shown that wild type and mutant *FGFR3* are associated with resistance to bortezomib, a commonly used treatment in MM[407]. Moreover, knockdown of *ANXA1* both *in vivo* and *in vitro* enhanced the anti-tumour effects of bortezomib[238]. This, alongside the data presented above, suggests a pro-tumour role for *ANXA1* in this disease and treatment response, perhaps through interaction with pathways that involve *FGFR3*. This is further supported by an upregulation of genes associated with cancer progression in the *ANXA1* high expressors, such as *TCN1*[408],and the calcium binding protein genes *S100A8, S100A9*[409]and *S100A12*[410]. However, as ANXA1 requires calcium to carry out its function[411], it is not entirely surprising that an upregulation of genes encoding calcium binding proteins coincides with an upregulation in *ANXA1* expression.

Data from correlation analysis provided further evidence for a role of *ANXA1* in MM progression, by showing that 22/28 genes with a positive correlation with *ANXA1* have been implicated in a form of cancer, and, moreover, 8 of these have been implicated specifically in MM (Figure 5.4). Notably, the gene encoding the Annexin family protein, Annexin A3 (*ANXA3*) correlated the most with *ANXA1*. Dysregulated activity of this protein has been implicated in several cancers, and has been associated with cancer progression, invasiveness, metastasis and resistance to therapy[389]. Results also showed that *FPR1* not only correlated with ANXA1 expression in this MM cohort but has also been implicated both in cancer and MM and, of course, ANXA1 signalling. This suggests that the effects of ANXA1 could be mediated by FPR1 (and not FPR2) in this MM cohort and prompts further investigation into the ANXA1-FPR1 signalling pathway.

The majority of the genes in Figure 5.4 that correlate with *ANXA1* expression encode proteins involved in cell motility and structural organisation or the

immune response. MM is a cancer involving immune cells, that relies on cell motility for dissemination throughout the body[412], and this data is suggestive of ANXA1 playing a role in this process. However, importantly, a correlation of *ANXA1* with certain genes does not necessarily mean an interaction between the two proteins. Thus, further functional studies are required to investigate these relationships and interactions. For instance, mass spectrometry experiments (which identify a protein of interest and other proteins physically associated with it) could identify ANXA1 interactions with the proteins encoded by the correlating genes. ANXA1 knock-out (K.O) mice models would also prove useful at determining whether K.O of ANXA1 gene is impacts any of the cellular functions associated with the correlating genes above (e.g., cell motility experiments or immunohistochemistry to assess the cell cytoskeleton structure).

Cytogenetic abnormalities are present in the majority of MM patients and can influence disease prognosis to different degrees depending on the particular abnormality present. Translocations t(4;14), t(14;16) and t(14;20) have been associated with worst prognosis in MM, however, t(11;14), t(6;14) translocations and/or trisomies are associated with a standard-risk disease[413](median overall survival of 7 years compared to 3 years with high risk disease[414]). Analysis of chromosomal abnormalities in the MM patients showed that high *ANXA1* expression was associated with the 1q21 chromosome amplification (Figure 5.5). Gain or amplification of 1q21 is the most frequent chromosomal abnormality in MM, occurring in around 40% of MM patients, with amplification(≥4 copies) being associated with a worst prognosis than gain (3 copies)[396]. This again, links *ANXA1* with a worse prognosis in MM.

Interestingly, the majority of the S100 calcium binding proteins are encoded by genes located at the 1q21 locus[397], including the *S100A8*, *S100A9* and *S100A12* genes that were shown to be upregulated in high *ANXA1* expressors in Figure 5.3. MM patients with the 1q21 chromosome amplification also had a lower baseline *FPR1* level compared to those that didn't have this abnormality, although this change was non-significant. This suggests a potential mechanism for aberrant ANXA1 signalling in MM, mediated through S100 proteins that could be

dysregulated due to an amplification chromosome abnormality at chromosome locus 1q21.

S100 proteins are a subgroup of calcium-binding proteins that interact with multiple signalling proteins involved in a range of biological processes, notably, proliferation and differentiation. Thus, the aberrant expression of S100 proteins seen in a range of cancers has been associated with dysregulated proliferation and promotion of pro-cancer processes such as angiogenesis and metastasis[410,415-417]. Importantly, S100 proteins have been shown to induce several of these biological pathways through interaction with nuclear factor kappa B (NF-κB) and MAP kinase and pathways, which are known to involve ANXA1 signalling[43,415,416]. More specific to cancer, ANXA1 has been shown to promote cancer invasiveness and metastasis through interaction with NF-κB[418].

Although the potential mechanism of S100 proteins in MM pathogenesis is unknown, research has implicated their aberrant expression to be associated with worst prognosis and poor response to proteosome inhibitor (PI) treatment[415]. Moreover, studies have shown a significant negative correlation between S100 family members *S100A8, S100A9*, and *S100A12* and sensitivity to PIs such as bortezomib and carfilzomib[415]. Interestingly, genes encoding these three S100 proteins were upregulated in MM patients in this study expressing high baseline ANXA1 (Figure 5.3). Additionally, ANXA1 activity can be linked to this S100-associated bortezomib resistance with studies showing ANXA1 knockdown enhanced bortezomib anti-tumour effects[238].

Bortezomib in particular functions to inhibit the breakdown of inhibitory kappa B (IκB), which works to inhibit the activity of NF-κB. This in turn, prevents NF-κB translocation into the nucleus and results in inactivation of several pathways associated with MM cell signalling (e.g., anti-apoptotic and proliferation pathways). Moreover, bortezomib in particular is associated with tiggering dysregulation of intracellular calcium metabolism, and research has suggested that this dysregulation is key for bortezomib cytotoxicity[419],which again links S100 proteins to PI treatment response pathways.

Based on the knowledge discussed above on how PIs such as bortezomib can work, alongside data presented in this chapter, it could be speculated that upregulation of ANXA1 and S100 proteins together in this MM cohort results in increased NF-κB-associated signalling. This, in turn, could lead to the overactivation of pathways associated with cancer pathogenesis, but also could reduce the effectiveness of treatment response to PIs, in particular, bortezomib. Further studies investigating the effect of S100 protein knockdown on both ANXA1 and NF-κB expression as well as treatment response to bortezomib could further characterise this pathway, its components and role in MM pathogenesis.

MM patients lower baseline *FPR1* expression were more likely to have the t(14;16) translocation. This translocation is present in only around 5% of MM patients and involves the *c-Maf* oncogene locus[420]. Overexpression of *c-Maf* is a frequent occurrence in MM, and is associated with increased proliferation and interaction with BM stromal cells[421]. The limited data that is available on this *c-Maf* t(14;16) translocation suggests that it is associated with more aggressive disease and worst survival outcomes[422,423]. The fact that both *ANXA1* and *FPR1* expression positively correlate in this MM cohort and that either high *ANXA1* or low *FPR1* is associated with worst prognosis in this disease, suggests that these proteins could have not only shared, but different functions in MM. FPR1 has been shown to be marker of poor prognosis in gastric cancer, independent of ANXA1, highlighting the differing roles of the two proteins in cancer[193].

The data presented in this chapter is not without its limitations. With lack of access to more MM patient samples, determining the role and expression of ANXA1 and FPR1 at the protein level is difficult. Moreover, with lack of access to clinical information from these patients, it was not possible to assess whether changes in ANXA1 and FPR1 between patients was due to factors such as disease activity or treatment. Additionally, although a wide range of data is available from the CoMMpass database, a lot of clinical information on the MM patients was missing and gene expression at baseline was only provided. This prevented investigation into whether *ANXA1* or *FPR1* gene expression changed over time in response to disease activity or treatment. Future investigations of this nature assessing *ANXA1* and *FPR1* gene expression levels would help define the role of ANXA1 and FPR1 in MM. In particular, it would be useful to track expression of

the *ANXA1* and *FPR1* genes at different timepoints; for instance, at baseline and at the time of disease flare/treatment relapse and compare these expression levels to patients exhibiting an optimal treatment response. This would allow for assessment of whether increased *ANXA1* and *FPR1* expression are associated with worse (treatment response) outcomes over time. Moreover, it would also be important to assess whether ANXA1 and FPR1 protein expression over time reflects what is evident at the gene level, through repetition of flow cytometric experiments carried out in this study (Figure 5.1). This would provide information on whether ANXA1/FPR1 protein and gene expression data have a correlative relationship and can both be used as markers of prognosis.

In summary, data presented in this chapter has provided preliminary evidence for a link between *ANXA1* and worse prognosis in MM, with associated roles in pathways such as angiogenesis and migration, that are relevant to cancer progression. Results also showed *FPR1* correlated with *ANXA1* expression in MM and showed low baseline *FPR1* to be associated with the (14;16) translocation linked with worst prognosis in MM, which warrants further investigation into ANXA1-FPR1 signalling in MM. This study has also suggested that high baseline *ANXA1* is associated with an amplification of the 1q21 chromosome and an upregulation in the S100 calcium binding protein genes located at this chromosome, some of which have been implicated in cancer pathogenesis. Moreover, a pathway for ANXA1 and S100 binding proteins in MM has been suggested which is associated with modulation of NK-KB signalling and bortezomib treatment resistance. Taken together, the data presented in this chapter adds to the genetic complexity of MM pathogenesis and highlights a role for ANXA1 and FPR1 in predicting prognosis and treatment response, however, further research is needed for this role to he fully defined.

Further experiments could include studies in MM cell lines assessing the effects of blockade of ANXA1 and S100 proteins individually and together on both cancerous processes (migration, angiogenesis, proliferation) and response to PIs such as bortezomib. This would aid in the understanding of whether aberrant ANXA1 signalling (through interactions with S100 proteins) could be linked to treatment response in MM. Moreover, confirmation of this study's findings in an independent cohort would provide more robust evidence for a role of ANXA1

signalling in MM progression and more rationale for further investigation into whether it could function as a prognostic biomarker in this disease.

Chapter 6 General Discussion

Aberrant expression of the GC-induced protein, ANXA1 and its receptors (FPR1 and FPR2) has been shown in range of inflammatory diseases[77,424,425] and cancers[197,426,427]. This thesis explored the ANXA1-FPR signalling axis in these two disease settings with particular focus on its role in PsA and MM. Moreover, the impact of manipulation of ANXA1 signalling through addition of a novel anti-ANXA1 antibody (MDX-124) to healthy cells was assessed.

MDX-124 is currently in development as a therapeutic, and this PhD has produced important data to aid in this process. Preliminary flow cytometric experiments presented in results chapter 3 allowed characterisation of MDX-124 binding to healthy and PsA immune cells, and identified high binding to cells of monocytic origin, supporting previous studies showing ANXA1 is highly expressed on these cells[29](Figure 3.5). This preliminary characterisation of ANXA1 expression informed decisions on which immune cells to focus on in a larger multi-colour panel aimed at investigating the expression of ANXA1 and its receptors (FPR1 and FPR2) in PsA. MDX-124 mechanisms of action were also explored, and preliminary results indicated that MDX-124 could be enhancing mitochondrial respiration in healthy cells (Figure 3.7), however, more samples are needed to confirm this. Additional analysis was conducted in chapter 4 to assess the impact of MDX-124 on the inflammatory response in healthy cells, which is further discussed below.

PsA is a chronic inflammatory disease of the skin and joints[295] associated with overactivation of various immune cells and overproduction of inflammatory cytokines[98]. Despite advances in research, there are still no approved diagnostic tests for PsA[272]. A better understanding of PsA pathogenesis is essential for achieving this. As numerous studies have indicated a role for ANXA1 and FPR signalling in chronic inflammation, it was of interest in this PhD to assess whether aberrant ANXA1 and/or FPR1/FPR2 was evident in PsA. Moreover, the vast amount of data suggesting role for the ANXA1 signalling pathway in inflammation is sourced from animal models, and this study aimed to transition this to humans by assessing ANXA1 and FPR expression in inflammatory disease (PsA) patient samples. The overarching hypothesis was that ANXA1 signalling

plays a role in PsA pathogenesis. In order to explore this hypothesis, several studies were conducted in chapter 4.

The trigger for transition of the inflammatory response in the skin to the widespread joint inflammation in PsA remains unknown, however, research has highlighted clear differences in the molecular pathways activated in PsO compared to PsA[356]. Chapter 4 aimed to explore these molecular pathways and focused on comparing genetic data from PsA L skin with that from HC skin. Results identified an upregulation of *FPR1* and *FPR2* in the PsA L skin. Furthermore, *FPR1* in particular had a significant positive correlation with other genes relevant to PsA pathogenesis, such as those involved in keratinocyte proliferation (Figure 4.1 and Figure 4.2). Further analysis revealed enriched pathways in the PsA skin lesions associated with FPR1 and FPR2 activity (Figure 4.4). Two of these pathways had previously been implicated in PsO (*S. aureus* infection pathway) and PsA (NET formation pathway) pathogenesis. This data highlighted key pathways where FPR1 and FPR2 are implicated, worthy of further investigation; analysis of how enrichment of these pathways in the PsA L skin affects disease activity and prognosis will prove vital in understanding the impact of upregulated FPR1 and FPR2 in the PsA skin lesions. Moreover, confirmation of this analysis in a larger patient cohort will help to corroborate this upregulation in FPR1 and FPR2 in the PsA L skin.

To transition analysis from the PsA L skin to the PsA peripheral blood, flow cytometric analysis of ANXA1, FPR1 and FPR2 surface expression on PsA and HC PBMCs was assessed. This analysis identified altered surface expression of both ANXA1 and the FPRs on PsA PBMCs that was cell-type specific. Surface ANXA1 and FPR1 was increased on disease-relevant cells in PsA (Tc17 populations) and FPR2 surface expression was both increased (Tc17) and decreased (unswitched memory B cells) in certain PsA immune cell subsets (Figure 4.6 and Figure 4.7). This led to the hypothesis that ANXA1 could play a dual role in PsA- associated inflammation depending on which cell type and receptor it signals through. Analysis of more PsA and HC samples from both the skin and peripheral blood are essential for investigating this concept further and confirming this study's results.

Flow cytometric analysis identified monocytes as high expressors of ANXA1 in both PsA and HC samples, therefore, these cells were considered the best candidates for assessing the effects of MDX-124 on the inflammatory response. Analysis in THP-1 cells showed that addition MDX-124 to these cells during their differentiation resulted in a downregulation of surface FPR1(Figure 4.13). To potential signalling pathways induced by MDX-124 that could be associated with this downregulation, analysis of phosphokinases was conducted. Results revealed that MDX-124-treatment during THP-1 differentiation was associated with an upregulation of intracellular phosphokinases and extracellular signalling proteins associated with cell survival, proliferation, differentiation and inflammation (Figure 4.14 and Figure 4.15). Of particular interest was that FPR1 downregulation was associated with an upregulation of components of the MAP Kinase pathway, which has been shown experimentally previously[341]. Moreover, ANXA1 is known to modulate inflammation through this pathway[56]. The MAP kinase pathway is involved in the regulation of range of biological processes, from apoptosis to inflammation. This data, alongside results from this study, allowed for speculation of a mechanism through which MDX-124 could trigger this pro-inflammatory, pro-survival response in the THP-1s; through regulation of MAP kinase signalling (Figure 4.17, chapter 4).

MDX-124- associated augmentation of the inflammatory response was also evident in studies conducted in HC primary monocytes, where treatment of MDX-124 was associated with an enhancement of LPS-associated TNF-α and IL-6 production (Figure 4.16). This response was particularly evident in $CD14^{+}CD16^{+}$ monocytes, which were shown to express higher surface FPR1 in the PsA samples assessed earlier in chapter 4. This highlights a pathway involving ANXA1 and FPR1 signalling, particularly in $CD14^{+}CD16^{+}$ monocytes, that could be involved in manipulation of the inflammatory response in PsA. More samples are needed to both confirm the results obtained in this chapter, but also explore the effects of addition of MDX-124 to the inflammatory response of PBMCs (particularly monocyte populations) obtained from PsA patients. This would improve understanding both of the role of ANXA1-FPR1 signalling in PsA, but also the effects of blockade of that signalling through MDX-124.

There is substantial evidence implicating a role for the ANXA1-FPR signalling axis in cancer progression, mainly through manipulation of processes such as angiogenesis, proliferation and apoptosis [180,193,274,404,428]. However, expression of ANXA1 is variable between cancer types[174,175,177,178], and the role of ANXA1 signalling in cancer is not fully defined.

MM is a form of cancer characterised by abnormal proliferation of plasma cells throughout the bone marrow[199]. Despite MM being the second most common haematological malignancy in Europe, diagnosis is often extremely delayed due to non-specific symptoms and lack of biomarkers to predict development from the asymptomatic MGUS phase that frequently precedes MM[200]. With a role for ANXA1 signalling being implicated in cancer, and some preliminary studies implicating ANXA1[238], FPR1[393] and FPR2[241] in MM, chapter 5 of this thesis was aimed at investigating expression of ANXA1 and FPR1/FPR2 in MM. The hypothesis was that ANXA1 signalling is involved in MM pathogenesis.

To investigate this hypothesis, ANXA1, FPR1 and FPR2 surface expression on MM and HC samples was assessed by flow cytometry. Preliminary results showed a substantial increase in ANXA1 and FPR1 on circulating B cells in MM samples compared to HCs. However, repetition of these experiments with two further MM samples did not replicate this result (Figure 5.1 and Figure 5.2). This data is therefore, inconclusive and more samples are needed to explore ANXA1/FPR1 surface expression in MM. However, based on data suggesting increased ANXA1 can limit response to certain MM treatments (bortezomib[238]), it could be speculated that differences in ANXA1 (and potentially the receptor it signals through, FPR1) could reflect response to treatment in the 3 MM patients assessed. Repeats of this analysis, as well as tracking ANXA1/FPR1 expression alongside clinical parameters (i.e., survival, treatment response, disease activity) would be vital for understanding the clinical significance of the differences in ANXA1/FPR1 surface expression shown in these samples.

MM disease progression has been linked to a range of genetic and chromosomal abnormalities[216,406,415]. Due to the flow cytometric data suggesting potential changes in ANXA1 and FPR1 surface expression in in MM and the restricted access to more MM samples due to the Covid-19 pandemic, the focus of the project

moved to analysing expression of ANXA1 and the FPRs in MM using a publicly available MM genetic database, the CoMMpass database[264]. Analysis of a cohort of 550 MM patients revealed that patients with a higher expression of the *ANXA1* gene at baseline had worse survival outcomes. Further analysis grouped these patients based on their *ANXA1* expression (high vs low) to assess the relevance of this expression to factors related to MM pathogenesis. Bioinformatic analysis identified pathways relevant to MM progression (angiogenesis and cell migration) enriched in patients with high baseline *ANXA1* compared to those with low baseline *ANXA*1. Additionally, differential gene expression analysis revealed that genes relevant to MM pathogenesis were upregulated in patients expressing high *ANXA1*(Figure 5.3). Namely, *FGFR3*, which is a commonly mutated gene in MM. Upregulation of this gene is linked with the t(4;14) chromosome translocation, which indicates poor prognosis in MM[206,406].

Several results presented in this thesis allowed for speculation that *ANXA1* expression levels could be linked to treatment resistance in MM, particularly to proteosome inhibitors such as bortezomib. Notably, both *FGFR3* and ANXA1 are associated with resistance bortezomib[238,407]. Additionally, the S100 family proteins S100A8, S100A9, and S100A12, which were upregulated in patients expressing high baseline *ANXA1* in this study, have been linked to treatment resistance to proteosome inhibitors, including bortezomib[415]. Interestingly, the S100 proteins (including S100A9 S100A8 and S10012) are located at the 1q21 chromosome locus, which is commonly amplified in MM and is associated with worse prognosis[396]. Additional analysis of chromosomal abnormalities in this cohort of MM patients revealed that baseline *ANXA1* expression was also associated with the 1q21 chromosome amplification (Figure 5.5). This data highlighted a potential signalling pathway involving ANXA1 and S100 proteins in MM (potentially triggered by the 1q21 chromosomal amplification) which warrants further investigation.

This data led to speculation that results linking high baseline *ANXA1* expression and worst survival outcomes in this cohort could be linked to treatment resistance, particularly to bortezomib. However, as most of the patients were on changing multi-treatment regimes, and ANXA1 expression levels were only taken at baseline, it was not possible to assess the correlative relationship between

ANXA1 expression and response bortezomib treatment only in this study. Future analysis assessing the expression of *ANXA1* before and after treatment, particularly with bortezomib, would be vital for understanding if there is a relationship between *ANXA1* and treatment resistance. Moreover, MM cell line studies assessing ANXA1-S100 protein interactions in response to bortezomib treatment would aid with understanding whether potential resistance bortezomib could be mediated through ANXA1-S100 protein signalling pathways.

In conclusion, this PhD has shown that ANXA1 and FPR receptor expression is altered in both inflammatory disease (PsA) and cancer (MM) settings. Throughout several chapters of this thesis, I have showed that ANXA1, FPR1 and FPR2 surface expression is altered on disease-relevant immune cell subsets in PsA, I have also showed that *FPR1* and *FPR2* gene expression is increased in PsA skin lesions and that expression these genes is correlated with enriched pathways in the PsA L skin relevant to disease pathogenesis. In addition, I have showed that increased baseline expression of the *ANXA1* gene is correlated with worst survival outcomes in a cohort of MM patients and that higher *ANXA1* expression is associated with an upregulation of genes associated with MM treatment resistance. I have also highlighted a prospective pathway that could be responsible for this resistance involving S100 calcium-binding proteins, which requires further investigation. Finally, this thesis has showed that manipulation of ANXA1 expression on monocytic cells using a novel anti-ANXA1 antibody results in increased activation of proteins involved in pathways associated with cell survival and inflammation. This preliminary data has, in turn, suggested a potential dual function of ANXA1 in both inflammation and cancer. Further work aimed at validating the preliminary results in this thesis and characterising the exact signalling pathways triggered as a result of aberrant ANXA1 expression is key to define the function of ANXA1 in both PsA and MM.

Impact of COVID-19

Due to the COVID-19 pandemic, healthy control and patient samples were unavailable. Moreover, access to the lab was limited. This meant that the project had to take a different (bioinformatics-based) approach than initially planned. Additionally, sample sizes are not as big as initially planned due to the reasons mentioned above.

Appendix

Media and Buffers

1X Phosphate Buffered Saline pH 7.4 (PBS):

8 g NaCl (Sodium chloride, MW
58.44 g/mol)
0.2 g KCl (potassium chloride, MW 74.5513 g/mol),
0.2 g KH2 PO4(Monopotassium phosphate, MW 136.086 g/mol)
and 1.74 g Na2 HPO 4 (Disodium phosphate, MW 141.96 g/mol)
in 1 litre of deionised water

Complete RPMI (cRPMI):

500ml RPMI (Gibco, Invitrogen)
50ml Heat Inactivated Fetal Bovine Serum (Invitrogen), 5ml Penicillin-Streptomycin (Sigma) , 5ml L-Glutamine (Invitrogen)

Cell Separation Buffer:

500ml dPBS (Invitrogen)
2mM EDTA (Invitrogen)
1% Heat Inactivated Fetal Bovine Serum (Invitrogen)

FACS buffer:

1 x dPBS
2% Heat Inactivated Fetal Bovine Serum
5mM EDTA

ELISA wash buffer:

250 µl Tween-20
0.2g EDTA
500mls PBS

ELISA Assay buffer:

2.5g BSA (ThermoFisher)

500µl Tween-20

2.5mls Proclin

Cell stimulation cocktail for proteome profiler assay

Per 1 million cells:

2.5 µl IFN-Y, final concentration=25ng

2µl IL-4, final concentration=20ng

1µl IL-6, final concentration=100ng

LPS- 4ul of 1/100 dilution from 1mg/ml stock, final concentration=10µg

Published papers

Review article- Kelly, L. et al. Annexin-A1: The culprit or the solution? Immunology (2022).

Supplementary tables

Table 1 Top 10 pathways upregulated in the PsA L skin

	GO.ID	Pathway	P.adj	Genes associated with each pathway
1	GO:0006959	Humoral immune response	1.23 E-38	IGLC7/IGHV1-3/IGHV3-7/MASP1/CXCL13/GNLY/GPR183/C9/PRSS3/CXCL8/CXCL2/IGLC2/IGLC3/BLNK/LTF/JCHAIN/CD83/PI3/SLPI/CXCL9/POU2AF1/IL6/PSMB10/IGHV4-28/IGHV3-33/IGHV4-39/IL17F/C1QC/TRBC1/TREM1/LTA/CCR7/IGHV4-31/SEMG2/IGHV5-10-1/CXCL3/CXCL5/CXCL1/IGKV3-20/KRT6A/CCL2/IGHV3-30/IL17A/CXCL6/LYZ/CXCL11/CXCL10/IL1B/FCN1/IGHV6-1/IGHV1-69/IL36RN/SH2D1A/PTPRC/IGHV1-69D/CD28/IGHV3-43/IGLL5/DMBT1/PAX5/IGHV3-11/IGHV3-21/IGHV3-20/IGHV1-18/IGHV3-23/S100A9/S100A12/CCR2/CR1/TRBC2/IGKC/BCL3/CAMP/PGLYRP4/DEFB4A/EXO1/NOD2/IGHA2/IGHG2/IGHG4/IGHA1/IGHG3/IGHG1/IFNG/TNFRSF21/S100A7/IGHV4-59/IGHV3-74/IFNE/IGHV3-48/IGHV3-53/IGHV5-51/EBI3/PGLYRP3/PDCD1/IGHV4-4/C1QB/CFB/IGHV2-5
2	GO:0042742	Defence response to bacterium	3.79 E-35	IL23R/IGLC7/FPR2/CLEC4D/CLEC4E/IGHV1-3/IGHV3-7/IL12B/CXCL13/IL23A/GNLY/SHC1/LCE3C/KLRK1/GRN/IGLC2/IGLC3/ARG2/LTF/JCHAIN/PI3/SLPI/LBP/IL7R/ACP5/IL6/IGHV4-28/IGHV3-33/IGHV4-39/IL17F/LCE3A/TRBC1/TREM1/LTA/IGHV4-31/S100A8/OAS3/OAS2/SEMG2/PGLYRP2/ZNFX1/ISG15/IGHV5-10-1/IRF8/IGKV3-20/KRT6A/IGHV3-30/IL17A/CXCL6/PYCARD/LYZ/IGHV6-1/LCN2/IGHV1-69/OAS1/IGHV1-69D/IGHV3-43/CCL20/IGLL5/CD36/DMBT1/IGHV3-11/IGHV3-21/IGHV3-20/IGHV1-18/IGHV3-23/S100A9/S100A12/GBP6/PLAC8/EPHA2/RNF213/TRBC2/NOS2/IGKC/BCL3/CAMP/PGLYRP4/PLA2G2A/MYD88/DEFB4A/NOD2/IGHA2/IGHG2/IGHG4/IGHA1/IGHG3/IGHG1/GSDMC/S100A7/IGHV4-59/GBP4/ADAM17/IGHV3-74/IFNE/IGHV3-48/IGHV3-53/IGHV5-51/PGLYRP3/IGHV4-4/TLR2/IGHV2-5
3	GO:0002443	Leukocyte mediated immunity	5.11 E-35	PIK3CG/IL23R/IGLC7/IGHV1-3/IGHV3-7/BATF/IL12B/RAC2/LYN/IL23A/DDX58/FUT7/C9/KLRK1/DDX21/IL4I1/JAK3/IGLC2/IGLC3/TNFRSF1B/GZMB/LAG3/SLAMF6/SASH3/RAB27A/LILRB4/IL7R/CLEC4G/IL6/SERPINB9/IGHV4-28/IGHV3-33/IGHV4-39/FZD5/IL9R/DNASE1L3/ICAM1/C1QC/RSAD2/CBL/TRBC1/TREM1/LTA/IGHV4-31/MYO1G/CD1B/ULBP1/IGHV5-10-1/KLRC1/PTAFR/CCL3/RAET1E/LILRB1/IGHV3-30/CXCL6/NLRP3/PRF1/IL1B/IRF7/SLAMF1/RASGRP1/IGHV6-1/IL21R/IGHV1-69/IL4R/FCGR3A/ARG1/CD40LG/SH2D1A/RNF168/FOXP3/PTPRC/IGHV1-69D/FCGR1A/CSF2RB/CD28/IGHV3-43/TBX21/CD96/ULBP3/ULBP2/IGLL5/CD27/SLA2/CD177/CRTAM/NR4A3/IGHV3-11/IGHV3-21/IGHV3-20/IGHV1-18/IGHV3-23/CTSC/CCR2/CR1/TLR8/IL12RB1/SERPINB4/KLRD1/KIR2DL4/TRBC2/HMOX1/NOS2/IGKC/BCL3/MYD88/RAET1G/EXO1/PLA2G3/NOD2/IGHA2/IGHG2/IGHG4/IGHA1/IGHG3/IGHG1/SLC22A13/CD226/CD8A/IGHV4-59/ADAM17/IGHV3-74/IGHV3-48/IGHV3-53/IGHV5-51/CLEC7A/IGHV4-4/NKG7/C1QB/SLAMF7/IGHV2-5

4	GO:0002449	Lymphocyte mediated immunity	7.47E-34	IL23R/IGLC7/IGHV1-3/IGHV3-7/BATF/IL12B/IL23A/FUT7/C9/KLRK1/IL4I1/IGLC2/IGLC3/TNFRSF1B/GZMB/LAG3/SLAMF6/SASH3/RAB27A/LILRB4/IL7R/CLEC4G/IL6/SERPINB9/IGHV4-28/IGHV3-33/IGHV4-39/FZD5/IL9R/ICAM1/C1QC/RSAD2/TRBC1/LTA/IGHV4-31/MYO1G/CD1B/ULBP1/IGHV5-10-1/KLRC1/RAET1E/LILRB1/IGHV3-30/NLRP3/PRF1/IL1B/IRF7/SLAMF1/RASGRP1/IGHV6-1/IL21R/IGHV1-69/IL4R/FCGR3A/ARG1/CD40LG/SH2D1A/RNF168/FOXP3/PTPRC/IGHV1-69D/FCGR1A/CSF2RB/CD28/IGHV3-43/TBX21/CD96/ULBP3/ULBP2/IGLL5/CD27/SLA2/CRTAM/IGHV3-11/IGHV3-21/IGHV3-20/IGHV1-18/IGHV3-23/CTSC/CCR2/CR1/TLR8/IL12RB1/SERPINB4/KLRD1/KIR2DL4/TRBC2/IGKC/BCL3/MYD88/RAET1G/EXO1/NOD2/IGHA2/IGHG2/IGHG4/IGHA1/IGHG3/IGHG1/SLC22A13/CD226/CD8A/IGHV4-59/IGHV3-74/IGHV3-48/IGHV3-53/IGHV5-51/IGHV4-4/NKG7/C1QB/SLAMF7/IGHV2-5
5	GO:0051249	Regulation of lymphocyte activation	8.32272E-34	IL23R/IGLC7/IGHV1-3/IGHV3-7/CD80/IL12B/RAC2/LYN/IL23A/GPR183/CTLA4/KLRK1/CD22/FLOT2/IL4I1/JAK3/LGALS9B/CD6/IGLC2/IGLC3/CD5/CAMK4/TNFRSF13B/ARG2/TNFRSF1B/CD83/ADAM8/CD24/LAG3/CCDC88B/IRF1/SASH3/PLA2G2F/LILRB4/CGAS/IL7R/CLEC4G/IL6/IGHV4-28/IGHV3-33/IGHV4-39/TRBC1/CD38/CCR7/IGHV4-31/ICOS/IDO1/PRKCQ/HSPH1/LCK/PGLYRP2/PTPN22/LGALS9C/IGHV5-10-1/SAMSN1/CD209/TNFSF14/CCL2/LILRB1/IGHV3-30/IL2RA/PYCARD/NLRP3/CD274/IL1B/IKZF3/CCL5/CARD11/SLAMF1/LILRB2/RASGRP1/IGHV6-1/FANCA/CD2/IGHV1-69/IL4R/FCGR3A/ARG1/CD40LG/TNFRSF4/PRDM1/EPHB2/FOXP3/PTPRC/IGHV1-69D/SIT1/CD28/IGHV3-43/TBX21/IGLL5/CD27/TIGIT/CRTAM/CD47/IGHV3-11/IGHV3-21/IGHV3-20/IGHV1-18/IGHV3-23/MZB1/CCR2/CR1/CD3E/ZC3H12A/SIRPG/RASAL3/NFKBIZ/IL12RB1/TRBC2/IGKC/HMGB3/PSG9/MYD88/PNP/SOCS1/NOD2/IGHA2/IGHG2/IGHG4/IGHA1/IGHG3/IGHG1/PLA2G2D/VNN1/TNFSF9/RHOH/FCRL3/IFNG/TNFRSF21/IGHV4-59/IGHV3-74/SIRPB1/IGHV3-48/IGHV3-53/IGHV5-51/EBI3/LAX1/CLEC7A/IGHV4-4/THY1/SLC7A1/LAPTM5/IGHV2-5
6	GO:0002460	Adaptive immune response based on somatic recombination of immune receptors built from immunoglobulin superfamily domains	1.3635E-33	IL23R/IGLC7/IGHV1-3/IGHV3-7/CD80/BATF/IL12B/CXCL13/IL23A/FUT7/C9/IL4I1/JAK3/IGLC2/IGLC3/RELB/TNFRSF1B/SLAMF6/SASH3/RAB27A/LILRB4/IL7R/CLEC4G/IL6/IGHV4-28/IGHV3-33/IGHV4-39/FZD5/IL9R/LY9/ICAM1/C1QC/RSAD2/TRBC1/CLEC6A/LTA/IGHV4-31/MYO1G/PRKCQ/CD1B/IGHV5-10-1/KLRC1/LILRB1/IGHV3-30/ENTPD7/NLRP3/PRF1/CD274/IL1B/IRF7/SLAMF1/KLHL6/IGHV6-1/IL21R/IGHV1-69/IL4R/FCGR3A/ARG1/CD40LG/EPHB2/RNF168/FOXP3/PTPRC/IGHV1-69D/FCGR1A/CSF2RB/CD28/IGHV3-43/TBX21/IGLL5/CD27/SLA2/IGHV3-11/IGHV3-21/IGHV3-20/IGHV1-18/IGHV3-23/CTSC/CCR2/CR1/ZC3H12A/NFKBIZ/TLR8/IL12RB1/KLRD1/TRBC2/IGKC/BCL3/PSG9/MYD88/EXO1/NOD2/IGHA2/IGHG2/IGHG4/IGHA1/IGHG3/IGHG1/SLC22A13/STAT3/CD226/CD8A/IGHV4-59/ADAM17/IGHV3-74/IGHV3-48/IGHV3-53/IGHV5-51/EBI3/CLEC7A/IGHV4-4/C1QB/IGHV2-5

7	GO:0002696	Positive regulation of leukocyte activation	1.70681E-33	IL23R/IGLC7/CLEC4D/IGHV1-3/IGHV3-7/CD80/IL12B/LYN/IL23A/GPR183/KLRK1/FLOT2/IL4I1/JAK3/CD6/IGLC2/IGLC3/CD5/TSLP/CD83/ADAM8/CD24/CCDC88B/SASH3/LILRB4/LBP/IL7R/IL6/IGHV4-28/IGHV3-33/IGHV4-39/TRBC1/CD38/CCR7/IGHV4-31/ICOS/CRLF2/PRKCQ/HSPH1/LCK/PTPN22/IGHV5-10-1/PTAFR/CD209/TNFSF14/CCL3/CCL2/LILRB1/IGHV3-30/IL2RA/PYCARD/NLRP3/CD274/IL1B/CCL5/CARD11/SLAMF1/LILRB2/RASGRP1/IGHV6-1/CD2/IGHV1-69/IL4R/FCGR3A/CD40LG/TNFRSF4/EPHB2/FOXP3/PTPRC/IGHV1-69D/CD28/IGHV3-43/TBX21/WNT5A/IGLL5/CD27/CD177/CD47/NR4A3/IGHV3-11/IGHV3-21/IGHV3-20/IGHV1-18/IGHV3-23/CTSC/CCR2/CR1/CD3E/SIRPG/RASAL3/NFKBIZ/IL12RB1/TRBC2/IGKC/MYD88/PLA2G3/PNP/SOCS1/NOD2/IGHA2/IGHG2/IGHG4/IGHA1/IGHG3/IGHG1/VNN1/TNFSF9/RHOH/FCRL3/IFNG/CD226/IGHV4-59/IGHV3-74/SIRPB1/IGHV3-48/IGHV3-53/IGHV5-51/EBI3/CLEC7A/IGHV4-4/THY1/SLC7A1/IGHV2-5
8	GO:0050867	Positive regulation of cell activation	2.22847E-33	IL23R/IGLC7/CLEC4D/IGHV1-3/IGHV3-7/CD80/IL12B/LYN/IL23A/GPR183/KLRK1/FLOT2/IL4I1/JAK3/CD6/IGLC2/IGLC3/CD5/TSLP/CD83/ADAM8/CD24/CCDC88B/SASH3/LILRB4/LBP/IL7R/IL6/IGHV4-28/IGHV3-33/IGHV4-39/TRBC1/CD38/CCR7/IGHV4-31/ICOS/CRLF2/PRKCQ/HSPH1/LCK/PTPN22/IGHV5-10-1/PTAFR/CD209/TNFSF14/CCL3/CCL2/LILRB1/IGHV3-30/IL2RA/PYCARD/NLRP3/CD274/IL1B/CCL5/CARD11/SLAMF1/LILRB2/RASGRP1/IGHV6-1/CD2/IGHV1-69/IL4R/FCGR3A/CD40LG/TNFRSF4/EPHB2/FOXP3/PTPRC/IGHV1-69D/CD28/IGHV3-43/TBX21/WNT5A/IGLL5/CD27/CD177/CD47/NR4A3/IGHV3-11/IGHV3-21/IGHV3-20/IGHV1-18/IGHV3-23/CTSC/CCR2/CR1/CD3E/SIRPG/RASAL3/NFKBIZ/IL12RB1/TRBC2/IGKC/MYD88/PLA2G3/PNP/SOCS1/NOD2/IGHA2/IGHG2/IGHG4/IGHA1/IGHG3/IGHG1/VNN1/TNFSF9/RHOH/FCRL3/IFNG/CD226/IGHV4-59/IGHV3-74/SIRPB1/IGHV3-48/IGHV3-53/IGHV5-51/EBI3/CLEC7A/IGHV4-4/THY1/SLC7A1/IGHV2-5
9	GO:0042110	T cell activation	5.46445E-31	CDH26/PIK3CG/IL23R/CLEC4D/CLEC4E/THEMIS/CD80/BATF/IL12B/RAC2/LYN/IL23A/ITGAL/FUT7/GPR183/CTLA4/KLRK1/FLOT2/IL4I1/CTSL/JAK3/WDFY4/LGALS9B/CD6/CD5/CAMK4/ARG2/RELB/TNFRSF1B/CD83/ADAM8/CD24/LAG3/CCDC88B/SLAMF6/IRF1/SASH3/RAB27A/PLA2G2F/LILRB4/CGAS/IL7R/TREML2/CLEC4G/IL6/PSMB10/FZD5/LY9/ICAM1/RSAD2/CCR7/ICOS/IDO1/PRKCQ/HSPH1/LCK/PTPN22/LGALS9C/KLRC1/CD209/TNFSF14/CCL2/EOMES/LILRB1/IL2RA/PYCARD/ENTPD7/ITK/NLRP3/CD274/IL1B/DOCK2/CCL5/CARD11/SLAMF1/CD48/LILRB2/RASGRP1/GPR18/FANCA/CD2/IL4R/ARG1/CD40LG/TNFRSF4/PRDM1/FOXP3/PTPRC/CD3G/SIT1/CD28/TBX21/CD27/SLA2/TIGIT/CRTAM/CD47/HSH2D/MICB/CCR2/CR1/CD3E/NLRC3/ZC3H12A/SIRPG/RASAL3/NFKBIZ/IL12RB1/CTPS1/BCL3/PSG9/CD3D/PNP/SOCS1/NOD2/PLA2G2D/STAT3/VNN1/TNFSF9/RHOH/IFNG/TNFRSF21/CD8A/ADAM17/SIRPB1/IFNE/CD7/EBI3/GBA/LAX1/CLEC7A/THY1/SLC7A1/NKG7/LAPTM5/SLAMF7

10	GO:0051251	Positive regulation of lymphocyte activation	1.52097E-30	IL23R/IGLC7/IGHV1-3/IGHV3-7/CD80/IL12B/LYN/IL23A/GPR183/KLRK1/FLOT2/IL4I1/JAK3/CD6/IGLC2/IGLC3/CD5/CD83/ADAM8/CD24/CCDC88B/SASH3/LILRB4/IL7R/IL6/IGHV4-28/IGHV3-33/IGHV4-39/TRBC1/CD38/CCR7/IGHV4-31/ICOS/PRKCQ/HSPH1/LCK/PTPN22/IGHV5-10-1/CD209/TNFSF14/CCL2/LILRB1/IGHV3-30/IL2RA/PYCARD/NLRP3/CD274/IL1B/CCL5/CARD11/SLAMF1/LILRB2/RASGRP1/IGHV6-1/IGHV1-69/IL4R/FCGR3A/CD40LG/TNFRSF4/EPHB2/FOXP3/PTPRC/IGHV1-69D/CD28/IGHV3-43/TBX21/IGLL5/CD27/CD47/IGHV3-11/IGHV3-21/IGHV3-20/IGHV1-18/IGHV3-23/CCR2/CR1/CD3E/SIRPG/RASAL3/NFKBIZ/IL12RB1/TRBC2/IGKC/MYD88/PNP/SOCS1/NOD2/IGHA2/IGHG2/IGHG4/IGHA1/IGHG3/IGHG1/VNN1/TNFSF9/RHOH/FCRL3/IFNG/IGHV4-59/IGHV3-74/SIRPB1/IGHV3-48/IGHV3-53/IGHV5-51/EBI3/CLEC7A/IGHV4-4/THY1/SLC7A1/IGHV2-5

Table 2 Top 10 pathways downregulated in the PsA L skin

		Pathway	P.adj	Genes associated with each pathway
1	GO:0006936	Muscle contraction	1.14E-44	IGLC7/IGHV1-3/IGHV3-7/MASP1/CXCL13/GNLY/GPR183/C9/PRSS3/CXCL8/CXCL2/IGKV1-5/IGLC2/IGLC3/BLNK/LTF/JCHAIN/CD83/PI3/SLPI/IGKV3-15/CXCL9/POU2AF1/IL6/PSMB10/IGKV2-30/IGHV4-28/IGHV3-33/IGHV4-39/C1QC/TRBC1/TREM1/LTA/CCR7/IGHV4-31/S100A8/SEMG2/PGLYRP2/IGHV5-10-1/CXCL3/CXCL5/CXCL1/IGKV3-20/KRT6A/IGKV1-17/CCL2/IGLV2-8/IGHV3-30/CXCL6/LYZ/CXCL11/CXCL10/IL1B/FCN1/IGLV1-51/IGLV6-57/IGLV1-47/IGHV6-1/LCN2/IGHV1-69/IL36RN/SH2D1A/PTPRC/IGHV1-69D/CD28/IGHV3-43/IGLL5/DMBT1/PAX5/IGHV3-11/IGHV3-21/IGHV3-20/IGHV1-18/IGHV3-23/S100A9/S100A12/CCR2/CR1/TRBC2/IGLV2-14/IGLV3-19/IGKV4-1/IGKC/BCL3/CAMP/PGLYRP4/PLA2G2A/DEFB4A/EXO1/IGHA2/IGHG2/IGHG4/IGHA1/IGHG3/IGHG1/IGLV1-40/IGLV1-44/IGLV3-25/IFNG/TNFRSF21/S100A7/IGHV4-59/IGHV3-74/IFNE/IGHV3-48/IGHV3-53/IGHV5-51/EBI3/PGLYRP3/PDCD1/IGHV4-4/C1QB/CFB/IGHV2-5

2	GO:0003012	Muscle system process	1.79E-37	IL23R/IGLC7/IGHV1-3/IGHV3-7/BATF/IL12B/IL23A/FUT7/C9/KLRK1/IGKV1-5/IL18RAP/IGLC2/IGLC3/TNFRSF1B/GZMB/IGKV3-15/LAG3/SLAMF6/SASH3/RAB27A/IL7R/CLEC4G/IL6/SERPINB9/IGKV2-30/IGHV4-28/IGHV3-33/IGHV4-39/FZD5/ICAM1/C1QC/RSAD2/TRBC1/LTA/IGHV4-31/MYO1G/CD1B/ULBP1/IGHV5-10-1/IGKV3-20/IGKV1-17/RAET1E/IGLV2-8/LILRB1/IGHV3-30/NLRP3/PRF1/IL1B/IRF7/IGLV1-51/IGLV6-57/IGLV1-47/RASGRP1/IGHV6-1/IGHV1-69/IL4R/ARG1/CD40LG/SH2D1A/RNF168/FOXP3/PTPRC/IGHV1-69D/CD28/IGHV3-43/TBX21/CD96/ULBP3/ULBP2/IGLL5/CD27/SLA2/CRTAM/IGHV3-11/IGHV3-21/IGHV3-20/IGHV1-18/IGHV3-23/CTSC/CCR2/CR1/TLR8/IL12RB1/SERPINB4/KLRD1/KIR2DL4/TRBC2/IGLV2-14/IGLV3-19/IGKV4-1/IGKC/BCL3/RAET1G/EXO1/IGHA2/IGHG2/IGHG4/IGHA1/IGHG3/IGHG1/SLC22A13/IGLV1-40/IGLV1-44/IGLV3-25/CD226/CD8A/IGHV4-59/IGHV3-74/IGHV3-48/IGHV3-53/IGHV5-51/IGHV4-4/C1QB/SLAMF7/IGHV2-5
3	GO:0050804	Modulation of chemical synaptic transmission	4.78E-34	IL23R/BTLA/IGLC7/CLEC4D/IGHV1-3/IGHV3-7/CD80/IL12B/LYN/IL23A/GPR183/CTLA4/KLRK1/FLOT2/JAK3/CD6/IGLC2/IGLC3/CD5/TSLP/CD83/ADAM8/CD24/CCDC88B/SASH3/LILRB4/LBP/IL7R/IL6/IGHV4-28/IGHV3-33/IGHV4-39/TRBC1/CD38/CCR7/IGHV4-31/ICOS/CRLF2/PRKCQ/HSPH1/LCK/PTPN22/IGHV5-10-1/PTAFR/CD209/TNFSF14/CCL3/CCL2/LILRB1/IGHV3-30/IL2RA/PYCARD/NLRP3/CD274/IL1B/CCL5/CARD11/LILRB2/RASGRP1/IGHV6-1/CD2/IGHV1-69/IL4R/GRAP2/CD40LG/TNFRSF4/FOXP3/PTPRC/IGHV1-69D/CD28/IGHV3-43/LILRA5/TBX21/WNT5A/IGLL5/CD27/CD177/CD47/NR4A3/IGHV3-11/IGHV3-21/IGHV3-20/IGHV1-18/IGHV3-23/PLEK/CTSC/PDPN/CCR2/CD3E/SIRPG/RASAL3/NFKBIZ/IL12RB1/TRBC2/IGKC/PLA2G3/PNP/SOCS1/NOD2/IGHA2/IGHG2/IGHG4/IGHA1/IGHG3/IGHG1/VNN1/TNFSF9/RHOH/FCRL3/IFNG/CD226/IGHV4-59/IGHV3-74/SIRPB1/IGHV3-48/IGHV3-53/IGHV5-51/EBI3/PDCD1/CLEC7A/IGHV4-4/THY1/SLC7A1/IGHV2-5
4	GO:0099177	Regulation of trans-synaptic signaling	6.15E-34	IL23R/IGLC7/IGHV1-3/IGHV3-7/CD80/BATF/IL12B/CXCL13/IL23A/FUT7/C9/JAK3/IGKV1-5/IL18RAP/IGLC2/IGLC3/RELB/TNFRSF1B/IGKV3-15/SLAMF6/SASH3/RAB27A/IL7R/CLEC4G/IL6/IGKV2-30/IGHV4-28/IGHV3-33/IGHV4-39/FZD5/LY9/ICAM1/C1QC/RSAD2/TRBC1/LTA/IGHV4-31/MYO1G/PRKCQ/CD1B/IGHV5-10-1/IGKV3-20/IGKV1-17/IGLV2-8/LILRB1/IGHV3-30/NLRP3/PRF1/CD274/IL1B/IRF7/IGLV1-51/IGLV6-57/IGLV1-47/KLHL6/IGHV6-1/IGHV1-69/IL4R/ARG1/CD40LG/RNF168/FOXP3/PTPRC/IGHV1-69D/CD28/IGHV3-43/TBX21/IGLL5/CD27/SLA2/IGHV3-11/IGHV3-21/IGHV3-20/IGHV1-18/IGHV3-23/CTSC/CCR2/CR1/ZC3H12A/NFKBIZ/TLR8/IL12RB1/TRBC2/IGLV2-14/IGLV3-19/IGKV4-1/IGKC/BCL3/EXO1/IGHA2/IGHG2/IGHG4/IGHA1/IGHG3/IGHG1/SLC22A13/STAT3/IGLV1-40/IGLV1-44/IGLV3-25/CD226/CD8A/IGHV4-59/ADAM17/IGHV3-74/IGHV3-48/IGHV3-53/IGHV5-51/EBI3/IGHV4-4/C1QB/IGHV2-5

5	GO:0042391	Regulation of membrane potential	9.15E-34	IL23R/BTLA/IGLC7/CLEC4D/IGHV1-3/IGHV3-7/CD80/IL12B/LYN/IL23A/GPR183/CTLA4/KLRK1/FLOT2/JAK3/CD6/IGLC2/IGLC3/CD5/TSLP/CD83/ADAM8/CD24/CCDC88B/SASH3/LILRB4/LBP/IL7R/IL6/IGHV4-28/IGHV3-33/IGHV4-39/TRBC1/CD38/CCR7/IGHV4-31/ICOS/CRLF2/PRKCQ/HSPH1/LCK/PTPN22/IGHV5-10-1/PTAFR/CD209/TNFSF14/CCL3/CCL2/LILRB1/IGHV3-30/IL2RA/PYCARD/NLRP3/CD274/IL1B/CCL5/CARD11/LILRB2/RASGRP1/IGHV6-1/CD2/IGHV1-69/IL4R/GRAP2/CD40LG/TNFRSF4/FOXP3/PTPRC/IGHV1-69D/CD28/IGHV3-43/TBX21/WNT5A/IGLL5/CD27/CD177/CD47/NR4A3/IGHV3-11/IGHV3-21/IGHV3-20/IGHV1-18/IGHV3-23/CTSC/CCR2/CD3E/SIRPG/RASAL3/NFKBIZ/IL12RB1/TRBC2/IGKC/PLA2G3/PNP/SOCS1/NOD2/IGHA2/IGHG2/IGHG4/IGHA1/IGHG3/IGHG1/VNN1/TNFSF9/RHOH/FCRL3/IFNG/CD226/IGHV4-59/IGHV3-74/SIRPB1/IGHV3-48/IGHV3-53/IGHV5-51/EBI3/PDCD1/CLEC7A/IGHV4-4/THY1/SLC7A1/IGHV2-5
6	GO:0034765	Regulation of ion transmembrane transport	2.00E-33	IL23R/BTLA/IGLC7/IGHV1-3/IGHV3-7/CD80/IL12B/RAC2/LYN/IL23A/GPR183/CTLA4/KLRK1/CD22/FLOT2/JAK3/LGALS9B/CD6/IGLC2/IGLC3/CD5/CAMK4/TNFRSF13B/ARG2/TNFRSF1B/CD83/ADAM8/CD24/LAG3/CCDC88B/IRF1/SASH3/PLA2G2F/LILRB4/CGAS/IL7R/CLEC4G/IL6/IGHV4-28/IGHV3-33/IGHV4-39/TRBC1/CD38/CCR7/IGHV4-31/ICOS/IDO1/PRKCQ/HSPH1/LCK/PGLYRP2/PTPN22/LGALS9C/IGHV5-10-1/SAMSN1/CD209/TNFSF14/CCL2/LILRB1/IGHV3-30/IL2RA/PYCARD/NLRP3/CD274/IL1B/IKZF3/CCL5/CARD11/LILRB2/RASGRP1/IGHV6-1/FANCA/CD2/IGHV1-69/IL4R/GRAP2/ARG1/CD40LG/TNFRSF4/PRDM1/FOXP3/PTPRC/IGHV1-69D/SIT1/CD28/IGHV3-43/TBX21/IGLL5/CD27/TIGIT/CRTAM/CD47/IGHV3-11/IGHV3-21/IGHV3-20/IGHV1-18/IGHV3-23/MZB1/CCR2/CR1/CD3E/ZC3H12A/SIRPG/RASAL3/NFKBIZ/IL12RB1/TRBC2/IGKC/HMGB3/PNP/SOCS1/NOD2/IGHA2/IGHG2/IGHG4/IGHA1/IGHG3/IGHG1/PLA2G2D/VNN1/TNFSF9/RHOH/FCRL3/IFNG/TNFRSF21/IGHV4-59/IGHV3-74/SIRPB1/IGHV3-48/IGHV3-53/IGHV5-51/EBI3/PGLYRP3/LAX1/PDCD1/CLEC7A/IGHV4-4/THY1/SLC7A1/IGHV2-5

7	GO:1903522	Regulation of blood circulation	1.63E-32	IL23R/IGLC7/IGHV3-7/CD80/IL12B/RAC2/LYN/IL23A/DDX58/FUT7/C9/KLRK1/CD22/DDX21/JAK3/IGKV1-5/HERC5/IL18RAP/GRN/IGLC2/IGLC3/MMP12/STAT1/TNFRSF1B/PARP9/AIM2/IGKV3-15/LAG3/SLAMF6/SASH3/LBP/CGAS/IL7R/CLEC4G/IL6/SERPINB9/IGKV2-30/IGHV3-33/IGHV4-39/FZD5/DNASE1L3/ICAM1/C1QC/RSAD2/LTA/DDX60/CD1B/PGLYRP2/PTPN22/PTAFR/IGKV3-20/TRIL/IGKV1-17/RAET1E/IGLV2-8/LILRB1/IGHV3-30/IL2RA/CXCL6/PYCARD/FFAR2/NLRP3/IL1B/IGLV1-51/IGLV6-57/IGLV1-47/RASGRP1/IGHV1-69/IL4R/ARG1/CD40LG/TNFRSF4/SH2D1A/SLC7A5/FOXP3/PTPRC/CD28/TBX21/CD96/WNT5A/IFIT1/CD177/CRTAM/CD47/CD36/NR4A3/IGHV3-11/IGHV3-23/MICB/TRIM15/MZB1/CCR2/CR1/ZC3H12A/NFKBIZ/IL12RB1/SERPINB4/KIR2DL4/HMOX1/NOS2/IGLV2-14/IGLV3-19/IGKV4-1/IGKC/IRAK3/BIRC3/DTX3L/RAET1G/PLA2G3/NOD2/IGHG2/IGHG4/IGHG3/IGHG1/SLC22A13/IGLV1-40/IGLV1-44/IGLV3-25/FCRL3/IFNG/CD226/IGHV4-59/IGHV3-48/IGHV3-53/PGLYRP3/NLRX1/C1QB/CFB/IGHV2-5
8	GO:0060047	Heart contraction	4.07E-32	IL23R/IGLC7/FPR2/CLEC4D/CLEC4E/IGHV1-3/IGHV3-7/IL12B/CXCL13/IL23A/GNLY/SHC1/LCE3C/KLRK1/GRN/IGLC2/IGLC3/ARG2/LTF/JCHAIN/PI3/SLPI/LBP/ACP5/IL6/IGHV4-28/IGHV3-33/IGHV4-39/LCE3A/TRBC1/LTA/IGHV4-31/S100A8/SEMG2/PGLYRP2/ISG15/IGHV5-10-1/IRF8/IGKV3-20/KRT6A/IGHV3-30/CXCL6/PYCARD/LYZ/NLRP3/IGHV6-1/LCN2/IGHV1-69/IGHV1-69D/IGHV3-43/CCL20/IGLL5/CD36/DMBT1/IGHV3-11/IGHV3-21/IGHV3-20/IGHV1-18/IGHV3-23/S100A9/S100A12/GBP6/PLAC8/EPHA2/TRBC2/NOS2/IGKC/BCL3/CAMP/PGLYRP4/PLA2G2A/MYD88/DEFB4A/NOD2/IGHA2/IGHG2/IGHG4/IGHA1/IGHG3/IGHG1/GSDMC/S100A7/IGHV4-59/GBP4/ADAM17/IGHV3-74/IFNE/IGHV3-48/IGHV3-53/IGHV5-51/PGLYRP3/IGHV4-4/TLR2/IGHV2-5
9	GO:0008016	Regulation of heart contraction	1.60E-30	IL23R/BTLA/IGLC7/IGHV1-3/IGHV3-7/CD80/IL12B/LYN/IL23A/GPR183/CTLA4/KLRK1/FLOT2/JAK3/CD6/IGLC2/IGLC3/CD5/CD83/ADAM8/CD24/CCDC88B/SASH3/LILRB4/IL7R/IL6/IGHV4-28/IGHV3-33/IGHV4-39/TRBC1/CD38/CCR7/IGHV4-31/ICOS/PRKCQ/HSPH1/LCK/PTPN22/IGHV5-10-1/CD209/TNFSF14/CCL2/LILRB1/IGHV3-30/IL2RA/PYCARD/NLRP3/CD274/IL1B/CCL5/CARD11/LILRB2/RASGRP1/IGHV6-1/IGHV1-69/IL4R/GRAP2/CD40LG/TNFRSF4/FOXP3/PTPRC/IGHV1-69D/CD28/IGHV3-43/TBX21/IGLL5/CD27/CD47/IGHV3-11/IGHV3-21/IGHV3-20/IGHV1-18/IGHV3-23/CCR2/CD3E/SIRPG/RASAL3/NFKBIZ/IL12RB1/TRBC2/IGKC/PNP/SOCS1/NOD2/IGHA2/IGHG2/IGHG4/IGHA1/IGHG3/IGHG1/VNN1/TNFSF9/RHOH/FCRL3/IFNG/IGHV4-59/IGHV3-74/SIRPB1/IGHV3-48/IGHV3-53/IGHV5-51/EBI3/PDCD1/CLEC7A/IGHV4-4/THY1/SLC7A1/IGHV2-5

10	GO:0030049	Muscle filament sliding	8.08E-29	IGLC7/IGHV1-3/IGHV3-7/C9/IGKV1-5/IGLC2/IGLC3/IGKV3-15/IGKV2-30/IGHV4-28/IGHV3-33/IGHV4-39/C1QC/TRBC1/LTA/IGHV4-31/IGHV5-10-1/IGKV3-20/IGKV1-17/IGLV2-8/IGHV3-30/IGLV1-51/IGLV6-57/IGLV1-47/IGHV6-1/IGHV1-69/PTPRC/IGHV1-69D/IGHV3-43/IGLL5/IGHV3-11/IGHV3-21/IGHV3-20/IGHV1-18/IGHV3-23/CR1/TRBC2/IGLV2-14/IGLV3-19/IGKV4-1/IGKC/BCL3/EXO1/IGHA2/IGHG2/IGHG4/IGHA1/IGHG3/IGHG1/IGLV1-40/IGLV1-44/IGLV3-25/IGHV4-59/IGHV3-74/IGHV3-48/IGHV3-53/IGHV5-51/IGHV4-4/C1QB/IGHV2-5

Table 3 List of genes that positively corelate with *FPR1* expression in PsA L skin

Gene name	Protein/gene	Protein/gene description	Spearman's correlation coefficient (R) value	P value	Associated diseases
PRAL	P53 Regulation Associated long-non-coding RNA(LncRNA)	P53 regulation-limited data available	0.976	0.0004	Lung cancer, Hepatocellular carcinoma
AL355304.1	HIVEP2-Divergent transcript, LncRNA	Unknown	0.97	6.55E-05	Unknown
RGS2	Regulator of G Protein Signalling 2	Regulates G protein-coupled receptor signalling cascades, mediator of myeloid differentiation	0.952	0.001	Renal cancer, breast cancer, may play a role in leukemogenesis
RPL38	Ribosomal protein L38	Component of the large ribosomal subunit, involved in protein synthesis	0.952	0.001	Tympanic membrane disease, renal cancer
TOMM7	Translocase of outer mitochondrial membrane 7	Regulates the assembly and stability of the translocase complex	0.952	0.001	Head and neck cancer
SLC6A10P	Solute Carrier Family 6 Member 10, Pseudogene	Unknown	0.952	0.001	Ovarian cancer, limited data.
RPL5P34	Ribosomal Protein L5 Pseudogene 34	Unknown	0.952	0.001	Unknown
AC090229.1	LncRNA	Unknown	0.952	0.001	Unknown
AC025181.2	GOLPH3 Divergent Transcript, LncRNA	Unknown	0.952	0.001	Unknown

Table 4 List of genes that negatively corelate with *FPR1* expression in PsA L skin

Gene name	Protein/gene	Protein/gene description	Spearman's correlation coefficient (R) value	P value	Associated diseases
SUDS3P1	SIN3A Corepressor Complex Component Pseudogene 1	Unknown	-0.976	0.0004	Unknown
TRIM46	Tripartite Motif Containing 46	Involved in microtubule bundle formation at the axon	-0.952	0.001	Neuropathy, associated with proliferation of multiple cancer cells, including lung and breast cancer.
SCG2	Secretogranin II	Neuroendocrine protein of the granin family, involved in secretory granule formation.	-0.952	0.001	Collagenous colitis, neuroendocrine tumours
AL137003.1	ATXN1 Antisense RNA 1, LncRNA	Unknown	-0.952	0.001	Unknown
UBE2SP1	Ubiquitin Conjugating Enzyme E2 S Pseudogene 1	Unknown	-0.952	0.001	Unknown

Table 5 List of genes that positively corelate with *FPR2* expression in PsA L skin

	Gene name	Protein/gene	Protein/gene description	Spearman's correlation coefficient (R) value	P value	Associated diseases
1	*DYNAP*	Dynactin associated protein	Involved in the regulation of cell proliferation. Promotes activation of the AKT1 signalling pathway	0.976	0.0004	Unknown
2	*SP5*	Sp5 Transcription Factor	Predicted to function as a transcription activator in the co-ordination of embryonic development	0.976	0.0004	Unknown
3	*ARIH2OS*	ARIH2 Opposite Strand LncRNA	Predicted to be a key component of the cell membrane	0.976	0.0004	Unknown
4	*AL451074.2*	TMCO1 Antisense RNA 1, LncRNA	Unknown	0.976	0.0004	Unknown
5	*AC020612.1*	Parkinsonism Associated Deglycase Pseudogene	Unknown	0.976	0.0004	Unknown
6	*KCNIP1*	Potassium Voltage-Gated Channel Interacting Protein 1	Regulatory subunit of the potassium voltage-gated channel, Kv4. Regulates channel density and inactivation in a calcium-dependent manner.	0.97	6.55E-05	Hypertension, Epilepsy,

7	*AL031722.1*	LncRNA	Unknown	0.97	6.55E-05	Unknown
8	*FBXO9*	F-Box Protein 9	Substrate recognition component of a SCF (SKP1-CUL1-F-box protein) E3 ubiquitin-protein ligase complex involved in the ubiquitination and degradation of proteins involved in mammalian target of rapamycin (rmTOR)	0.952	0.001	Ovarian and pancreatic cancer, epilepsy
9	*MDH1B*	Malate Dehydrogenase 1B	Predicted to be involved in NADH metabolism.	0.952	0.001	Unknown
10	*GALNT11*	Polypeptide N-Acetylgalactosaminyltransferase 11	Promotes Notch binding activity and polypeptide N-acetylgalactosaminyltransferase activity	0.952	0.001	Heart disease, Hemochromatosis,renal cancer
11	*NBEAP2*	Neurobeachin pseudogene 2	Unknown	0.952	0.001	Unknown
12	*LUCAT1*	Lung Cancer Associated Transcript 1, LncRNA	Unknown	0.952	0.001	Squamous cell carcinoma, head and neck cancer
13	*AC006160.1*	MED-28-divergent transcript, LncRNA	Unknown	0.952	0.001	Unknown
14	*MIR3142HG*	LncRNA	Unknown	0.952	0.001	Unknown

Table 6 List of genes that negatively corelate with *FPR2* expression in PsA L skin

	Gene name	Protein/gene	Protein/gene description	Spearman's correlation coefficient (R) value	P value	Associated diseases
1	TCFL5	Transcription Factor Like 5	Promotes DNA-binding transcription repressor activity	-0.976	0.0004	Chagas disease, bile duct cancer, endometrial cancer
2	RPTOR	Regulatory associated protein of MTOR complex 1	Involved in the regulation of the mammalian target of rapamycin complex 1 (mTORC1) activity which regulates cell growth and survival	-0.976	0.0004	Ependymoma, Kidney Angiomyolipoma
3	UBTD2	Ubiquitin Domain Containing 2	Unknown	-0.976	0.0004	Liver cancer, colorectal cancer
4	GNG12	G Protein Subunit Gamma 12	Involved in G protein signalling	-0.976	0.0004	Unknown
5	SLCO3A1	Solute Carrier Organic Anion Transporter Family Member 3A1	Predicted to be involved in sodium-independent organic anion transmembrane transporter activity, involved in NF-κB signalling	-0.976	0.0004	Primary Hypertrophic Osteoarthropathy, bone cyst formation, endometrial cancer, cervical cancer,
6	KRT8P38	Keratin 8 Pseudogene 38	Unknown	-0.976	0.0004	Unknown

7	KIAA2026	Uncharacterized Protein	Unknown	-0.952	0.001	Unknown
8	CENPBD1P1	CENPB DNA-Binding Domains Containing 2, Pseudogene	Unknown	-0.952	0.001	Unknown
9	AC093673.1	Uncategorized gene	Unknown	-0.952	0.001	Unknown
10	GAPDHP49	Glyceraldehyde 3 Phosphate Dehydrogenase Pseudogene 49	Unknown	-0.952	0.001	Unknown
11	AC025171.3	LncRNA	Unknown	-0.952	0.001	Unknown
12	AL359397.1	LncRNA	Unknown	-0.952	0.001	Unknown
13	KC6	Keratoconus Gene 6, LncRNA	Unknown	-0.952	0.0003	Keratoconus

Table 7 Pathways associated with genes that are upregulated in high ANXA1 expressors

GO.ID	Pathway	P.adj	Gene list
GO:0050900	Leukocyte migration	1.15E-38	**ANXA1/**S100A8/S100A12/S100A9/TREM1/CSF3R/C5AR1/CXCL8/ITGAX/BST1/JAML/DYSF/DEFA1/CD177/FPR2/PADI2/HCK/CEACAM8/ADGRE2/EPX/ITGAM/FFAR2/FCER1G/ELANE/ITGB2/NLRP12/CXCR1/CEACAM3/IL1B/C3AR1/AIF1/PRTN3/THBS1/CXCL1/CSF1R/GYPA/CXCR2/CXCL2/CEACAM6/THBD/HMOX1/AZU1/SDC3/PLA2G7/IL10/CMKLR1/IL1R1/VCAM1/ITGA2B/F2RL1/PROS1/CXCL3/PTAFR/PPBP/CCN3/CCL8/TRPV4/SLC7A8/GPR183/FUT7/PF4/ITGA9/CCL2/TNFSF14/SELL/FN1/CXCL12/IGHV3-11/ITGA1/BMP5/CXCL9/SDC2/ITGA5/GYPB/CSF1/DOK2/IGLV1-40/CCL13/CCL24/P2RY12/KITLG/LBP/ADORA1/CD34/CXCL16/SLAMF8/SELP/CD84/LGMN/IGLV2-11/KLRK1/KLRC4-KLRK1/HRH1/PIK3CD/CXCL6/IGHV2-5/SWAP70/IGLV7-43/CORO1A/IGLV1-51/CCL20/LCK/ATP1B2/IGHV3-7/CD2/SDC4/TREM2/RIPOR2/LGALS3/IGHV3-23/THY1/CCR7/TNF/NBL1/IGLC7/GPR18/SERPINE1/SLC7A10/PREX1/ITGB3/STAT5B/CYP19A1/CH25H/PDGFB/IGLV3-27/IL33/JAM3/RARRES2/CXCL10/MPP1/CXCL5/ITGA2/CRTAM/IGHV333/DEFA1B/IL23A/ANGPT4/CXCL11/SIRPA/IGLL1/GPR15/TEK/IGKV2-30/ADAM8/IGHV4-34/IGLV3-19/IGLV1-47/IGKV3-15/VPREB1/CX3CL1/L1CAM/IGKV41/XCL2/PF4V1/CX3CR1/SIRPG/PLVAP/IGHV353/MYO1G/IL34/IGLV144/ITGB7/ADD2/PTGER4/SELE/MMP14/IGHA2/DPP4/IGKV1-16/CD81/IL6/CXCL13/HSD3B7/TGFB2/XG/FYN/TNFSF11/DAPK2/CCL7/CXCL14/S100A14/GCSAML/CHGA/CD99/CNR2/IGLV3-21/IGKV1-17/CCL19/CYP7B1/IGKV3D 11/MMP1/IGHA1/CEACAM5/EDN2/IGKV2D-30/S1PR1/EPCAM/IGLC2

GO:0006959	Humoral immune response	2.08E-38	S100A8/S100A12/S100A9/PGLYRP1/TREM1/LCN2/C5AR1/FCN1/LTF/CXCL8/BST1/LYZ/BPI/SLC11A1/DEFA1/CR1/ELANE/DEFA4/CTSG/IL1B/C3AR1/RNASE3/PRTN3/CXCL1/CFP/CXCL2/C1QA/DEFA3/CLU/SLPI/VSIG4/AZU1/SERPING1/A2M/EBI3/C3/PROS1/CXCL3/CD5L/CD83/PPBP/C1QC/HLA-DRB1/CAMP/GPR183/GNLY/PI3/PF4/CCL2/TRBC2/C1QB/IGHV3-11/CXCL9/C7/IGLV1-40/CCL13/CFD/HLA-DQB1/TF/IGLV2-11/SH2D1A/CXCL6/CR1L/IGHV2-5/CD55/IGLV7-43/IGLV1-51/ITLN1/IGHV3-7/TREM2/IGHV3-21/IL7/IGHV3-23/CCR7/TNF/IGLC7/C4BPA/PTPRC/IGLV3-27/RARRES2/CXCL10/CXCL5/IGHV1-3/IGHV1-18/C1S/IGHV3-33/IGHE/DEFA1B/CXCL11/IGLL1/KRT1/IGKV2-30/IGHV3-74/IGHV4-34/IGLV3-19/CPN2/IGLV1-47/IGHV3-20/IGKV3-15/IGHV2-70D/IGKV4-1/PF4V1/IGHV3-53/IGLV1-44/IGHV2-26/FCN2/IGHA2/IGKV1-16/CD81/IL6/IGHV3-73/IGHD/CXCL13/IGHV3-49/IGHV1-24/IGHV3-66/IGHV4-61/CFH/FCN3/CXCL14/IGHV6-1/CHGA/IGLV3-21/IGHV1-58/DMBT1/IGKV1-17/IGKV3D-11/CFHR1/RNASE6/IGHA1/MASP1/IGHV4-28/HRG/ACOD1/IGKV2D-30/DEFB4A/SUSD4/CFI/BPIFB1/IGHV7-81/IGHV1-45/IGHV3-38/IGLC2
GO:0042742	Defence response to bacteria	2.61E-27	S100A8/S100A12/S100A9/FGR/PGLYRP1/LCN2/C5AR1/LTF/TLR2/CLEC4E/LYZ/NLRP3/BPI/SLC11A1/DEFA1/HP/CLEC4D/FPR2/EPX/MPO/FCER1G/CD36/ELANE/DEFA4/CTSG/RNASE3/PRG2/CFP/ANXA3/DEFA3/CEBPE/IRF8/SYT11/SLPI/AZU1/STAB1/IL10/HAVCR2/F2RL1/PPBP/CAMP/GNLY/PI3/TRBC2/IGHV3-11/COLEC12/NLRC4/LBP/TF/SLAMF8/SELP/KLRK1/KLRC4-KLRK1/GSDMA/CXCL6/IGHV2-5/TLR5/CCL20/IGHV3-7/TREM2/IGHV3-21/TNFRSF1A/IGHV3-23/TNF/IGLC7/SERPINE1/CD4/MPEG1/RARRES2/STAB2/IGHV1-3/IGHV1-18/IGHV3-33/GBP2/IGHE/DEFA1B/IL23A/SIGLEC16/IGLL1/TLR4/IGHV3-74/IGHV4-34/IGHV3-20/LPO/IGHV2-70D/RAG2/IGHV3-53/IGHV2-26/FCN2/IGHA2/IL6/IGHV3-73/IGHD/CXCL13/IGHV3-49/IGHV1-24/IGHV3-66/IGHV4-61/IGHV6-1/EPHA2/S100A14/CHGA/IGHV1-58/DMBT1/ADAMTS5/IL12B/RNASE6/IGHA1/IGHV4-28/DEFB4A/IGHV7-81/IGHV1-45/IGHV3-38/IGLC2

GO:0001525	Angiogenesis	2.95E-26	**ANXA1**/C5AR1/CXCL8/ITGAX/DYSF/PROK2/ITGB2/MMP19/IL1B/C3AR1/THBS1/CHI3L1/CXCR2/ANXA3/CYP1B1/HMOX1/SPRY2/STAB1/TAL1/IL10/NOTCH3/ACVRL1/C3/PPARG/ENPP2/CCN3/NRP1/DCN/GPNMB/PF4/NGFR/CCL2/PLXND1/IL18/EREG/ANPEP/FN1/SASH1/ADGRA2/GLUL/ESM1/ITGA5/EGFL7/ANGPTL4/ADAMTS1/AQP1/CCL24/COL15A1/TGFBI/DLL1/COL4A2/ADAMTS9/SRPX2/COL4A1/TNFRSF12A/MMP2/FOXC1/ANXA2/CD34/CDH5/PLXDC1/NRP2/SERPINF1/PDGFRA/CLDN5/APLNR/PARVA/FGFR1/KDR/FBLN5/VASH1/EFNA1/ARHGAP22/TIE1/EGF/FLT4/ENG/AGT/SULF1/SFRP1/SAT1/THY1/TNF/SERPINE1/NPR1/GATA2/ITGB3/EPHB2/AMOTL2/NIBAN2/CLEC14A/JAM3/STAB2/CXCL10/CNMD/HMGA2/EPHA1/ANGPT4/HHEX/CCN1/PDE3B/HSPB1/COL8A2/SHB/TEK/ENPEP/TNFAIP2/ECSCR/EFNB2/KRT1/ADAM8/ROBO4/HSPB6/PTGIS/RASIP1/RAMP1/ADAM12/FZD8/EDNRA/CHRNA7/PDGFRB/ANGPTL2/CX3CL1/COL18A1/HPSE/FGFR2/CX3CR1/COL8A1/TWIST1/SPHK1/SH2D2A/NOS3/FGF9/ISM1/LRG1/MMP14/FASLG/UNC5B/IL6/HIF1A/CTSH/RHOJ/JCAD/CARD10/CXCL13/JUP/TGFBR3/SEMA3E/EMP2/TGFB2/MCAM/SFRP2/CSPG4/GPR4/SMOC2/AGTR1/CCBE1/EPHA2/SOX17/MEIS1/GATA6/CMA1/PRL/FUT1/AMOTL1/IL12B/SOX18/CDH13/HRG/TMIGD2/NOX5/ACKR3/S1PR1/RAMP3/GATA4/MEOX2/OVOL2
GO:0006956	Complement activation	1.92E-25	C5AR1/FCN1/CR1/IL1B/C3AR1/CFP/C1QA/CLU/VSIG4/SERPING1/A2M/C3/PROS1/CD5L/C1QC/TRBC2/C1QB/IGHV3-11/C7/IGLV1-40/CFD/IGLV2-11/CR1L/IGHV2-5/CD55/IGLV7-43/IGLV1-51/IGHV3-7/IGHV3-21/IGHV3-23/IGLC7/C4BPA/IGLV3-27/IGHV1-3/IGHV1-18/C1S/IGHV3-33/IGHE/IGLL1/KRT1/IGKV2-30/IGHV3-74/IGHV4-34/IGLV3-19/CPN2/IGLV1-47/IGHV3-20/IGKV3-15/IGHV2-70D/IGKV4-1/IGHV3-53/IGLV1-44/IGHV2-26/FCN2/IGHA2/IGKV1-16/CD81/IGHV3-73/IGHD/IGHV3-49/IGHV1-24/IGHV3-66/IGHV4-61/CFH/FCN3/IGHV6-1/IGLV3-21/IGHV1-58/IGKV1-17/IGKV3D-11/CFHR1/IGHA1/MASP1/IGHV4-28/IGKV2D-30/SUSD4/CFI/IGHV7-81/IGHV1-45/IGHV3-38/IGLC2
GO:0043062	Extracellular structure organisation	2.37E-25	MMP9/MMP8/MMP25/ITGAX/ITGAM/PTX3/CRISPLD2/ELANE/ITGB2/CTSG/MMP19/TNFRSF1B/THBS1/CYP1B1/COL17A1/ITGAD/FSCN1/VCAM1/NID1/ITGA2B/A2M/NTNG2/VCAN/LOXL3/LAMA4/DCN/ADAMTS2/ITGA9/VWF/LUM/ELF3/FN1/BGN/MYO1E/ITGA1/ITGA5/FBLN1/TNC/HTRA1/ADAMTS1/COL3A1/HPN/COL15A1/TGFBI/COL4A2/ADAMTS9/COL4A1/MMP2/FOXC1/LOXL1/ANXA2/SH3PXD2B/SPP1/COL16A1/PDGFRA/COL12A1/KDR/FBLN5/COL5A3/VWA1/MFAP5/MMP17/CTSL/CAPN2/ENG/TNFRSF1A/EGFLAM/AGT/SULF1/LAMB3/COL6A2/ADAMTS7/TEX14/LCP1/TNF/SERPINE1/POSTN/ITGB3/PDGFB/MATN3/JAM3/LAMB1/HAS1/ITGA2/ITGB5/SOX9/ADAMTSL4/CCN1/COL8A2/CTSV/ADAM8/THSD4/FBN2/ADAM12/FLRT2/TPSAB1/COL18A1/LRP1/COL8A1/MMP27/COL27A1/CST3/ITGB7/FMOD/LAMB2/MMP14/TIMP1/DPP4/HAS2/IL6/FBN1/TNFRSF11B/MMP13/COL14A1/COL9A1/NTN4/ELN/TGFB2/SFRP2/ADAMTS12/LAMA1/MMP15/ADAMTS10/ITGA11/HPSE2/SMOC2/ACAN/ECM2/VIT/FERMT1/DPT/TMPRSS6/COL11A1/CDH1/CMA1/ADAMTS5/ADAMTS3/PRSS1/MMP1/MFAP2/MATN4/WT1/EGFL6/IBSP/TCF15/TLL1

GO:0030335	Positive regulation of cell migration	2.92E-25	**ANXA1**/FGR/MMP9/C5AR1/CXCL8/ITGAX/DYSF/FPR2/DOCK5/ELANE/IL1B/C3AR1/AIF1/THBS1/CSF1R/CXCR2/ANXA3/CEACAM6/HMOX1/SPRY2/PLA2G7/CMKLR1/IL1R1/ITGA2B/F2RL1/ENPP2/PTAFR/PLAU/NRP1/CCL8/TNFAIP6/TRPV4/FUT7/RIN2/GPNMB/TNFSF14/FN1/CXCL12/SASH1/ADGRA2/IGFBP5/ITGA5/CSF1/ADAMTS1/SMO/CCL24/P2RY12/KITLG/LBP/SRPX2/SDCBP/CXCL16/CDH5/SYDE1/DOCK1/NRP2/SELP/LGMN/PDGFRA/FGFR1/PIK3CD/ZNF703/KDR/HBEGF/EGFR/MAP2K3/SWAP70/S100A11/CORO1A/EGF/CCL20/GLIPR2/LPAR1/FLT4/TREM2/FLNA/RIPOR2/LGALS3/AGT/CLEC7A/THY1/CLDN4/SEMA6B/CCR7/TNF/SERPINE1/GATA2/PREX1/POSTN/ITGB3/BMP2/PDGFB/PTPRC/RARRES2/LAMB1/CXCL10/ITGA2/IRS2/SOX9/ATOH8/EPHA1/CASS4/TMSB4X/IL23A/ANGPT4/CCN1/RHOC/FAM107A/HSPB1/TEK/ADAM8/CGA/PDGFRB/CX3CL1/COL18A1/LRP1/DMTN/XCL2/SEMA7A/CX3CR1/PLVAP/IL34/SPHK1/NOS3/LRRC15/FGF9/MYADM/SELE/MMP14/HAS2/TWIST2/CLDN1/IL6/HIF1A/CTSH/RHOJ/JCAD/EPB41L4B/SNAI2/CXCL13/WNT11/SEMA3G/PAK3/VIL1/SEMA3F/SEMA3E/TGFB2/MCAM/CCN4/INSL3/PDGFC/SEMA6D/XG/DAPK2/CCL7/SHTN1/SMOC2/ADRA2A/TAC1/CXCL14/CCBE1/SEMA3C/S100A14/CD99/DAB2/SH3RF2/FUT1/AMOTL1/CCL19/CDH13/EDN2/ACKR3/NOX4/S1PR1/CLDN3/RAB25/PROX1/INSM1
GO:0030198	Extracellular matrix organisation	4.58E-25	MMP9/MMP8/MMP25/ITGAX/ITGAM/PTX3/CRISPLD2/ELANE/ITGB2/CTSG/MMP19/TNFRSF1B/THBS1/CYP1B1/COL17A1/ITGAD/FSCN1/VCAM1/NID1/ITGA2B/A2M/NTNG2/VCAN/LOXL3/LAMA4/DCN/ADAMTS2/ITGA9/VWF/LUM/ELF3/FN1/BGN/MYO1E/ITGA1/ITGA5/FBLN1/TNC/HTRA1/ADAMTS1/COL3A1/HPN/COL15A1/TGFBI/COL4A2/ADAMTS9/COL4A1/MMP2/FOXC1/LOXL1/ANXA2/SH3PXD2B/SPP1/COL16A1/PDGFRA/COL12A1/KDR/FBLN5/COL5A3/VWA1/MFAP5/MMP17/CTSL/CAPN2/ENG/TNFRSF1A/EGFLAM/AGT/SULF1/LAMB3/COL6A2/ADAMTS7/LCP1/TNF/SERPINE1/POSTN/ITGB3/PDGFB/MATN3/JAM3/LAMB1/HAS1/ITGA2/ITGB5/SOX9/ADAMTSL4/CCN1/COL8A2/CTSV/ADAM8/THSD4/FBN2/ADAM12/FLRT2/TPSAB1/COL18A1/LRP1/COL8A1/MMP27/COL27A1/CST3/ITGB7/FMOD/LAMB2/MMP14/TIMP1/DPP4/HAS2/IL6/FBN1/TNFRSF11B/MMP13/COL14A1/COL9A1/NTN4/ELN/TGFB2/SFRP2/ADAMTS12/LAMA1/MMP15/ADAMTS10/ITGA11/HPSE2/SMOC2/ACAN/ECM2/VIT/FERMT1/DPT/TMPRSS6/COL11A1/CDH1/CMA1/ADAMTS5/ADAMTS3/PRSS1/MMP1/MFAP2/MATN4/WT1/EGFL6/IBSP/TCF15/TLL1
GO:0060326	Cell chemotaxis	7.01E-25	**ANXA1**/S100A8/S100A12/S100A9/CSF3R/C5AR1/CXCL8/BST1/JAML/DYSF/DEFA1/FPR2/PADI2/ADGRE2/FFAR2/FCER1G/ITGB2/CXCR1/IL1B/C3AR1/AIF1/THBS1/CXCL1/CSF1R/CXCR2/CXCL2/AZU1/PLA2G7/IL10/CMKLR1/F2RL1/CXCL3/ARRB2/PPBP/CCN3/NRP1/CCL8/TRPV4/GPR183/PF4/ITGA9/CCL2/TNFSF14/CXCL12/ITGA1/CXCL9/CSF1/CCL13/CCL24/LBP/CXCL16/SLAMF8/LGMN/PDGFRA/KLRK1/KLRC4-KLRK1/HRH1/PARVA/FGFR1/PIK3CD/KDR/CXCL6/HBEGF/SWAP70/CORO1A/CCL20/LPAR1/RIPOR2/LGALS3/CCR7/NBL1/GPR18/SERPINE1/PREX1/CYP19A1/CH25H/PDGFB/JAM3/RARRES2/CXCL10/MPP1/CXCL5/CCR4/TMSB4X/DEFA1B/IL23A/CXCL11/HSPB1/ADAM8/PDGFRB/CX3CL1/XCL2/PF4V1/CX3CR1/IL34/DPP4/IL6/CXCL13/HSD3B7/TGFB2/PLXNB3/TNFSF11/DAPK2/CCL7/SMOC2/AGTR1/CXCL14/EPHA2/S100A14/CHG

			A/CNR2/CCL19/CYP7B1/HRG/EDN2/ACKR3/DEFB4A/S1PR1
GO:0030595	Leukocyte chemotaxis	3.48E-24	**ANXA1**/S100A8/S100A12/S100A9/CSF3R/C5AR1/CXCL8/BST1/JAML/DYSF/DEFA1/FPR2/PADI2/ADGRE2/FFAR2/FCER1G/ITGB2/CXCR1/IL1B/C3AR1/AIF1/THBS1/CXCL1/CSF1R/CXCR2/CXCL2/AZU1/PLA2G7/IL10/CMKLR1/F2RL1/CXCL3/PPBP/CCN3/CCL8/TRPV4/GPR183/PF4/ITGA9/CCL2/TNFSF14/CXCL12/ITGA1/CXCL9/CSF1/CCL13/CCL24/LBP/CXCL16/SLAMF8/LGMN/KLRK1/KLRC4-KLRK1/HRH1/PIK3CD/CXCL6/SWAP70/CORO1A/CCL20/RIPOR2/LGALS3/CCR7/NBL1/GPR18/SERPINE1/PREX1/CYP19A1/CH25H/PDGFB/JAM3/RARRES2/CXCL10/MPP1/CXCL5/DEFA1B/IL23A/CXCL11/ADAM8/CX3CL1/XCL2/PF4V1/IL34/DPP4/IL6/CXCL13/HSD3B7/TGFB2/TNFSF11/DAPK2/CCL7/CXCL14/S100A14/CHGA/CNR2/CCL19/CYP7B1/EDN2/S1PR1

Table 8 Pathways associated with genes that are downregulated in high ANXA1 expressors

GO.ID	Pathway	P.adj	Gene list
GO:0035249	Synaptic transmission, glutamatergic	1.15 E-38	**ANXA1**/S100A8/S100A12/S100A9/TREM1/CSF3R/C5AR1/CXCL8/ITGAX/BST1/JAML/DYSF/DEFA1/CD177/FPR2/PADI2/HCK/CEACAM8/ADGRE2/EPX/ITGAM/FFAR2/FCER1G/ELANE/ITGB2/NLRP12/CXCR1/CEACAM3/IL1B/C3AR1/AIF1/PRTN3/THBS1/CXCL1/CSF1R/GYPA/CXCR2/CXCL2/CEACAM6/THBD/HMOX1/AZU1/SDC3/PLA2G7/IL10/CMKLR1/IL1R1/VCAM1/ITGA2B/F2RL1/PROS1/CXCL3/PTAFR/PPBP/CCN3/CCL8/TRPV4/SLC7A8/GPR183/FUT7/PF4/ITGA9/CCL2/TNFSF14/SELL/FN1/CXCL12/IGHV3-11/ITGA1/BMP5/CXCL9/SDC2/ITGA5/GYPB/CSF1/DOK2/IGLV1-40/CCL13/CCL24/P2RY12/KITLG/LBP/ADORA1/CD34/CXCL16/SLAMF8/SELP/CD84/LGMN/IGLV2-11/KLRK1/KLRC4-KLRK1/HRH1/PIK3CD/CXCL6/IGHV2-5/SWAP70/IGLV7-43/CORO1A/IGLV1-51/CCL20/LCK/ATP1B2/IGHV3-7/CD2/SDC4/TREM2/RIPOR2/LGALS3/IGHV3-23/THY1/CCR7/TNF/NBL1/IGLC7/GPR18/SERPINE1/SLC7A10/PREX1/ITGB3/STAT5B/CYP19A1/CH25H/PDGFB/IGLV3-27/IL33/JAM3/RARRES2/CXCL10/MPP1/CXCL5/ITGA2/CRTAM/IGHV3-33/DEFA1B/IL23A/ANGPT4/CXCL11/SIRPA/IGLL1/GPR15/TEK/IGKV2-30/ADAM8/IGHV4-34/IGLV3-19/IGLV1-47/IGKV3-15/VPREB1/CX3CL1/L1CAM/IGKV4-1/XCL2/PF4V1/CX3CR1/SIRPG/PLVAP/IGHV3-53/MYO1G/IL34/IGLV1-44/ITGB7/ADD2/PTGER4/SELE/MMP14/IGHA2/DPP4/IGKV1-16/CD81/IL6/CXCL13/HSD3B7/TGFB2/XG/FYN/TNFSF11/DAPK2/CCL7/CXCL14/S100A14/GCSAML/CHGA/CD99/CNR2/IGLV3-21/IGKV1-17/CCL19/CYP7B1/IGKV3D-11/MMP1/IGHA1/CEACAM5/EDN2/IGKV2D-30/S1PR1/EPCAM/IGLC2
GO:0051966	Regulation of synaptic transmission, glutamatergic	2.08 E-38	S100A8/S100A12/S100A9/PGLYRP1/TREM1/LCN2/C5AR1/FCN1/LTF/CXCL8/BST1/LYZ/BPI/SLC11A1/DEFA1/CR1/ELANE/DEFA4/CTSG/IL1B/C3AR1/RNASE3/PRTN3/CXCL1/CFP/CXCL2/C1QA/DEFA3/CLU/SLPI/VSIG4/AZU1/SERPING1/A2M/EBI3/C3/PROS1/CXCL3/CD5L/CD83/PPBP/C1QC/HLA-DRB1/CAMP/GPR183/GNLY/PI3/PF4/CCL2/TRBC2/C1QB/IGHV3-11/CXCL9/C7/IGLV1-40/CCL13/CFD/HLA-DQB1/TF/IGLV2-11/SH2D1A/CXCL6/CR1L/IGHV2-5/CD55/IGLV7-43/IGLV1-51/ITLN1/IGHV3-7/TREM2/IGHV3-21/IL7/IGHV3-23/CCR7/TNF/IGLC7/C4BPA/PTPRC/IGLV3-27/RARRES2/CXCL10/CXCL5/IGHV1-3/IGHV1-18/C1S/IGHV3-33/IGHE/DEFA1B/CXCL11/IGLL1/KRT1/IGKV2-30/IGHV3-74/IGHV4-34/IGLV3-19/CPN2/IGLV1-47/IGHV3-20/IGKV3-15/IGHV2-70D/IGKV4-1/PF4V1/IGHV3-53/IGLV1-44/IGHV2-26/FCN2/IGHA2/IGKV1-16/CD81/IL6/IGHV3-73/IGHD/CXCL13/IGHV3-49/IGHV1-24/IGHV3-66/IGHV4-61/CFH/FCN3/CXCL14/IGHV6-1/CHGA/IGLV3-21/IGHV1-58/DMBT1/IGKV1-17/IGKV3D-11/CFHR1/RNASE6/IGHA1/MASP1/IGHV4-28/HRG/ACOD1/IGKV2D-30/DEFB4A/SUSD4/CFI/BPIFB1/IGHV7-81/IGHV1-45/IGHV3-38/IGLC2

Table 9 List of genes that positively corelate with ANXA1 expression in MM CoMMpass database cohort

	Gene name	Protein	**Protein/gene description**	**Associated diseases**
1	*ACTN1*	Actin Alpha 1	Roles in cell motility, structure and integrity. Found in skeletal muscle.	Myopathies. Unfavourable prognostic marker in renal, lung, head and neck and urothelial cancer.
2	*AHR*	Aromatic Hydrocarbon Receptor	Involved in a range of biological processes, including angiogenesis, haematopoiesis, drug and lipid metabolism, cell motility and immune modulation.	Retinitis Pigmentosa
3	*ANXA3*	Annexin A3	Signalling protein, inhibitor of phospholipase A2.	Favourable prognostic marker in renal cancer. Unfavourable prognostic marker in pancreatic cancer.
4	*APOBR*	Apolipoprotein B Receptor	Macrophage receptor that binds apolipoprotein B48.	Atherosclerosis. Favourable prognostic marker in endometrial cancer.
5	*CDA*	Cytidine deaminase	Enzyme involved in pyrimidine salvaging	Acute leukaemia, unfavourable prognostic marker in pancreatic and cervical cancer
6	*CLEC7A*	C-type lectin domain containing 7A	Plays a role in innate immunity by acting as a pattern recognition receptor that binds beta glucans.	Unfavourable prognostic marker in renal cancer

7	*COTL1*	Coactosin like F-actin binding protein 1	Binds to F-actin. Involved in the regulation of the actin cytoskeleton.	Unfavourable prognostic marker in renal cancer.
8	*EMP1*	Epithelial membrane protein 1	Involved in bleb assembly and cell death	Blount disease. Unfavourable prognostic marker in ovarian, urothelial and pancreatic cancer.
9	*ETS2*	ETS proto-oncogene 2	Transcription factor/activator. Regulates genes involved in development and apoptosis.	Associated with choriocarcinoma and Acute Megakaryocytic Leukaemia (AML).
10	*FGR*	FGR proto-oncogene.	Non-receptor tyrosine-protein kinase involved in regulation of the immune response. Negative regulator of cell migration and adhesion.	Pre-eclampsia, placental insufficiency.
11	*FPR1*	Formyl Peptide Receptor 1	G-protein-coupled receptor on mammalian phagocytic cells. Plays a role in chemotaxis, host defence and inflammation.	Peridontitis. Unfavourable prognostic marker in renal cancer. Enhanced RNA expression in glioma.
12	*GNAQ*	G protein subunit alpha q	Membrane signalling, regulates B cell selection and survival.	Platelet aggregation and activation disorders Favourable prognostic marker in renal cancer.

13	*LILRA2*	Leukocyte immunoglobulin like receptor A2	Receptor expressed predominantly on B cells and monocytes. Suppresses the innate immune response, dendritic cell differentiation and antigen presentation.	Tuberculoid leprosy
14	*LILRA5*	Leukocyte Immunoglobulin Like Receptor A5	Believed to play a role in activation of the innate immune response.	Hemophagocytic lymphohistiocytosis. Unfavourable prognostic marker in renal cancer
15	*MYO1F*	Myosin IF	Actin-based motor believed to be involved in intracellular movement of membrane-enclosed compartments	Sensorineural hearing loss. Unfavourable prognostic marker in renal cancer.
16	*PIK3R5*	Phosphoinositide-3-Kinase Regulatory Subunit 5	Regulatory subunit of the class I Phosphatidylinositol 3-kinase (PI3K) gamma complex. PI3Ks are involved in a range of functions from cellular proliferation to survival.	Spinocerebellar ataxia
17	*PIK3R5-DT*	N/A- RNA gene	PIK3R5 Divergent Transcript. Long noncoding RNA (lncRNA). Function unknown. High expression in bone marrow.	Unknown.
18	*PYGL*	Glycogen Phosphorylase L	Enzyme involved in carbohydrate metabolism.	Glycogen storage disease. Unfavourable prognostic marker in pancreatic and head and neck cancer.

19	*RASGRP2*	RAS guanyl releasing protein 2	Activates small GTPases. Functions in the aggregation platelets and adhesion of T cells and neutrophils.	Bleeding disorders, leukocyte adhesion disorders. Unfavourable prognostic marker in renal cancer.
20	*RIN3*	Ras And Rab Interactor 3	Binds small GTPases. Enhanced expression in the bone marrow.	Paget's disease of bone.
21	*SERPINA1*	Serpin family A member 1	Serine protease inhibitor. Involved in haemostasis and coagulation.	Bleeding disorders, Chronic obstructive pulmonary disease (COPD). Favourable prognostic marker in breast and colorectal cancer.
22	*SLA*	Src Like Adaptor	Adaptor protein which negatively regulates T cell receptor signalling. Believed to be involved in T cell differentiation and the innate immune response.	Unknown.
23	*SLC2A3*	Solute Carrier Family 2 Member 3	Involved in glucose transport.	Huntington disease. Unfavourable prognostic marker for stomach, renal and colorectal cancer.
24	*SLPI*	Secretory Leukocyte Peptidase Inhibitor	Inhibitor which protects epithelial cells from serine proteases. Has antimicrobial and wound-healing activities.	Pustular psoriasis. Unfavourable prognostic marker in renal cancer.
25	*TLR2*	Toll like receptor 2	Involved in pathogen recognition and innate immunity.	Leprosy. Autoimmunity. Unfavourable prognostic marker in renal cancer.

26	*TNFRSF1B*	TNF receptor superfamily member 1B	Involved in apoptosis.	Unfavourable prognostic marker in renal and testicular cancer. T cell lymphoma (Sezary syndrome).
27	*TREM1*	Triggering Receptor Expressed on Myeloid Cells 1	Cell surface receptor involved in adaptive immunity and activation of inflammation. Amplifies inflammatory signals that are initially triggered by TLR and NOD-like receptors (NLRs).	Cholangitis, septic arthritis.
28	*TUBA1A*	Tubulin alpha 1a	Major component of the microtubules that comprise the eukaryotic cytoskeleton.	Unfavourable prognostic marker in renal cancer.

List of References

1. Parkin, J. & Cohen, B. An overview of the immune system. *Lancet*. **357**, 1777–1789 (2001).

2. Chaplin, D. D. Overview of the immune response. *J. Allergy Clin. Immunol*. (2010).

3. OpenStax. 21.2 Barrier Defenses and the Innate Immune Response. (2013).

4. Patel, P. & Chatterjee, S. Innate and adaptive immunity: Barriers and receptor-based recognition. in Immunity and Inflammation in Health and Disease: Emerging Roles of Nutraceuticals and Functional Foods in Immune Support. Elsevier: 3–13 (2017).

5. Amarante-Mendes, G. P. *et al*. Pattern recognition receptors and the host cell death molecular machinery. *Frontiers in Immunology*. **9,** 2379 (2018).

6. Mak, T., Saunders, M. & Jett, B. Chapter 3: Innate Immunity. *Prim. to Immune Response* 55–83 (2014).

7. Wherry, E. J. & Masopust, D. Adaptive Immunity: Neutralizing, Eliminating, and Remembering for the Next Time. in *Viral Pathogenesis: From Basics to Systems Biology: Third Edition* 57–69 (Elsevier Inc., 2016).

8. Chiu, S. & Bharat, A. Role of monocytes and macrophages in regulating immune response following lung transplantation. *Current Opinion in Organ Transplantation*. **21**, 239–245 (2016).

9. Barker, R. N. *et al*. Antigen presentation by macrophages is enhanced by the uptake of necrotic, but not apoptotic, cells. *Clin. Exp. Immunol*. **127**, 220–225 (2002).

10. Moticka, E. J. Hallmarks of the Adaptive Immune Responses. in *A Historical Perspective on Evidence-Based Immunology* 9–19 (Elsevier, 2016).

11. Alberts, B. *et al*. The Adaptive Immune System. (2002).

12. B cells immunophenotyping | Abcam. https://www.abcam.com/primary-antibodies/b-cells-basic-immunophenotyping.

13. Kaminski, D. A., Wei, C., Rosenberg, A. F., Lee, F. E. H. & Sanz, I. Multiparameter flow cytometry and bioanalytics for B cell profiling in systemic lupus erythematosus. *Methods Mol. Biol*. **900**, 109–134 (2012).

14. Marshall, J. S., Warrington, R., Watson, W. & Kim, H. L. An introduction to immunology and immunopathology. *Allergy, Asthma and Clinical Immunology*. **14**, 49 (2018).

15. Kumar, B. V., Connors, T. J. & Farber, D. L. Human T Cell Development, Localization, and Function throughout Life. *Immunity*. **48,** 202–213 (2018).

16. Koch, S. *et al*. Multiparameter flow cytometric analysis of CD4 and CD8 T cell subsets in young and old people. *Immun. Ageing* **5**, 6 (2008).

17. Farber, D. L., Yudanin, N. A. & Restifo, N. P. Human memory T cells: Generation, compartmentalization and homeostasis. *Nature Reviews Immunology*. **14**, 24–35 (2014).

18. Chatzileontiadou, D. S. M., Sloane, H., Nguyen, A. T., Gras, S. & Grant, E. J. The Many Faces of CD4+ T Cells: Immunological and Structural Characteristics. *Int. J. Mol. Sci.* **22**, 73 (2020).

19. Pennock, N. D. *et al*. T cell responses: Naïve to memory and everything in between. *Am. J. Physiol. - Adv. Physiol. Educ.* **37**, 273–283 (2013).

20. St. Paul, M. & Ohashi, P. S. The Roles of CD8+ T Cell Subsets in Antitumor Immunity. *Trends in Cell Biology*. **30**, 695–704 (2020).

21. Loyal, L. *et al*. SLAMF7 and IL-6R define distinct cytotoxic versus helper memory CD8+ T cells. *Nat. Commun.* **11**, 1–12 (2020).

22. Mirsaeidi, M., Gidfar, S., Vu, A. & Schraufnagel, D. Annexins family: Insights into their functions and potential role in pathogenesis of sarcoidosis. *Journal of Translational Medicine*. **14**, 89 (2016).

23. Sheikh, M. H. & Solito, E. Annexin A1: Uncovering the many talents of an old protein. *International Journal of Molecular Sciences*. **19**, 1045 (2018).

24. Gavins, F. N. E., Yona, S., Kamal, A. M., Flower, R. J. & Perretti, M. Leukocyte antiadhesive actions of annexin 1: ALXR- and FPR-related anti-inflammatory mechanisms. *Blood* **101**, 4140–4147 (2003).

25. Perretti, M., Getting, S. J., Solito, E., Murphy, P. M. & Gao, J. L. Involvement of the receptor for formylated peptides in the in vivo anti-migratory actions of annexin 1 and its mimetics. *Am. J. Pathol.* **158**, 1969–1973 (2001).

26. Spurr, L. *et al*. Comparative analysis of Annexin A1-formyl peptide receptor 2/ALX expression in human leukocyte subsets. *Int. Immunopharmacol.* **11**, 55–66 (2011).

27. D'Acquisto, F., Perretti, M. & Flower, R. J. Annexin-A1: A pivotal regulator of the innate and adaptive immune systems. *British Journal of Pharmacology*. **155**, 152–169 (2008).

28. Sugimoto, M. A. *et al*. Annexin A1 and the Resolution of Inflammation: Modulation of Neutrophil Recruitment, Apoptosis, and Clearance. *J. Immunol. Res.* **2016**, 8239258 (2016).

29. Gavins, F. N. E. E. & Hickey, M. J. Annexin A1 and the regulation of innate and adaptive immunity. *Front. Immunol.* **3**, 354 (2012).

30. Patel, H. B. *et al*. The impact of endogenous annexin A1 on glucocorticoid control of inflammatory arthritis. *Ann. Rheum. Dis.* **71**, 1872–1880 (2012).

31. Wein, S. *et al*. Mediation of annexin 1 secretion by a probenecid-sensitive ABC-transporter in rat inflamed mucosa. *Biochem. Pharmacol.* **67**, 1195–1202 (2004).

32. Perretti, M. *et al*. Mobilizing lipocortin 1 in adherent human leukocytes downregulates their transmigration. *Nat. Med.* **2**, 1259–1262 (1996).

33. Perretti, M. & D'Acquisto, F. Annexin A1 and glucocorticoids as effectors of the resolution of inflammation. *Nature Reviews Immunology*. **9**, 62–70 (2009).

34. D'Acquisto, F. *et al*. Annexin-1 modulates T-cell activation and differentiation. *Blood* **109**, 1095–1102 (2007).

35. Pupjalis, D., Goetsch, J., Kottas, D. J., Gerke, V. & Rescher, U. Annexin A1 released from apoptotic cells acts through formyl peptide receptors to dampen inflammatory monocyte activation via JAK/STAT/SOCS signalling. *EMBO Mol. Med.* **3**, 102–114 (2011).

36. Perretti, M., Ahluwalia, A., Harris, J. G., Goulding, N. J. & Flower, R. J. Lipocortin-1 fragments inhibit neutrophil accumulation and neutrophil-dependent edema in the mouse. A qualitative comparison with an anti-CD11b monoclonal antibody. *J. Immunol.* **151**, 4306–4314 (1993).

37. Walther, A., Riehemann, K. & Gerke, V. A novel ligand of the formyl peptide receptor: annexin I regulates neutrophil extravasation by interacting with the FPR. *Mol. Cell* **5**, 831–40 (2000).

38. Williams, S. L. *et al*. A Proinflammatory Role for Proteolytically Cleaved Annexin A1 in Neutrophil Transendothelial Migration. *J. Immunol.* **185**, 3057–3063 (2010).

39. He, H. Q. & Ye, R. D. The formyl peptide receptors: Diversity of ligands and mechanism for recognition. *Molecules* (2017).

40. Zhuang, Y. *et al*. Structure of formylpeptide receptor 2-Gi complex reveals insights into ligand recognition and signaling. *Nat. Commun.* **11**, (2020).

41. Ansari, J., Kaur, G. & Gavins, F. N. E. Therapeutic potential of annexin A1 in ischemia reperfusion injury. *International Journal of Molecular Sciences*. **19** (2018).

42. D'Acunto, C. W., Gbelcova, H., Festa, M. & Ruml, T. The complex understanding of Annexin A1 phosphorylation. *Cellular Signalling*. **26**, 173–178 (2014).

43. Shao, G., Zhou, H., Zhang, Q., Jin, Y. & Fu, C. Advancements of Annexin A1 in inflammation and tumorigenesis. *Onco. Targets. Ther.* (2019).

44. D'Acquisto, F., Piras, G. & Rattazzi, L. Pro-inflammatory and pathogenic properties of Annexin-A1: The whole is greater than the sum of its parts. *Biochemical Pharmacology*. **85,** 1213–1218 (2013).

45. Yang, Y. H. *et al*. Modulation of inflammation and response to dexamethasone by Annexin 1 in antigen-induced arthritis. *Arthritis Rheum*. **50**, 976–984 (2004).

46. Gavins, F. N. E., Kamal, A. M., D'Amico, M., Oliani, S. M. & Perretti, M. Formyl-peptide receptor is not involved in the protection afforded by annexin 1 in murine acute myocardial infarct. *FASEB J.* **19**, 100–102 (2005).

47. Gavins, F. N. E., Sawmynaden, P., Chatterjee, B. E. & Perretti, M. A twist in anti-inflammation: Annexin 1 acts via the lipoxin A4 receptor. *Prostaglandins Leukot. Essent. Fat. Acids* **73**, 211–219 (2005).

48. Araújo, T. G. *et al*. Annexin a1 as a regulator of immune response in cancer. *Cells* vol. 10 (2021).

49. Saito, N. *et al*. An annexin A1-FPR1 interaction contributes to necroptosis of keratinocytes in severe cutaneous adverse drug reactions. *Sci. Transl. Med.* (2014).

50. Baracco, E. E. *et al*. Contribution of annexin A1 to anticancer immunosurveillance. *Oncoimmunology* **8**, e1647760 (2019).

51. Schloer, S. *et al*. The annexin A1/FPR2 signaling axis expands alveolar macrophages, limits viral replication, and attenuates pathogenesis in the murine influenza A virus infection model. *FASEB J.* **33**, 12188–12199 (2019).

52. Perretti, M. & Solito, E. Annexin 1 and neutrophil apoptosis. in *Biochemical Society Transactions*. **32**, 507–510 (Biochem Soc Trans, 2004).

53. Maderna, P., Yona, S., Perretti, M. & Godson, C. Modulation of Phagocytosis of Apoptotic Neutrophils by Supernatant from Dexamethasone-Treated Macrophages and Annexin-Derived Peptide Ac 2–26 . *J. Immunol.* (2005).

54. Hannon, R. *et al*. Aberrant inflammation and resistance to glucocorticoids in annexin 1-/- mouse. *FASEB J.* **17**, 253–255 (2003).

55. Grewal, T., Wason, S. J., Enrich, C. & Rentero, C. Annexins-insights from knockout mice. *Biological Chemistry* (2016).

56. Han, P. F. *et al*. Annexin A1 involved in the regulation of inflammation and cell signaling pathways. *Chinese Journal of Traumatology - English Edition* **23**, 96–101 (2020).

57. Hirata, F. & Iwata, M. Role of lipomodulin, a phospholipase inhibitory protein, in immunoregulation by thymocytes. *J. Immunol.* **130**, 1930–1936

(1983).

58. Yang, Y. H. *et al*. Deficiency of Annexin A1 in CD4 + T Cells Exacerbates T Cell–Dependent Inflammation . *J. Immunol.* **190**, 997–1007 (2013).

59. Kelly, L. *et al*. Annexin-A1: The culprit or the solution? *Immunology* (2022).

60. Bruschi, M. *et al*. Glomerular Autoimmune Multicomponents of Human Lupus Nephritis In Vivo: α-Enolase and Annexin AI. *J. Am. Soc. Nephrol.* **25**, 2483–2498 (2014).

61. Bruschi, M. *et al*. Glomerular Autoimmune Multicomponents of Human Lupus Nephritis In Vivo (2): Planted Antigens. *J. Am. Soc. Nephrol.* **26**, 1905–1924 (2015).

62. Osei-Owusu, P., Charlton, T. M., Kim, H. K., Missiakas, D. & Schneewind, O. FPR1 is the plague receptor on host immune cells. *Nature* (2019).

63. Duan, L., Rao, X. & Sigdel, K. R. Regulation of Inflammation in Autoimmune Disease. *J. Immunol. Res.* **2019**, (2019).

64. Lacy, P. & Stow, J. L. Cytokine release from innate immune cells: Association with diverse membrane trafficking pathways. *Blood* (2011).

65. Rodrigues, P. R. S. *et al*. Innate immunology in COVID-19—a living review. Part II: dysregulated inflammation drives immunopathology. *Oxford Open Immunol.* **1**, 5 (2020).

66. Canacik, O. *et al*. Annexin A1 as a potential prognostic biomarker for COVID-19 disease: Case–control study. *Int. J. Clin. Pract.* **75**, e14606 (2021).

67. Probst-Cousin, S. *et al*. Expression of annexin-1 in multiple sclerosis plaques. *Neuropathol. Appl. Neurobiol.* **28**, 292–300 (2002).

68. Perretti, M. Editorial: To resolve or not to resolve: Annexin A1 pushes resolution on track. *J. Leukoc. Biol.* (2012).

69. Vago, J. P. *et al*. Annexin A1 modulates natural and glucocorticoid-induced resolution of inflammation by enhancing neutrophil apoptosis. *J. Leukoc. Biol.* **92**, 249–258 (2012).

70. Qin, C. *et al*. Reperfusion-induced myocardial dysfunction is prevented by endogenous annexin-A1 and its N-terminal-derived peptide Ac-ANX-A12-26. *Br. J. Pharmacol.* **168**, 238–252 (2013).

71. Purvis, G. S. D., Solito, E. & Thiemermann, C. Annexin-A1: Therapeutic Potential in Microvascular Disease. *Front. Immunol.* **10**, 938 (2019).

72. Drechsler, M. *et al*. Annexin A1 counteracts chemokine-induced arterial myeloid cell recruitment. *Circ. Res.* **116**, 827–835 (2015).

73. Kusters, D. H. M. *et al*. Pharmacological treatment with annexin A1

reduces atherosclerotic plaque burden in LDLR-/- mice on Western Type Diet. *PLoS One* **10**, (2015).

74. Marwaha, A. K., Leung, N. J., McMurchy, A. N. & Levings, M. K. TH17 cells in autoimmunity and immunodeficiency : Protective orpathogenic? *Frontiers in Immunology*. **3**, 129 (2012).

75. Townsend, M. J., Monroe, J. G. & Chan, A. C. B-cell targeted therapies in human autoimmune diseases: An updated perspective. *Immunological Reviews* (2010).

76. Khan, U. & Ghazanfar, H. T Lymphocytes and Autoimmunity. *Int. Rev. Cell Mol. Biol.* (2018).

77. Yang, Y. H. *et al*. Deficiency of Annexin A1 in CD4+ T Cells Exacerbates T Cell–Dependent Inflammation. *J. Immunol.* **190**, 997–1007 (2013).

78. Yazid, S. *et al*. Annexin-A1 restricts Th17 cells and attenuates the severity of autoimmune disease. *J. Autoimmun.* **58**, 1–11 (2015).

79. Tagoe, C. E. *et al*. Annexin-1 Mediates TNF-α-Stimulated Matrix Metalloproteinase Secretion from Rheumatoid Arthritis Synovial Fibroblasts. *J. Immunol.* **181**, 2813–2820 (2008).

80. A, C. *et al*. Reduced Annexin A1 Expression Associates with Disease Severity and Inflammation in Multiple Sclerosis Patients. **203**, 1753–1765 (2019).

81. Kao, W. *et al*. A formyl peptide receptor agonist suppresses inflammation and bone damage in arthritis. *Br. J. Pharmacol.* **171**, 4087–4096 (2014).

82. Stevens, T. R. J., Smith, S. F. & Rampton, D. S. Antibodies to human recombinant lipocortin-I in inflammatory bowel disease. *Clin. Sci.* **84**, 381–386 (1993).

83. Jeong, Y. S. & Bae, Y. S. Formyl peptide receptors in the mucosal immune system. *Experimental and Molecular Medicine* (2020).

84. Luan, L., Ding, Y., Han, S., Zhang, Z. & Liu, X. An increased proportion of circulating Th22 and Tc22 cells in psoriasis. *Cell. Immunol.* **290**, 196–200 (2014).

85. Psoriasis - NHS. https://www.nhs.uk/conditions/psoriasis/.

86. Mease, P. J. *et al*. Secukinumab Inhibition of Interleukin-17A in Patients with Psoriatic Arthritis. *N. Engl. J. Med.* **373**, 1329–1339 (2015).

87. Brockbank, J. & Gladman, D. D. Psoriatic arthritis. *Expert Opinion on Investigational Drugs*. **9,** 1511–1522 (2000).

88. Versus Arthritis. *Psoriatic arthritis*. [online].Available at<http://www.versusarthritis.org/about-arthritis/conditions/psoriatic-

arthritis/>. (2022).

89. Chimenti, M. S. *et al*. Immunomodulation in psoriatic arthritis: Focus on cellular and molecular pathways. *Autoimmunity Reviews* (2013).

90. Chimenti, M. S. *et al*. Auto-reactions, autoimmunity and psoriatic arthritis. *Autoimmun. Rev.* **14**, 1142–1146 (2015).

91. Myers, W. A., Gottlieb, A. B. & Mease, P. Psoriasis and psoriatic arthritis: clinical features and disease mechanisms. *Clin. Dermatol.* **24**, 438–447 (2006).

92. Veale, D. J., Ritchlin, C. & FitzGerald, O. Immunopathology of psoriasis and psoriatic arthritis. in *Annals of the Rheumatic Diseases*. **64**,ii26–ii29 (BMJ Publishing Group Ltd, 2005).

93. Veale, D. J., Barnes, L., Rogers, S. & FitzGerald, O. Immunohistochemical markers for arthritis in psoriasis. *Ann. Rheum. Dis.* **53**, 450–454 (1994).

94. Laloux, L. *et al*. Immunohistological study of entheses in spondyloarthropathies: Comparison in rheumatoid arthritis and osteoarthritis. *Ann. Rheum. Dis.* (2001)

95. Costello, P., Bresnihan, B., O'Farrelly, C. & Fitzgerald, O. Predominance of CD8+ T lymphocytes in psoriatic arthritis. *J. Rheumatol.* **26**, 1117–1124 (1999).

96. Lowes, M. A. *et al*. Psoriasis vulgaris lesions contain discrete populations of Th1 and Th17 T cells. *J. Invest. Dermatol.* **128**, 1207–1211 (2008).

97. Schön, M. P. Adaptive and Innate Immunity in Psoriasis and Other Inflammatory Disorders. *Frontiers in immunology*. **10**,1764 (2019).

98. Diani, M., Altomare, G. & Reali, E. *T cell responses in psoriasis and psoriatic arthritis. Autoimmunity Reviews*. **14**, 286–292 (2015).

99. Kagami, S., Rizzo, H. L., Lee, J. J., Koguchi, Y. & Blauvelt, A. Circulating Th17, Th22, and Th1 cells are increased in psoriasis. *J. Invest. Dermatol.* **130**, 1373–83 (2010).

100. Furue, M., Furue, K., Tsuji, G. & Nakahara, T. Interleukin-17A and keratinocytes in psoriasis. *International Journal of Molecular Sciences* (2020).

101. Leipe, J. *et al*. Role of Th17 cells in human autoimmune arthritis. *Arthritis Rheum.* **62**, 2876–2885 (2010).

102. Res, P. C. M. *et al*. Overrepresentation of IL-17A and IL-22 Producing CD8 T Cells in Lesional Skin Suggests Their Involvement in the Pathogenesis of Psoriasis. *PLoS One* **5**, e14108 (2010).

103. Raychaudhuri, S. P. S. K., Abria, C., Mitra, A. & Raychaudhuri, S. P. S. K. Functional significance of MAIT cells in psoriatic arthritis. *Cytokine* **125**,

154855 (2020).

104. Mavropoulos, A. *et al*. Apremilast increases IL-10-producing regulatory B cells and decreases proinflammatory T cells and innate cells in psoriatic arthritis and psoriasis. *Rheumatol. (United Kingdom)* **58**, 2240–2250 (2019).

105. Mizumaki, K., Horii, M., Kano, M., Komuro, A. & Matsushita, T. Suppression of IL-23-mediated psoriasis-like inflammation by regulatory B cells. *Sci. Rep.* (2021).

106. Christophers, E. & Kerkhof, P. C. M. Severity, heterogeneity and systemic inflammation in psoriasis. *J. Eur. Acad. Dermatology Venereol.* **33**, 643–647 (2019).

107. Lin, A. M. *et al*. Mast Cells and Neutrophils Release IL-17 through Extracellular Trap Formation in Psoriasis. *J. Immunol.* **187**, 490–500 (2011).

108. Ritchlin, C. T., Haas-Smith, S. A., Li, P., Hicks, D. G. & Schwarz, E. M. Mechanisms of TNF-α– and RANKL-mediated osteoclastogenesis and bone resorption in psoriatic arthritis. *J. Clin. Invest.* **111**, 821–831 (2003).

109. Chiu, Y. G. *et al*. CD16 (FcRγIII) as a potential marker of osteoclast precursors in psoriatic arthritis. *Arthritis Res. Ther.* **12**, R14 (2010).

110. Golden, J. B. *et al*. Chronic Psoriatic Skin Inflammation Leads to Increased Monocyte Adhesion and Aggregation. *J. Immunol.* **195**, 2006–2018 (2015).

111. Pennington, S. R. & FitzGerald, O. *Early Origins of Psoriatic Arthritis: Clinical, Genetic and Molecular Biomarkers of Progression From Psoriasis to Psoriatic Arthritis. Frontiers in Medicine*. **8**, 1344 (Frontiers Media S.A., 2021).

112. Gialouri, C. G. & Fragoulis, G. E. Disease activity indices in psoriatic arthritis: current and evolving concepts. *Clinical Rheumatology*. **40,** 4427–4435 (2021).

113. Gladman, D. D. *et al*. Outcome measures in psoriatic arthritis. in *Journal of Rheumatology* (2007).

114. Sengul, I., Akcay-Yalbuzdag, S., Ince, B., Goksel-Karatepe, A. & Kaya, T. Comparison of the DAS28-CRP and DAS28-ESR in patients with rheumatoid arthritis. *Int. J. Rheum. Dis.* **18**, 640–645 (2015).

115. Schoels, M. M., Aletaha, D., Alasti, F. & Smolen, J. S. Disease activity in psoriatic arthritis (PsA): Defining remission and treatment success using the DAPSA score. *Ann. Rheum. Dis.* **75**, 811–818 (2016).

116. Alenius, G. M., Eriksson, C. & Dahlqvist, S. R. Interleukin-6 and soluble interleukin-2 receptor alpha - Markers of inflammation in patients with psoriatic arthritis? *Clin. Exp. Rheumatol.* **27**, 120–123 (2009).

117. Paek, S. Y. *et al*. Emerging biomarkers in psoriatic arthritis. *IUBMB Life* (2015).

118. Chandran, V. *et al*. Soluble biomarkers differentiate patients with psoriatic arthritis from those with psoriasis without arthritis. *Rheumatology* (2010).

119. Cretu, D. *et al*. Differentiating Psoriatic Arthritis From Psoriasis Without Psoriatic Arthritis Using Novel Serum Biomarkers. *Arthritis Care Res*.

120. Integration of Clinical and Protein Markers Through Machine Learning to Distinguish Patients with Psoriasis Arthritis from Those with Psoriasis Without Psoriatic Arthritis - ACR Meeting Abstracts. https://acrabstracts.org/abstract/integration-of-clinical-and-protein-markers-through-machine-learning-to-distinguish-patients-with-psoriasis-arthritis-from-those-with-psoriasis-without-psoriatic-arthritis/.

121. Leijten, E. *et al*. Broad proteomic screen reveals shared serum proteomic signature in patients with psoriatic arthritis and psoriasis without arthritis. *Rheumatol. (United Kingdom)* (2021.

122. Bogliolo, L., Crepaldi, G. & Caporali, R. Biomarkers and prognostic stratification in psoriatic arthritis. *Reumatismo* (2012).

123. Frasca, L. *et al*. Anti-LL37 antibodies are present in psoriatic arthritis (PsA) patients: New biomarkers in PsA. *Front. Immunol.* **9**, (2018).

124. Magee, C., Jethwa, H., FitzGerald, O. M. & Jadon, D. R. Biomarkers predictive of treatment response in psoriasis and psoriatic arthritis: a systematic review. *Ther. Adv. Musculoskelet. Dis.* **13**, 1759720X211014010 (2021).

125. Treatment Guidelines for Psoriatic Arthritis | Arthritis Foundation. https://www.arthritis.org/health-wellness/treatment/treatment-plan/you-your-doctor/treatment-guidelines-for-psoriatic-arthritis-arthr.

126. Ogdie, A., Coates, L. C. & Gladman, D. D. Treatment guidelines in psoriatic arthritis. *Rheumatol. (United Kingdom)* (2021) .

127. Uva, L. *et al*. Mechanisms of action of topical corticosteroids in psoriasis. *International Journal of Endocrinology* (2012.

128. Chen, M., Dai, S. M. & Guo, L. S. A novel treatment for psoriatic arthritis: Janus kinase inhibitors. *Chinese Medical Journal*. **133**, 959–967 (2020).

129. Jacobs, M. E., Pouw, J. N., Welsing, P., Radstake, T. R. D. J. & Leijten, E. F. A. First-line csDMARD monotherapy drug retention in psoriatic arthritis: Methotrexate outperforms sulfasalazine. *Rheumatol. (United Kingdom)* (2021).

130. Boehncke, W.-H. & Menter, A. Burden of Disease: Psoriasis and Psoriatic Arthritis. *Am. J. Clin. Dermatol.* **14**, 377–388 (2013).

131. Gladman, D. D., Antoni, C., Mease, P., Clegg, D. O. & Nash, P. Psoriatic arthritis: epidemiology, clinical features, course, and outcome. *Ann. Rheum. Dis.* **64 Suppl 2**, ii14-7 (2005).

132. Mease, P. J. *et al.* Brodalumab, an Anti-IL17RA Monoclonal Antibody, in Psoriatic Arthritis. *N. Engl. J. Med.* **370**, 2295–2306 (2014).

133. Papp, K. *et al.* Safety and efficacy of brodalumab for psoriasis after 120 weeks of treatment. *J. Am. Acad. Dermatol.* **71**, 1183-1190.e3 (2014).

134. Bauer, E., Lucier, J. & Furst, D. E. Brodalumab-an IL-17RA monoclonal antibody for psoriasis and psoriatic arthritis. *Expert Opin. Biol. Ther.* **15**, 883–893 (2015).

135. Liu, T. *et al.* The IL-23/IL-17 Pathway in Inflammatory Skin Diseases: From Bench to Bedside. *Frontiers in Immunology* (2020) .

136. Johnsson, H. J. & McInnes, I. B. Interleukin-12 and interleukin-23 inhibition in psoriatic arthritis. *Clin. Exp. Rheumatol.* (2015).

137. Schurich, A., Raine, C., Morris, V. & Ciurtin, C. The role of IL-12/23 in T cell-related chronic inflammation: Implications of immunodeficiency and therapeutic blockade. *Rheumatology (United Kingdom)* (2018) .

138. Gossec, L. *et al.* Persistence and effectiveness of the IL-12/23 pathway inhibitor ustekinumab or tumour necrosis factor inhibitor treatment in patients with psoriatic arthritis: 1-year results from the real-world PsABio Study. *Ann. Rheum. Dis.* (2022).

139. Mortezavi, M. & Ritchlin, C. IL12/IL23 Inhibition in the Treatment of Psoriatic Arthritis. *Curr. Treat. Options Rheumatol.* **1**, 197–209 (2015).

140. Varma, A. & Han, G. JAK Inhibitors for Psoriasis and Psoriatic Arthritis. *Current Dermatology Reports.* **9** ,107–113 (2020).

141. Ly, K., Beck, K. M., Smith, M. P., Orbai, A.-M. & Liao, W. Tofacitinib in the management of active psoriatic arthritis: patient selection and perspectives. *Psoriasis Targets Ther.* **9**, 97–107 (2019).

142. Mease, P. J. *et al.* Upadacitinib for psoriatic arthritis refractory to biologics: SELECT-PsA 2. *Ann. Rheum. Dis.* **80**, 312–320 (2021).

143. Reed, M. & Crosbie, D. Apremilast in the treatment of psoriatic arthritis: a perspective review. *Therapeutic Advances in Musculoskeletal Disease* (2017).

144. Zamora, N. V., Valerio-Morales, I. A., Lopez-Olivo, M. A., Pan, X. & Suarez-Almazor, M. E. Phosphodiesterase 4 inhibitors for psoriatic arthritis. *Cochrane Database Syst. Rev.* (2016).

145. Maejima, H. *et al*. Moesin and stress-induced phosphoprotein-1 are possible sero-diagnostic markers of psoriasis. *PLoS One* **9**, 101773 (2014).

146. Sato-Matsumura, K. C. *et al*. Localization of annexin I (lipocortin I, p35) mRNA in normal and diseased human skin by in situ hybridization. *Arch. Dermatol. Res.* (1996).

147. Kitajima, Y., Koji Owada, M., Mitsui, H. & Yaoita, H. Lipocortin I (Annexin I) is preferentially localized on the plasma membrane in keratinocytes of psoriatic lesional epidermis as shown by immunofluorescence microscopy. *J. Invest. Dermatol.* (1991).

148. Ademowo, O. S. *et al*. Discovery and confirmation of a protein biomarker panel with potential to predict response to biological therapy in psoriatic arthritis. *Ann. Rheum. Dis.* **75**, 234–241 (2016).

149. Paschalidis, N. *et al*. Modulation of experimental autoimmune encephalomyelitis by endogenous Annexin A1. *J. Neuroinflammation* **6**, 33 (2009).

150. Headland, S. *et al*. A novel mechanism for protecting the arthritic joint: microparticles deliver Annexin A1 into cartilage (146.8). *FASEB J.* (2014) .

151. Alhasan, H. *et al*. Inhibitory role of Annexin A1 in pathological bone resorption and therapeutic implications in periprosthetic osteolysis. *Nat. Commun.* **13**, 3919 (2022).

152. Sobolev, V. *et al*. Analysis of PPARγ signaling activity in psoriasis. *Int. J. Mol. Sci.* (2021).

153. Korinek, M. *et al*. Randialic acid B and tomentosolic acid block formyl peptide receptor 1 in human neutrophils and attenuate psoriasis-like inflammation in vivo. *Biochem. Pharmacol.* (2021).

154. Salamah, M. F. *et al*. The antimicrobial cathelicidin cramp augments platelet activation during psoriasis in mice. *Biomolecules* (2020).

155. Spill, F., Reynolds, D. S., Kamm, R. D. & Zaman, M. H. Impact of the physical microenvironment on tumor progression and metastasis. *Current Opinion in Biotechnology*. **40**, 41–48 (2016).

156. Gonzalez, H., Hagerling, C. & Werb, Z. Roles of the immune system in cancer: From tumor initiation to metastatic progression. *Genes and Development*. **32,** 1267–1284 (2018).

157. Iannello, A., Thompson, T. W., Ardolino, M., Marcus, A. & Raulet, D. H. Immunosurveillance and immunotherapy of tumors by innate immune cells. *Current Opinion in Immunology*. **38**, 52–58 (2016).

158. Coca, S. *et al*. The prognostic significance of intratumoral natural killer cells in patients with colerectal carcinoma. *Cancer* **79**, 2320–2328 (1997).

159. Hanson, H. L. *et al*. Eradication of established tumors by CD8+ T cell adoptive immunotherapy. *Immunity* (2000).

160. Michaud, D., Steward, C. R., Mirlekar, B. & Pylayeva-Gupta, Y. Regulatory B cells in cancer. *Immunological Reviews*. **299**, 74–92 (2021).

161. De Visser, K. E., Korets, L. V. & Coussens, L. M. De novo carcinogenesis promoted by chronic inflammation is B lymphocyte dependent. *Cancer Cell* (2005).

162. Hollern, D. P. *et al*. B Cells and T Follicular Helper Cells Mediate Response to Checkpoint Inhibitors in High Mutation Burden Mouse Models of Breast Cancer. *Cell* **179**, 1191-1206.e21 (2019).

163. Helmink, B. A. *et al*. B cells and tertiary lymphoid structures promote immunotherapy response. *Nature* **577**, 549–555 (2020).

164. Schmidt, H. *et al*. Elevated neutrophil and monocyte counts in peripheral blood are associated with poor survival in patients with metastatic melanoma: A prognostic model. *Br. J. Cancer* **93**, 273–278 (2005).

165. Rao, H.-L. *et al*. Increased Intratumoral Neutrophil in Colorectal Carcinomas Correlates Closely with Malignant Phenotype and Predicts Patients' Adverse Prognosis. *PLoS One* **7**, e30806 (2012).

166. Zhao, J. jing *et al*. The prognostic value of tumor-infiltrating neutrophils in gastric adenocarcinoma after resection. *PLoS One* (2012.
)
167. Donskov, F. Immunomonitoring and prognostic relevance of neutrophils in clinical trials. *Seminars in Cancer Biology* (2013).

168. Governa, V. *et al*. The interplay between neutrophils and CD8+ T cells improves survival in human colorectal cancer. *Clin. Cancer Res.* (2017) .

169. Houghton, A. M. G. *et al*. Neutrophil elastase-mediated degradation of IRS-1 accelerates lung tumor growth. *Nat. Med.* (2010).

170. Zhang, Q. wen *et al*. Prognostic Significance of Tumor-Associated Macrophages in Solid Tumor: A Meta-Analysis of the Literature. *PLoS One* **7**, (2012).

171. Mantovani, A., Marchesi, F., Malesci, A., Laghi, L. & Allavena, P. Tumour-associated macrophages as treatment targets in oncology. *Nature Reviews Clinical Oncology*. **14**, 399–416 (2017).

172. Qian, B. Z. *et al*. FLT1 signaling in metastasis-associated macrophages activates an inflammatory signature that promotes breast cancer metastasis. *J. Exp. Med.* **212**, 1433–1448 (2015).

173. DeNardo, D. G. *et al*. Leukocyte complexity predicts breast cancer survival and functionally regulates response to chemotherapy. *Cancer Discov.* **1**,

54–67 (2011).

174. Biaoxue, R. *et al*. Upregulation of Hsp90-beta and annexin A1 correlates with poor survival and lymphatic metastasis in lung cancer patients. *J. Exp. Clin. Cancer Res.* **31**, 1–14 (2012).

175. Oliveira-Cunha, M., Byers, R. J. & Siriwardena, A. K. Poly(A) RT-PCR measurement of diagnostic genes in pancreatic juice in pancreatic cancer. *Br. J. Cancer* **104**, 514–519 (2011).

176. Roth, U. *et al*. Differential expression proteomics of human colorectal cancer based on a syngeneic cellular model for the progression of adenoma to carcinoma. *Proteomics* **10**, 194–202 (2010).

177. Silistino-Souza, R. *et al*. Annexin 1: Differential expression in tumor and mast cells in human larynx cancer. *Int. J. Cancer* **120**, 2582–2589 (2007).

178. Kang, J. S. *et al*. Dysregulation of annexin I protein expression in high-grade prostatic intraepithelial neoplasia and prostate cancer. *Clin. Cancer Res.* **8**, 117–123 (2002).

179. Moghanibashi, M. *et al*. Proteomics of a new esophageal cancer cell line established from Persian patient. *Gene* **500**, 124–133 (2012).

180. Fu, Z. *et al*. *Annexin A1: A double-edged sword as novel cancer biomarker*. *Clinica Chimica Acta*. **504**, 36–42 (Elsevier B.V., 2020).

181. Ganesan, T., Sinniah, A., Ibrahim, Z. A., Chik, Z. & Alshawsh, M. A. Annexin A1: A bane or a boon in cancer? A systematic review. *Molecules*. **25** (2020).

182. Ang, E. Z. F., Nguyen, H. T., Sim, H. L., Putti, T. C. & Lim, L. H. K. Annexin-1 regulates growth arrest induced by high levels of estrogen in MCF-7 breast cancer cells. *Mol. Cancer Res.* **7**, 266–274 (2009).

183. Yang, Y. *et al*. Annexin 1 released by necrotic human glioblastoma cells stimulates tumor cell growth through the formyl peptide receptor 1. *Am. J. Pathol.* **179**, 1504–1512 (2011).

184. De Graauw, M. *et al*. Annexin A1 regulates TGF-ß signaling and promotes metastasis formation of basal-like breast cancer cells. *Proc. Natl. Acad. Sci. U. S. A.* **107**, 6340–6345 (2010).

185. Maschler, S. *et al*. Annexin A1 attenuates EMT and metastatic potential in breast cancer. *EMBO Mol. Med.* **2**, 401–414 (2010).

186. Liang, Z. & Li, X. Identification of ANXA1 as a potential prognostic biomarker and correlating with immune infiltrates in colorectal cancer. *Autoimmunity* (2021).

187. Liu, Y. F., Zhang, P. F., Li, M. Y., Li, Q. Q. & Chen, Z. C. Identification of annexin A1 as a proinvasive and prognostic factor for lung adenocarcinoma. *Clin. Exp. Metastasis* (2011) .

188. Hongsrichan, N. *et al*. Annexin A1: A new immunohistological marker of cholangiocarcinoma. *World J. Gastroenterol*. **19**, 2456–2465 (2013).

189. Wang, Y. *et al*. Annexin-I expression modulates drug resistance in tumor cells. *Biochem. Biophys. Res. Commun*. **314**, 565–570 (2004).

190. Liu, Q. H. *et al*. Reduced expression of annexin A1 promotes gemcitabine and 5-fluorouracil drug resistance of human pancreatic cancer. *Invest. New Drugs* **38**, 350–359 (2020).

191. Manai, M. M. *et al*. Overexpression of annexin A1 is an independent predictor of longer overall survival in epithelial ovarian cancer. *In Vivo (Brooklyn)*. **34**, 177–184 (2020).

192. Snapkov, I. *et al*. The role of formyl peptide receptor 1 (FPR1) in neuroblastoma tumorigenesis. *BMC Cancer* **16**, 490 (2016).

193. Cheng, T. Y. *et al*. Formyl peptide receptor 1 expression is associated with tumor progression and survival in gastric cancer. *Anticancer Res*. (2014).

194. Sztupinszki, Z. *et al*. A major genetic accelerator of cancer diagnosis: rs867228 in FPR1. *OncoImmunology*. **10** (2021).

195. Xiang, Y. *et al*. The G-protein coupled chemoattractant receptor FPR2 promotes malignant phenotype of human colon cancer cells. *Am. J. Cancer Res*. **6**, 2599–2610 (2016).

196. Xie, X., Yang, M., Ding, Y., Yu, L. & Chen, J. Formyl peptide receptor 2 expression predicts poor prognosis and promotes invasion and metastasis in epithelial ovarian cancer. *Oncol. Rep*. **38**, 3297–3308 (2017).

197. Hou, X. L. *et al*. FPR2 promotes invasion and metastasis of gastric cancer cells and predicts the prognosis of patients. *Sci. Rep*. **7**, 1–11 (2017).

198. Boudhraa, Z., Bouchon, B., Viallard, C., D'Incan, M. & Degoul, F. Annexin A1 localization and its relevance to cancer. *Clin. Sci*. **130**, 205–220 (2016).

199. Albagoush, S. A. & Azevedo, A. M. *Cancer, Multiple Myeloma*. *StatPearls* (StatPearls Publishing, 2018).

200. Seesaghur, A. *et al*. Clinical features and diagnosis of multiple myeloma: A population-based cohort study in primary care. *BMJ Open* **11**, 52759 (2021).

201. Fairfield, H., Falank, C., Avery, L. & Reagan, M. R. Multiple myeloma in the marrow: Pathogenesis and treatments. *Annals of the New York Academy of Sciences* (2016).

202. Nakaya, A. *et al*. Impact of CRAB symptoms in survival of patients with symptomatic myeloma in novel agent era. *Hematol. Rep*. **9**, 16–18 (2017).

203. Myeloma symptoms | Cancer Research UK.

https://www.cancerresearchuk.org/about-cancer/myeloma/symptoms.

204. Bianchi, G. & Munshi, N. C. Pathogenesis beyond the cancer clone(s) in multiple myeloma. *Blood* **125**, 3049–3058 (2015).

205. Yang, P. *et al*. Pathogenesis and treatment of multiple myeloma. *MedComm* **3**, e146 (2022).

206. Kalff, A. & Spencer, A. The t(4;14) translocation and FGFR3 overexpression in multiple myeloma: Prognostic implications and current clinical strategies. *Blood Cancer Journal*. **2**, e89 (2012).

207. Kuehl, W. M. & Bergsagel, P. L. Multiple myeloma: Evolving genetic events and host interactions. *Nature Reviews Cancer*. **2**, 175–187 (2002).

208. Talamo, G. *et al*. Beyond the CRAB Symptoms: A study of presenting clinical manifestations of multiple myeloma. *Clin. Lymphoma, Myeloma Leuk*. **10**, 464–468 (2010).

209. Kaiser, M. F. *et al*. Global methylation analysis identifies prognostically important epigenetically inactivated tumor suppressor genes in multiple myeloma. *Blood* **122**, 219–226 (2013).

210. Vrábel, D., Pour, L. & Ševčíková, S. The impact of NF-κB signaling on pathogenesis and current treatment strategies in multiple myeloma. *Blood Reviews*. **34**, 56–66 (2019).

211. Raje, N. S., Bhatta, S. & Terpos, E. Role of the RANK/RANKL pathway in multiple myeloma. *Clinical Cancer Research*. **25**, 12–20 (2019).

212. Zhang, L. *et al*. Regulatory B cell-myeloma cell interaction confers immunosuppression and promotes their survival in the bone marrow milieu. *Blood Cancer Journal* (2017).

213. Ludwig, H. *et al*. Current Multiple Myeloma Treatment Strategies with Novel Agents: A European Perspective. *Oncologist* **15**, 6–25 (2010).

214. Soliman, A. M., Das, S. & Teoh, S. L. Next-generation biomarkers in multiple myeloma: Understanding the molecular basis for potential use in diagnosis and prognosis. *International Journal of Molecular Sciences*. **22** (2021).

215. Li, Y. *et al*. Classify Hyperdiploidy Status of Multiple Myeloma Patients Using Gene Expression Profiles. *PLoS One* **8**, 58809 (2013).

216. Bustoros, M., Mouhieddine, T. H., Detappe, A. & Ghobrial, I. M. Established and Novel Prognostic Biomarkers in Multiple Myeloma. *Am. Soc. Clin. Oncol. Educ. B.* 548–560 (2017).

217. Avet-Loiseau, H. *et al*. Bortezomib Plus Dexamethasone Induction Improves Outcome of Patients With t(4;14) Myeloma but Not Outcome of Patients With del(17p). *J Clin Oncol* **28**, 4630–4634 (2010).

218. Walker, B. A. *et al*. Mutational spectrum, copy number changes, and outcome: Results of a sequencing study of patients with newly diagnosed myeloma. *J. Clin. Oncol.* **33**, 3911–3920 (2015).

219. Chapman, M. A. *et al*. Initial genome sequencing and analysis of multiple myeloma. *Nature* **471**, 467–472 (2011).

220. Lohr, J. G. *et al*. Widespread genetic heterogeneity in multiple myeloma: Implications for targeted therapy. *Cancer Cell* **25**, 91–101 (2014).

221. Sharman, J. P. *et al*. Vemurafenib response in 2 patients with posttransplant refractory BRAF V600E-mutated multiple myeloma. *Clin. Lymphoma, Myeloma Leuk.* **14**, e161–e163 (2014).

222. Chen, L. *et al*. Identification of early growth response protein 1 (EGR-1) as a novel target for JUN-induced apoptosis in multiple myeloma. *Blood* **115**, 61–70 (2010).

223. Zhu, Y. X. *et al*. Identification of cereblon-binding proteins and relationship with response and survival after IMiDs in multiple myeloma. *Blood* **124**, 536–545 (2014).

224. Bettegowda, C. *et al*. Detection of circulating tumor DNA in early- and late-stage human malignancies. *Sci. Transl. Med.* **6**, (2014).

225. Reinert, T. *et al*. Analysis of circulating tumour DNA to monitor disease burden following colorectal cancer surgery. *Gut* **65**, 625–634 (2016).

226. Gonsalves, W. I. *et al*. Quantification of clonal circulating plasma cells in relapsed multiple myeloma. *Br. J. Haematol.* **167**, 500–505 (2014).

227. Garcia-Murillas, I. *et al*. Mutation tracking in circulating tumor DNA predicts relapse in early breast cancer. *Sci. Transl. Med.* **7**, (2015).

228. Manier, S. *et al*. Whole-Exome Sequencing and Targeted Deep Sequencing of cfDNA Enables a Comprehensive Mutational Profiling of Multiple Myeloma. *Blood* **128**, 197–197 (2016).

229. Ansell, S. M. *et al*. PD-1 Blockade with Nivolumab in Relapsed or Refractory Hodgkin's Lymphoma. *N. Engl. J. Med.* **372**, 311–319 (2015).

230. Wallington-Beddoe, C. T. & Pitson, S. M. Novel therapies for multiple myeloma. *Aging* vol. 9 1857–1858 (2017).

231. Obeng, E. A. *et al*. Proteasome inhibitors induce a terminal unfolded protein response in multiple myeloma cells. *Blood* **107**, 4907–4916 (2006).

232. El-Ghammaz, A. M. S. & Abdelwahed, E. Bortezomib-based induction improves progression-free survival of myeloma patients harboring 17p deletion and/or t(4;14) and overcomes their adverse prognosis. *Ann. Hematol.* **95**, 1315–1321 (2016).

233. Miguel, J. F. S. *et al*. Persistent overall survival benefit and no increased risk of second malignancies with bortezomib-melphalan-prednisone versus melphalan-prednisone in patients with previously untreated multiple myeloma. *J. Clin. Oncol.* **31**, 448–455 (2013).

234. Dimopoulos, M. A. *et al*. Carfilzomib and dexamethasone versus bortezomib and dexamethasone for patients with relapsed or refractory multiple myeloma (ENDEAVOR): And randomised, phase 3, open-label, multicentre study. *Lancet Oncol.* **17**, 27–38 (2016).

235. Holstein, S. A. & McCarthy, P. L. Immunomodulatory Drugs in Multiple Myeloma: Mechanisms of Action and Clinical Experience. *Drugs*. **77**, 505–520 (2017).

236. Zhang, T. *et al*. Systematic review and meta-analysis of the efficacy and safety of novel monoclonal antibodies for treatment of relapsed/ refractory multiple myeloma. *Oncotarget*. **8**, 34001–34017 (2017).

237. Landgren, O. & Rajkumar, S. V. New developments in diagnosis, prognosis, and assessment of response in multiple myeloma. *Clinical Cancer Research*. **22**, 5428–5433 (2016).

238. Jia, C., Kong, D., Guo, Y., Li, L. & Quan, L. Enhanced antitumor effect of combination of annexin A1 knockdown and bortezomib treatment in multiple myeloma in vitro and in vivo. *Biochem. Biophys. Res. Commun.* **505**, 720–725 (2018).

239. Ria, R. *et al*. HIF-1a of bone marrow endothelial cells implies relapse and drug resistance in patients with multiple myeloma and may act as a therapeutic target. *Clin. Cancer Res.* **20**, 847–858 (2014).

240. Jibril,A *et al*.Myeloma Derived Mitochondrial Damage Associated Molecular Patterns Promote Pro-Tumoral Expansion By Inducing a Pro-Inflammatory Signature in the Bone Marrow Microenvironment. *Blood*. **136** (2020).

241. Yang, Q., Li, K., Li, X. & Liu, J. Identification of Key Genes and Pathways in Myeloma side population cells by Bioinformatics Analysis. *Int. J. Med. Sci.* **2020**, 2063–2076 (2020).

242. CD14 protein expression summary - The Human Protein Atlas. https://www.proteinatlas.org/ENSG00000170458-CD14.

243. Qin, Z. The use of THP-1 cells as a model for mimicking the function and regulation of monocytes and macrophages in the vasculature. *Atherosclerosis*. **221**, 2–11 (2012).

244. Dadouch, M., Ladner, Y. & Perrin, C. Analysis of Monoclonal Antibodies by Capillary Electrophoresis: Sample Preparation, Separation, and Detection. *Separations* **8**, 4 (2021).

245. Mason, M., Sweeney, B., Cain, K., Stephens, P. & Sharfstein, S. T. Identifying bottlenecks in transient and stable production of recombinant

monoclonal-antibody sequence variants in chinese hamster ovary cells. *Biotechnol. Prog.* **28**, 846–855 (2012).

246. Fus-Kujawa, A. *et al.* An Overview of Methods and Tools for Transfection of Eukaryotic Cells in vitro. *Frontiers in Bioengineering and Biotechnology*. **9**, 634 (2021).

247. Size Exclusion Chromatography (SEC) for Antibody Aggregation Analysis - Creative Biolabs. https://www.creative-biolabs.com/drug-discovery/therapeutics/size-exclusion-chromatography-sec-for-antibody-aggregation-analysis.htm.

248. Benoit, D. S. W., Gray, W., Murthy, N., Li, H. & Duvall, C. L. pH-responsive polymers for the intracellular delivery of biomolecular drugs. in *Comprehensive Biomaterials*. **4**,357–375 (Elsevier, 2011).

249. Kubiak, R. J. *et al.* Storage Conditions of Conjugated Reagents Can Impact Results of Immunogenicity Assays. *J. Immunol. Res.* **2016**, (2016).

250. Alexa Fluor™ 647 Antibody Labeling Kit. https://www.thermofisher.com/order/catalog/product/A20186#/A20186.

251. Annexin V Staining | Thermo Fisher Scientific - UK. https://www.thermofisher.com/uk/en/home/life-science/cell-analysis/cell-viability-and-regulation/apoptosis/annexin-v-staining.html?ef_id=EAIaIQobChMIz--nldTo9AIVDZ53Ch3Arwj1EAAYAiAAEgJmjfD_BwE:G:s&s_kwcid=AL!3652!3!358436904933!p!!g!!annexin v apoptosis&cid=bid_pca_frg_r01_co_cp1359_pjt0000_bid00000_0se_gaw_nt_pur_con&gclid=EAIaIQobChMIz--nldTo9AIVDZ53Ch3Arwj1EAAYAiAAEgJmjfD_BwE.

252. Rieger, A. M., Nelson, K. L., Konowalchuk, J. D. & Barreda, D. R. Modified annexin V/propidium iodide apoptosis assay for accurate assessment of cell death. *J. Vis. Exp.* (2011).

253. BestProtocols: Annexin V Staining Protocol for Flow Cytometry - UK.

254. EasySep™ Human Monocyte Isolation Kit. https://www.stemcell.com/products/easysep-human-monocyte-isolation-kit.html.

255. Agilent Seahorse XF Instruments Overview and Selection Guide | Agilent. https://www.agilent.com/en/products/cell-analysis/seahorse-xf-instruments-selection-guide.

256. Mitochondrial Respiration XF Cell Mito Stress Test | Agilent. https://www.agilent.com/en/support/cell-analysis/mitochondrial-respiration-xf-cell-mito-stress-test.

257. Human Annexin A1 ELISA Kit - Invitrogen. https://www.thermofisher.com/elisa/product/Human-Annexin-A1-ELISA-Kit/EH31RB.

258. Langan, T. J. & Chou, R. C. Chapter 5 Synchronization of Mammalian Cell Cultures by Serum Deprivation.
.
259. Pierce™ BCA Protein Assay Kit. https://www.thermofisher.com/order/catalog/product/23225.

260. Array Analysis Tool. https://www.wvision.com/QuickSpots.html.

261. Bioconductor - DESeq2. https://bioconductor.org/packages/release/bioc/html/DESeq2.html.

262. Count normalization with DESeq2 | Introduction to DGE - ARCHIVED. https://hbctraining.github.io/DGE_workshop/lessons/02_DGE_count_normalization.html.

263. Anders, S. & Huber, W. Differential expression analysis for sequence count data. *Genome Biol.* **11**, R106 (2010).

264. The MMRF CoMMpass Study | The MMRF. https://themmrf.org/finding-a-cure/our-work/the-mmrf-commpass-study/.

265. Bioconductor - clusterProfiler. https://bioconductor.org/packages/release/bioc/html/clusterProfiler.html.

266. stats package - RDocumentation. https://www.rdocumentation.org/packages/stats/versions/3.6.2.

267. Create Elegant Data Visualisations Using the Grammar of Graphics • ggplot2. https://ggplot2.tidyverse.org/.

268. Ye, R. D. *et al.* International union of basic and clinical pharmacology. LXXIII. Nomenclature for the formyl peptide receptor (FPR) family. *Pharmacological Reviews.***61** 119–161 (2009).

269. Okano, M. *et al.* Triple-negative breast cancer with high levels of annexin a1 expression is associated with mast cell infiltration, inflammation, and angiogenesis. *Int. J. Mol. Sci.* (2019).

270. Boudhraa, Z. *et al.* Annexin A1 in primary tumors promotes melanoma dissemination. *Clin. Exp. Metastasis* **31**, 749–760 (2014).

271. Gladman, D. D. Psoriatic arthritis. in *Moderate-to-Severe Psoriasis, Third Edition.* **8 ,** 239–258 (CRC Press, 2008).

272. NG, B. C. K. & Jadon, D. R. Unmet needs in psoriatic arthritis. *Best Practice and Research: Clinical Rheumatology* . **35**, 101693 (2021).

273. Ito, R. *et al.* Involvement of IL-17A in the pathogenesis of DSS-induced colitis in mice. *Biochem. Biophys. Res. Commun.* **377**, 12–16 (2008).

274. Rohwer, N. *et al*. Annexin A1 sustains tumor metabolism and cellular proliferation upon stable loss of HIF1A. *Oncotarget* **7**, 6693–6710 (2016).

275. Wang, B., Kankanamalage, S. G., Dong, J. & Liu, Y. Optimization of therapeutic antibodies. *Antibody Therapeutics*. **4,** 45–54 (2021).

276. Hallmaier-Wacker, L. K., Lueert, S., Roos, C. & Knauf, S. The impact of storage buffer, DNA extraction method, and polymerase on microbial analysis. *Sci. Rep.* **8**, 1–9 (2018).

277. Lazar, K. L., Patapoff, T. W. & Sharma, V. K. Cold denaturation of monoclonal antibodies. *MAbs* **2**, 42–52 (2010).

278. Bumbaca, D. *et al*. Highly specific off-target binding identified and eliminated during the humanization of an antibody against FGF receptor 4. *MAbs* **3**, 376–386 (2011).

279. Mulder, M. L. M. *et al*. Blood-based immune profiling combined with machine learning discriminates psoriatic arthritis from psoriasis patients. *Int. J. Mol. Sci.* **22**, 10990 (2021).

280. Wu, Z. *et al*. Effect of Monoclonal Antibody Blockade of Long Fragment Neurotensin on Weight Loss, Behavior, and Metabolic Traits After High-Fat Diet Induced Obesity. *Front. Endocrinol. (Lausanne).* **12**, 1179 (2021).

281. Suzuki, M., Kato, C. & Kato, A. Therapeutic antibodies: Their mechanisms of action and the pathological findings they induce in toxicity studies. *Journal of Toxicologic Pathology*. **28**, 133–139 (2015).

282. Culture Collections. https://www.culturecollections.org.uk/news/ecacc-news/co2-concentration-and-ph-control-in-the-cell-culture-laboratory.aspx.

283. Minocha, S. C. PH of the Medium and the Growth and Metabolism of Cells in Culture. in 125–141 (Springer, Dordrecht, 1987).

284. Smolina, N., Bruton, J., Kostareva, A. & Sejersen, T. Assaying mitochondrial respiration as an indicator of cellular metabolism and fitness. in *Methods in Molecular Biology* .**1601**, 79–87 (Humana Press Inc., 2017).

285. Louie, M. C. *et al*. Total Cellular ATP Production Changes With Primary Substrate in MCF7 Breast Cancer Cells. *Front. Oncol.* **10**, 1703 (2020).

286. Alldridge, L. C. & Bryant, C. E. Annexin 1 regulates cell proliferation by disruption of cell morphology and inhibition of cyclin D1 expression through sustained activation of the ERK1/2 MAPK signal. *Exp. Cell Res.* **290**, 93–107 (2003).

287. Chen, L. *et al*. Inflammatory responses and inflammation-associated diseases in organs. *Oncotarget*. **9**, 7204–7218 (2018).

288. Sugimoto, M. A., Sousa, L. P., Pinho, V., Perretti, M. & Teixeira, M. M. Resolution of inflammation: What controls its onset? *Frontiers in Immunology*. **7**, 160 (2016).

289. Rosenblum, M. D., Remedios, K. A. & Abbas, A. K. Mechanisms of human autoimmunity. *J. Clin. Invest*. **125**, 2228–2233 (2015).

290. Michael Pollard, K. *et al*. Mechanisms of Environment-Induced Autoimmunity. *Annu. Rev. Pharmacol. Toxicol*. **61**, 135–157 (2021).

291. Wu, H. J. *et al*. Gut-residing segmented filamentous bacteria drive autoimmune arthritis via T helper 17 cells. *Immunity* **32**, 815–827 (2010).

292. Kuwabara, T., Ishikawa, F., Kondo, M. & Kakiuchi, T. The Role of IL-17 and Related Cytokines in Inflammatory Autoimmune Diseases. *Mediators Inflamm*. **2017**, (2017).

293. Piras, G. *et al*. Immuno-moodulin: A new anxiogenic factor produced by Annexin-A1 transgenic autoimmune-prone T cells. *Brain. Behav. Immun.* (2020).

294. Hampe, C. S. B Cells in Autoimmune Diseases. **2012**, (2012).

295. Suzuki, E., Mellins, E. D., Gershwin, M. E., Nestle, F. O. & Adamopoulos, I. E. The IL-23/IL-17 axis in psoriatic arthritis. *Autoimmunity Reviews*. **13**,496–502 (2014).

296. Wang, Y. *et al*. Monocytes/Macrophages play a pathogenic role in IL-23 mediated psoriasis-like skin inflammation. *Sci. Rep*. **9**, 1–9 (2019).

297. Abji, F. *et al*. Proteinase-Mediated Macrophage Signaling in Psoriatic Arthritis. *Front. Immunol*. **11**, 3914 (2021).

298. Novelli, L., Chimenti, M. S., Chiricozzi, A. & Perricone, R. The new era for the treatment of psoriasis and psoriatic arthritis: Perspectives and validated strategies. *Autoimmunity Reviews*l. **13**, 64–69 (2014).

299. Mease, P. J. Tumour necrosis factor (TNF) in psoriatic arthritis: Pathophysiology and treatment with TNF inhibitors. *Annals of the Rheumatic Diseases*. **61**, 298–304 (2002).

300. Chiricozzi, A. *et al*. Integrative responses to IL-17 and TNF-α in human keratinocytes account for key inflammatory pathogenic circuits in psoriasis. *J. Invest. Dermatol*. **131**, 677–687 (2011).

301. Cretu, D. *et al*. Quantitative tandem mass-spectrometry of skin tissue reveals putative psoriatic arthritis biomarkers. *Clin. Proteomics* (2015) .

302. He, J. *et al*. Weighted gene co-expression network analysis identifies RHOH and TRAF1 as key candidate genes for psoriatic arthritis. *Clin. Rheumatol*. **40**, 1381–1391 (2021).

303. The Human Protein Atlas. https://www.proteinatlas.org/.

304. GeneCards - Human Genes | Gene Database | Gene Search. https://www.genecards.org/.

305. Mathy, N. W. & Chen, X. M. Long non-coding RNAs (lncRNAs) and their transcriptional control of inflammatory responses. *Journal of Biological Chemistry*.**292**, 12375–12382 (2017).

306. Rapicavoli, N. A. *et al*. A mammalian pseudogene lncRNA at the interface of inflammation and antiinflammatory therapeutics. *Elife* **2013**, 762 (2013).

307. RPL38 Gene - GeneCards | RL38 Protein | RL38 Antibody. https://www.genecards.org/cgi-bin/carddisp.pl?gene=RPL38.

308. TOMM7 Gene - GeneCards | TOM7 Protein | TOM7 Antibody. https://www.genecards.org/cgi-bin/carddisp.pl?gene=TOMM7&keywords=TOMM7.

309. Swindell, W. R. *et al*. Proteogenomic analysis of psoriasis reveals discordant and concordant changes in mRNA and protein abundance. *Genome Med.* **7**, 1–22 (2015).

310. Thorslund, K., El-Nour, H. & Nordlind, K. The serotonin transporter protein is expressed in psoriasis, where it may play a role in regulating apoptosis. *Arch. Dermatol. Res.* **301**, 449–457 (2009).

311. RGS2 - Regulator of G-protein signaling 2 - Homo sapiens (Human) - RGS2 gene & protein. https://www.uniprot.org/uniprot/P41220.

312. Liszewska, A., Robak, E., Bernacka, M., Bogaczewicz, J. & Woźniacka, A. Methotrexate use and NAD+/NADH metabolism in psoriatic keratinocytes. *Postepy Dermatologii i Alergologii*. **37**, 19–22 (2020).

313. Xu, X. *et al*. Annexin A1 protects against cerebral ischemia–reperfusion injury by modulating microglia/macrophage polarization via FPR2/ALX-dependent AMPK-mTOR pathway. *J. Neuroinflammation* **18**, 119 (2021).

314. Tylek, K. *et al*. Formyl peptide receptor 2, as an important target for ligands triggering the inflammatory response regulation: a link to brain pathology. *Pharmacological Reports*. **73**, 1004–1019 (2021).

315. Ulgen, E., Ozisik, O. & Sezerman, O. U. PathfindR: An R package for comprehensive identification of enriched pathways in omics data through active subnetworks. *Front. Genet.* **10**, 858 (2019).

316. Kanehisa, M., Sato, Y. & Kawashima, M. KEGG mapping tools for uncovering hidden features in biological data. *Protein Sci.* **31**, 47–53 (2022).

317. Varley, C. D. *et al*. Persistence of Staphylococcus aureus colonization among individuals with immune-mediated inflammatory diseases treated with TNF-α inhibitor therapy. *Rheumatol. (United Kingdom)* (2014) doi:10.1093/rheumatology/ket351.

318. Prat, C., Bestebroer, J., de Haas, C. J. C., van Strijp, J. A. G. & van Kessel, K. P. M. A New Staphylococcal Anti-Inflammatory Protein That Antagonizes the Formyl Peptide Receptor-Like 1. *J. Immunol.* **177**, 8017–8026 (2006).

319. Hu, S. C. S. *et al*. Neutrophil extracellular trap formation is increased in psoriasis and induces human β-defensin-2 production in epidermal keratinocytes. *Sci. Rep.* **6**, (2016).

320. Carey, K. D. & Stork, P. J. S. Nonisotopic methods for detecting activation of small G proteins. in *Methods in Enzymology* (2002).

321. Salinas, G. F. *et al*. Sustained Rap1 activation in autoantigen-specific T lymphocytes attenuates experimental autoimmune encephalomyelitis. *J. Neuroimmunol.* **250**, 35–43 (2012).

322. Mavropoulos, A., Rigopoulou, E. I., Liaskos, C., Bogdanos, D. P. & Sakkas, L. I. The role of p38 mapk in the aetiopathogenesis of psoriasis and psoriatic arthritis. *Clinical and Developmental Immunology* . **2013**, (2013).

323. Flow cytometry recommended controls | Abcam. https://www.abcam.com/protocols/recommended-controls-for-flow-cytometry.

324. Domingues, R. G. *et al*. CD5 expression is regulated during human T-cell activation by alternative polyadenylation, PTBP1, and miR-204. *Eur. J. Immunol.* **46**, 1490–1503 (2016).

325. Rouxel, O. & Lehuen, A. Mucosal-associated invariant T cells in autoimmune and immune-mediated diseases. *Immunology and Cell Biology* (2018).

326. Lai, T. *et al*. Annexin A1 is elevated in patients with COPD and affects lung fibroblast function. *Int. J. Chron. Obstruct. Pulmon. Dis.* **13**, 473–486 (2018).

327. Wang, G., Liang, X. S., He, C. J., Zhou, Y. F. & Chen, S. H. Ability of serum annexin A1 to predict 6-month poor clinical outcome following aneurysmal subarachnoid hemorrhage. *Clin. Chim. Acta* **519**, 142–147 (2021).

328. Tsai, W. H., Shih, C. H., Yu, Y. Bin & Hsu, H. C. Plasma levels in sepsis patients of annexin A1, lipoxin A4, macrophage inflammatory protein-3a, and neutrophil gelatinase-associated lipocalin. *J. Chinese Med. Assoc.* **76**, 486–490 (2013).

329. Sadofsky, L. R. *et al*. Characterisation of a New Human Alveolar Macrophage-Like Cell Line (Daisy). *Lung* **197**, 687–698 (2019).

330. Ni, Q., Titov, D. V. & Zhang, J. Analyzing protein kinase dynamics in living cells with FRET reporters. *Methods* **40**, 279–286 (2006).

331. Proteome Profiler Human Phospho-Kinase Array Kit ARY003C: R&D Systems. https://www.rndsystems.com/products/proteome-profiler-human-phospho-kinase-array-kit_ary003c.

332. Xiao, K. *et al*. Global phosphorylation analysis of β-arrestin-mediated signaling downstream of a seven transmembrane receptor (7TMR).

333. Lawson, S. K., Dobrikova, E. Y., Shveygert, M. & Gromeier, M. p38α Mitogen-Activated Protein Kinase Depletion and Repression of Signal Transduction to Translation Machinery by miR-124 and -128 in Neurons. *Mol. Cell. Biol.* **33**, 127–135 (2013).

334. Ivashkiv, L. B. & Hu, X. Signaling by STATs. *Arthritis Res. Ther.* **6**, 159 (2004).

335. Bartek, J. & Lukas, J. Chk1 and Chk2 kinases in checkpoint control and cancer. *Cancer Cell.* **3**, 421–429 (2003).

336. Harada, H., Andersen, J. S., Mann, M., Terada, N. & Korsmeyer, S. J. p70S6 kinase signals cell survival as well as growth, inactivating the pro-apoptotic molecule BAD. *Proc. Natl. Acad. Sci. U. S. A.* (2001).

337. PI3K / Akt Signaling | Cell Signaling Technology. https://www.cellsignal.co.uk/pathways/pathways-akt-signaling.

338. Patel, S. & Werstuck, G. H. Macrophage function and the role of GSK3. *Int. J. Mol. Sci.* **22**, 1–13 (2021).

339. JNK Signaling Pathway - Creative Diagnostics. https://www.creative-diagnostics.com/JNK-Signaling-Pathway.htm.

340. Wortzel, I. & Seger, R. The ERK cascade: Distinct functions within various subcellular organelles. *Genes and Cancer.* **2**, 195–209 (2011).

341. Chen, H. & Zhang, L. Downregulation of FPR1 abates lipopolysaccharide-induced inflammatory injury and apoptosis by upregulating MAPK signaling pathway in murine chondrogenic ATDC5 cells. *Allergol. Immunopathol. (Madr).* **49**, 57–63 (2021).

342. Li, Y. *et al*. Resistin, a Novel Host Defense Peptide of Innate Immunity. *Frontiers in Immunology*. **12,** 2436 (2021).

343. Tsiotra, P. C., Boutati, E., Dimitriadis, G. & Raptis, S. A. High insulin and leptin increase resistin and inflammatory cytokine production from human mononuclear cells. *Biomed Res. Int.* **2013**, (2013).

344. Boulakirba, S. *et al*. IL-34 and CSF-1 display an equivalent macrophage differentiation ability but a different polarization potential. *Sci. Rep.* **8**, 256 (2018).

345. Lendemans, S. *et al*.GM-CSF priming of human monocytes is dependent on ERK1/2 activation. *J. Endotoxin.* **12**, 10-20 (2006).

.

346. Niu, J. *et al*. Keratinocyte growth factor/fibroblast growth factor-7-regulated cell migration and invasion through activation of NF-κB transcription factors. *J. Biol. Chem.* **282**, 6001–6011 (2007).

347. Darling, M. R., Tsai, S., Jackson-Boeters, L., Daley, T. D. & Diamandis, E. P. Human kallikrein 3 (prostate-specific antigen) and human kallikrein 5 expression in salivary gland tumors. *Int. J. Biol. Markers* **21**, 201–205 (2006).

348. Yang, Y., Lin, Z., Lin, Q., Bei, W. & Guo, J. Pathological and therapeutic roles of bioactive peptide trefoil factor 3 in diverse diseases: recent progress and perspective. *Cell Death and Disease*.**13** (2022).

349. THP-1 ATCC® TIB-202™. https://www.lgcstandards-atcc.org/products/all/TIB-202.aspx?geo_country=gb.

350. Tucureanu, M. M. *et al*. Lipopolysaccharide-induced inflammation in monocytes/macrophages is blocked by liposomal delivery of G_i-protein inhibitor. *Int. J. Nanomedicine*. **13**, 63–76 (2017).

351. Ngkelo, A., Meja, K., Yeadon, M., Adcock, I. & Kirkham, P. A. LPS induced inflammatory responses in human peripheral blood mononuclear cells is mediated through NOX4 and G iα dependent PI-3kinase signalling. *J. Inflamm.* **9**, 1 (2012).

352. Van Der Bruggen, T., Nijenhuis, S., Van Raaij, E., Verhoef, J. & Van Asbeck, B. S. Lipopolysaccharide-induced tumor necrosis factor alpha production by human monocytes involves the Raf-1/MEK1-MEK2/ERK1-ERK2 pathway. *Infect. Immun.* **67**, 3824–3829 (1999).

353. Vecellio, M. *et al*. The IL-17/IL-23 Axis and Its Genetic Contribution to Psoriatic Arthritis. *Frontiers in Immunology*. **11**, 3418 (2021).

354. Laborde, C. M., Larzabal, L., González-Cantero, Á., Castro-Santos, P. & Díaz-Peña, R. Personalized Medicine Advances of Genomic Medicine in Psoriatic Arthritis. *J. Pers. Med. 2022* **12**, 35 (2022).

355. Shi, C., Rattray, M., Barton, A., Bowes, J. & Orozco, G. Using functional genomics to advance the understanding of psoriatic arthritis. *Rheumatology (United Kingdom)* (2020).

356. Caputo, V. *et al*. Overview of the molecular determinants contributing to the expression of Psoriasis and Psoriatic Arthritis phenotypes. *Journal of Cellular and Molecular Medicine* (2020).

357. de Vlam, K. *et al*. Skin Involvement in Psoriatic Arthritis Worsens Overall Disease Activity, Patient-Reported Outcomes, and Increases Healthcare Resource Utilization: An Observational, Cross-Sectional Study. *Rheumatol. Ther*. (2018).

358. Diani, M. *et al*. Increased frequency of activated CD8+ T cell effectors in patients with psoriatic arthritis. *Sci. Rep*. (2019) .

359. Choy, E. T cells in psoriatic arthritis. *Current Rheumatology Reports*. **9,**437–441 (2007).

360. Ng, C. Y., Huang, Y. H., Chu, C. F., Wu, T. C. & Liu, S. H. Risks for Staphylococcus aureus colonization in patients with psoriasis: a systematic review and meta-analysis. *British Journal of Dermatology* (2017).

361. Grice, E. A. & Segre, J. A. The skin microbiome. *Nature Reviews Microbiology*. **9**, 244–253 (2011).

362. Van Avondt, K. & Hartl, D. Mechanisms and disease relevance of neutrophil extracellular trap formation. *European Journal of Clinical Investigation*.**48** (2018).

363. Hutchinson, J. L., Rajagopal, S. P., Sales, K. J. & Jabbour, H. N. Molecular regulators of resolution of inflammation: Potential therapeutic targets in the reproductive system. *Reproduction*. **142**, 15–28 (2011).

364. Elkon, K. & Casali, P. Nature and functions of autoantibodies. *Nature Clinical Practice Rheumatology*. **4**, 491–498 (2008).

365. Zhu, J., Shi, X. F. & Chu, C. Q. Autoantibodies in psoriatic arthritis: Are they of pathogenic relevance? *Chinese Medical Journal*. **133**, 2899–2901 (2020).

366. Simon, D. *et al*. Increased Frequency of Activated Switched Memory B Cells and Its Association With the Presence of Pulmonary Fibrosis in Diffuse Cutaneous Systemic Sclerosis Patients. *Front. Immunol*. (2021) .

367. Stansky, E. *et al*. B cell anomalies in autoimmune retinopathy (AIR). *Investig. Ophthalmol. Vis. Sci*. **58**, 3600–3607 (2017).

368. Zhou, Y. *et al*. Transitional B cells involved in autoimmunity and their impact on neuroimmunological diseases. *Journal of Translational Medicine*. **18**, 131 (2020).

369. Liu, M. *et al*. Type I interferons promote the survival and proinflammatory properties of transitional B cells in systemic lupus erythematosus patients. *Cell. Mol. Immunol*. **16**, 367–379 (2019).

370. Cappellen, D. *et al*. Transcriptional program of mouse osteoclast differentiation governed by the macrophage colony-stimulating factor and the ligand for the receptor activator of NFκB. *J. Biol. Chem*. **277**, 21971–

21982 (2002).
371. Boudhraa, Z., Bouchon, B., Viallard, C., D'Incan, M. & Degoul, F. Annexin A1 localization and its relevance to cancer. *Clin. Sci.* (2016) .

372. Jeon, C. *et al*. Monoclonal antibodies inhibiting IL-12, -23, and -17 for the treatment of psoriasis. *Hum. Vaccines Immunother.* **13**, 2247–2259 (2017).

373. Treating Psoriatic Arthritis: Inside the New Biologic Monoclonal Antibodies. https://www.practicalpainmanagement.com/treatments/pharmacological/new-biological-agents-psoriatic-arthritis-monoclonal-antibody-primer.

374. Starr, T., Bauler, T. J., Malik-Kale, P. & Steele-Mortimer, O. The phorbol 12-myristate-13-acetate differentiation protocol is critical to the interaction of THP-1 macrophages with Salmonella Typhimurium. *PLoS One* **13**, e0193601 (2018).

375. Yang, Y. H., Morand, E. & Leech, M. Annexin A1: potential for glucocorticoid sparing in RA. *Nat. Rev. Rheumatol.* **9**, 595–603 (2013).

376. Chanput, W., Peters, V. & Wichers, H. THP-1 and U937 cells. in *The Impact of Food Bioactives on Health: In Vitro and Ex Vivo Models* 147–159 (Springer International Publishing, 2015).

377. Kapellos, T. S. *et al*. Human monocyte subsets and phenotypes in major chronic inflammatory diseases. *Frontiers in Immunology*. **10**, 2035 (2019).

378. Tsubota, Y., Frey, J. M. & Raines, E. W. Technical Advance: Novel ex vivo culture method for human monocytes uses shear flow to prevent total loss of transendothelial diapedesis function. *J. Leukoc. Biol.* **95**, 191–195 (2014).

379. Liu, Y., Li, H., Czajkowsky, D. M. & Shao, Z. Monocytic THP-1 cells diverge significantly from their primary counterparts: a comparative examination of the chromosomal conformations and transcriptomes. *Hereditas* **158**, 43 (2021).

380. (US), N. I. of H. & Study, B. S. C. Understanding Cancer. (2007).

381. Cheng, T. Y. *et al*. Annexin A1 is associated with gastric cancer survival and promotes gastric cancer cell invasiveness through the formyl peptide receptor/extracellular signal-regulated kinase/integrin beta-1-binding protein 1 pathway. *Cancer* **118**, 5757–5767 (2012).

382. Prinja, S., Gupta, N. & Verma, R. Censoring in clinical trials: Review of survival analysis techniques. *Indian Journal of Community Medicine*. **35**, 217–221 (2010).

383. Huynh, M. *et al*. Hyaluronan and proteoglycan link protein 1 (HAPLN1) activates bortezomib-resistant NF-B activity and increases drug resistance in multiple myeloma. *J. Biol. Chem.* **293**, 2452–2465 (2018).

384. Xiang, Y., Zhang, L., Xiang, P. & Zhang, J. Circulating miRNAs as Auxiliary Diagnostic Biomarkers for Multiple Myeloma: A Systematic Review, Meta-Analysis, and Recommendations. *Frontiers in Oncology* (2021) .

385. Klein, C. A. Cancer progression and the invisible phase of metastatic colonization. *Nature Reviews Cancer*. **20**, 681–694 (2020).

386. Roussos, E. T., Condeelis, J. S. & Patsialou, A. Chemotaxis in cancer. *Nature Reviews Cancer* (2011).

387. Crupi, R., Impellizzeri, D. & Cuzzocrea, S. Role of metabotropic glutamate receptors in neurological disorders. *Frontiers in Molecular Neuroscience*. **12**, 20 (2019).

388. Egan, P. A., Elder, P. T., Deighan, W. I., O'Connor, S. J. M. & Alexander, H. D. Multiple myeloma with central nervous system relapse. *Haematologica*. **105**, 1780–1790 (2020).

389. Yang, L., Lu, P., Yang, X., Li, K. & Qu, S. Annexin A3, a Calcium-Dependent Phospholipid-Binding Protein: Implication in Cancer. *Front. Mol. Biosci.* **8**, 700 (2021).

390. Zatula, A. *et al*. Proteome alterations associated with transformation of multiple myeloma to secondary plasma cell leukemia. *Oncotarget* **8**, 19427–19442 (2017).

391. Gu, Z. Y. *et al*. Maintenance of cellular annexin a1 level is essential for pi3k/akt/mtor-mediated proliferation of pancreatic beta cells. *J. Biol. Regul. Homeost. Agents* (2021).

392. Bode, K. *et al*. Dectin-1 Binding to Annexins on Apoptotic Cells Induces Peripheral Immune Tolerance via NADPH Oxidase-2. *Cell Rep.* (2019) .

393. Jibril, A. *et al*. Myeloma Derived Mitochondrial Damage Associated Molecular Patterns Promote Pro-Tumoral Expansion By Inducing a Pro-Inflammatory Signature in the Bone Marrow Microenvironment. *Blood* **136**, 1–1 (2020).

394. Gene Set - Multiple Myeloma. https://maayanlab.cloud/Harmonizome/gene_set/Multiple+Myeloma/CTD+Gene-Disease+Associations.

395. Rajan, A. M. & Rajkumar, S. V. Interpretation of cytogenetic results in multiple myeloma for clinical practice. *Blood Cancer Journal*. **5**, e365 (2015).

396. Hanamura, I. Gain/amplification of chromosome arm 1q21 in multiple myeloma. *Cancers*. **13**,1–16 (2021).

397. Weisz, J. & Uversky, V. N. Zooming into the dark side of human annexin-s100 complexes: Dynamic alliance of flexible partners. *International Journal of Molecular Sciences* (2020).

398. Ohshima, K. *et al*. Integrated analysis of gene expression and copy number identified potential cancer driver genes with amplification-dependent overexpression in 1,454 solid tumors. *Sci. Rep.* **7**, 1–13 (2017).

399. Common Symptoms of Multiple Myeloma | The MMRF. https://themmrf.org/multiple-myeloma/symptoms-and-side-effects/.

400. Rajkumar, S. V. MGUS and smoldering multiple myeloma: update on pathogenesis, natural history, and management. *Hematology Am. Soc. Hematol. Educ. Program* (2005).

401. Avilés, A. *et al*. Prognostic importance of beta-2-microglobulin in multiple myeloma. *Rev. Invest. Clin.* (1992).

402. Bergsagel, P. L., Masellis Smith, A., Belch, A. R. & Pilarski, L. M. The blood B-cells and bone marrow plasma cells in patients with multiple myeloma share identical IgH rearrangements. in *Current Topics in Microbiology and Immunology* (1994).

403. Thiago, L. S. *et al*. Circulating clonotypic B cells in multiple myeloma and monoclonal gammopathy of undetermined significance. *Haematologica* (2014).

404. Yi, M. & Schnitzer, J. E. Impaired tumor growth, metastasis, angiogenesis and wound healing in annexin A1-null mice. *Proc. Natl. Acad. Sci. U. S. A.* **106**, 17886–17891 (2009).

405. Prideaux, S. M., Conway O'Brien, E. & Chevassut, T. J. The genetic architecture of multiple myeloma. *Advances in Hematology* (2014) .

406. Benard, B. *et al*. FGFR3 Mutations Are an Adverse Prognostic Factor in Patients with t(4;14)(p16;q32) Multiple Myeloma: An Mmrf Commpass Analysis. *Blood* **130**, 3027–3027 (2017).

407. Guan, M. *et al*. Bortezomib therapeutic effect is associated with expression of FGFR3 in multiple myeloma cells. *Anticancer Res.* (2009).

408. Liu, G. jie *et al*. High expression of TCN1 is a negative prognostic biomarker and can predict neoadjuvant chemosensitivity of colon cancer. *Sci. Rep.* **10**, 1–11 (2020).

409. Gebhardt, C., Németh, J., Angel, P. & Hess, J. S100A8 and S100A9 in inflammation and cancer. *Biochem. Pharmacol.* (2006) .

410. Wang, X. *et al*. S100A12 is a promising biomarker in papillary thyroid cancer. *Sci. Rep.* (2020.

411. Moss, S. E. & Morgan, R. O. The annexins. *Genome Biology*. **5**, 219 (2004).

412. Samart, P., Luanpitpong, S., Rojanasakul, Y. & Issaragrisil, S. O-GlcNAcylation homeostasis controlled by calcium influx channels regulates multiple myeloma dissemination. *J. Exp. Clin. Cancer Res.* **40**, 100 (2021).

413. Abdallah, N. *et al*. Cytogenetic abnormalities in multiple myeloma: association with disease characteristics and treatment response. *Blood Cancer J.* (2020).

414. Rajkumar, S. V. Multiple myeloma: 2016 update on diagnosis, risk-stratification, and management. *Am. J. Hematol.* **91**, 719–734 (2016).

415. Liu, M. *et al*. S100 Calcium Binding Protein Family Members Associate With Poor Patient Outcome and Response to Proteasome Inhibition in Multiple Myeloma. *Front. Cell Dev. Biol.* **9**, 2261 (2021).

416. Donato, R. *et al*. Functions of S100 Proteins. *Curr. Mol. Med.* **13**, 24–57 (2012).

417. Grebhardt, S., Müller-Decker, K., Bestvater, F., Hershfinkel, M. & Mayer, D. Impact of S100A8/A9 expression on prostate cancer progression in vitro and in vivo. *J. Cell. Physiol.* **229**, 661–671 (2014).

418. Kang, H., Ko, J. & Jang, S. W. The role of annexin A1 in expression of matrix metalloproteinase-9 and invasion of breast cancer cells. *Biochem. Biophys. Res. Commun.* **423**, 188–194 (2012).

419. Landowski, T. H., Megli, C. J., Nullmeyer, K. D., Lynch, R. M. & Dorr, R. T. Mitochondrial-mediated disregulation of Ca2+ is a critical determinant of velcade (PS-341/Bortezomib) cytotoxicity in myeloma cell lines. *Cancer Res.* **65**, 3828–3836 (2005).

420. Narita, T. *et al*. T(14;16)-positive multiple myeloma shows negativity for CD56 expression and unfavorable outcome even in the era of novel drugs. *Blood Cancer Journal* vol. 5 e285 (2015).

421. Hurt, E. M. *et al*. Overexpression of c-maf is a frequent oncogenic event in multiple myeloma that promotes proliferation and pathological interactions with bone marrow stroma. *Cancer Cell* (2004) .

422. Caro, J. *et al*. How to Treat High-Risk Myeloma at Diagnosis and Relapse. *Am. Soc. Clin. Oncol. Educ. B.* (2021).

423. Sonneveld, P. *et al*. Treatment of multiple myeloma with high-risk cytogenetics: A consensus of the International Myeloma Working Group. *Blood* (2016.

424. Asahina, Y. *et al*. Discovery of BMS-986235/LAR-1219: A Potent Formyl Peptide Receptor 2 (FPR2) Selective Agonist for the Prevention of Heart Failure. *J. Med. Chem.* **63**, 9003–9019 (2020).

425. Giebeler, A. *et al*. Deficiency of Formyl Peptide Receptor 1 and 2 Is Associated with Increased Inflammation and Enhanced Liver Injury after LPS-Stimulation. *PLoS One* **9**, e100522 (2014).

426. Han, G. H. *et al*. Association of serum annexin A1 with treatment response and prognosis in patients with esophageal squamous cell carcinoma. *J. Cancer Res. Ther*. **14**, S667–S674 (2018).

427. Morris, S. *et al*. Whole blood FPR1 mRNA expression predicts both non-small cell and small cell lung cancer. *Int. J. Cancer* **142**, 2355–2362 (2018).

428. Zhang, J., Yang, C., Zhou, F. & Chen, X. PDK1 inhibitor GSK2334470 synergizes with proteasome inhibitor MG-132 in multiple myeloma cells by inhibiting full AKT activity and increasing nuclear accumulation of the PTEN protein. *Oncol. Rep.* **39**, 2951–2959 (2018).